MATHEMATICAL MODELING AND OPTIMAL CONTROL TO BIOLOGICAL MODELS

A Thesis Submitted to

DELHI TECHNOLOGICAL UNIVERSITY

In Partial Fulfillment of the Requirements of the Award of the Degree of

DOCTOR OF PHILOSOPHY

In

MATHEMATICS

By

SUDHAKAR YADAV, M.Sc.

Under the Supervision of

Dr. Vivek Kumar Aggarwal, Ph.D.

DEPARTMENT OF APPLIED MATHEMATICS

DELHI TECHNOLOGICAL UNIVERSITY

(Formerly Delhi College of Engineering)

BAWANA ROAD, DELHI-110 042, INDIA.

June, 2022   **Enroll. No. : 2K16/PHDAM/07**

DECLARATION

I declare that the work included in this thesis entitled "**Mathematical Modeling and Optimal Control to Biological Models**" has been completed by me for the award of the degree of *Doctor of Philosophy in Mathematics* under the supervision of *Dr. Vivek Kumar Aggarwal*, Department of Applied Mathematics, Delhi Technological University, Delhi, India.

   The research content of this thesis is an authentic work and has not been submitted to any other University or Institute for the award of any degree or diploma.

Date :   **(Sudhakar Yadav)**

CERTIFICATE

This is to certify that the thesis titled **"Mathematical Modeling and Optimal Control to Biological Models"** submitted by **Ms. Sudhakar Yadav**, student of Ph.D., to the Department of Applied Mathematics, Delhi Technological University, Delhi for the award of the degree of *Doctor of Philosophy in Mathematics*. The thesis embodies authentic research work completed by his under my supervision.

It is further stated that the content of the thesis is original and has not been submitted to any University or Institution for the award of any Degree or Diploma.

(Dr. Vivek Kumar Aggarwal)
Supervisor
Department of Applied Mathematics
Delhi Technological University
Delhi, India.

(Dr. S. Sivaprasad Kumar)
Professor & Head
Department of Applied Mathematics
Delhi Technological University
Delhi, India.

ACKNOWLEDGEMENTS

Date :   **(SUDHAKAR YADAV)**

Place : Delhi, India.

Dedicated to My Brother

Martyred Sanjay Kumar Yadav

Contents

6 Preventing the Spread of Locust Swarm and Pest in Agriculture: Mathematical Modeling and Qualitative Analysis **175**

Preface

The thesis entitled **"Mathematical Modeling and Optimal Control to Biological Models"** comprises of six chapters followed by conclusion, future scope and a bibliography. The abstract at the start of each chapter provides a quick overview of the research work done in that chapter. The core objective of this dissertation is to construct and establish mathematical models of crop, pest, and natural enemies of pests, with a strong attention on pests' detrimental effects on crops. As a consequence, This allows us to explain, recommend, propose, and provide the best pest treatment approach and optimal pest control technique needed to remove or reduce pest density while enhancing agricultural output. The following is the framework of the thesis:

Chapter 1 introduces the motivation, biological backgrounds, a mathematical model, the relevance of functional responses, several ways for obtaining stability, the concept of optimal control, and a numerical methodology.

Chapter 2 addresses the concepts, methodologies, and implementations of mathematical models in farming. A mathematical study of two prey and one predator model has been performed in agriculture. Furthermore, an ecosystem consists of two prey and their predator; here, the prey–I, such as sugarcane crops, which require more time to develop, and the prey–II, such as vegetables, which have a shorter lifespan, are cultivated alongside sugarcane crops, with predators harming both prey–I and prey–II. The actual data of some parameters and the experimental data of other parameters have been used for model verification. The content of this chapter is published in the form of a research paper entitled **"A Prey–Predator Model Approach to Increase the Production of Crops: Mathematical Modelling and Qualitative Analysis"** in *International Journal of Biomathematics* (World Scientific).

In chapter 3, a mathematical model of an ecological perspective of prey, pest, and natural enemies of pest is addressed. The existence and stability of the steady–state

conditions of various equilibrium points are studied. Furthermore, in the presence of the control variable, a mathematical model is formed for designing optimal pest control problems and studying the effects on crop pests. Then, the existence, characterization, and necessary conditions of the optimal control are determined using Pontryagin's maximum principle. Numerical simulations are then used to validate analytical results and to depict a better approach. The content of this chapter is published in the form of a research paper entitled **"Study of a Prey–Predator Model with Preventing Crop Pest Using Natural Enemies and Control"** in *American Institute of Physics, Conference Proceedings*.

In Chapter 4, the effectiveness of additional food has been investigated in this study of the prey–predator interaction. Providing additional food to predators has been considered significant to balance the biological system and ecosystem. A mathematical model of a prey-predator ecology is provided, which contains a crop, a susceptible pest, an infected pest, and a natural enemy of the pest. Further, the dynamic behavior of the framework, the description of steady–state equilibrium behavior, and pest control are discussed. The basic reproduction number and sensitivity analysis are addressed to determine the most influential parameters. Furthermore, a comprehensive analysis of the optimal control strategy is performed. Pontryagin's maximum principle is used to develop an optimal strategy for pest control. Finally, numerical simulations are carried out to support the analytical results and to explain various dynamic systems that are used in the model. The results of this chapter are in the form of a communicated research paper entitled **"Study of Prey Predator System with Additional Food and Effective Pest Control Techniques in Agriculture"**.

Chapter 5 develops a mathematical model for describing the dynamics of the banana–nematodes and its pest detection method to help banana farmers. There are two criteria that are addressed: the mathematical model and the type of nematode pest management technique. The sensitivity analysis, local stability, global stability, and the dynamic behavior of the mathematical model are performed. Further, the mathematical model for optimal control is developed and discussed. This mathematical model describes various management strategies, such as the initial release of infected predators and the destruction of nematodes. Theoretical results are demonstrated and validated via numerical simulations. The content of this chapter is published in the form of a research paper entitled **"A Prey Predator Model and Control of a Ne-**

matodes Pest Using Control in Banana: Mathematical Modelling and Qualitative Analysis" in *International Journal of Biomathematics* (World Scientific).

Chapter 6 presents an interaction between the prey predator model consisting of three species: crop, pest and locust swarms. Under specific circumstances, all possible existence of the biological equilibrium points of the model is described. To study the dynamics of the system, the local asymptotic stability of several equilibrium points is illustrated. Different criteria are addressed for the coexistence of equilibrium solutions. Further, we present numerical results to illustrate some biologically important circumstances. This study investigates the appropriate use of management measures to reduce the spread of the swarm through optimal control techniques. Two types of control variables are used: first, the application of pesticide, and second, the application of creating awareness. The content of this chapter are in the form of a communicated research paper entitled **"Preventing the Spread of Locust Swarm and Pest in Agriculture: Mathematical Modeling and Qualitative Analysis"**.

Subsequently, the conclusion of the work carried out in the thesis is presented. We have also discussed the future scope of the current work.

List of Figures

List of Tables

Chapter 1

Introduction

"Nature is written in mathematical language."

Galileo

1.1 Motivation

Mathematical modelling has a diversity of applications due to its collaboration with different disciplines of study. The field gets revitalised and improved with each subsequent interaction. System models have been ingrained in our culture. Mathematical biology, often known as biomathematics, is a field of mathematical modelling that analyses real-world issues in biological systems and health fields using mathematics and computation. From a philosophical standpoint, mathematical logic and precision give a paradigm for argument creation. Fractal mathematics has contributed in the successful establishment of fractal image compression systems that need little storage for incredibly precise pictures. Physical sciences, medicine, and social sciences are among additional fields of applicability. Mathematical models are widely employed in ecosystems to investigate population changes, water drainage basins, erosion, and

contaminant distribution. Another broad field of study is fluid dynamics, which has applications ranging from the modelling of developing tsunamis over the ocean to the flow of candy mixture into containers. This tendency is expected to continue since modelling results in a more efficient and cost-effective method of studying, analysing, and creating processes. Additionally, the wide range of applications in which mathematical models are utilised implies an attraction to many disciplines of mathematics as well as many different types of models. Some models can forecast quite accurately, but some may be more open to a variety of interpretations. The utilisation of facts from this modelling technique to make choices is now well publicised, particularly in the case of climate impacts, as demonstrated by the 1998 international summit on Global Warming in Kyoto. Because biological sciences are so complicated, multidisciplinary participation is required. Environmental protection concepts that have arisen in contemporary agriculture establish tight boundaries for the agricultural techniques that have been implemented. At the same time, solving the food supply issue for the globe's rising population continues to be a significant task. As a result, numerous resource-saving measures are becoming increasingly important for the development of sustainable agriculture. Agriculture has always been the backbone of the country's economy, providing both food for the growing population and raw materials for industry. The application of mathematics in agricultural growth has clearly become both necessary and beneficial. Many interesting issues in biological models and optimal management of biological systems may be framed as optimization with differential equation constraints and other restrictions. Supervision of biological models that are extremely valuable in real life. As with the SIR Model, optimum control techniques are used to establish a vaccination schedule that minimize the number of infected humans and the total cost of the vaccine over a set time period. Optimal control approaches in cancer decrease tumour density and treatment adverse effects over a particular time span. In the predator–prey model, a pesticide destroys both the prey and the predator on a timely basis. In HIV treatment, the use of optimal control to establish a chemotherapy technique for the diagnosis. To establish the insulin injection level (control) in the Glucose Model that minimizes the discrepancy between the concentration of blood glucose and the desired constant glucose level. To prevent the transmission of infectious illnesses, there are two types of control techniques available: pharmaceutical treatments (drugs, vaccines) and nonpharmaceutical therapies

2

(Social isolation, containment, and an awareness and education movement). There are various variables that may be optimally controlled to maximise the epidemic illness. Thus, engineering, environment and industry, health sciences, and other fields have all benefited from mathematical modelling. Its use in various domains is growing, and it is now an unique instrument for quantitative and qualitative analysis.

1.2   Mathematical Models and Optimal Control in Agriculture

Many of the latest pest control approaches have concentrated on organic insecticides. As stated by [58], the use of chemical insecticides is an effort to control the pest directly at a minimal price. However, these chemicals have been identified to have a variety of negative effects on the environment, including chemical residues in crops and agricultural habitats. Efficient management of these pests can be achieved using living organisms, reducing their abundance. There are many species and birds whose feed is these insects, but they cannot affect farming. Thus, such inhabitants could be used by some of the biological controls. Usage of predator species to kill pests can be seen in the research work [10, 16, 111, 153, 173, 196, 203]. Therefore, the pest may be an infection with certain bacterial or viral diseases. For example, baculovirus normally develops in plants, so these viruses do not have any direct impact on crop yield, but they can be used to decrease the pest population [60, 128, 154]. The possible approaches to addressing this problem have been a subject of considerable discussion between investigators at a minimum of four decades [29, 39], and discussions are still underway on this issue [60, 128, 154, 241].

In the specific field of agricultural pest control, the challenge is to develop reliable mathematical models capable of at least describing different techniques of pest control qualitatively. As from roots of the idea of integrated pest control models in the late 1950s, the study has provided a valuable selection of mathematical models that focuses on the different characteristics of application–based pest–integrated management models [236]. [29] considered appropriate biological and chemical pest control combinations to be used in specific ecosystems of plants, pests, and parasites. Parasites can manage the pest population on their own accord to some extent, but this effect

3

is negatively affected by the use of pesticides, as [29] has also found that the chemicals harm the parasites. Successive studies of mathematical models for pest control have been carry out by [78, 115]. Interactions between crop, pest, diseases, and pest predators have also been studied in [115, 236]. [78, 171] presented the relationships among both hosts and parasites. [22] explained pest control by adding an infected insect. [57] also implemented mathematical models to monitor infected pests in a plant population. Moreover, the development of effective control measures to battle insect populations and boost crop output is discussed [12, 14, 104, 105, 221]. [15, 130] explored into ecological modelling, focusing about the methods and relevance of analysing insect movement, as well as the benefits for agriculture.

Thus, infection with the insect population has also become one of the ways in which they can be effectively eliminated from farm crops. The impetuous pest control model has been chosen and reformed as a hybrid dynamic system [171], enabling the parametric analysis of the system's response periodically via numerical continuation methods [22]. In this way, it has been possible to address concerns such as increasing the effectiveness of impetuous pest control while minimizing production costs and environmental damages.

1.3   What Is Mathematical Modelling?

A mathematical model is a mathematical approach, method, or collection of equations that is used to describe or explain ecosystems and their behaviors, functions, or different elements of real-life issues. Mathematical modelling refers to the event or way of achieving the aforesaid situation. Models express our assumptions about how the world works. We transfer such views into mathematical terms in mathematical modelling. A mathematical model can differ depending on the type of model or what it is addressing, and some of the applications of mathematical models include:

- Quantity relationships in real–life scenarios

- Creating future forecasts

- Comprehending a system's beginnings

- Displaying data,

- Acquiring knowledge about a system

Furthermore, mathematical models provide novel approaches to understand the increasingly complicated behaviour of technology, which is at the basis of today's industrial output, according [7]. They are essential in simulation, investigation, analysis, and decision–making. As a consequence, they play a significant role in technological progress. Moreover, mathematical models may generate unique answers and solutions in a relatively short amount of time, enabling faster innovation cycles [149].

1.3.1 Classifications of Models

Many various forms of mathematical models can be utilised based on the goals of the scientist, such as analysing relationships or generating forecasting. This is useful to categorise models while examining them. Individual model classification into such groups quickly reveals some of the most important structural characteristics. The type of outcome that models suggest is one way to distinguish them. [182] defines the categorisation in the following way:

- **Empirical models:** Empirical modelling describes the connection of observations between one or two variables using current data, according to [38]. In animal husbandry, empirical models are commonly utilised, and caution must be exercised when projecting beyond the data's constraints. Empirical modelling includes looking at data linked to the problem in order to formulate or establish a mathematical correlation between different variables in the issue using the data provided.

- **Simulation models:** Simulation modelling is the process of creating a scenario based on a set of rules using a computer programme or other technical instrument. These guidelines are based on how a process is expected to grow or improve.

- **Deterministic models:** In general, deterministic modelling entails using an equation or collection of equations to model or forecast the result of an event or the value of a quantity.

- **Stochastic models:** When formulating equations in stochastic models, unpre-

dictability and probability of events occurring are taken into account.

- **Mechanistic models:** Mechanistic equations are those generated from a theory or hypothesis about the system's underlying nature. A mechanistic model presupposes full understanding of the system's casual interactions, and calculated findings should be applicable to a wide range of situations.

Deterministic models avoid random fluctuation and, as a result, always anticipate the same result from a given beginning point. The model, on the other hand, may be statistical in character and therefore forecast the distribution of possible results. These models are described as stochastic.

1.3.2 Stages of Modelling

It is beneficial to split the modelling process into four major areas of activity: constructing, researching, testing, and application. Although it would be wonderful to believe that modelling projects go easily from conception to completion, this is rarely the case. Defects discovered during the research and testing phases are often addressed by returning to the construction stage. It is worth noting that if the model is changed, the research and testing processes must be redone.

1.3.3 Building Models

- **Getting started:** We must have a clear understanding of our goals before beginning a modelling effort. In two ways, these influence the project's future course. Firstly, the quantity of information included in the model is determined by the model's intended usage. Secondly, we must distinguish between the simulated system and its surroundings. This distinction is clear if the environment influences the system's behaviour but the system does not influence the environment.

- **Systems analysis**

  - **Making assumptions:** After determining the system to be simulated, we must build the model's fundamental structure. This reflects our perceptions of how the system works. Underlying assumptions can be used to

6

express these views. Future system analysis takes these assumptions as true, but the outcomes are only as good as the assumptions. In epidemiological studies, it is commonly assumed that, in the absence of limiting circumstances, a population would expand at a pace proportionate to its size. The differential equation is a deterministic framework that illustrates such a population over time.

$$\frac{dP}{at} = aP$$

where $P(t)$ denotes the population size at time t and a denotes a constant. The integration of this equation yields

$$P(t) = P(0)e^{at},$$

where $P(0)$ denotes the population size at time zero. When $a > 0$, this is an exponential growth model, and when $a < 0$, this is an exponential decay model. Populations expand at an exponential rate, as per this answer. Obviously, not all populations expand at an exponential rate. Because the differential equation was derived from an understanding of the presumption, we must look to the presumption to demonstrate this mismatch.

– **Flow diagrams:** When modelling a more complicated system, we cannot simply move from a hypothesis to an equation. Flow diagrams can help with this visually. In their most fundamental sense, they are made up of a succession of boxes connected by an arrow network. Physical entities are represented by the boxes that exist in the system, and the arrows show how these entities interact with one another.

- **Choosing mathematical equations:** After determining the design of a model, mathematical expressions must be utilised to characterise the system. It is critical to select such equations with caution since they may have unanticipated impacts on the model's functioning.

- **Solving equations:** Finding an analytical solution to a model may be quite beneficial. This will allow us to carry out all of the model's inferred adjustments with little hassle. Obtaining an analytical answer is rarely easy. It is feasible to acquire a mathematical approach to a system of equations in some particular in-

stances. If we considered a comparable system with only one non-linear factor, we would be unable to use this strategy. If an analytical answer exists, it must be sought in other methods. However, when models feature nonlinearity, as most attractive models do, obtaining analytic solutions is often more difficult than for the comparable deterministic system. If the model is more complex, and particularly if the framework is likely to change, it is unlikely that an analytic solution will be found. When analytical approaches are ineffective, numerical methods might be used to get approximate answers. Though they will never have the identical generality as analytical answers, they can be just as effective in any given situation. In general, numerical solutions to model equations approximate the processes stated in the model.

1.3.4 Studying models:

It is essential to understand that the actions of a model may be characterised in two approaches: qualitatively and quantitatively. In general, qualitative behaviour is the same for entire families of models, but quantitative behaviour is typically only appropriate for a particular scenario.

1.3.5 Testing Models

Once we have analyzed our model and are satisfied with its effectiveness, we can begin testing it against observations from the physical system that it describes. This is often known as validation. The model's hypotheses, framework, parameters, and predictions should all be tested in mathematical models.

1.3.6 Discussion of a Model

This module emphasises the range of activities associated with mathematical modelling. It is essential to provide a clear representation of the range across which the model is regarded to be reliable. This range is dependent on the information used to develop the model as well as the data used to test it.

1.4 History of the Study

T. Malthus argued in his book "An essay on the principle of population" [215] in 1798 that population increase is an exponential approach, i.e. always rising or declining, generally known as the Malthusian model or exponential model. The rate of population increase, as per this concept, is proportionate to the current population at the moment. If $P_1(t)$ represents the population at any moment t, then the population change rate is dP_1/dt, and $(1/P_1)(dP_1/dt)$ signifies the population change rate per capita. Considering that only births r_1 and deaths r_2, affect growth rate change, the per capita rate of change is given by,

$$\frac{dP_1(t)}{dt} = (r_1 - r_2)P_1.$$

If the initial population at time $t = t_0$ is P_{10}, then the model is,

$$\frac{dP_1(t)}{dt} = rP_1, \; P_1(t_0) = P_{10}, \tag{1.4.1}$$

where, $r = r_1 - r_2$ is the intrinsic growth rate. The solution is $P_1 = P_{10}e^{r(t-t_0)}$. Because of the following conclusions, the model is restricted [189].

I. The rate of per capita growth is constant and is not affected by density.

II. The rate of increase is either exponential or exponential decline.

III. When the birth and death rates are same, the population is constant, and $r = 0$.

Despite this, the model has several applications in the study of plant or insect populations, microbiology, fisheries, and so on [189] and may be regarded as a basic model in understanding population dynamics. On population growth [160], Pierre-François Verhulst presented a logistic model in 1838. Following the debate by [160], the model became recognized as the Verhulst–Pearl model. It was discovered that the per capita growth rate is dependent on total population, and that population rises exponentially in the presence of ample food; nevertheless, as the population develops, competition for food ensues, which is known as the *crowding effect*. If the initial population at time

$t = t_0$ is P_{10}, the model is

$$\frac{dP_1(t)}{dt} = rP_1(1 - \frac{P_1}{K}), \; P_1(t_0) = P_{10}.$$

Writing the initial value problem as,

$$\frac{dP_1(t)}{dt} = rP_1(1 - \frac{P_1}{K}), \; P_1(t_0) = P_{10} \tag{1.4.2}$$

where $r = r_1 - r_2$ represents the intrinsic growth rate and Carrying capacity is governed by available information and is denoted by K. The result is $P_1 = \frac{K}{1 - e^{-rt}\frac{P_{10}-K}{P_{10}}}$.
The model is limited because of the following implications [189]

I. The per capita growth rate is affected linearly by P_1.

II. Variations in growth rate occur spontaneously in response to changes in population, with no regard for time lag.

III. The model does not take into account external circumstances.

The approach has numerous uses in both the human and animal populations [30]. Furthermore, the logistic model was transformed into a Theta–Logistic model in order to investigate the several types of nonlinear interactions between the rate of population change and its densities. As a result, the model appears in the form:

$$\frac{dP_1}{dt} = rP_1 \left[1 - \left(\frac{P_1}{K} \right)^\theta \right]. \tag{1.4.3}$$

In the analysis of the connection between population and per capita growth rate, the $'\theta'$ factor is the decisive factor. As an example, if θ is big with $P_1 < K$, the system grows exponentially; if $P_1 > K$, the growth rate reduces; and if $P_1 = K$, the population does not change. Warder Clyde Allee researched biological organisms from the standpoint of ecology in 1931 and discovered that the life expectancy is frequently influenced by populationof the same species, resulting in low population densities. Because of lower rates of reproduction and survival, population rates might reach zero or even be negative [231, 232]. The Allee effect demonstrates that a certain level of population density is essential for a population to exist or sustain itself. The Allee effect occurs when the population growth rate initially climbs and then declines to zero at a greater population rate. The exponential system is transformed into the restricted growth model by introducing the idea of overcrowding, which causes conflict among

species owing to a shortage of resources. The model has the following structure:

$$\frac{dP_1}{dt} = r_1 P_1 - r_2 P_1 - \gamma P_1^2, \qquad (1.4.4)$$

where γ is the mortality rate caused to species overpopulation. Ecological modelling comprises two species, one predator and one prey, and the study of their connection is an important element of ecology. The predator's feeding rate on prey is the most important factor in prey predator contact, and there is an increase or decrease in prey density owing to a rise or reduction in predator density. Furthermore, there is a dynamic between prey decline and predator growth, and studying this dynamic is an essential subject of study in ecology [124, 189]. Beginning in the twentieth century, Umberto D'Ancona, an Italian marine researcher, completed a 13-year quantitative examination of fish species. The density of Selachians (predators) surged during the First World War (1914-1918), but declined when hunting was done [136], and prey population followed the opposite direction. Later, Vito Volterra, an Italian physicist and mathematician, and [224] designed and implemented a mathematical model illustrating the eating of one species by the other. Let $P_1(t)$ and $P_2(t)$ be the prey and predator population densities, respectively. Volterra's system is structured as follows:

$$\begin{cases} \frac{dP_1}{dt} = P_1(t)(\alpha - \beta P_2(t)), \\ \frac{dP_2}{dt} = P_2(t)(\gamma P_1(t) - \delta), \end{cases} \qquad (1.4.5)$$

where, $\alpha, \beta, \gamma, \delta$ are the positive constants. The first equation of (1.4.5) states that the rate of change in prey population is a function of the rate of growth in prey population minus the damage due to predator population, while the second equation of (1.4.5) states that the rate of change in predator population is a function of the existing prey population minus the predator death rate [1, 2, 189]. Lotka [1] and subsequently Volterra [229] developed the model, which became recognized as the Lotka-Volterra (L-V) model. The L-V model, according to [133], is based on certain unsustainable biological hypotheses, like the fact that both prey and predator populations do not constrain their development rate.

Kermack and Mckendrick produced an important publication on the Susceptible–Infectious–Recovered (SIR) model in 1927, which was extensively recognised by numerous

11

scholars. The SIR model looks like this:

$$
\begin{cases}
\frac{dP_1}{dt} = -\beta P_1 P_2, \\
\frac{dP_2}{dt} = \beta P_1 P_2 - \gamma P_2, \\
\frac{dP_3}{dt} = \gamma P_2,
\end{cases}
\tag{1.4.6}
$$

where $P_1(t)$, $P_2(t)$, and $P_3(t)$ denote the susceptible, infected, and recovered populations at any given time t, and β, γ denote the infection and recovery rates, respectively. The Kermack–Mckendrick (K-M) model looked at how the number of infectious agents increased and decreased throughout epidemics. In the subject of eco–epidemiology, the two basic models are L-V and K-M, which are integrated to establish an eco–epidemological system. Let $P_1(t), P_2(t),$ and $P_3(t)$ be the population concentrations of healthy prey, sick prey, and predator populations, respectively, and the model be written as:

$$
\begin{cases}
\frac{dP_1}{dt} = rP_1 - \beta P_1 P_2, \\
\frac{dP_2}{dt} = \beta P_1 P_2 - \gamma P_3 P_2 - c_1 P_2, \\
\frac{dP_3}{dt} = \gamma \delta P_3 P_2 - c_2 P_3,
\end{cases}
\tag{1.4.7}
$$

where r, β, γ, δ, c_1, and c_2 are positive constants. Only the prey population is infected in the previous scenario. Hadeler and Freedman study the predator-prey relationship with pathogens in the prey population, which infects the predator population as well [116]. Prey become frail as a result of infection, making them more vulnerable to predators. [108] was inspired by [116] to investigate an eco–epidemiological model comprising three populations as vulnerable prey, diseased prey, and predators. The prey population is supposed to obey the logistic rule, and illness occurs by the basic law of mass action with no recovery. The system becomes:

$$
\begin{cases}
\frac{dP_1}{dt} = r(P_1 + P_2)(1 - \frac{P_1 + P_2}{K}) - \beta P_1 P_2 - \eta \gamma_1 P_1 P_3, \\
\frac{dP_2}{dt} = \beta P_1 P_2 - \gamma(P_2) P_3 - C P_2, \\
\frac{dP_3}{dt} = (\varepsilon \gamma P_2 + \eta \varepsilon \gamma_1 P_1 - d) P_3,
\end{cases}
\tag{1.4.8}
$$

where r, β, η, γ_1, γ, C, ε, γ and d are positive constants. Further, P_1, P_2, and P_3 are the populations of susceptible prey, infected prey, and predators, respectively. The model described above is the most often cited [74] and a fundamental model in eco-

epidemiology. The prey predator system is defined as follows in [136, 195]:

$$\begin{cases} \frac{dP_1}{dt} = B(P_1) - g(P_1, P_2)P_2, \\ \frac{dP_2}{dt} = -dP_2 + e\, g(P_1, P_2)P_2, \end{cases} \quad (1.4.9)$$

In the absence of predators, $B(P_1)$ is the growth rate of the prey population. Predator effectiveness, predator population mortality rate, and functional response are all represented by e, d, and $g(P_1, P_2)$, respectively. An important characteristic of this discipline is choosing a desirable functional response for the prey predator system.

The functional response is described as the connection between the predation rate, which may be defined as the amount of prey eaten per predator in unit time, and the prey density [82]. The linear functional response, also recognised as the L–V type functional response or Holling type I functional response, is taken into account in Lotka Volterra type prey predator systems where the predator's intake is directly proportionate to prey density, i.e., attack rate rises linearly with prey population, then it acquires a fixed value when the predator's population reaches saturation [108, 177] and consists of following structure:

$$g(P) = P. \quad (1.4.10)$$

[26, 27, 114] modified the Lotka Volterra model and another functional response known as Holling type II was formed where the consumption rate by predators increases with decreasing prey population density till it satisfies with the following form::

$$g(P_1) = \frac{\alpha_1 P_1}{\alpha_2 + P_1}, \quad (1.4.11)$$

where α_1, α_2 are constants and P_1 denotes species density. Many articles with Holling type II functional response in the literature [113, 238]. Furthermore, Holling type III [112] denotes that the consumption rate first rises, then declines until easily assessed is reached, and the functional response has the form:

$$g(P_1) = \frac{\alpha_1 P_1^2}{\alpha_2 + P_1^2}. \quad (1.4.12)$$

Holling type IV [186] was first assigned by [106], indicating that the rate of predation

reduces at high prey populations and the functional response adopts the following structure:

$$g(P_1) = \frac{\alpha_1 P_1}{\alpha_2 + P_1 + \frac{P_1^2}{\alpha_3}}. \tag{1.4.13}$$

Many scientists criticised the addition of prey dependent functional responses in prey predator models, arguing that functional responses in ecology must be depending on the population size of both prey and predator as predators seek or struggle for food. A prey predator model was discovered to include 'ratio dependent' theory, which asserts that per individual predator growth rate is the ratio of prey density to predator density. Several authors strongly supported this notion. So, [181] presented a ratio-dependent functional response based on the Holling type-II functional response, which has the form:

$$g(P_1) = \frac{\alpha_1 \frac{P_1}{P_2}}{\alpha_2 + \frac{P_1}{P_2}} = \frac{\alpha_1 P_1}{P_1 + \alpha_2 P_2}. \tag{1.4.14}$$

In 1969, Hassell-Varley in his paper [132] defined the functional response as,

$$g(P_1, P_2) = \frac{\alpha P_1}{P_2^\sigma}, \tag{1.4.15}$$

where α reflects the efficacy of hunting and σ denotes the predator's interference. The functional response of Hassel-Verley type can be characterised as follows:

$$g(P_1, P_2) = \frac{\alpha P_1}{P_2^\sigma + P_1}. \tag{1.4.16}$$

[40] was published in 1975 with a functional response depending on predator density termed as the Beddington-DeAngelis response, which takes the shape of

$$g(P_1, P_2) = \frac{\beta P_1}{\gamma + \alpha P_2 + \delta P_1}, \tag{1.4.17}$$

where γ represents the atmosphere's safety to the prey population, α represents predator involvement, and δ represents the intensity with which the feeding rate approaches the saturation level β. The Beddington–DeAngelis functional response is

represented by the following model:

$$
\begin{cases}
\frac{dP_1(t)}{dt} = P_1(t)\left(a - bP_1(t) - \frac{cP_2(t)}{a_1+b_1P_1(t)+c_1P_2(t)}\right), \\
\frac{dP_2(t)}{dt} = P_2(t)\left(-d + \frac{fP_2(t)}{a_1+b_1P_2(t)+c_1P_2(t)}\right).
\end{cases} \tag{1.4.18}
$$

Where the prey and predator population densities are P_1 and P_2, respectively. Several mathematical problems have been studied in literature using Beddington–DeAngelis functional responses [81,183]. [163] reevaluated the Beddington–DeAngelis type model, allowing predator interference regardless of whether predators are handling prey or looking for prey, and provided the following functional response:

$$
g(P_1, P_2) = \frac{\alpha_2 P_1}{\alpha_3 + P_2 + \delta P_1 + \alpha_1 P_1 P_2}. \tag{1.4.19}
$$

This is referred to as a Crowley–Martin (C–M)functional response. Many studies utilising the C-M type response have been reported in the literature [70]. The broadening scope of investigating eco-epidemiological models has been highlighted in the literature. The fundamental models stated previously are updated in this thesis, and the analysis is then carried out using positivity, boundedness, permanence, stability criteria, bifurcation, and other criteria.

1.5 Mathematical Preliminaries

The preliminaries utilised in the subsequent chapters are acknowledged in the following section. The majority of the results are stated in the next part without proof but supported by various sources.

1.5.1 Dynamical System

The mathematical explanation of a systematic, experimental, and predictable process is referred to as a dynamical system. It may be expressed as a system that grows over time in accordance with a set principle. The present situation and the mathematically expressed law of any physical, chemical, biological, or ecological system predict its past and future states, provided that the rules do not change through time. As a result, the dynamical system includes specified states and rules that evolve

over time.

1.5.2 Phase Plane Analysis

Because there is frequently no analytical approach to solve for a nonlinear system, phase plane analysis is among the most essential tools for investigating its behaviour. [88, 165] describe the phase plane approach. Let

$$\dot{P_1} = f_1(P_1, P_2), \ \dot{P_2} = f_2(P_1, P_2) \tag{1.5.1}$$

where P_1 and P_2 denote system state variables and f_1 and f_2 denote nonlinear functions of the states. The phase plane is defined by the state space of the P_1 and P_2 functions. Let $P(t) = (P_1(t), P_2(t))$ be the solution of (1.5.1) starting from a given initial state $P_0 = (P_{10}, P_{20})$. For any $t \geqslant 0$, the locus in the $P_1 - P_2$–plane of the solution $P(t)$ is a curve that runs through the point P_{10}. This curve is referred to be the trajectory or orbit of (1.5.1) from P_0. A solution of (1.5.1), $P(t) = (P_1(t), P_2(t))$ produces a phase plane trajectory, and a family of these trajectories forms a phase representation of the system (1.5.1). A unique point is an essential notion in phase plane analysis. A unique point in the phase plane is an equilibrium point that implies the requirements

$$\dot{P_1} = 0, \ \dot{P_2} = 0 \tag{1.5.2}$$

From conditions (1.5.2) and (1.5.1), the equilibrium relationships are obtained.

$$f_1(P_1, P_2) = 0, \ f_2(P_1, P_2) = 0 \tag{1.5.3}$$

The variables P_1, P_2 that determine the equilibrium point are obtained from (1.5.3). The matrix A is the Jacobian of $f_1(P_1, P_2)$ and $f_2(P_1, P_2)$, and it has the form

$$A = \begin{pmatrix} \frac{\partial f_1}{\partial P_1} & \frac{\partial f_1}{\partial P_2} \\ \frac{\partial f_2}{\partial P_1} & \frac{\partial f_2}{\partial P_2} \end{pmatrix}$$

Table 1.1 depicts the behaviour of the system as it relates to the eigenvalues of A.

16

Table 1.1: Stability Conditions Using Eigenvalues

Eigenvalues of A	Behavior	Stability
$\lambda_1 > \lambda_2 > 0$	node,outgoing	unstable
$\lambda_1 > 0 > \lambda_2$	saddle point	unstable
$0 > \lambda_1 > \lambda_2$	node, ingoing	stable
$\lambda_1 = \lambda_2 > 0$	node(degenerate)	unstable
$\lambda_1 = \lambda_2 < 0$	node(degenerate)	stable
$\lambda = \alpha \pm \beta, \alpha > 0$	spiral, outgoing	unstable
$\lambda = \alpha \pm \beta, \alpha < 0$	spiral, ingoing	stable
$\lambda = \pm \beta, \alpha = 0$	ellipse	stable

When the system is of the type $\dot{P} = AP$ for some matrix A with constant coefficients [44]. There is the following theorem in specific.

Theorem 1.5.1. In the system $\dot{P} = AP$, let A be a constant matrix having eigenvalues λ_i, $i = 1, 2, 3, ..., n$.

1. If the system is stable, then $\text{Re}(\lambda_i) \leqslant 0$, $i = 1, 2, 3, ..., n$.

2. If either $\text{Re}(\lambda_i) < 0$, $i = 1, 2, 3, ..., n$; or if $\text{Re}(\lambda_i) \leqslant 0$, $i = 1, 2, 3, ..., n$ and there are no zero repeating eigenvalues, then the system is uniformly stable.

3. The system is asymptotically stable if and only if $\text{Re}(\lambda_i) < 0$, $i = 1, 2, 3, ..., n$.

1.5.3   Stability Analysis Using Routh–Hurwitz Criteria

Routh's work [49] was a watershed moment in the understanding of dynamic system stability and became a cornerstone of control theory. Routh is widely credited for developing a criteria for evaluating the stability of a system. The criteria is applied by analysing the characteristic equation, and methods for interpreting and applying the criterion are well recognised and utilised, particularly in control systems analysis. The criteria gives an analytical method for evaluating the stability of a system of any order without requiring the roots of the characteristic equation to be obtained. The characteristic equation is required in this criteria to determine the stability of control systems. For linear system stability, the Routh–Hurwitz criteria is both required and sufficient. This criteria is based on the sequence of the characteristic equation's coefficients [67, 143, 235]. We investigate a multiple variables model with continuous

time in this work. As a result, the following stages are used to conduct the stability analysis [121]:

- **Step 1: Calculating a Jacobian matrix.**

$$
J = \begin{pmatrix}
\frac{\partial f_1}{\partial P_1}(P_1, P_2, \ldots, P_n) & \frac{\partial f_1}{\partial P_2}(P_1, P_2, \ldots, P_n) & \cdots & \frac{\partial f_1}{\partial P_n}(P_1, P_2, \ldots, P_n) \\
\frac{\partial f_2}{\partial P_1}(P_1, P_2, \ldots, P_n) & \frac{\partial f_2}{\partial P_2}(P_1, P_2, \ldots, P_n) & \cdots & \frac{\partial f_2}{\partial P_n}(P_1, P_2, \ldots, P_n) \\
\vdots & \vdots & \ddots & \vdots \\
\frac{\partial f_n}{\partial P_1}(P_1, P_2, \ldots, P_n) & \frac{\partial f_n}{\partial P_2}(P_1, P_2, \ldots, P_n) & \cdots & \frac{\partial f_n}{\partial P_n}(P_1, P_2, \ldots, P_n)
\end{pmatrix}
$$

where $\frac{\partial f_i}{\partial P_j}(P_1, P_2, \ldots, P_n)$ is the partial derivative of f_i with respect to its variable, $P_j (i, j = 1, 2, \ldots, n)$.

- **Step 2: Find the Jacobian matrix.** The equilibrium value, P_1^*, P_2^*, $\ldots$, P_n^*, is used to calculate the Jacobian matrix. A local stability matrix, $\hat{J} = J|_{P_1 = P_1^*,\ P_2 = P_2^*,\ \ldots, P_n = P_n^*}$, is obtained. Then, using $\det(\hat{J} - \lambda I) = 0$, get the characteristic polynomial. Where I stands for the identity matrix, and rewrite as follows:

$$
Q(\lambda) = \lambda^n + b_1 \lambda^{n-1} + \ldots + b_{n-1} \lambda + b_n
$$

with real coefficients b_i for $i = 1, 2, , \ldots, n$.

- **Step 3: Routh–Hurwiz criteria.** The following are the values for the n Hurwitz matrices:

$$
H_1 = (b_1),\ H_2 = \begin{pmatrix} b_1 & 1 \\ b_3 & b_2 \end{pmatrix},\ \text{and } H_n = \begin{pmatrix}
b_1 & 1 & 0 & 0 & \cdots & 0 \\
b_3 & b_2 & b_1 & 1 & \cdots & 0 \\
b_5 & b_4 & b_3 & b_2 & \cdots & 0 \\
\vdots & \vdots & \vdots & \vdots & \cdots & \vdots \\
0 & 0 & 0 & 0 & \cdots & b_n
\end{pmatrix}
$$

Note that if $j > n$, then $b_j = 0$. If and only if all $\det H_j > 0$ with $j = 1, 2, \ldots, n$, then $Q(\lambda)$ has roots that are negative or have negative real part and the equilibrium point is thus described as asymptotically stable. The Routh–Hurwitz criteria for polynomials of degree, $n = 4$ are $b_1 > 0$, $b_3 > 0$, $b_4 > 0$, and $b_1 b_2 b_3 > b_3^2 + b_1^2 b_4$.

18

1.5.4 Global Stability

The direct approach of Lyapunov is covered in this section.

1.5.5 Lyapunov Stability Analysis

The stability of a dynamic process is illustrated using Lyapunov stability. A. M. Lyapunov was a forerunner in the successful development of a method for analysing the stability of nonlinear dynamical systems from a global perspective in compared to the widely used local method of linearizing them around points of equilibrium.

Lyapunov's direct method: Lyapunov suggested two approaches for establishing stability in his 1892 work [4]. The first method developed a set of solutions that were later shown to be convergent within specific parameters. The Lyapunov stability criterion, often known as the Direct Method, is the second technique, which employs a Lyapunov function $V(P)$ that is analogous to the potential function in classical dynamics. Let the following dynamical continuous system be:

$$\dot{P}(t) = f(P), \tag{1.5.4}$$

with $f \in C[\Omega, \mathbb{R}^n]$, where Ω is a connected and open subset of $\mathbb{R}^n$ containing the origin. The function f is smooth which assures the uniqueness and existence of the solutions of the system (1.5.4). Assuming that,

$$\left.\begin{array}{l} f(P) = 0, P = 0, \\ f(P) \neq 0, P \neq 0. \end{array}\right\}$$

Without loss of generality, a trivial equilibrium point of the system (1.5.4), i.e., the origin is considered.

Definition 1.5.1. If $V : \mathbb{R}^n \to \mathbb{R}$ is a continuous scalar function. V is said to be a Lyapunov function if it is positive definite, i.e.,

(i) $V(0) = 0$,

(ii) $V(P) > 0$, $\forall P \in \Omega - \{0\}$,

where, Ω is a region in the neighborhood of $P = 0$.

Theorem 1. *Let $P = 0$ be an equilibrium point of the system given by (1.5.4). If $V : \Omega \to \mathbb{R}$ is*

a continuously differentiable function such that the following holds,

(i) $V(0) = 0$,

(ii) $V(P) > 0$, in $\Omega - \{0\}$,

(iii) $\dot{V}(P) = \frac{d}{dt}V(P) = \sum_{i=1}^{n} \frac{\partial V}{\partial P_i} f_i(P) = \nabla V.f(P) \leqslant 0$ in $\Omega - \{0\}$.

Then, the equilibrium point $P = 0$ is said to be stable.

Theorem 2. *Let $P = 0$ be an equilibrium point of the system given by (1.5.4). If $V : \Omega \to \mathbb{R}$ is a continuously differentiable function such that the following holds,*

(i) $V(0) = 0$,

(ii) $V(P) > 0$, in $\Omega - \{0\}$,

(iii) $\dot{V}(x) = \frac{d}{dt}V(x) = \sum_{i=1}^{n} \frac{\partial V}{\partial P_i} f_i(P) = \nabla V.f(P) < 0$ in $\Omega - \{0\}$.

So, the equilibrium point $P = 0$ is said to be asymptotically stable.

Theorem 3. *Let $P = 0$ be an equilibrium point of the system given by (1.5.4). If $V : \Omega \to \mathbb{R}$ is a continuously differentiable function such that the following holds,*

(i) $V(0) = 0$,

(ii) $V(P) > 0$, in $\Omega - \{0\}$,

(iii) $\dot{V}(x) = \frac{d}{dt}V(x) = \sum_{i=1}^{n} \frac{\partial V}{\partial P_i} f_i(P) = \nabla V.f(P) < 0$ in $\Omega - \{0\}$.

(iv) $V(X)$ is radially unbounded.

Then, the equilibrium point $P = 0$ is said to be globally asymptotically stable.

Theorem 4. *(Krasowskii's approach for the formation of Lyapunov function)*

If the matrix function defined by $M(P) = J(P) + J^T(P)$ is negative definite function $\forall\ P \in \Omega (0 \in \Omega)$, where J is the Jacobian matrix with respect to the dynamical system described by (1.5.4). As a result, the point $P = 0$ is stated to be a locally asymptotically stable equilibrium point for the system (1.5.4), with the Lyapunov function $V(P) = M^T(P)M(P)$. Furthermore, the equilibrium point $P = 0$ is said to be globally asymptotically stable if $\Omega = \mathbb{R}^n$ and $V(P)$ is radially unbounded.

1.5.6 LaSalle's Invariance Principle

Definition 1.5.2. (Invariant set). For a dynamic system $\dot{P} = f(P)$, a set Q is an invariant set if every trajectory $P(t)$ starting from a point in Q remains in Q for all time.

Definition 1.5.3. For a dynamic system $\dot{P} = f(P)$, a set Q is an invariant set if every trajectory $P(t)$ with a point in Q remains in Q for all time. A set Q is a positively invariant set if any trajectory $P(t)$ that starts at a point $P(0)$ in Q remains in Q for all time $t > 0$.

Theorem 1.5.2. Let $V(P) : \mathbb{R}^n \to \mathbb{R}$ be such that on $\Omega_l = \{P \in \mathbb{R}^n : V(t) \leqslant l\}$, we have $\dot{V}(t) \leqslant 0$. Define $R = \{P \in \mathbb{R}^n : \dot{V}(t) = 0\}$. Then, If R consists only $P = 0$ trajectories, then the zero solution is asymptotically stable.

1.5.7 Basic Reproduction Number

The epidemiological term of fundamental reproduction number is an essential measure of success of illness transmissibility [109]. It serves as an invasion criteria for the virus's early propagation in a susceptible population. Now we present the basic reproduction number, which is defined as the number of secondary infected persons created by a single infected individual throughout the duration of the entire time. In the case of a single infected compartment, R_0 is just the infection rate multiplied by the mean duration of the illness. This basic heuristic definition of R_0, however, is insufficient for more complex models with several infected compartments. Furthermore, the technique proposed by [110, 158] may be applied to derive the fundamental reproduction number expression. The next–generation matrix technique [156, 158, 159, 167] is used to obtain the basic reproduction number. We calculate the pest reproduction number at pest–free equilibrium points. Let G be the next generation matrix, which includes $f_i(t)$, $v_i^+(t)$, and $v_i^-(t)$, $i = 1, 2, 3, ..., n \in N$; where $f_i(t)$ is the rate of presence of new infections in the compartment i, $v_i^+(t)$ is the rate of immigration of individuals into the compartment i, and $v_i^-(t)$ is the rate at which new individuals are transferred from compartment i. In this process, the matrices $f(t)$ and $v(t) = v^-(t) - v^+(t)$. The Jacobian matrices of $f(t)$ and of $v(t)$ are, at disease–free equilibrium point , respectively, given by F and V. Now the next generation matrix is defined as $G = FV^{-1}$ and the basic reproduction number R_0 of the system is defined by the spectral radius of the matrix FV^{-1}. If $R_0 < 1$, then an infected individual generates fewer than one newly infected individual on average during the life of his illness. In this situation, the infection may eventually die off. If $R_0 > 1$, on average, each infected individual creates more than one new infection, the virus can spread in a community. Several variables influence the basic reproduction number, including the persistence of infectivity of infected persons, the infectiousness of the germ, and the number of susceptible people in the population that the infected people come into touch with.

1.5.8 Sensitivity Analysis

The examination of the relative impact of various input elements on model output. Sensitivity analysis gives developers of mathematical and simulation models tools to comprehend the model's influence on model input, as well as to investigate the importance of each model input in determining the model's output. The sensitivity analysis reveals us how essential each parameter is in the spread of illness. Such knowledge is essential not just for layout of experiments, but also for data assimilation and the reduction of complicated nonlinear models [46]. Because there are sometimes errors in data collection and assumed parameter values, sensitivity analysis is widely performed to test the robustness of model predictions to parameter values. It is utilised to find parameters with a lot of influence on R_0 that should be addressed by intervention tactics. When a parameter changes, sensitivity indices allow us to quantify the relative change in a variable. The ratio of the relative change in the variable to the relative change in the parameter is the normalised forward sensitivity index of a variable with regard to a parameter. When the variable is a differentiable function of the parameter, partial derivatives can be used to determine the sensitivity index. We investigate the effect of the basic reproduction number R_0 for certain key parameters in order to do a sensitivity analysis of the model. Following [34,151,155], we calculate the normalized forward sensitivity index of the reproduction number, which estimates the relative change in a variable with respect to the relative change in its parameter.

Definition. The normalized forward sensitivity index of a variable h that depend differentially on a parameter, l, is defined as: $\Gamma_l^h = \frac{1}{h} \times \frac{\partial h}{\partial l}$.

1.6 Optimal Control Theory

The challenge of determining a control scheme for a given system that meets a specified optimality condition is addressed by optimal control theory. An optimal control issue is an optimization problem in the largest context. The distinction between the two is that the optimizer in optimal control theory is a function rather than a single value. This optimising function is known as optimal control. An optimal control problem is defined as the process of designing control and state trajectories for a dynamic system over time in order to minimise a performance index. The collection of vari-

ables (functions) used to represent the mathematical state of the system is referred to as the state variable (or function). A control operation, also known as a control function, is one that regulates the recording, processing, or transmission of data. These two roles govern how the system operates and where the needed control may be located. A basic optimal control issue may be defined using these concepts. This fundamental issue will be referred to as our standard issue (SP). Optimal control theory is concerned with creating control signals that maximize (or minimize) a specific performance index or criteria while also causing the process to meet some physical restrictions [20]. In other words, it is a method for determining control function(s) and state trajectories for a dynamical system over time in order to maximize (or minimize) a productivity criterion [5, 20]. It is based on the calculus of variations and is an extension of it [5]. Lev Pontryagin (1908–1988) and his colleagues–V. G. Boltyanskii, R. V. Gamkrelidz, and E. F. Misshchenko established the maximum principle (Pontryagin's maximum principle), Richard Bellman (1920–1984) invented dynamic programming, and Rudolf Kalman (1930–2016) developed the Kalman filter and built the linear quadratic regulator [5, 122]. The rising popularity of the Pontryagin's maximum principle signifies the beginning of a new era in optimal control theory since it offers mathematicians with suitable circumstances in optimization problems with differential equations as constraints, laying the groundwork for extensive research [122]. Addressing optimization issues with restrictions on the derivatives of functions is difficult; consequently, optimal control is used to develop solutions [69]. Economic and management theory, biomedical engineering, business, ecology and medical sciences, aerospace and aerospace engineering, control theory, robotics, and other disciplines of study all make substantial use of optimal control theory. The development of fast and high–resolution computers aids in the application of optimal control approaches to tough and intricate issues [5].

1.6.1 Optimal Control Problem

The state and control variables make up a cost functional in an optimal control issue. The formulation of an optimal control issue necessarily requires:

- A mathematical representation (or model) of the controllable process

- A description of the physical limitations

- Effectiveness evaluation specification

The collection of variables used to represent the mathematical state of the system is known as the state variable (or function). A basic optimal control issue may be defined using these concepts. Let $u(t)$ be the control variable that is used on the state variable $P(t)$, and the state variable constitutes the differential equation that is dependent on the control variable: $P'(t) = g(t, P(t), u(t))$. The goal is to find a piecewise continuous control $u(t)$ and its corresponding state variable $P(t)$. The objective functional, which is maximize/minimize, is

$$\max_{u}/\min \int_{t_o}^{t_1} f(t, P(t), u(t))dt,$$

$$\text{subject to } P'(t) = g(t, P(t), u(t)), \tag{1.6.1}$$

$$P(t_o) = P_o \text{ and } P(t_1) \ free.$$

An optimal control is one that maximizes/minimizes. $f(t)$ and $g(t)$ will always be continuously differentiable functions in all three parameters for our requirements.

1.6.2 Necessary and Sufficient Conditions

Pontryagin and his colleagues in Moscow discovered the Necessary criteria in the 1950s [122].

Necessary Conditions Let $u(t)$ be a control and state function $P(t)$ satisfies differential equations(DE), control affect the DE. Define Hamiltonin H as

$$H(t, P, u, \lambda) = f(t, P, u) + \lambda g(t, P, u)$$

Let u^* is an optimal control and P^* corresponding state. Then following conditions hold:

$\frac{\partial H}{\partial u} = 0$ at $u^* \implies f_u + \lambda g_u = 0$ (optimality condition),

$\lambda' = -\frac{\partial H}{\partial p} \implies \lambda' = -(f_p + \lambda g_p)$ (adjoint equation),

$\lambda(t_1) = 0$(transversality condition)

Sufficient Conditions

Theorem 1.6.1. Consider

$$J(u) = \int_{t_o}^{t_1} f(t, p(t), u(t)) dt,$$

$$\text{subject to } p'(t) = g(t, p(t), u(t)), \; p(t_0) = p_0.$$

Assume that $f(t, P, u)$ and $g(t, P, u)$ are both continuously differentiable functions in their arguments and concave in P and u. Consider u^* is a control with associated states p^*, and λ, which are piecewise differentiable functions, and u^*, P^* and λ fulfil on $t_0 \leqslant t \leqslant t_1$:

$$f_u + \lambda g_u = 0,$$

$$\lambda' = -(f_P + \lambda g_P),$$

$$\lambda(t_1) = 0,$$

$$\lambda(t) \geqslant 0.$$

Then for all controls u, we have $J(u^*) \geqslant J(u)$.

1.6.3   Pontryagin's Maximum Principle

If $u^*(t)$ and $P^*(t)$ are optimal for (1.6.1), then there exists a piecewise differentiable adjoint variable $\lambda(t)$ such that

$$H(t, P^*(t), u(t), \lambda(t)) \leqslant H(t, P^*, u^*(t), \lambda(t))$$

for all controls $u(t)$ at each time t, where the Hamiltonian H is

$$H = f(t, P(t), u(t)) + \lambda(t) g(t, P(t), u(t)),$$

and

$$\lambda'(t) = -\frac{\partial H(t, P^*(t)), u^*(t), \lambda(t))}{\partial P}$$

$$\lambda(t_1) = 0$$

When the issue is minimization rather than maximizing, a similar approach gives the same required conditions. We minimise the Hamiltonian pointwise in a minimization problem, and the inequality in Pontryagin's Maximum Principle is reversed. However,

for a minimization problem with f and g that are convex in u, we can obtain

$$H(t, P^*(t), u(t), \lambda(t)) \geqslant H(t, P^*, u^*(t), \lambda(t))$$

1.6.4   Existence of Optimal Control

Before addressing and identifying an optimal control, we must first establish that the solution, and specifically the optimal control, exists. To begin, what criteria may ensure the existence of a limited objective functional value at optimal control and state? We present some results findings from [107, 123, 200, 233].

Theorem 1.6.2. Let the set of control for the problem (1.6.1) be lebesgue integrable functions on $t_0 \leqslant t \leqslant t_1$ with values in R. Let $f(t, P(t), u(t))$ is convex in u, and there exist constant M_1 and M_2, M_3, $M_4 > 0$ and $\beta > 1$ such that;

1. The class that includes all initial conditions that have a control u and each state equation that is fulfilled in the admissible control set is nonempty.

2. $g(t, P, u) = \alpha(t, P) + \beta(t, P)u$

3. $| g(t, P, u) | \leqslant M_1(1 + | P | + | u |)$

4. $| g(t, P_1, u) - g(t, P, u) | \leqslant M_2 | P_1 - P | (1 + | u |)$

5. $f(t, P, u) \geqslant M_3 | u |^{\beta} - M_4$

for all t with $t_0 \leqslant t \leqslant t_1$, P, P_1, u in R. Then there exists an optimal u^* minimizing $J(u)$, with $J(u^*)$ finite.

1.6.5   Bounded Controls

To arrive at a reasonable solution, many issues need control bounds. Consider the amount of a chemical utilised in a system as an application of a control. The amount must then be nonnegative, i.e., $u \geqslant 0$. Control must frequently be bounded. There may be physical limitations on the amount of chemicals that may be utilised, or environmental restrictions that make some levels of use inappropriate. Then there is the possibility of an issue if the control is a percentage of a strength or use. Then our bounds would be $0 \leqslant u \leqslant 1$ [200]. We must design other required conditions to solve issues with boundaries on the control in order to solve problems with bounds on the

control. Take into account the issue

$$\max_u J(u) = \max_u \int_{t_o}^{t_1} f(t, P(t), u(t))dt + \phi(P(t_1)),$$

$$\text{subject to } P'(t) = g(t, P(t), u(t)), \; P(t_0) = p_0. \tag{1.6.2}$$

$$c \leqslant u(t) \leqslant d, \tag{1.6.3}$$

where c, d are fixed, real constant and $c < d$. Let $J(u)$ be the objective functional's value at control u, and $P(t)$ be the related state. Forming the Hamiltonian

$$\begin{cases} u^* = c & \text{if } \frac{\partial H}{\partial u} < 0, \\ c \leqslant u^* \leqslant d & \text{if } \frac{\partial H}{\partial u} = 0, \\ u^* = d & \text{if } \frac{\partial H}{\partial u} > 0. \end{cases} \tag{1.6.4}$$

Thus, the optimal control u^* maximizes H pointwise with regard to $c \leqslant u \leqslant d$. If there is a problem with minimization, u^* is used to minimize H pointwise. This causes the $<$ and $>$ in the first and third lines of (1.6.4) to be reversed.

1.6.6 Numerical Methods for Solving Optimal Control Problems

There are a variety of numerical procedures that may be used to approximate an optimal control issue. Though most issues have a theoretical solution, finding it analytically is extremely difficult in reality. As a result, numerical techniques are required. The most important analytical approach is Pontryagin's maximum principle, which specifies the requirements that the control and state must meet. These conditions may be handled in a straightforward manner; but, for the majority of cases, the conditions are too complex to be addressed explicitly. This is particularly true for issues with extra state or control limitations. Numerical techniques are utilised to develop approximations to these complicated equations as a result of these factors. All of the approaches require one of these numerical procedures. A technique for solving ordinary differential equations and systems of differential equations is required.

Forward Backward Sweep: This is a form of indirect approach for finding the optimality conditions of an optimal control problem numerically. When the maximum principle is used, the problem is reduced to a multiple point boundary value problem (optimal-

27

ity system). The ideal values for the original control issue are determined by solving the optimality system. The presence of adjoint equations, transversality criteria, and control equations is necessary in indirect techniques. The Forward Backward Sweep (FBS) is used to find an approximate solution to these difficult equations. Given a control function approximation, FBS solves the state 'ahead' in time (from t_0 to t_1) before solving the adjoint 'backward' (from t_1 to t_0). Once the state and adjoint functions have been identified, the control is updated, and the state, control, and adjoint functions are checked for convergence against a user-specified tolerance. Depending on the result, the algorithm either repeats the process with the updated control or stops with the final approximations for the state, adjoint, and control functions considered as the solution to the optimal control problem. The control vector requires an initial value before it can be used. This starting value is always a $N + 1$ vector of zeros. A basic Runge–Kutta 4 (RK4) approach is used to solve the state ODE, however the RK4 method must be modified to allow for working backwards in time while solving the adjoint ODE. The first method is the RK4 equipped for three inputs, while the second is a reverse solution from the RK4 equipped for four inputs.

Runge–Kutta 4 (with 3 input update) Algorithm:

$$K_1 = f(t_i, P_i, u_i)$$
$$K_2 = f(t_i + \frac{h}{2}, P_i + \frac{h}{2}K_1, \frac{1}{2}(u_i + u_{i+1}))$$
$$K_3 = f(t_i + \frac{h}{2}, P_i + \frac{h}{2}K_2, \frac{1}{2}(u_i + u_{i+1}))$$
$$K_4 = f(t_i + h, P_i + hK_3, u_{i+1})$$
$$P_{i+1} = P_i + \frac{h}{6}(K_1 + 2K_2 + 2K_3 + K_4)$$

Backward Runge–Kutta 4:

$$j = N + 2 - i$$

$$K_1 = f(t_j, \lambda_j, P_j, u_j)$$

$$K_2 = f(t_j - \frac{h}{2}, \lambda_j - \frac{h}{2}K_1, \frac{1}{2}(P_j + P_{j-1}), \frac{1}{2}(u_j + u_{j-1}))$$

$$K_3 = f(t_j - \frac{h}{2}, \lambda_j - \frac{h}{2}K_2, \frac{1}{2}(P_j + P_{j-1}), \frac{1}{2}(u_j + u_{j-1}))$$

$$K_4 = f(t_j - h, \lambda_j - hK_3, P_{j-1}, u_{j-1})$$

$$\lambda_{j-1} = \lambda_j - \frac{h}{6}(K_1 + 2K_2 + 2K_3 + K_4)$$

Now that the algorithm has a state and a control for the current step, the programme must compute the actual control before it can test for convergence. This indicates that the control for the current step is a combination of the current control, u_{new}, and the control from the previous step, u_{old}. This can be accomplished in a variety of ways. To verify convergence, the algorithm computes the error terms. At the end of each iteration, the FBS compares the newly computed state, control, and adjoint vector to the old state, control, and adjoint vector to determine whether the change is small enough to cause the algorithm to stop. When the test variable gets positive, the FBS function performs this. The test variable is the sum of all the state, adjoint, and control relative errors. The test variable is the minimum of all of the relative errors of the state, adjoint, and control. The relative error, P, for the state vector is shown in Equation $(1.6.5)$. It is essential to emphasise that the k signifies the iteration step, not the kth element of P.

$$\frac{||P^k - P^{k+1}||_1}{||P^k||_1} \leqslant \delta. \tag{1.6.5}$$

When $||P^k|| \approx 0$. Then, the result is Equation $(1.6.6)$

$$\delta ||P^k||_1 - ||P^k - P^{k+1}||_1 \geqslant 0 \tag{1.6.6}$$

When this is true for all three vectors being examined, the process terminates and the present control is the best approximation to the optimal control.

Chapter 2

A Prey–Predator Model Approach to Increase the Production of Crops: Mathematical Modelling and Qualitative Analysis

This chapter presents the concept, approaches, and uses of mathematical models in farming. Prey–I, such as sugarcane crops, which take a long time to grow, and prey–II, such as vegetables, which have a short time for crop yields, are planted alongside sugarcane crops and predators that harm both prey–I and prey–II. The various equilibria of the system are obtained, and the stability conditions are analyzed. Furthermore, a comprehensive analysis of the optimal control strategy is also performed. The optimal control model includes the use of three control variables, such as pesticide application rate, biomass application rate, and control of the Cassava mosaic virus in the system. Finally, Pontryagin's maximum principle is used to determine the optimal control. Further, analytical results are verified by numerical simulations.

2.1 Introduction

Population constitutes the key elements of human geography. Due to the dynamic phenomenon of the population, it has been increasing at an alarming rate. India is the second most populous country, and it constitutes over 16% of the total population of the world. India has seen four distinct phases of demographic change during the twentieth century: the phase of the stagnant population (during 1901–1921, the population of India increased from 238 million to 251 million), phase of steady growth (a period 1921–51, the population of India increased from 251 million to 361 million), a phase of rapid high growth (during 1951–1981, the population of India increased from 361 million in 1951 to 683 million in 1981 recording on the increase of 89.36 percentage in a short span of thirty years.), phase of high growth rate but with a sign of slowing down (during 1981–2001, the population increased from 683 million to 1028 million). While the total population of India was 361 million in 1951, it boomed to 1210 million in 2011 [142]. The population continues to increase at an alarming rate , which is simply mind boggling. It is estimated that if this trend continues, the population will be 1400 million in 2025, thus surpassing China's population in that year to become the most densely populated country in the world. The current growth rate of India's population is 17.64% (2011). In the last two decades, the Gross Domestic Product of India and per capita consumption has increased 4.5 times and 3 times, respectively [249]. However, the effects of population explosion have resulted in increasing poverty and shortage of food. The main objective of agriculture was developed to produce food for human consumption. Although, agricultural production has increased almost 2 times but it is unable to provide access to food to a large section of the population. Thus, despite the increase in food production and tremendous economic growth, we are unable to eliminate the need for food in India. According to FAO (Food and Agriculture Organization UN) approximately calculated in the state of food security and nutrition in the world, 2019 report, 194.4 million people have insufficient food in India which is 14.5% of the total population. Further, according to the report, 37.9% of the children aged below five in India are stunted, while 20.8% suffer from wasting. These children are more likely to die from common pediatric diseases including malaria, pneumonia, and diarrhoea. India has rank 103 in the global hunger index–2018 out of 119 countries as per the 2018 Global Hunger Index. The index is based on three

parameters–existence of wasting and stunting in children below 5 years, the child mortality rate (below 5 years), and the percentage of undernourished people in the population. However, it is found that about one–third of the crop produced for human consumption gets lost or wasted per year. About 40% of the vegetables and fruits and 30% of cereals are lost every year. Figure 2.1 demonstrates the output of grain from 2013–14 to 2017–18 and the prediction for the 2018–19 and 2019–20 in India.
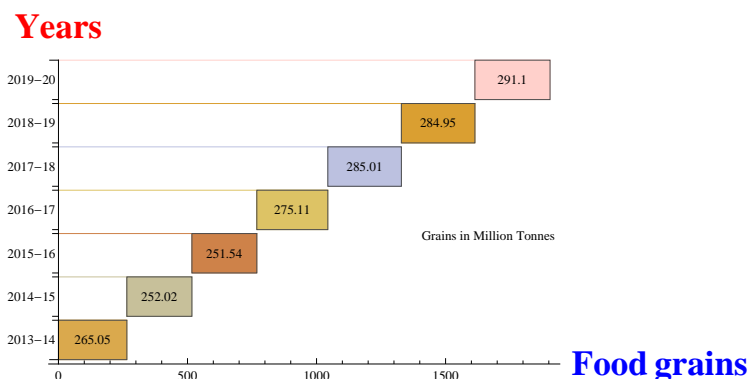
Figure 2.1: Crop production of food grains in India.
(Source: Ministry of Agriculture & Farmers Welfare, Govt. of India.)

Table 2.1 indicates the total annual production of sugarcane in India for four years.

Table 2.1: Sugarcane production in India

Years	2013–14	2014–15	2015–16	2016–17
Production (tonnes/ha)	70.5	71.5	70.7	69.0

Source: Directorate of Economics and Statistics, Ministry of Agriculture & Farmers Welfare, Govt. of India.

Table 2.2 displays the production of vegetables in India.

Table 2.2: Vegetables Production in India

Years	2015–16	2016–17	2017–18
Vegetables Production (in '000 MT)	169064	178172	184394
Area (in '000 Ha)	10106	10238	10259

Source: Directorate of Economics and Statistics, Ministry of Agriculture & Farmers Welfare, Govt. of India.

The Use of chemical fertilizers in India is shown in Table 3.1.

Table 2.3: Consumption of chemical fertiliser products in India (in'000 Tonne) [223]

Years	Urea	AS	ACI	CAN	SSP	TSP	MOP	SOP	DAP
2011-12	29565.3	509.39	58.01	109.20	4746.01	78.13	3028.93	30.79	10191.20
2012-13	30002.20	529.71	3.11	89.99	4030.36	39.56	2211.02	34.46	9154.08
2013-14	30600.50	480.66	2.38	51.90	3879.32	3.59	2280.41	30.53	7357.42
2014-15	30610.00	508.55	0.89	7.68	3989.30	1.84	2853.35	18.95	7625.56
2015-16	30634.77	448.87	5.17	12.33	4252.74	5.386	2466.93	16.83	9107.22
2016-17	29613.58	426.09	4.13	7.14	3756.81	5.00	2863.20	5.68	8963.51
2017-18	29894.44	573.57	19.26	0.14	3439.38	3.76	3158.18	5.19	9294.1

Abbr.: AS: Ammonium Sulphate, CAN: Calcium Ammonium Nitrate, ACI: Ammonium Chloride, DAP: Diammonium Phosphate, MOP: Muriate of Potash, TSP: Triple Super Phosphate, SOP: Sulphate of Potash and Potassium Sulphate, SSP: Single Super Phosphate.

According to the Indian Council of Agricultural Research (ICAR)–2010 survey, about 120.40 million ha, which is (37%) of total geographical area, has been subjected to different kinds of land degradation. Alkalinity and salinity have affected about 1.73 million hectares of areas in agriculture led states of Haryana, Punjab & Uttar Pradesh in India. One of the main causes of such a problem is the improper use of chemical fertilizers. As per land uses, barren land includes lands covered by deserts, mountains, etc. that are not suitable for cultivation except at a high input cost. There is a lack of a comprehensive program for transforming barren land into fertile land. However, many watershed development programs have been started for developing degraded land by India's government. There is an effort to bring parts of such developed land under cultivation for various crops including food crops. Figure 2.2 and Figure 2.3 show areas under nonagricultural uses, barren unculturable land & culturable wasteland.
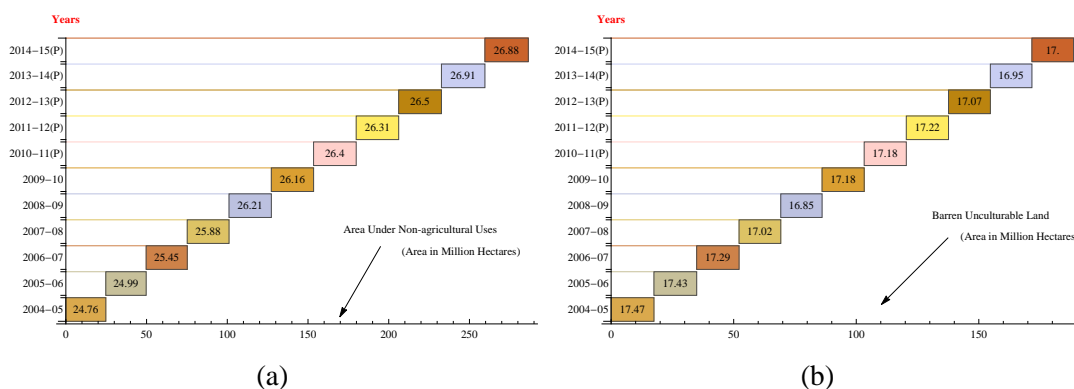
Figure 2.2: Agricultural land in India during 2004–05 to 2014–15 [9].

34
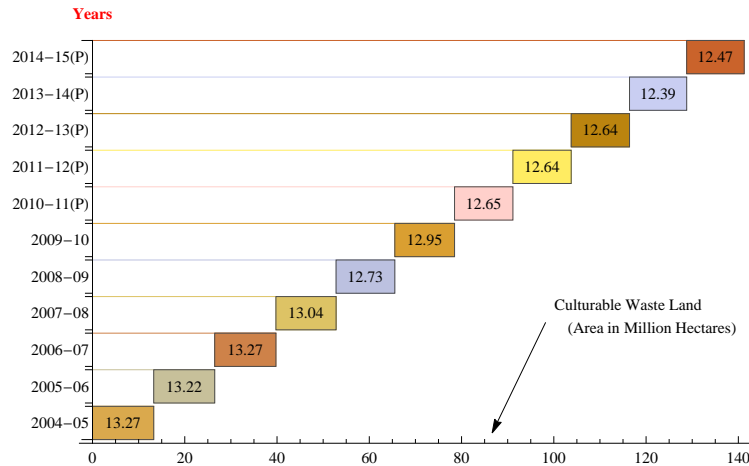
Figure 2.3: Agricultural land in India during 2004–05 to 2014–15 [9].

P: Provisional except Geographical Area.

Source: Directorate of Economics & Statistics, DAC & FW.

It is estimated that agricultural production should grow by approximately 40% in the coming 20 years to meet the consumption demand of an increased population (OECD and FAO of the UN, 2009). However, the global capacity to increase agricultural production is endangered by vast land degradation across regions. Since land for the cultivation of crops is limited. Thus, we cannot destroy the fertility of the land as well as cannot afford to destroy the crops. Some organisms consume crops. It is found that few small insects, weeds, and animals are destroying the many valuable crops. Simultaneously, there are some bacteria, fungi, etc. that also harm trees and plants. Plant diseases are transmitted by various insects. Some examples of viral pathogens are Begomoviruses, carried by the whitefly, Bemisia tabaci, etc. They have drastically reduced crop productivity for crops like tomato, cotton, soybean, etc. [198, 199]. The damage caused by agricultural pests is a worldwide problem. For instance, about 37% of all agricultural production in the US is destroyed by pests, causing a loss of approximately $122 billion a year. So it is very clear why the control of the pest is one of the major global problems. Due to the huge loss in food crops, pesticides are commonly used to try solving the problem. Currently, chemical insecticides are widely used as the most common technique of pest control to prevent the pest population directly at low cost [58]. Pesticides are used to kill or control pest populations. There are various types of pesticides available today, but insecticides and herbicides are commonly used pesticides that kill or balance unwanted insects and plants. The use

35

of pesticides has increased fourfold in the past half-century. Figure 2.4 demonstrates the use of agricultural pesticides in India during 2010–11 to 2016–17 [76].
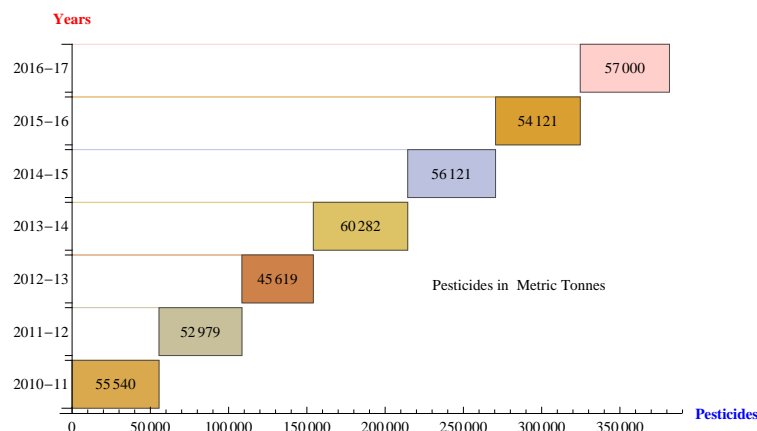
Figure 2.4: Consumption of chemical pesticides in India during 2010–11 to 2016–17

The use of pesticides benefits farmers by increasing food production and preventing crop diseases. It prevents the loss of a higher percentage of crops due to pests. However, despite the benefits, many problems are associated with the use of pesticides. Research studies have found that improper use of pesticides has led to many negative environmental effects. Some of those problems are loss of impact on pest populations due to their improved resistance, harm the beneficial non-pest population, loss of natural pest control due to destruction of natural enemies of the pests, and increase in new and more destructive pest, chemical residues in crops and chemical insecticide residues in the agricultural ecosystem for long–duration [18]. There are various studies regarding the use of optimal control theory to control pest populations [18, 64, 147, 153, 213, 214]. [19] applied optimal control theory to design optimal feedback mechanisms for a few models. As pesticides often move to different locations from where it is applied, through water, air, and soil. Therefore, it can harm other organisms. On many occasions, when a pesticide is applied, it also destroys non–pest organisms that are either non–harming or restrict the growth of pests. This can radically change the natural balance of an ecosystem. Removal of non–pest organisms may create favorable situations for the growth of the pest. Apart from harming the ecology, pesticides also cause harm to humans when they move from their original target. People's exposure to pesticides creates a high number of accidents that intoxicate human beings, which results in the growth of life–threatening diseases like cancer leading to deaths of people between 20,000 and 40,000 worldwide each year.

Other harmful effects of pesticide use are bioaccumulation and biological magnification. The pesticides accumulated in the organisms body can cause many harmful effects on the body. These pesticides get transferred when consumed by organisms. For example, DDT as a pesticide was sprayed on crops to kill pests. It entered the bodies of zooplankton, which were then consumed by fish. The consumption of such fish by predatory birds led to their death due to the biomagnification of the pesticide in their body. This resulted in the near extinction of predatory birds such as peregrine falcons and bald eagles. In a recent model, a complex model has been developed based on cropping weather for the study of corn lethal necrosis, crop disease due to co–infection with two viruses. However, as there is a possibility of a virus being transmitted via a vector, soil, and seed, few control techniques were developed including the use of the clean seed, crop rotation, implicit control of vectors, and removing plants with undesirable characteristics [62, 230]. A plant–vector–virus model for crops showed that rouging has only a little impact on crop disease incidence [94, 140, 208, 209] . Further, [63] worked on the control of crop pests using the importance of farming awareness. Today there is no appropriate method for limiting the pest population. One of the effective strategies to control the population of pests can also be achieved by using natural enemies under the prey-predator model. For instance, many animals and birds eat pests without hampering agriculture. Thus, they can be used as biological controls for the pest. The pest populations may also be affected due to some viral or bacterial infection. Thus, it can be used as another important natural strategy to control the targeted pest population [174, 196]. The use of predator populations to control pests can be found in [196, 217]. The interactions among crop, pest, infection, and predator of pests were analyzed in [43, 77]. [37, 86] also worked on a prey-predator model with the disease in the prey populations. In their studies, a systematic approach has been used to control the pest population using a combination of various possible methods; say, (i) productive application of predator population, (ii) application of infection among the pest population, and (iii) use of balanced chemicals. In this study, our modelling approach is based on prey–predator system, therefore our proposed model is analysed using the concepts of prey–predator model. We have considered two types of prey populations and their predator as a pest. Prey is considered as crops and who damage the crops considered as predators (pest). Mathematical modeling has made a significant role in

these types of pest and pesticide problems. Pest problems, expressing the relationship between prey–predator forms, are popular and have been widely analyzed in recent times. The vision is to meet the food demand of the people and create enough food surplus. In eliminating hunger, agriculture can play a significant role. It is essential to use agricultural work systemically to solve the problems related to hunger and food crop waste. Increasing the population leads to the development of a food crisis. For this reason, ensuring sustainable agriculture and increasing domestic production become essential to meet the growing demands of the population as well as reduce undernutrition among the major section of the population. So, this paper develops the techniques and methods to manage agriculture effectively and ensure food security. A systematic approach to managing the pest population using pesticide control and increasing crop productivity as well as the fertility of land using biomass control has been discussed in this study. The model description is covered in Section 2.2. In Section 2.3–2.5, positiveness, boundedness, and the criteria for the existence of local stability analysis surrounding all equilibria of the model system are examined. In Section 2.7, the numerical simulation of the system is discussed. In Section 2.8, we carry out mathematical formulation and analysis in the presence of controls. Section 2.9 is devoted for numerical simulations and discussions of the model in the presence and absence of controls. The conclusion is presented in Section 2.10.

2.2 Proposed Mathematical Model

In this chapter, a significant mathematical model is studied to address the same. The mathematical model is a prey–predator type system, namely prey-I, prey–II, and pests. The prey–I like sugarcane crops, which take a long time to grow, Prey–II like vegetables such as beans, peppers, pumpkins, and corn, which have a short lifetime, are grown with sugarcane crops and the pest that damage both the prey–I and prey–II. Due to the longer time taken by prey–I(sugarcane) to grow, the space available in the same field can be easily used for growing prey–II (vegetables) without impacting

the growth of sugarcane. The proposed model takes the form

$$
\begin{cases}
\frac{dP_1}{dt} = r_1 P_1 - i_1 P_1{}^2 - c_1 \left(1 - m_1\right) P_3 P_1 - \alpha_1 P_1 P_2, \\[2mm]
\frac{dP_2}{dt} = r_2 P_2 - i_2 P_2{}^2 - c_2 \left(1 - m_2\right) P_3 P_2 - \alpha_2 P_1 P_2, \\[2mm]
\frac{dP_3}{dt} = r_3 P_3 - i_3 P_3{}^2 + c_3 \left(1 - m_1\right) P_3 P_1 + c_4 \left(1 - m_2\right) P_3 P_2,
\end{cases}
\tag{2.2.1}
$$

with initial data $P_1(0) > 0$, $P_2(0) > 0$ and $P_3(0) > 0$. Here, $P_1(t)$ represent density of crops (prey–I) at time t, $P_2(t)$ represent density of crops (prey–II) at time t, and $P_3(t)$ represent density of pest (predators) at time t. The parameters are defined in Table 3.3.

Table 2.4: Parameters of the model (2.2.1)

Parameter	Meaning
r_1	Growth rate of prey–I in the absence of predation
i_1	The level of competition among prey–I
c_1	The number of prey-I that a predators consume in a given time unit
m_1	Special threshold value or the minimal feasible prey–I population
α_1	Competition among prey–I and prey–II
r_2	Growth rate of prey–II
i_2	The level of competition among prey–II
c_2	The number of prey-II that a predators consume in a given time unit
m_2	Special threshold value or the minimal feasible prey–II population
α_2	Competition among prey–II and prey–I
r_3	Growth rate of predator
i_3	The level of competition among predators
c_3	The rate at which pests transform ingested prey-I into new pests
c_4	The rate at which pests transform ingested prey-II into new pests

To fulfill our model, we make some assumptions that the predator species depends on a prey–I and prey–II species as its only food supply, and there is no threat to crops other than the pest. The parameters, r_1 is the growth rate of prey–I (P_1), r_2 is the growth rate of prey–II (P_2) in the absence of predator (P_3). The prey–I and prey–II populations are diminished by predators. The term r_3 is the natural growth rate of predators. The term i_1 is a positive parameter of competition among prey–I and the term $i_1 P_1^2(t)$ decreases the prey–I population due to competition with each other in a particular habitat. Similarly, the term i_2 is a positive parameter of competition among prey–II and the term $i_2 P_2^2(t)$ decreases the prey–II population. Like the minerals, light, amount of food, space, and water that are available which are limited. The term i_3 is

39

a positive parameter of competition among predators and the term $i_3 P_3^2(t)$ decreases the predator populations. The term m_1, $0 < m_1 < 1$, m_2, $0 < m_2 < 1$ is a special threshold value of prey–I and prey–II respectively. To understand better m_1, let us consider one example. Say, there are 100 preys and out of 100 only 80 are available for predation, then m_1 will be $\frac{1}{5}$. It means 20 prey are safe by different means. The terms $c_1(1 - m_1)P_3$ and $c_2(1 - m_3)P_3$ denote the net rate of death of the prey–I and prey–II population in response to the size of the predator populations. Similarly, the term $c_3(1 - m_1)P_1$ and $c_4(1 - m_2)P_2$ denotes the net rate of growth of the predator populations in response to the size of the prey–1 and prey–II populations. $\alpha_1 P_1 P_2$ and $\alpha_2 P_1 P_2$ denote the death rate of the prey–I and prey–II respectively due to competition between prey–I and prey–II.

2.3 Positiveness and Boundedness of the System

2.3.1 Positivity

It is important to demonstrate that all the solutions of the system with positive initial data will remain positive for model (2.2.1). The following theorem will demonstrate this.

Theorem 2.3.1. The solutions of $(P_1(t),\ P_2(t),\ P_3(t))$ of the system (2.2.1) with the initial data $P_1(0) > 0$, $P_2(0) > 0$, and $P_3(0) > 0$ are positive for all $t \geqslant 0$.

Proof. (i) Positivity of $P_1(t)$: from the model (2.2.1)

$$\frac{dP_1}{dt} = r_1 P_1 - i_1 P_1{}^2 - c_1 (1 - m_1) P_3 P_1 - \alpha_1 P_1 P_2. \tag{2.3.1}$$

Without loss of generality, removing all the positive terms from the right–hand side of the differential equation (2.3.1), the differential inequality can be written as:

$$\frac{dP_1}{dt} \geqslant -P_1(i_1 P_1 + c_1 (1 - m_1) P_3 + \alpha_1 P_2)$$

Assume that $c_1 (1 - m_1) P_3 + \alpha_1 P_2 = C$, then the differential inequality is reduced to

$$\frac{dP_1}{dt} \geqslant -P_1(i_1 P_1 + C).$$

This inequality can be arranged for integration by partial fraction and then integrating the integral inequality,

$$\frac{1}{C} \ln|(\frac{P_1}{i_1 P_1 + C})| \geqslant -t + Q,$$

where Q is integration constant. Finally, solving for P_1 will give us

$$P_1(t) \geqslant \frac{ACe^{-Ct}}{1 - i_1 Ae^{-Ct}},$$

where $A = e^{CQ}$. Therefore $P_1(t) > 0$ for $1 - i_1 Ae^{-Ct} > 0$. That is, $P_1(t)$ is nonnegative for $t > \frac{1}{C} \ln(i_1 A)$.

(ii) Positivity of $P_2(t)$: from the model (2.2.1),

$$\frac{dP_2}{dt} = r_2 P_2 - i_2 P_2^2 - c_2(1 - m_2) P_3 P_2 - \alpha_2 P_1 P_2, \tag{2.3.2}$$

After removing all the positive terms from the right–hand side of the differential equation (2.3.2), the differential inequality is as follows:

$$\frac{dP_2}{dt} \geqslant -i_2 P_2^2 - c_2(1 - m_2) P_3 P_2 - \alpha_2 P_1 P_2,$$

Assume that $c_2(1 - m_2) P_3 + \alpha_2 P_1 = C_1$, then the differential inequality is reduced to

$$\frac{dP_2}{dt} \geqslant -P_2(i_2 P_2 + C_1).$$

This inequality can be arranged for integration by partial fraction and then integrating the integral inequality,

$$\frac{1}{C_1} \ln|(\frac{P_2}{i_2 P_1 + C_1})| \geqslant -t + Q_1,$$

where Q_1 is integration constant. Finally, solving for P_2 will give us

$$P_2(t) \geqslant \frac{ACe^{-C_1 t}}{1 - i_2 Ae^{-C_1 t}},$$

where $A_1 = e^{C_1 Q_1}$. Therefore $P_2(t) > 0$ for $1 - i_2 A_1 e^{-Ct} > 0$. That is, $P_2(t)$ is nonnegative for $t > \frac{1}{C_1} \ln(i_2 A)$. (iii) Positivity of $P_3(t)$: from the model (2.2.1),

$$\frac{dP_3}{dt} = r_3 P_3 - i_3 P_3^2 + c_3(1 - m_1) P_3 P_1 + c_4(1 - m_2) P_3 P_2, \tag{2.3.3}$$

41

After removing the some positive terms from the right–hand side of the differential equation (2.3.3), the differential inequality is as follows:

$$\frac{dP_3}{dt} \geqslant r_3 P_3 - i_3 P_3{}^2.$$

This inequality can be arranged for integration by partial fraction and then integrating the integral inequality,

$$\frac{1}{r_3} \ln |(\frac{i_3 P_3 - r_3}{P_3})| \geqslant -t + Q_2,$$

where Q_2 is integration constant. Finally, solving for P_3 will give us

$$P_3(t) \geqslant \frac{r_3}{i_3 - A_2 e^{-tr_3}},$$

where $A_2 = e^{r_3 Q_2}$. Therefore $P_3(t) > 0$ for $i_3 - A_2 e^{-tr_3} > 0$. That is, $P_3(t)$ is nonnegative for $t > \frac{1}{r_3} \ln(\frac{A_2}{i_3})$.

$\square$

Theorem 2.3.2. All solutions of the model system (2.2.1) that initiate in R_+^3 are uniformly bounded.

Proof. We define the function $w(P_1, P_2, P_3) = P_1 + P_2 + P_3$. For $\eta > 0$, adding ηw and derivative of $w(P_1, P_2, P_3)$ with respect to time is

$$\frac{dw}{dt} + \eta w = \frac{dP_1}{dt} + \frac{dP_2}{dt} + \frac{dP_3}{dt} + \eta(P_1 + P_2 + P_3),$$
$$= r_1 P_1 - i_1 P_1{}^2 - c_1(1 - m_1)P_3 P_1 - \alpha_1 P_1 P_2 + r_2 P_2 - i_1 P_2{}^2$$
$$- c_2(1 - m_2)P_3 P_2 - \alpha_2 P_1 P_2 + r_3 P_3 - i_3 P_3{}^2 + c_3(1 - m_1)P_3 P_1$$
$$+ c_4(1 - m_2)P_3 P_2 + \eta(P_1 + P_2 + P_3),$$
$$\Rightarrow \frac{dw}{dt} + \eta w \leqslant P_1 \left[(1 - \frac{P_1}{\frac{r_1}{i_1}}) + \eta \right] + P_2 \left[(1 - \frac{P_2}{\frac{r_2}{i_2}}) + \eta \right] + P_3 \left[(1 - \frac{P_3}{\frac{r_3}{i_3}}) + \eta \right],$$
$$\Rightarrow \frac{dw}{dt} + \eta w \leqslant \frac{(r_1 + \eta)^2}{4i_1} + \frac{(r_2 + \eta)^2}{4i_2} + \frac{(r_3 + \eta)^2}{4i_3},$$

for $c_1 > c_3$, $c_2 > c_4$. Thus, we select a value $k > 0$ such that $k = \frac{(r_1 + \eta)^2}{4i_1} + \frac{(r_2 + \eta)^2}{4i_2} + \frac{(r_3 + \eta)^2}{4i_3}$,

$$\frac{dw}{dt} + \eta w \leqslant k.$$

42

Applying the theory of differential inequality [65],

$$0 < w(P_1, P_2, P_3) \leqslant \frac{k}{\eta}(1 - e^{-\eta t}) + \frac{w(P_1(0), P_2(0), P_3(0))}{e^{\eta t}},$$

for $t \to \infty$,

$$0 < w(P_1, P_2, P_3) \leqslant \frac{k}{\eta}.$$

Hence all the solution of system (2.2.1) are

$$\Theta = \{(P_1, P_2, P_3) \in R_+^3 : 0 < w \leqslant \frac{k}{\eta}\}.$$

$\square$

2.4   Equilibrium Points of the System

Prey–predator model system (2.2.1) has following equilibrium points:

1. The trivial equilibrium point $E_0(P_1^*, P_2^*, P_3^*)$, where

$$P_1^* = 0,\ P_2^* = 0,\ P_3^* = 0.$$

2. The prey–I and prey–II free equilibrium point $E_1(P_1^*, P_2^*, P_3^*)$, where

$$P_1^* = 0, P_2^* = 0, P_3^* = \frac{r_3}{i_3}.$$

3. The prey–I free equilibrium point $E_2(P_1^*, P_2^*, P_3^*)$, where

$$P_1^* = 0,\ P_2^* = \frac{f_3 - f_4}{f_1 - f_2},\ P_3^* = \frac{f_3 - f_4}{f_1 - f_2},$$

where $f_1 = c_2 c_4 + i_2 i_3 + + c_2 c_4 m_2^2$, $f_2 = 2 c_2 c_4 m_2, f_3 = i_3 r_2 + c_2 m_2 r_3$, $f_4 = c_2 r_3, f_5 = c_4 r_2 + i_2 r_3, f_6 = c_4 m_2 r_2$, which is biologically feasible if (i) $f_1 > f_2$ and $f_3 > f_4$ or $f_1 < f_2$ and $f_3 < f_4$, (ii) $f_1 < f_2$ and $f_3 < f_4$, or $f_1 > f_2$ and $f_3 > f_4$.

4. The prey–II free equilibrium point $E_3(P_1^*, P_2^*, P_3^*)$, where

$$P_1^* = \frac{i_3 r_1 + c_1 m_1 r_3 - c_1 r_3}{c_1 c_3 + i_1 i_3 + c_1 c_3 m_1^2 - 2 c_1 c_3 m_1},\ P_2^* = 0,\ P_3^* = \frac{c_3 r_1 + i_1 r_3 - c_3 m_1 r_1}{c_1 c_3 + i_1 i_3 - 2 c_1 c_3 m_1 + c_1 c_3 m_1^2},$$

43

which is biologically feasible if (i) $i_3 r_1 + c_1 m_1 r_3 > c_1 r_3$ and $c_1 c_3 + i_1 i_3 + c_1 c_3 m_1^2 > 2 c_1 c_3 m_1$, or $i_3 r_1 + c_1 m_1 r_3 < c_1 r_3$ and $c_1 c_3 + i_1 i_3 + c_1 c_3 m_1^2 < 2 c_1 c_3 m_1$. (ii) $c_3 r_1 + i_1 r_3 > c_3 m_1 r_1$ and $c_1 c_3 + i_1 i_3 + c_1 c_3 m_1^2 > 2 c_1 c_3 m_1$, or $c_3 r_1 + i_1 r_3 < c_3 m_1 r_1$ and $c_1 c_3 + i_1 i_3 + c_1 c_3 m_1^2 < 2 c_1 c_3 m_1$.

5. The prey–I and predator free equilibrium $E_4(P_1^*, P_2^*, P_3^*)$, where

$$P_1^* = 0, \ P_2^* = \frac{r_2}{i_2}, \ P_3^* = 0,$$

which is biologically feasible.

6. The predator free equilibrium $E_5(P_1^*, P_2^*, P_3^*)$, where

$$P_1^* = \frac{i_2 r_1 - r_2 \alpha_1}{i_1 i_2 - \alpha_1 \alpha_2}, \ P_2^* = \frac{i_1 r_2 - r_1 \alpha_2}{i_1 i_2 - \alpha_1 \alpha_2}, \ P_3^* = 0,$$

which is biologically feasible if (i) $i_2 r_1 > r_2 \alpha_1$ and $i_1 i_2 > \alpha_1 \alpha_2$ or $i_2 r_1 < r_2 \alpha_1$ and $i_1 i_2 < \alpha_1 \alpha_2$, (ii) $i_1 r_2 > r_1 \alpha_2$ and $i_1 i_2 > \alpha_1 \alpha_2$ or $i_1 r_2 < r_1 \alpha_2$ and $i_1 i_2 < \alpha_1 \alpha_2$.

7. The prey-II and predator free equilibrium $E_6(P_1^*, P_2^*, P_3^*)$, where

$$P_1^* = \frac{r_1}{i_1}, \ P_2^* = 0, \ P_3^* = 0,$$

which is biologically feasible.

8. The interior equilibrium $E_7(P_1^*, P_2^*, P_3^*)$ is the point of intersection of the following equations:

$$r_1 - i_1 P_1 - c_1 (1 - m_1) P_3 - \alpha_1 P_2 = 0, \tag{2.4.1}$$

$$r_2 - i_2 P_2 - c_2 (1 - m_2) P_3 - \alpha_2 P_1 = 0, \tag{2.4.2}$$

$$r_3 - i_3 P_3 + c_3 (1 - m_1) P_1 + c_4 (1 - m_2) P_2 = 0, \tag{2.4.3}$$

from (2.4.1),

$$P_1 = \frac{-c_1 P_3 + c_1 m_1 P_3 + r_1 - P_2 \alpha_1}{i_1}, \tag{2.4.4}$$

from (2.4.4) and (2.4.2),

$$h_2 P_3 + h_3 P_2 + h_1 = 0, \tag{2.4.5}$$

44

where $h_1 = r_2 - \frac{r_1\alpha_2}{i_1}$, $h_2 = \left(-c_2(1-m_2) + \frac{c_1\alpha_2}{i_1} - \frac{c_1 m_1 \alpha_2}{i_1} \right)$, $h_3 = \left(-i_2 + \frac{\alpha_1\alpha_2}{i_1} \right)$, from (2.4.4) and (2.4.3),

$$h_6 P_3 + h_5 P_2 + h_4 = 0, \tag{2.4.6}$$

where $h_4 = \frac{c_3(1-m_1)r_1}{i_1} + r_3$, $h_5 = \left(c_4(1-m_2) - \frac{c_3(1-m_1)\alpha_1}{i_1} \right)$,
$h_6 = \left(-i_3 - \frac{c_1 c_3(1-m_1)}{i_1} + \frac{c_1 c_3(1-m_1)m_1}{i_1} \right)$,
from (2.4.5) and (2.4.6),

$$P_2^* = \frac{h_1 h_6 - h_2 h_4}{h_2 h_5 - h_3 h_6}, \quad P_3^* = \frac{h_3 h_4 - h_1 h_5}{h_2 h_5 - h_3 h_6}, \tag{2.4.7}$$

from (2.4.4) and (2.4.7),

$$P_1^* = \frac{h_7 - h_8}{(h_2 h_5 - h_3 h_6)i_1}, \tag{2.4.8}$$

where $h_7 = c_1 h_1 h_5 + c_1 h_3 h_4 m_1 + h_2 h_5 r_1 + h_2 h_4 \alpha_1$, and $h_8 = h_1 h_6 \alpha_1 + c_1 h_3 h_4 + c_1 h_1 h_5 m_1 + h_3 h_6 r_1$, which is biologically feasible if following conditions are satisfy (i) $h_1 h_6 > h_2 h_4$ and $h_2 h_5 > h_3 h_6$ or $h_1 h_6 < h_2 h_4$ and $h_2 h_5 < h_3 h_6$, (ii) $h_3 h_4 > h_1 h_5$ and $h_2 h_5 > h_3 h_6$ or $h_3 h_4 < h_1 h_5$ and $h_2 h_5 < h_3 h_6$, (iii) $h_7 > h_8$ and $h_2 h_5 > h_3 h_6$ or $h_7 < h_8$ and $h_2 h_5 < h_3 h_6$.

2.5 Local Stability Analysis

In this section, we analyze the local stability behaviour of the mathematical model that is determined by constructing the Jacobian matrix relating to every equilibrium point. The Jacobian matrix of the system (2.2.1) is given by

$$J(P_1, P_2, P_3) = \begin{pmatrix} X & -P_1\alpha_1 & -c_1(1-m_1)P_1 \\ -P_2\alpha_2 & Y & -c_2(1-m_2)P_2 \\ c_3(1-m_1)P_3 & c_4(1-m_2)P_3 & Z \end{pmatrix},$$

where $X = -2i_1 P_1 - c_1(1-m_1)P_3 + r_1 - P_2\alpha_1$, $Y = -2i_2 P_2 - c_2(1-m_2)P_3 + r_2 - P_1\alpha_2$ and $Z = c_3(1-m_1)P_1 + c_4(1-m_2)P_2 - 2i_3 P_3 + r_3$.

45

(1) The Jacobian matrix at E_0 is

$$J(E_0) = \begin{pmatrix} r_1 & 0 & 0 \\ 0 & r_2 & 0 \\ 0 & 0 & r_3 \end{pmatrix},$$

the eigenvalues of $J(E_0)$ are r_1, r_2, and r_3. Hence, E_0 is unstable since all eigenvalues are always positive.

(2) The Jacobian matrix at E_1 is

$$J(E_1) = \begin{pmatrix} r_1 & 0 & 0 \\ 0 & r_2 & 0 \\ c_3(1-m_1)\frac{r_3}{i_3} & c_3(1-m_1)\frac{r_3}{i_3} & -r_3 \end{pmatrix},$$

the eigenvalues of $J(E_1)$ are r_1, r_2, and $-r_3$. Since two eigenvalues are always positive and one is negative, therefore E_1 is unstable(saddle).

(3) The Jacobian matrix using system (2.2.1) at equilibrium point E_2 is

$$J(E_2) = \begin{pmatrix} -c_1(1-m_1)P_3^* + r_1 - P_2^*\alpha_1 & 0 & 0 \\ -P_2^*\alpha_2 & -i_2P_2^* & -c_2(1-m_2)P_2^* \\ c_3(1-m_1)P_3^* & c_4(1-m_2)P_3^* & -i_3P_3^* \end{pmatrix},$$

the characteristic polynomial of the Jacobian matrix $J(E_2)$ is

$$x^3 + a_1x^2 + a_2x + a_3 = 0,$$

where $a_1 = i_2P_2^* + i_3P_3^* + c_1(1-m_1)P_3^* - r_1 - P_2^*\alpha_1$, $a_2 = i_2i_3P_2^*P_3^* + c_1i_2(1-m_1)P_2^*P_3^* - c_2c_4(1-m_2)^2P_2^*P_3^* + c_1i_3(1-m_1)(P_3^*)^2 - i_2P_2^*r_1 - i_3P_3^*r_1 + i_2(P_2^*)^2\alpha_1 + i_3P_2^*P_3^*\alpha_1$,
$a_3 = c_1i_2i_3(1-m_1)P_2^*(P_3^*)^2 - c_1c_2c_4(1-m_1)(1-m_2)^2P_2^*(P_3^*)^2 - i_2i_3P_2^*P_3^*r_1 + c_2c_4(1-m_2)^2P_2^*P_3^*r_1 + i_2i_3(P_2^*)^2P_3^*\alpha_1 - c_2c_4(1-m_2)^2(P_2^*)^2P_3^*\alpha_1$.

For the local asymptotically stable of the system, the following Routh–Hurwitz criterion must be satisfied:

$$(1)\ a_1 > 0,\ a_2 > 0,\ a_3 > 0,\ \text{and}\ (2)\ a_1a_2 - a_3 > 0. \tag{2.5.1}$$

46

(4) The Jacobian matrix at E_3 is

$$J(E_3) = \begin{pmatrix} -i_1 P_1^* & -P_1^* \alpha_1 & -c_1(1-m_1)P_1^* \\ 0 & -c_2(1-m_2)P_3^* + r_2 - P_1^* \alpha_2 & 0 \\ c_3(1-m_1)P_3^* & c_4(1-m_2)P_3^* & -i_3 P_3^* \end{pmatrix},$$

$$\lambda_1 = \frac{1}{2}\left(-i_1 P_1^* + i_3 P_3^* - \sqrt{i_1^2(P_1^*)^2 + 2i_1 i_3 P_1^* P_3^* + P_3^*\left(-4c_1 c_3(-1+m_1)^2 P_1^* + i_3^2 P_3^*\right)}\right)$$

$$\lambda_2 = \frac{1}{2}\left(-i_1 P_1^* + i_3 P_3^* + \sqrt{i_1^2(P_1^*)^2 + 2i_1 i_3 P_1^* P_3^* + P_3^*\left(-4c_1 c_3(-1+m_1)^2 P_1^* + i_3^2 P_3^*\right)}\right)$$

$$\lambda_3 = c_2(-1+m_2)P_3^* + r_2 - P_1^* \alpha_2.$$

The eigenvalues $\lambda_1 < 0$, $\lambda_2 < 0$ and $\lambda_3 < 0$, if

$$i_3 P_3^* < \left(i_1 P_1^* + \sqrt{i_1^2(P_1^*)^2 + 2i_1 i_3 P_1^* P_3^* + P_3^*\left(-4c_1 c_3(-1+m_1)^2 P_1^* + i_3^2 P_3^*\right)}\right),$$

$$i_1 P_1^* > i_3 P_3^* + \sqrt{i_1^2(P_1^*)^2 + 2i_1 i_3 P_1^* P_3^* + P_3^*\left(-4c_1 c_3(-1+m_1)^2 P_1^* + i_3^2 P_3^*\right)},$$

$$\text{and } r_2 < c_2(1-m_2)P_3^* + P_1^* \alpha_2, \tag{2.5.2}$$

in this case system is locally asymptotically stable.

(5) The Jacobian matrix at E_4

$$J(E_4) = \begin{pmatrix} r_1 - \frac{r_2}{i_2}\alpha_1 & 0 & 0 \\ -\frac{r_2}{i_2}\alpha_2 & -r_2 & -c_2(1-m_2)\frac{r_2}{i_2} \\ 0 & 0 & c_4(1-m_2)\frac{r_2}{i_2} + r_3 \end{pmatrix},$$

thus the eigenvalues of the Jacobian matrix $J(E_4)$ are $\lambda_1 = -r_2$, $\lambda_2 = \frac{-c_4(-1+m_2)r_2 + i_1 r_3}{i_1}$, $\lambda_3 = r_1 - \frac{r_2 \alpha_1}{i_1}$. Since $0 < m_2 < 1$, and all parameters are positive, therefore, $\frac{-c_4(-1+m_2)r_2 + i_1 r_3}{i_1} > 0$, hence eigenvalue λ_2 is always positive. In this case system is not locally asymptotically stable.

(6) The Jacobian matrix $J(E_5)$ at E_5 is

$$\begin{pmatrix} -2i_1 P_1^* + r_1 - P_2^* \alpha_1 & -P_1^* \alpha_1 & -c_1(1-m_1)P_1^* \\ -P_2^* \alpha_2 & -2i_2 P_2^* + r_2 - P_1^* \alpha_2 & -c_2(1-m_2)P_2^* \\ 0 & 0 & c_3(1-m_1)P_1^* + c_4(1-m_2)P_2^* + r_3 \end{pmatrix},$$

and the simplification of the Jacobian matrix using system (2.2.1), we can find

$$J(E_5) = \begin{pmatrix} -i_1 P_1^* & -P_1^* \alpha_1 & -c_1 (1-m_1) P_1^* \\ -P_2^* \alpha_2 & -i_2 P_2^* & -c_2 (1-m_2) P_2^* \\ 0 & 0 & c_3 (1-m_1) P_1^* + c_4 (1-m_2) P_2^* + r_3 \end{pmatrix},$$

thus the eigenvalues of the Jacobian matrix $J(E_5)$ are $\lambda_1 = -c_3 (-1+m_1) P_1^* - c_4 (-1+m_2) P_2^* + r_3$,

$$\lambda_2 = \tfrac{1}{2} \left(-i_1 P_1^* - i_2 P_2^* - \sqrt{i_1^2 (P_1^*)^2 - 2 i_1 i_2 P_1^* \, P_2^* + i_2^2 (P_2^*)^2 + 4 P_1^* \, P_2^* \alpha_1 \alpha_2} \right),$$

$$\lambda_3 = \tfrac{1}{2} \left(-i_1 P_1^* - i_2 P_2^* + \sqrt{i_1^2 (P_1^*)^2 - 2 i_1 i_2 P_1^* \, P_2^* + i_2^2 (P_2^*)^2 + 4 P_1^* \, P_2^* \alpha_1 \alpha_2} \right).$$

Since $0 < m_1 < 1, 0 < m_2 < 1$ and all parameters are positive, therefore, $-c_3 (-1+m_1) P_1 - c_4 (-1+m_2) P_2^* + r_3 > 0$, hence eigenvalue λ_1 is always positive and

$$\lambda_2 = \tfrac{1}{2} \left(-i_1 P_1^* - i_2 P_2^* - \sqrt{i_1^2 (P_1^*)^2 - 2 i_1 i_2 P_1^* \, P_2^* + i_2^2 (P_2^*)^2 + 4 P_1^* \, P_2^* \alpha_1 \alpha_2} \right) < 0.$$ So the system is not locally asymptotically stable.

(7) The Jacobian matrix at E_6 is

$$J(E_6) = \begin{pmatrix} -r_1 & -\alpha_1 \frac{r_1}{i_1} & -c_1 (1-m_1) \frac{r_1}{i_1} \\ 0 & r_2 - \alpha_2 \frac{r_1}{i_1} & 0 \\ 0 & 0 & c_3 (1-m_1) \frac{r_1}{i_1} + r_3 \end{pmatrix},$$

the eigenvalues of $J(E_6)$ are $\lambda_1 = -r_1$, $\lambda_2 = r_2 - \alpha_2 \frac{r_1}{i_1}$, and $\lambda_3 = c_3 (1-m_1) \frac{r_1}{i_1} + r_3$. Since $0 < m_1 < 1$ and all parameters are positive, therefore, $\lambda_3 = c_3 (1-m_1) \frac{r_1}{i_1} + r_3 > 0$, thus some eigenvalues are positive and some are negative. So in this case equilibrium point is saddle point.

(8) The Jacobian matrix at E_7 is

$$J(E_7) = \begin{pmatrix} -i_1 P_1^* & -P_1^* \alpha_1 & -c_1 (1-m_1) P_1^* \\ -P_2^* \alpha_2 & -i_2 P_2^* & -c_2 (1-m_2) P_2^* \\ c_3 (1-m_1) P_3^* & c_4 (1-m_2) P_3^* & -i_3 P_3^* \end{pmatrix},$$

the characteristic equation of system around the equilibrium is

$$x^3 + a_1 x^2 + a_2 x + a_3 = 0,$$

where

$$a_1 = i_1 P_1^* + i_2 P_2^* + i_3 P_3^*, \quad a_2 = i_1 i_2 P_1^* P_2^* + c_1 c_3 P_1^* P_3^* + i_1 i_3 P_1^* P_3^* - 2 c_1 c_3 m_1 P_1^* P_3^* + c_1 c_3 m_1^2 P_1^* P_3^* +$$

$$c_2 c_4 P_2^* P_3^* + i_2 i_3 P_2^* P_3^* - 2 c_2 c_4 m_2 P_2^* P_3^* + c_2 c_4 m_2^2 P_2^* P_3^* - P_1^* P_2^* \alpha_1 \alpha_2,$$

$$a_3 = c_2 c_4 i_1 P_1^* P_2^* P_3^* + i_1 i_2 i_3 P_1^* P_2^* P_3^* + c_1 c_3 i_2 (-1 + m_1)^2 P_1^* P_2^* P_3^* - 2 c_2 c_4 i_1 m_2 P_1^* P_2^* P_3^*$$

$$+ c_2 c_4 i_1 m_2^2 P_1^* P_2^* P_3^* - c_2 c_3 P_1^* P_2^* P_3^* \alpha_1 + c_2 c_3 m_1 P_1^* P_2^* P_3^* \alpha_1 + c_2 c_3 m_2 P_1^* P_2^* P_3^* \alpha_1$$

$$- c_2 c_3 m_1 m_2 P_1^* P_2^* P_3^* \alpha_1 - c_1 c_4 P_1^* P_2^* P_3^* \alpha_2 + c_1 c_4 m_1 P_1^* P_2^* P_3^* \alpha_2 + c_1 c_4 m_2 P_1^* P_2^* P_3^* \alpha_2$$

$$- c_1 c_4 m_1 m_2 P_1^* P_2^* P_3^* \alpha_2 - i_3 P_1^* P_2^* P_3^* \alpha_1 \alpha_2.$$

For the local asymptotically stable of the system, the following Routh–Hurwitz criterion must be satisfied:

$$(i) \; a_i > 0 \; (i = 1, 2, 3) \text{ and } (ii) \; a_1 a_2 > a_3. \tag{2.5.3}$$

2.6 Global Stability

Theorem 2.6.1. The positive interior equilibrium point $E_7(P_1^*, P_2^*, P_3^*)$ is globally asymptotically stable if $\frac{i_1 i_2 i_3 c_1 c_4}{c_2^2} > \frac{i_3 c_3}{4 c_2} \left(\alpha_1 + \alpha_2 \frac{c_1 c_4}{c_2 c_3} \right)^2$.

Proof. Firstly, we define a Lyapunov function

$$V(P_1, P_2, , P_3) = (P_1 - P_1^* - P_1^* \ln \frac{P_1}{P_1^*}) + h_1 (P_2 - P_2^* - P_2^* \ln \frac{P_2}{P_2^*}) + h_2 (P_3 - P_3^* - P_3^* \ln \frac{P_3}{P_3^*}),$$

where h_1 and h_2 are positive constants to be determined later. It can be easily seen that the function V is zero at the equilibrium point $(P_1^*, P_2^*, , P_3^*)$ and is positive for all other values of P_1, P_2, and P_3. The derivative of Lyapunov function V is

$$\frac{dV}{dt} = (1 - \frac{P_1^*}{P_1}) \frac{dP_1}{dt} + h_1 (1 - \frac{P_2^*}{P_2}) \frac{dP_2}{dt} + h_2 (1 - \frac{P_3^*}{P_3}) \frac{dP_3}{dt},$$

putting the values of $\frac{dP_1}{dt}$, $\frac{dP_2}{dt}$ and $\frac{dP_3}{dt}$ from the (2.2.1), we have

$$\frac{dV}{dt} = (1 - \frac{P_1^*}{P_1})(r_1 P_1 - i_1 P_1^2 - c_1 (1 - m_1) P_3 P_1 - \alpha_1 P_1 P_2)$$

$$+ h_1 (1 - \frac{P_2^*}{P_2})(r_2 P_2 - i_2 P_2^2 - c_2 (1 - m_2) P_3 P_2 - \alpha_2 P_1 P_2)$$

$$+ h_2 (1 - \frac{P_3^*}{P_3})(r_3 P_3 - i_3 P_3^2 + c_3 (1 - m_1) P_3 P_1 + c_4 (1 - m_2) P_2 P_3),$$

49

$$\frac{dV}{dt} = -i_1(P_1 - P_1^*)^2 - c_1(1-m_1)(P_3 - P_3^*)(P_1 - P_1^*) - \alpha_1(P_2 - P_2^*)(P_1 - P_1^*)$$

$$- i_2 h_1(P_2 - P_2^*)^2 - c_2 h_1(1-m_2)(P_3 - P_3^*)(P_2 - P_2^*) - \alpha_2 h_1(P_1 - P_1^*)(P_2 - P_2^*)$$

$$- i_3 h_2(P_3 - P_3^*)^2 + c_3 h_2(1-m_1)(P_1 - P_1^*)(P_3 - P_3^*)$$

$$+ c_4 h_2(1-m_2)(P_2 - P_2^*)(P_3 - P_3^*).$$

Choosing $h_1 = \frac{c_1 c_4}{c_3 c_2}$, $h_2 = \frac{c_3}{c_2}$, and then simplifies

$$\frac{dV}{dt} = -i_1(P_1 - P_1^*)^2 - \alpha_1(P_2 - P_2^*)(P_1 - P_1^*) - i_2 \frac{c_1 c_4}{c_3 c_2}(P_2 - P_2^*)^2$$

$$- \alpha_2 \frac{c_1 c_4}{c_3 c_2}(P_1 - P_1^*)(P_2 - P_2^*) - i_3 \frac{c_3}{c_2}(P_3 - P_3^*)^2$$

$$= -i_1(P_1 - P_1^*)^2 - i_2 \frac{c_1 c_4}{c_3 c_2}(P_2 - P_2^*)^2 - i_3 \frac{c_3}{c_2}(P_3 - P_3^*)^2$$

$$- (\alpha_1 + \alpha_2 \frac{c_1 c_4}{c_3 c_2})(P_1 - P_1^*)(P_2 - P_2^*),$$

let $x = ((P_1 - P_1^*), (P_2 - P_2^*), (P_3 - P_3^*))$. Thus, right–hand side of $\frac{dV}{dt}$ is a quadratic form which can be expressed as $-x^T Q x$, Here Q is the symmetric quadratic form given by

$$\begin{pmatrix} A & H & G \\ H & B & F \\ G & F & C \end{pmatrix},$$

where, $A = i_1$, $B = i_2 \frac{c_1 c_4}{c_2 c_3}$, $C = i_3 \frac{c_3}{c_2}$, $H = \frac{1}{2}(\alpha_1 + \alpha_2 \frac{c_1 c_4}{c_2 c_3})$, $F = 0$, $G = 0$. We need all of the principal minors of Q, namely $A_1 = A$, $A_2 = AB - H^2$, $A_3 = ABC + 2FGH - AF^2 - BG^2 - CH^2$, to be positive, i.e., $A_1 = i_1$, $A_2 = i_1 i_2 \frac{c_1 c_4}{c_2^2}$, $A_3 = \frac{i_1 i_2 i_3 c_1 c_4}{c_2^2} - \frac{i_3 c_3}{4 c_2}\left(\alpha_1 + \alpha_2 \frac{c_1 c_4}{c_2 c_3}\right)$ to be positive. Since $A_1 > 0$, $A_2 > 0$, and $A_3 > 0$ if $\frac{i_1 i_2 i_3 c_1 c_4}{c_2^2} > \frac{i_3 c_3}{4 c_2}\left(\alpha_1 + \alpha_2 \frac{c_1 c_4}{c_2 c_3}\right)^2$. It then follows that, $\frac{dV}{dt} < 0$, if $\frac{i_1 i_2 i_3 c_1 c_4}{c_2^2} > \frac{i_3 c_3}{4 c_2}\left(\alpha_1 + \alpha_2 \frac{c_1 c_4}{c_2 c_3}\right)^2$. Also, $\frac{dV}{dt} = 0$ at (P_1^*, P_2^*, P_3^*). We then define the invariant set as

$$\Omega = \{(P_1, P_2, P_3) \in R_3^+ : \frac{dV}{dt} = 0\}.$$

Hence, by LaSalles Invariance Principle [92], it follows that the $E_7(P_1^*, P_2^*, P_3^*)$ is said to be globally asymptotically stable. $\qquad\square$

2.7 Numerical Simulation

For the simulation purposes, we perform numerical simulations to analyze the dynamical behavior of the system. The mathematical parameters of the models representing a certain pattern can be modified to achieve a stronger agreement between the performance of the model and the observations. The modification should, however, obtain model parameters within its complexity. The computational parameters used throughout models to describe actual processes are sometimes ambiguous since these parameters are empirically defined. In addition, the initial conditions of the model may not be well recognized. Despite these limitations, models are very effective tools for representing natural processes. Models are also the only way of extrapolating to broad spatial scales or forecasting the future. Because of their significance in ecology, we are trying to determine precision by validating models. For the same, the land area of the globe is 13,003 million hectares and 4,889 million ha are classified as agricultural area by the FAO. The estimation of the prey-I growth rate is proportional to the yield of sugarcane and can be computed using Table 2.1. Similarly, the estimation of prey–II growth rate is proportional to vegetables production and can be derived by using Table 2.2. The growth rate of prey–I can be estimated by taking the average annual production between 2013–14 and 2016–17. Thus, the average annual production is 70.425 tons per hectares. Therefore, the growth rate of prey–I=$\frac{70.425 \text{ tons}}{\text{hectares}}$ per year i.e. r_1=0.59 $month^{-1}$. The growth rate of prey–II can be estimated by taking the average annual production of vegetables between 2015–16 and 2017–18. Thus, the average annual production of vegetables is 177,210 thousand metric tons over 10,201 thousand hectares. Therefore, the growth rate of prey–II=$\frac{177210 \text{ thousands metric tons}}{10201 \text{ thousands hectares}}$ per year i.e. r_2=0.144 $month^{-1}$. Further, due to the limitations of the availability of data, in this study, we take some experimental values for other parameters to meet the requirement of the proposed model. By this data set of parameters, we justify our theoretical results, which reflect the effectiveness of our proposed study. In this work, to see how proposed models react to changes in model data, initial conditions, or parameter values. Understanding the extent of the change in model results to changes in parameters is often referring to as susceptibility tests. We perform numerical simulations to analyze the dynamical behaviour of the model (2.2.1). Parameters used in this model are taken assumed feasible values which are shown in Table 2.5.

Table 2.5: Parameter value used in simulation.

Parameter	Values	Parameter	Values
r_1	$0.59\ month^{-1}$(estimated)	c_2	$0.01\ kg^{-1}m^2\ month^{-1}$
i_1	$0.12\ kg^{-1}m^2\ month^{-1}$	m_2	0.9
c_1	$0.2\ kg^{-1}m^2\ month^{-1}$	α_2	$0.2\ kg^{-1}m^2\ month^{-1}$
m_1	0.7	c_4	$0.35\ kg^{-1}m^2\ month^{-1}$
α_1	$0.2\ kg^{-1}m^2\ month^{-1}$	r_3	$0.5\ month^{-1}$
r_2	$0.144\ month^{-1}$(estimated)	i_3	$0.4\ kg^{-1}m^2\ month^{-1}$
i_2	$0.2\ kg^{-1}m^2\ month^{-1}$	c_3	$0.4\ kg^{-1}m^2\ month^{-1}$

We take a simulated set of parameters from Table 2.5 and let the initial population density $P_{10} = 2\ kg/m^2$, $P_{20} = 1.5\ kg/m^2$, $P_{30} = 1\ kg/m^2$ in Figure 2.5a. Figure 2.5a shows the graph of prey–I, prey–II, and predator (pest) with respect to time $t = 5$. The density of prey–I and pest increases while prey–II decreases. Further, Figure 2.5b is plotted using (2.7.1) for the time t=5. Figure 2.5b describes that both prey–I and prey-II decrease rapidly while initially P_3 increases. The P_3 increases but, later on, the P_3 decreases slowly as P_3 depends on P_1 and P_2.

$$r_1 = 0.59,\ i_1 = 0.3,\ c_1 = 0.9,\ m_1 = 0.5,\ \alpha_1 = 0.4,\ r_2 = 0.14,\ i_2 = 0.3,\ c_2 = 0.8,$$

$$m_2 = 0.4,\ \alpha_2 = 0.2,\ r_3 = 0.35,\ i_3 = 0.64,\ c_3 = 0.45,\ c_4 = 0.3. \qquad (2.7.1)$$

(a)　　　　　　　　　(b)
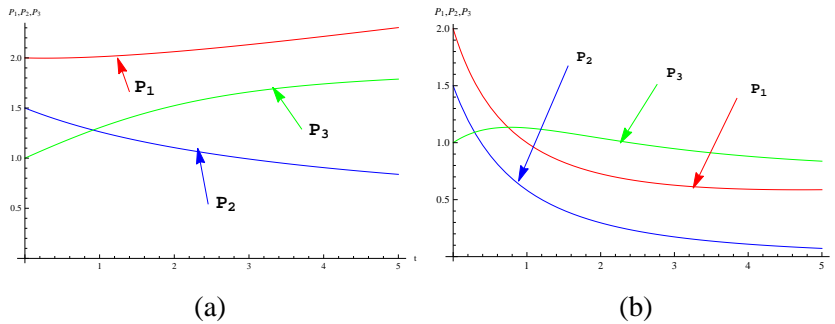
Figure 2.5: Solution curves for the system (2.2.1) the parameter values for (a) from Table 2.5, and (b) from the (2.7.1).

The equilibrium points, corresponding eigenvalues and the nature of the equilibrium points of the model are presented in Section 2.5. It is difficult to interpret the theoretical results due to complicated equilibrium points. To visualize the theoretical and stability results obtained in Section 2.5, we use numerical simulation to validate

the theoretical aspects. In this section, we discuss only those equilibrium points, which have biological feasible and asymptotically stable. For the set of parametric values given in (2.7.2), the stability condition (2.5.1), is fulfilled and the equilibrium point $E_2(0,0.3046,0.6337)$ is stable. Figure 2.6a shows that for parametric values given in (2.7.2), the density of P_1 and P_2 decrease, and P_3 increases. Finally, all three species eventually get their steady states $E_2(0,0.3046,0.6337)$. Ultimately, the density of P_1 tends to zero. Figure 2.8a represent phase portrait of the model system (2.2.1) with parametric values given in (2.7.2). Starting from various initial conditions, all the solution approach toward $(0,0.3046,0.6337)$. The different initial conditions are shown in Figure 2.8a. Thus, all three finally attain their steady states and achieve asymptotically stability. Since these groups share the same ecosystem, they can be cooperative or compete with one another depending on the situation.

$$r_1 = 0.5, \ i_1 = 0.3, \ c_1 = 0.9, \ m_1 = 0.2, \ \alpha_1 = 0.4, \ r_2 = 0.4, \ i_2 = 0.3, \ c_2 = 0.8,$$
$$m_2 = 0.4, \ \alpha_2 = 0.2, \ r_3 = 0.35, \ i_3 = 0.64, \ c_3 = 0.45, \ c_4 = 0.3. \qquad (2.7.2)$$

For the set of parametric values given in (2.7.3), the stability condition (2.5.2), is fulfilled and the equilibrium point $E_3(0.7412,0,0.8112)$ is stable. Figure 2.6b shows that for parametric values given in (2.7.3), the density of P_1 and P_2 decreases while P_3 increases. Finally, all three species finally get their steady states $E_3(0.7412,0,0.8112)$. Ultimately, the density of P_2 approaches to zero. Figure 6.4a represent phase portrait of the model system (2.2.1) with parametric values given in (2.7.3). Starting from various initial conditions, all the solution approach toward $E_3(0.7412,0,0.8112)$. The different initial conditions are shown in Figure 6.4a. Thus, all three eventually attain their steady states and achieve asymptotically stability.

$$r_1 = 0.59, \ i_1 = 0.3, \ c_1 = 0.9, \ m_1 = 0.5, \ \alpha_1 = 0.4, \ r_2 = 0.14, \ i_2 = 0.3, \ c_2 = 0.8,$$
$$m_2 = 0.4, \ \alpha_2 = 0.2, \ r_3 = 0.35, \ i_3 = 0.64, \ c_3 = 0.45, \ c_4 = 0.3. \qquad (2.7.3)$$

For the set of parametric values given in Table 2.5 and (2.7.4) , the stability condition (2.5.3), is fulfilled and the equilibrium point E_7 is stable. Figure 2.7a shows that the population density of P_1 and P_3 increase while P_2 decreases. Finally, all three species finally get their steady states $E_7(3.26879,0.383026,2.01899)$. Figure 2.7b

shows that for parametric values given in (2.7.4), the density of crop P_1 decreases rapidly while P_2 and P_3 increase. Finally, all three species eventually get their steady states $E_7(0.2563, 2.0768, 2.3979)$. Further, Figure 2.7a and Figure 2.7b coverage to the endemic equilibrium points $(3.26879, 0.383026, 2.01899)$ and (0.256354,2.07679,2.39799), respectively, for the model system (2.2.1). Figure 2.9 represent phase portrait of the model system (2.2.1) with parametric values given in Table 2.5. Starting from various initial conditions, all the solution approach toward $(3.26879, 0.383026, 2.01899)$ for Figure 2.9a and (0.256354,2.07679,2.39799) for Figure 6.4b. The different initial conditions are shown in Figure 2.9. Thus, all three finally attain their steady states and achieve asymptotically stability.

$$r_1 = 0.59, \ i_1 = 0.12, \ c_1 = 0.2, \ m_1 = 0.7, \ \alpha_1 = 0.2, \ r_2 = 0.44, \ i_2 = 0.2,$$

$$c_2 = 0.01, \ m_2 = 0.4, \ \alpha_2 = 0.04, \ r_3 = 0.5, \ i_3 = 0.4, \ c_3 = 0.3, \ c_4 = 0.35. \tag{2.7.4}$$

(a) Equilibrium point(0,0.3046,0.6337)   (b) Equilibrium point(0.7412,0,0.8112)
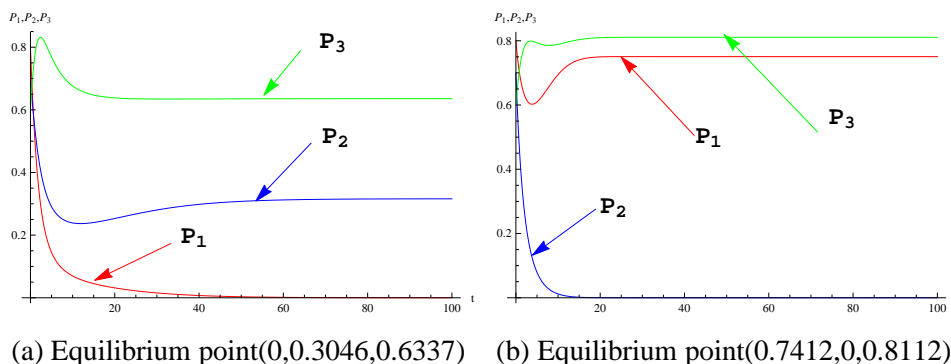
Figure 2.6: Asymptotic stable solution at equilibrium points for the model system (2.2.1).

(a)   (b)
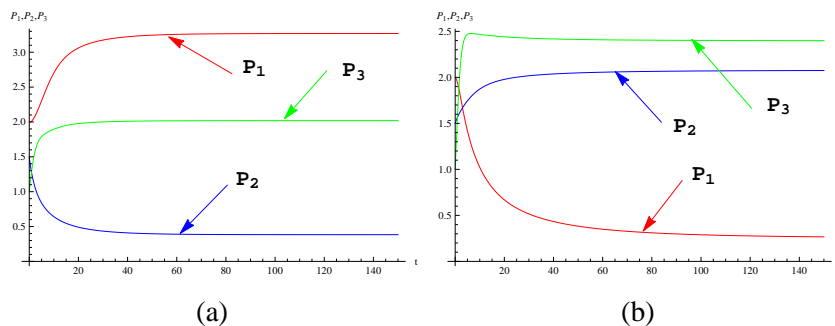
Figure 2.7: Solution curves coverage to the endemic equilibrium for the model system (2.2.1), showing that all species survive and ultimately evolve to their steady states, the parameter values are taken for (a) from Table 2.5 and (b) $r_2 = 0.44$, $m_2 = 0.4$, $\alpha_2 = 0.04$, remaining from Table 2.5.

(a) Stable point(0,0.3046,0.6337)   (b) Stable point(0.7412,0,0.8112)
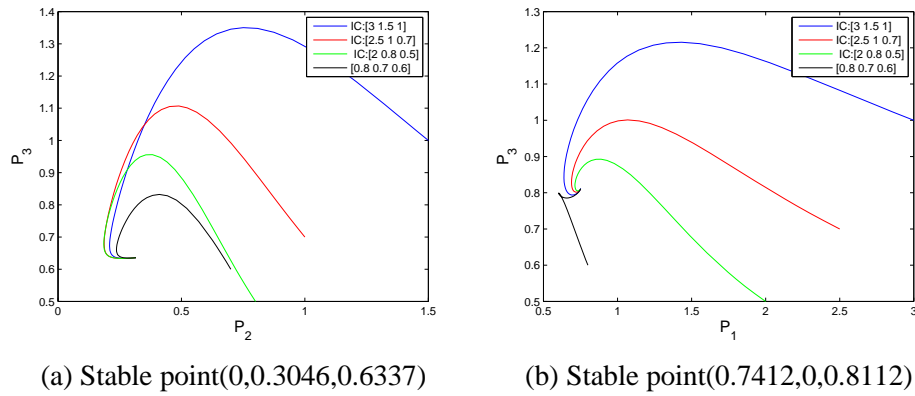
Figure 2.8: Phase portrait of model system (2.2.1).

(a)   Stable (b)   Stable
point(3.26879,0.383026,2.01899)   point(0.256354,2.07679,2.39799)
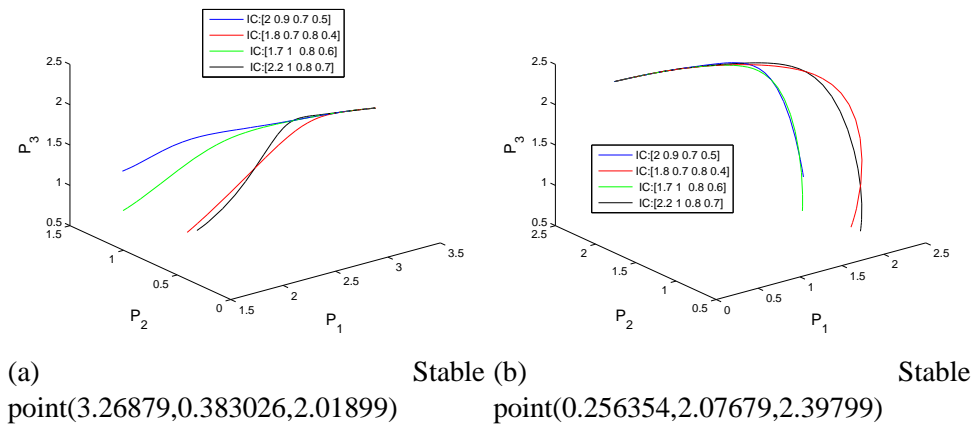
Figure 2.9: Phase portrait of model system (2.2.1), the parameter values are taken for (a) from Table 2.5 and (b) $r_2 = 0.44$, $m_2 = 0.4$, $\alpha_2 = 0.04$, remaining from Table 2.5.

2.7.1   Biological Interpretation of the Parameters

A mathematical model includes the parameters that increase the complexity of the model and make it more complicated to analyze the parameters that occur in the model. Therefore, parameter helps us determine the importance of the parameter. Thus, several factors influence the agriculture production. Figure 2.10 and Figure 2.11 represent the dynamic behavior of P_1, P_2, and P_3, of the system (2.2.1), when the value of one parameter varies and the other parameters remain constant. We study parameters that relate one variable to another, i.e., c_1, m_1, α_1, c_4, α_2, c_3 and m_2. Figure 2.10a–2.10c indicate that population density P_1 grows when the value of c_1 lowers, whereas population density P_2 declines when the value of c_1 decreases, and population density P_3 increases when the value of c_1 changes. Similarly, we notice that the population

density of P_1 grows when the values of m_1 and α_2 increase, whereas the population density of P_1 increases approximately equally when the values of c_3 and m_2 increase in Figure 2.10 and Figure 2.11. Further, Figure 2.10 and Figure 2.11 show that density P_2 decreases approximately equally when the value of m_1, c_4, c_2, and m_2 increases while the population density of P_2 decreases when c_1 and α_1 decrease. Further, when the value of m_1, α_1, and m_2 increases, population density P_3 decreases, and when the value of c_1, c_2 and α_2 changes, population density P_3 nearly remains the same.
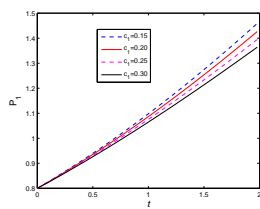
(a) Variation of P_1 when c_1 varies
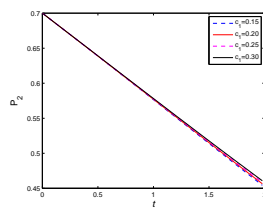
(b) Variation of P_2 when c_1 varies
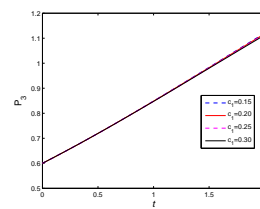
(c) Variation of P_3 when c_1 varies
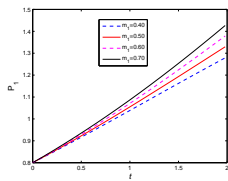
(d) Variation of P_1 when m_1 varies
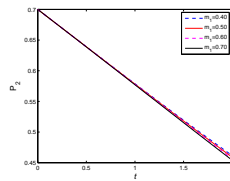
(e) Variation of P_2 when r_1 varies
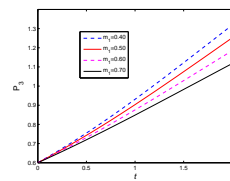
(f) Variation of P_3 when m_1 varies
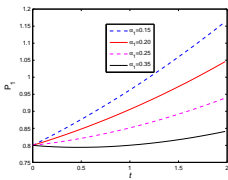
(g) Variation of P_1 when α_1 varies
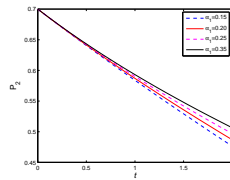
(h) Variation of P_2 when α_1 varies
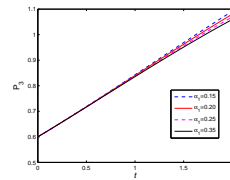
(i) Variation of P_3 when α_1 varies
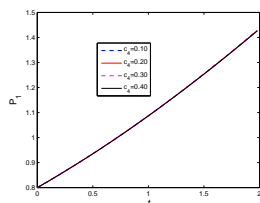
(j) Variation of P_1 when c_4 varies
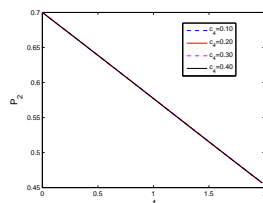
(k) Variation of P_2 when c_4 varies
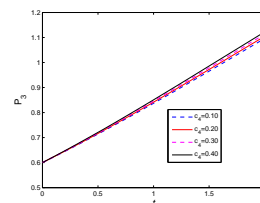
(l) Variation of P_3 when c_4 varies

Figure 2.10: Dynamical behavior of the P_1, P_2, and P_3 of the system (2.2.1) and parameter values are taken from Table 2.5.
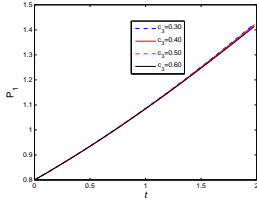
(a) Variation of P_1 when c_3 varies
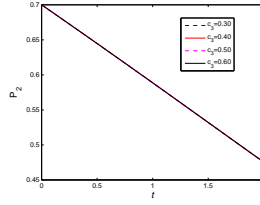
(b) Variation of P_2 when c_3 varies
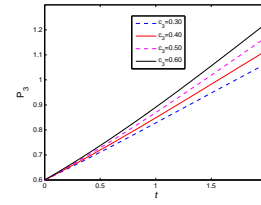
(c) Variation of P_3 when c_3 varies
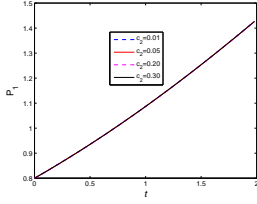
(d) Variation of P_1 when c_2 varies
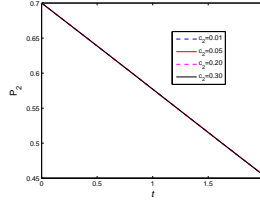
(e) Variation of P_2 when c_2 varies
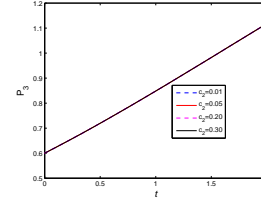
(f) Variation of P_3 when c_2 varies
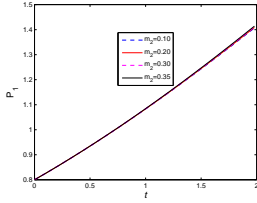
(g) Variation of P_1 when m_2 varies
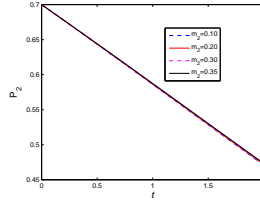
(h) Variation of P_2 when m_2 varies
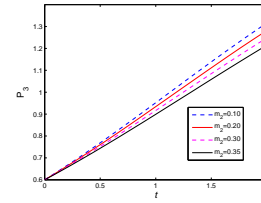
(i) Variation of P_3 when m_2 varies
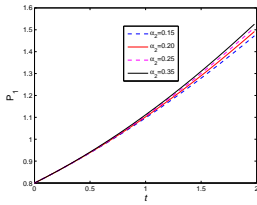
(j) Variation of P_1 when α_2 varies
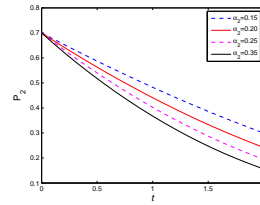
(k) Variation of P_2 when α_2 varies
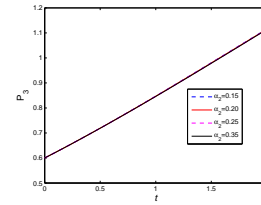
(l) Variation of P_3 when α_2 varies

Figure 2.11: Dynamical behavior of the P_1, P_2, and P_3 of the system (2.2.1) and parameter values are taken from Table 2.5.

2.8 Mathematical Model in the Presence of Control Variables

Biomass is animal manure and plant substance used for fertilizing the land. For instance, woods or forest leftovers, garbage from crop production (bagasse, straw), horticulture, food manufacturing, animal farming (nitrogen and phosphorus–rich manure), or human excrement from sewage treatment plants [25]. Despite the fact that burn-

ing plant–based biomass emits CO_2, it is still considered a renewable energy source since photosynthesis recycles CO_2 into new crops. Because a considerable amount of CO_2 is transported to the soil during each cycle, the efficient emission of CO_2 into the atmosphere can turn negative in certain instances [244]. The microbial biomass decomposes biotic and abiotic residues to release CO2 and existing plant nutrients. Microbial biomass tends to rise in agricultural systems that yield plant wastes. The size of the microbial biomass is influenced by soil parameters such as pH, clay, and the accessibility of organic carbon. Bacteria and fungus make up the majority of the microbial biomass, which decompose agricultural wastes and organic materials in the soil. This process makes nutrients like nitrogen (N) accessible for plant absorption in the soil. Approximately half of a soils profile's microbial biomass is found in the top 10 cm [239]. Thus, biomass control work as fertilizer, increase the fertility of land and production of crops is proportional to biomass quantity. According to [94], The application of phytosanitation technologies or the planting of resistant cultivars are the two major control options for African cassava mosaic disease (ACMD). Phytosanitation is the process of removing contaminated plants or utilising virus–free cuttings. Insecticide–based vector strategy is usually inadequate, and roguing may merely contain rather than reduce illness [140]. To control the Cassava mosaic disease, we do management by removing and destroying infected plants, plant–resistant varieties like H–97, H–165, H–2304 and to eradicate the Cassava mosaic virus from infected plants, apply meristem tip culture technique. Insecticide control kills predators, causing prey populations to suffer. Insecticide control kills the predator population that damages the prey population. Generally, there are some techniques to reduce losses caused by CMD (Cassava Mosaic Disease): (i) reduce the portion of crops that have become infected; (ii) prevent infection until losses become insignificant; (iii) reduce the level of damage incurred when infection has occurred; (iv) usage of pesticide. These goals can be met in a variety of methods, with phytosanitation, disease-resistant cultivars, cultural practices, vector management, and mild-strain preservation being the primary options for managing CMD. Thus, $u_2(t)$ is a control variable, which is a technique to control CMD. Though in this section, our primary objective is to reduce the predator population by using insecticides, We need to consider both the negative consequences on the environment and the expense. Furthermore, if it is applied more regularly, the crops may become toxic. Also, certain pesticides are so dangerous that their harmful

effects persist on the crops for a long period of time after applications, affecting the human body directly. As a result, we make pest management more economically and socially feasible by using the perfect mixture of pesticides and biological control. We should reduce the square of the pesticide we are spraying so that we may reduce not only the pesticide application expense but also the adverse effects [79].

In this regard, we modify our system (2.2.1) based on the assumption that $u_1(t)$ be the rate of application of biomass, $u_2(t)$ be the control that acts on Cassava mosaic disease of prey–II and $u_3(t)$ is the rate of application of insecticides. Finally, controls that are used to both the prey–I and prey–II as well as predator. Prey–I and prey–II populations are increased by control u_1 and u_2, and predator population is reduced by the control u_3. Thus, our proposed control mathematical model of two prey and one predator is

$$
\begin{cases}
\frac{dP_1}{dt} = r_1 P_1 - i_1 P_1{}^2 - c_1 (1 - m_1) P_3 P_1 - \alpha_1 P_1 P_2 + b_1 u_1 P_1, \\
\frac{dP_2}{dt} = r_2 P_2 - i_2 P_2{}^2 - c_2 (1 - m_2) P_3 P_2 - \alpha_2 P_1 P_2 + b_2 u_1 P_2 + b_3 u_2 P_2, \\
\frac{dP_3}{dt} = r_3 P_3 - i_3 P_3{}^2 + c_3 (1 - m_1) P_3 P_1 + c_4 (1 - m_2) P_3 P_2 - b_4 u_3 P_3,
\end{cases}
\tag{2.8.1}
$$

where $b_1 > 0$, $b_2 > 0$, $b_3 > 0$, $b_4 > 0$ and initial data $P_1(0) = P_{10} > 0$, $P_2(0) = P_{20} > 0$, $P_3(0) = P_{30} > 0$, $t \in [0, T_f]$. $u_1(t)$, $u_2(t)$, and $u_3(t)$ are measurable function with $0 \leqslant u_1(t) \leqslant 1$, $0 \leqslant u_2(t) \leqslant 1$, $0 \leqslant u_3(t) \leqslant 1$. Our main objective is to maximize the prey–I and prey–II population using biomass control while reducing cost and these costs are the control strategies that are applied in agriculture, such as the cost of biomass. We assume that the prey–I and prey–II populations are to maximize at the final time with different weights applied to the preys population. Thus, the objective functional is defined as

$$
J(u_1, u_2, u_3) = \int_0^{T_f} (A_1 P_1(t) + A_2 P_2(t) - A_3 u_1^2(t) - A_4 u_2^2(t) - A_5 u_3^2(t)) dt,
\tag{2.8.2}
$$

where A_1, A_2, A_3, A_4, and A_5 are positive weights. A_1 and A_2 are taken corresponding to the prey–I and prey–II and the term $A_3 u_1^2$, $A_4 u_2^2$, and $A_5 u_3^2$ are the cost of control effects on system. The weights of state variables are assigned depending on their

relative importance. To find a optimal control such that

$$J(u_1^*, u_2^*, u_3^*) = max\{J(u_1, u_2, u_3)|u_1, u_2, u_3 \in U\}, \qquad (2.8.3)$$

where control set U is defined as

$$U = \{u_i(t)|u_i(t) \text{ are lebesgue measurable with } 0 \leqslant t \leqslant 1, i = 1, 2\ 3; t \in [0, T_f]\}. \quad (2.8.4)$$

With the help of Pontryagins maximum principle [122], we obtain the necessary conditions for evaluating a positive control value for which the J is optimized.

2.8.1 Existence of Optimal Control

To determine the existence of optimal control to the system, we take a result from [148, 233, 240]. The following theorem gives the existence of optimal control.

Theorem 2.8.1. Let the objective functional $J(u_1, u_2, u_3)$, where $u_1(t)$, $u_2(t)$, and $u_3(t)$ are measurable with $0 \leqslant u_1(t) \leqslant 1$, $0 \leqslant u_2(t) \leqslant 1$ and $0 \leqslant u_3(t) \leqslant 1$ respectively, subject to the system of equation (2.8.1) with initial condition $P_1(0) = P_{10} > 0$, $P_2(0) = P_{20} > 0$, $P_3(0) = P_{30} > 0$, $t \in [0, T_f]$, then there exists control u_1^*, u_2^* and u_3^* such that

$$J(u_1^*, u_2^*, u_3^*) = max\{J(u_1, u_2, u_3)|u_1, u_2, u_3 \in U\}.$$

Proof. To prove the existence of optimal control using the result [200, 233, 242], if the following conditions are hold

(1). The initial condition and control variables u_1, u_2, u_3 with state equations are not empty.

(2). The admissible control set U are closed and convex.

(3). Each right-hand side of system (2.8.1) are continuous, bounded above by a sum of the state and bounded control, which can be written as a linear function of control u_1, u_2 and u_3 with coefficients depending on time and the state.

(4). The integrand of $J(u_1, u_2, u_3)$ is concave on U and is bounded above by $C_1 - C_2 u_1^{n_1} - C_3 u_2^{n_2} - C_4 u_3^{n_3}$ with $C_2 > 0$, $C_3 > 0$, $C_4 > 0$ and $n_1, n_2, n_3 > 1$.

The state and control variables are non–empty and non-negative. The control variables u_1, u_2 and u_2 are also convex and closed by the given definition. The integrand of $J(u_1, u_2, u_3)$ in the term of $A_1 P_1(t) + A_2 P_2(t) - A_3 u_1^2(t) - A_4 u_2^2(t) - A_5 u_3^2(t)$ is concave on U. For the third

60

condition (3), right–hand side of the equation (2.8.1) can be written as

$$
\begin{bmatrix}
r_1 - i_1 P_1 & -\alpha_1 P_1 & -c_1(1-m_1)P_1 \\
-\alpha_2 P_2 & r_2 - i_2 P_2 & -c_2(1-m_2)P_2 \\
c_3(1-m_1)P_3 & c_4(1-m_2)P_3 & r_3 - i_3 P_3
\end{bmatrix}
\begin{bmatrix}
P_1 \\ P_2 \\ P_3
\end{bmatrix}
+
\begin{bmatrix}
b_1 u_1 P_1 \\
(b_2 u_1 + b_3 u_2)P_2 \\
-b_3 u_3 P_3
\end{bmatrix}
$$

$$
\overrightarrow{g}(t,\overrightarrow{P},u) = \overrightarrow{\alpha}(t,\overrightarrow{P}) + \overrightarrow{\beta}(t,\overrightarrow{P})u,
$$

where $\overrightarrow{\alpha}(t,\overrightarrow{P}) =
\begin{bmatrix}
r_1 - i_1 P_1 & -\alpha_1 P_1 & -c_1(1-m_1)P_1 \\
-\alpha_2 P_2 & r_2 - i_2 P_2 & -c_2(1-m_2)P_2 \\
c_3(1-m_1)P_3 & c_4(1-m_2)P_3 & r_3 - i_3 P_3
\end{bmatrix}
\begin{bmatrix}
P_1 \\ P_2 \\ P_3
\end{bmatrix}$,

and $\overrightarrow{\beta}(t,\overrightarrow{P}) =
\begin{bmatrix}
b_1 u_1 P_1 \\
(b_2 u_1 + b_3 u_2)P_2 \\
-b_4 u_3 P_3
\end{bmatrix}$,

and $\overrightarrow{P} = (P_1,\ P_2,\ P_3)$, $\overrightarrow{\alpha}$ and $\overrightarrow{\beta}$ is a vector valued function of $\overrightarrow{P}$.

The bound of the right–hand side of the state system can be obtained as follows:

$$
\left\|
\begin{bmatrix}
r_1 - i_1 P_1 & -\alpha_1 P_1 & -c_1(1-m_1)P_1 \\
-\alpha_2 P_2 & r_2 - i_2 P_2 & -c_2(1-m_2)P_2 \\
c_3(1-m_1)P_3 & c_4(1-m_2)P_3 & r_3 - i_3 P_3
\end{bmatrix}
\begin{bmatrix}
P_1 \\ P_2 \\ P_3
\end{bmatrix}
+
\begin{bmatrix}
b_1 u_1 P_1 \\
(b_2 u_1 + b_3 u_2)P_2 \\
-b_4 u_3 P_3
\end{bmatrix}
\right\|
$$

$$
\leqslant
\left\|
\begin{bmatrix}
r_1 & 0 & 0 \\
0 & r_2 & 0 \\
c_3\frac{r_3}{i_3} & c_4\frac{r_3}{i_3} & r_3
\end{bmatrix}
\begin{bmatrix}
P_1 \\ P_2 \\ P_3
\end{bmatrix}
\right\|
+
\left\|
\begin{bmatrix}
b_1 u_1 P_1 \\
(b_2 u_1 + b_3 u_2)P_2 \\
-b_4 u_3 P_3
\end{bmatrix}
\right\|
\leqslant C_1|\overrightarrow{P}| + C_2|u|,
$$

where C_1 depends on the coefficients of the system and C_2 is maximum norm value. For the forth condition (4), the integrand $J(u_1,\ u_2,\ u_3)$ is concave, there exist a constant B_1 and B_2 such that $0 \leqslant |P_1| \leqslant B_1$ and $0 \leqslant |P_2| \leqslant B_2$.

$$
A_1 P_1 + A_2 P_2 - A_3 u_1^2 - A_4 u_2^2 - A_5 u_3^2 \leqslant A_1 B_1 + A_2 B_2 - A_3 u_1^2 - A_4 u_2^2 - A_5 u_3^2,
$$

$$
\leqslant C_1 - C_2|u_1|^2 - C_3|u_2|^2 - C_4|u_3|^2.
$$

We choose $C_1 = A_1 B_1 + A_2 B_2$, $C_2 = A_2$, $C_3 = A_3$, $C_4 = A_4$. Thus, the integrand J of the objective functional is concave on U and is bounded above by $C_1 - C_2|u_1|^2 - C_3|u_2|^2 - C_4|u_3|^2$ with $C_1 > 0$ and $n > 1$. We see that control and state variables are non-negatives values, the

concavity of the objective function in $u(t)$ is satisfied in the maximization problem and control set $\{u(t)|u(t)$ is measurable and $0 \leqslant u(t) \leqslant 1\}$ is convex and closed by definition. The optimal system is bounded, which determines the compactness, and state systems are bounded by a linear function in the control and condition (5), all conditions determine the existence of the optimal control. From the boundedness of the state system, the adjoint system, and the result of Lipschitz condition of the ordinary differential equation, we can obtain the uniqueness of the optimal control variable for small–time t. The uniqueness of the optimality system implies the uniqueness of optimal control. $\qquad\square$

2.8.2   Characterization of Optimal Control

Pontryagin's maximum principle is used to find the necessary conditions and characterization of optimal control [122].

Theorem 2.8.2. If u_1^*, u_2^* and u_3^* be an optimal control which maximizes $J(u_1, u_2, u_3)$. Let $P_1^*(t)$, $P_2^*(t)$ and $P_3^*(t)$ are optimal state solutions for the control system (2.8.1), then there exist adjoint variables $\lambda_1(t)$, $\lambda_1(t)$ and $\lambda_2(t)$ satisfying the following

$$
\frac{d\lambda_1}{dt} = -A_1 - \lambda_1 r_1 + 2i_1\lambda_1 P_1 + \lambda_1 c_1(1-m_1)P_3 + \lambda_1\alpha_1 P_2 + \lambda_2\alpha_2 P_2
$$
$$
\quad - \lambda_3 c_3(1-m_1)P_3 - \lambda_1 b_1 u_1,
$$
$$
\frac{d\lambda_2}{dt} = -A_2 + \alpha_1\lambda_1 P_1 - \lambda_2 r_2 + 2i_2\lambda_2 P_2 + \lambda_2 c_2(1-m_2)P_3
$$
$$
\quad + \lambda_2\alpha_2 P_1 - \lambda_3 c_4(1-m_2)P_3 - \lambda_2 b_2 u_1 - \lambda_2 b_3 u_2,
$$
$$
\frac{d\lambda_3}{dt} = \lambda_1 c_1(1-m_1)P_1 + \lambda_2 c_2(1-m_2)P_2 - \lambda_3 r_3 + 2\lambda_3 i_3 P_3
$$
$$
\quad - \lambda_3 c_3(1-m_1)P_1 - \lambda_3 c_4(1-m_2)P_2 + \lambda_3 b_4 u_3,
$$

with transversality conditions are

$$
\lambda_i(T_f) = 0, \ i = 1,2,3. \tag{2.8.5}
$$

Further, the optimal control variable $u_1^*(t)$, $u_2^*(t)$ and $u_3^*(t)$ that maximize $J(u_1, u_2, u_3)$ are

given by

$$u_1^*(t) = min\,\{max\,\{0,\,\frac{\lambda_1 b_1 P_1^* + \lambda_2 b_2 P_2^*}{2A_3}\},\,1\},\;u_2^*(t) = min\,\{max\,\{0,\,-\frac{\lambda_2 b_3 P_2^*(t)}{2A_4}\},\,1\},$$

$$u_3^*(t) = min\,\{max\,\{0,\,-\frac{\lambda_3 b_4 P_3^*(t)}{2A_5}\},\,1\}.$$

Proof. The transversality and adjoint conditions are given by [89, 122, 200]. Using the Hamiltonian function $H(t,\,\vec{P},\,\vec{u}) = f(t,\,\vec{P},\,\vec{u}) + \sum_{i=1}^{3} g_i(t,\,\vec{P},\,\vec{u})$, where $f(t,\,\vec{P},\,\vec{u})$ is integrand of the functional and $g_i(t,\,\vec{P},\,\vec{u})$ are state equations. $H = A_1 P_1(t) + A_2 P_2(t) - A_3 u_1^2(t) - A_4 u_2^2(t) - A_5 u_3^2(t) + \lambda_1(r_1 P_1 - i_1 P_1^2 - c_1(1-m_1)P_3 P_1 - \alpha_1 P_1 P_2 + b_1 u_1 P_1) + \lambda_2(r_2 P_2 - i_2 P_2^2 - c_2(1-m_2)P_3 P_2 - \alpha_2 P_1 P_2 + b_2 u_1 P_2 + b_3 u_2 P_2) + \lambda_3(r_3 P_3 - i_3 P_3^2 + c_3(1-m_1)P_3 P_1 + c_4(1-m_2)P_3 P_2 - b_4 u_3 P_3)$, where $\lambda_1(t)$, $\lambda_2(t)$ and $\lambda_3(t)$ are adjoint functions and the Pontryagin's maximum principle [122] provides adjoint system which can be followed as

$$\frac{d\lambda_1}{dt} = -(\frac{\partial H}{\partial P_1}) = -A_1 - \lambda_1 r_1 + 2i_1 \lambda_1 P_1$$
$$+ \lambda_1 c_1(1-m_1)P_3 + \lambda_1 \alpha_1 P_2 + \lambda_2 \alpha_2 P_2 - \lambda_3 c_3(1-m_1)P_3 - \lambda_1 b_1 u_1,$$

$$\frac{d\lambda_2}{dt} = -(\frac{\partial H}{\partial P_2})$$
$$= -A_2 + \alpha_1 \lambda_1 P_1 - \lambda_2 r_2 + 2i_2 \lambda_2 P_2 + \lambda_2 c_2(1-m_2)P_3$$
$$+ \lambda_2 \alpha_2 P_1 - \lambda_3 c_4(1-m_2)P_3 - \lambda_2 b_2 u_1 - \lambda_2 b_3 u_2,$$

$$\frac{d\lambda_3}{dt} = -(\frac{\partial H}{\partial P_3}) = \lambda_1 c_1(1-m_1)P_1 + \lambda_2 c_2(1-m_2)P_2 - \lambda_3 r_3$$
$$+ 2\lambda_3 i_3 P_3 - \lambda_3 c_3(1-m_1)P_1 - \lambda_3 c_4(1-m_2)P_2 + \lambda_3 b_4 u_3.$$

The transversality conditions are $\lambda_i(T_f) = 0$ for $i = 1,\,2,\,3$. The optimality condition provides

$$\frac{\partial H}{\partial u_1} = -2A_3 u_1 + \lambda_1 b_1 P_1 + \lambda_2 b_2 P_2 = 0 \; at \; u_1 = u_1^*(t),$$

$$\Rightarrow -2A_3 u_1^* + \lambda_1 b_1 P_1^* + \lambda_2 b_2 P_2^* = 0,\; \Rightarrow u_1^*(t) = \frac{.\lambda_1 b_1 P_1^* + \lambda_2 b_2 P_2^*}{2A_3}.$$

Since controls are bounded, we consider three cases, $set\{t|0 < u^*(t) < 1\}$, $set\{t|u^*(t) = 1\}$, $set\{t|u^*(t) = 0\}$. To determine the characterization of an optimal control. Hence, the optimal

control is

$$u_1^*(t) = \begin{cases} \frac{.\lambda_1 b_1 P_1^* + \lambda_2 b_2 P_2^*}{2A_3}, & \text{if } 0 \leqslant \frac{.\lambda_1 b_1 P_1^* + \lambda_2 b_2 P_2^*}{2A_3} \leqslant 1, \\ 0, & \text{if } \frac{.\lambda_1 b_1 P_1^* + \lambda_2 b_2 P_2^*}{2A_3} < 0, \\ 1, & \text{if } \frac{.\lambda_1 b_1 P_1^* + \lambda_2 b_2 P_2^*}{2A_3} > 1. \end{cases}$$

Further, $u_1^*(t)$ can be represented in a compact form by combining the above three cases, hence optimal control is characterized as

$$u_1^*(t) = min \left\{ max \left\{ 0, \frac{.\lambda_1 b_1 P_1^* + \lambda_2 b_2 P_2^*}{2A_3} \right\}, 1 \right\}.$$

Hence, the optimal control is

$$\frac{\partial H}{\partial u_2} = -2A_4 u_2 + \lambda_2 b_3 P_2 = 0 \text{ at } u_2 = u_2^*(t), \Rightarrow u_2^*(t) = \frac{\lambda_2 b_3 P_2^*}{2A_4}.$$

Hence, the optimal control is

$$u_2^*(t) = \begin{cases} \frac{\lambda_2 b_3 P_2^*}{2A_4}, & \text{if } 0 \leqslant \frac{\lambda_2 b_3 P_2^*}{2A_4} \leqslant 1, \\ 0, & \text{if } \frac{\lambda_2 b_3 P_2^*}{2A_4} < 0, \\ 1, & \text{if } \frac{\lambda_2 b_3 P_2^*}{2A_4} > 1. \end{cases}$$

Further, u_2^* can be written in compact form by combining above three cases, the optimal control is characterized as

$$u_2^*(t) = min \{ max \{ 0, \frac{\lambda_2 b_3 P_2^*}{2A_4} \}, 1 \}.$$

$$\frac{\partial H}{\partial u_3} = -2A_5 u_3 - \lambda_3 b_4 P_3 = 0 \text{ at } u_3 = u_3^*(t), \Rightarrow u_3^*(t) = -\frac{\lambda_3 b_4 P_3^*}{2A_5},$$

$$u_3^*(t) = \begin{cases} -\frac{\lambda_3 b_4 P_3^*}{2A_5}, & \text{if } 0 \leqslant -\frac{\lambda_3 b_4 P_3^*}{2A_5} \leqslant 1, \\ 0, & \text{if } -\frac{\lambda_3 b_4 P_3^*}{2A_5} < 0, \\ 1, & \text{if } -\frac{\lambda_3 b_4 P_3^*}{2A_5} > 1. \end{cases}$$

Further, u_3^* can be written in compact form by combining all the three cases, the optimal control is

$$u_3^*(t) = min \{ max \{ 0, -\frac{\lambda_3 b_4 P_3^*}{2A_5} \}, 1 \}.$$

$\square$

2.8.3 Optimality System

The optimality system consists of the adjoint system, state system, initial and transversality conditions together with the characterization of optimal control. The following optimality system characterizes the optimal control.

$$
\begin{cases}
\frac{dP_1}{dt} = r_1 P_1 - i_1 P_1{}^2 - c_1 (1-m_1) P_3 P_1 - \alpha_1 P_1 P_2 + b_1 P_1 \left(min \left\{ max \left\{ 0, \frac{\lambda_1 b_1 P_1^* + \lambda_2 b_2 P_2^*}{2A_3} \right\}, 1 \right\} \right), \\[2mm]
\frac{dP_2}{dt} = r_2 P_2 - i_2 P_2{}^2 - c_2 (1-m_2) P_3 P_2 - \alpha_2 P_1 P_2 + b_2 P_2 \left(min \left\{ max \left\{ 0, \frac{\lambda_1 b_1 P_1^* + \lambda_2 b_2 P_2^*}{2A_3} \right\}, 1 \right\} \right) \\[2mm]
\quad + b_3 P_2 \left(min \left\{ max \left\{ 0, -\frac{\lambda_2 b_3 P_2^*(t)}{2A_4} \right\}, 1 \right\} \right), \\[2mm]
\frac{dP_3}{dt} = r_3 P_3 - i_3 P_3{}^2 + c_3 (1-m_1) P_3 P_1 + c_4 (1-m_2) P_3 P_2 - b_4 P_3 \left(min \left\{ max \left\{ 0, -\frac{\lambda_3 b_4 P_3^*(t)}{2A_5} \right\}, 1 \right\} \right), \\[2mm]
\frac{d\lambda_1}{dt} = -A_1 - \lambda_1 r_1 + 2 i_1 \lambda_1 P_1 + \lambda_1 c_1 (1-m_1) P_3 + \lambda_1 \alpha_1 P_2 + \lambda_2 \alpha_2 P_2 - \lambda_3 c_3 (1-m_1) P_3 \\[2mm]
\quad - \lambda_1 b_1 \left(min \left\{ max \left\{ 0, \frac{\lambda_1 b_1 P_1^* + \lambda_2 b_2 P_2^*}{2A_3} \right\}, 1 \right\} \right), \\[2mm]
\frac{d\lambda_2}{dt} = -A_2 + \alpha_1 \lambda_1 P_1 - \lambda_2 r_2 + 2 i_2 \lambda_2 P_2 + \lambda_2 c_2 (1-m_2) P_3 + \lambda_2 \alpha_2 P_1 - \lambda_3 c_4 (1-m_2) P_3 - \lambda_2 b_2 u_1 \\[2mm]
\quad - \lambda_2 b_3 \left(min \left\{ max \left\{ 0, \frac{\lambda_2 b_3 P_2^*}{2A_4} \right\}, 1 \right\} \right), \\[2mm]
\frac{d\lambda_3}{dt} = \lambda_1 c_1 (1-m_1) P_1 + \lambda_2 c_2 (1-m_2) P_2 - \lambda_3 r_3 + 2 \lambda_3 i_3 P_3 - \lambda_3 c_3 (1-m_1) P_1 - \lambda_3 c_4 (1-m_2) P_2 \\[2mm]
\quad + \lambda_3 b_4 \left(min \left\{ max \left\{ 0, -\frac{\lambda_3 b_4 P_3^*}{2A_5} \right\}, 1 \right\} \right),
\end{cases}
$$

$$(2.8.6)$$

and subject to the following conditions

$$P_1(0) = P_{10}, \; P_2(0) = P_{20}, \; P_3(0) = P_{30}, \; \lambda_1(T_f) = 0, \; \lambda_2(T_f) = 0 \text{ and } \lambda_3(T_f) = 0.$$

2.9 Numerical Simulations for Optimal Control Problem

Because this study is qualitative, and it is not based on any survey and census. This is one of the limitations of our model and the same is persistent in the huge published literature. For the simulation purposes, we conduct numerical simulations to evaluate the behavior of the model $(2.8.1)$ in the presence and absence of control. We take a simulated set of parameters from Table 2.5, which describes the numerical values of the parameters that have been used in computational models. Let the initial population density $P_{10} = 0.8 \, kg/m^2$, $P_{20} = 0.7 \, kg/m^2$, and $P_{30} = 0.6 \, kg/m^2$. Furthermore,

our goal in this system is to maximize the prey-I and prey-II sample size, to reduce the predator population. Therefore, we take a simulated set of parameters to apply these controls in the model at a time of $t = 1$ month. Next, we get the solution of optimal control problems numerically using the fourth–order of the Runge–Kutta procedure [50, 65, 200]. Starting with an initial guess for the adjoint variables, the state equations are solved forward in time by the forward Runge–Kutta fourth-order method. Then, using these state values, the backward fourth–order Runge–Kutta procedure is used to solve the adjoint equations backward in time, and the iterations continue until convergence. Figure 3.2 describe the solution curves of the state variables prey–I, prey–II, and predator in the presence and without the presence of the control variables. The observations show that the application of optimal control variables reduces a much larger number of predator populations than in the absence of control. Further, Figure 3.2 shows that the prey–I and prey–II population increase. Again from Figure 3.2, it can be seen that the prey–I population increases from 0.8 kg/m^2 to more than 1 kg/m^2, the prey–II population increases from 0.7 kg/m^2 to 1.75 kg/m^2 approximately and the predator population is also significantly affected by the use of pesticide control. Figure 3.2(d), Figure 3.2(e) and Figure 3.2(f) represent variations in the control variables of the biomass application rate, control of the Cassava mosaic virus and insecticide rate with respect to time. Figure 3.2(g), Figure 3.2(h), and Figure 3.2(i) show the variation of adjoint variables λ_1, λ_2, and λ_3 with respect to time. In Figure 3.4, some different parameters values are taken compared to Figure 3.2, the good improvements occur in prey–I, prey–II, and predator populations. Figure 3.4(d), Figure 3.4(e) and Figure 3.4(f) show the variation of control variables with respect to time t that are convergent. Figure 3.4(g), Figure 3.4(h) and Figure 3.4(i) show the variation of adjoint variables with respect to time t. From the Figure 3.4, we observe that production of crop increases and predator population decreases compared to Figure 3.2. In Figure 3.4(c), the application of optimal control variable reduces a larger number of predator populations 0.6 kg/m^2 to 0.05 kg/m^2 approximately in the presence of the control. This is happening with the use of biomass, the control of the cassava mosaic virus, and the use of pesticides. Thus, we observe that the application of optimal control not only increases the number of prey populations but also reduces predator populations.
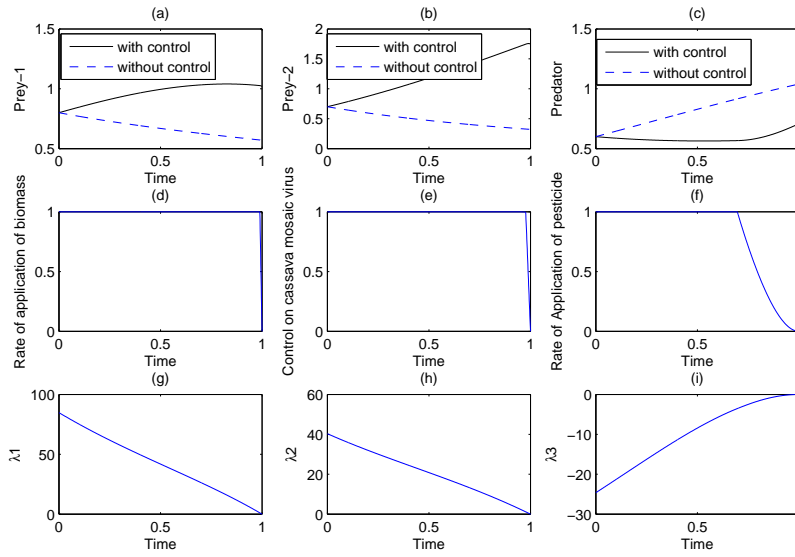
Figure 2.12: Plots represent the results of the comparison between the curves of the prey–predator individuals with control versus the non-control, control, and adjoint variables for the time, where the values of the parameters are $A_1 = 100$, $A_2 = 50$, $A_3 = 1$, $A_4 = 1$, $A_5 = 1$, $r_1 = 0.59$, $i_1 = 0.35$, $c_1 = 1$, $m_1 = 0.5$, $\alpha_1 = 0.6$, $r_2 = 0.144$, $i_2 = 0.25$, $c_2 = 1$, $m_2 = 0.6$, $\alpha_2 = 0.7$, $r_3 = 0.5$, $i_3 = 0.43$, $c_3 = 0.8$, $c_4 = 0.7$, $b_1 = 1$, $b_2 = 1$, $b_3 = 1$, $b_4 = 1$, $P_{10} = 0.8\,kg/m^2$, $P_{20} = 0.7\,kg/m^2$, $P_{30} = 0.6\,kg/m^2$ and $T_f = 1\,month$.
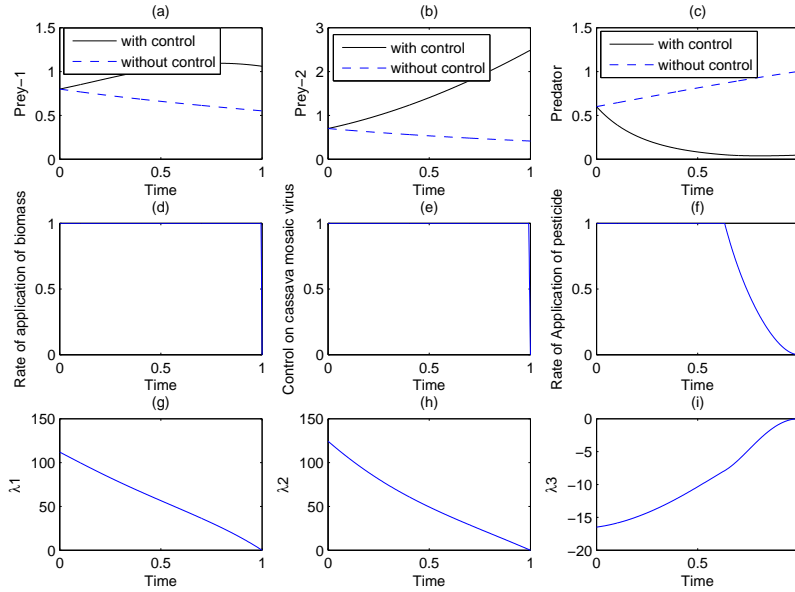
Figure 2.13: Plots represent the results of the comparison between the curves of prey–predator individuals with control versus without control, and adjoint variables for the time, where the values of parameters are $A_1 = 150$, $A_2 = 100$, $A_3 = 1$, $A_4 = 1$, $A_5 = 1$, $r_1 = 0.59$, $i_1 = 0.35$, $c_1 = 1$, $m_1 = 0.5$, $\alpha_1 = 0.6$, $r_2 = 0.4$, $i_2 = 0.25$, $c_2 = 1$, $m_2 = 0.6$, $\alpha_2 = 0.7$, $r_3 = 0.5$, $i_3 = 0.5$, $c_3 = 0.8$, $c_4 = 0.7$, $b_1 = 1$, $b_2 = 1$, $b_3 = 1$, $b_4 = 5$, $P_{10} = 0.8\,kg/m^2$, $P_{20} = 0.7\,kg/m^2$, $P_{30} = 0.6\,kg/m^2$ and $t = 1\,month$.

2.10   Discussion

In this study, a mathematical study of two prey and one predator model has been performed in agriculture. The positivity of the solutions and the boundedness of the model have been discussed. Under certain conditions, it has been observed that all equilibrium points are conditionally biologically feasible, locally asymptotically, and globally asymptotically stable. Figure 2.5 and Figure 2.7 showed the dynamics of population interactions. Also, we discussed the mathematical model in the presence and absence of control variables. Furthermore, the existence of optimal control and the characterization of optimal control have been discussed. The actual data of r_1, r_2, and the experimental data of other parameters have been used for model verification. Our numerical results show that the application of three control measures: biomass, cassava mosaic virus control, and pesticides have a great impact on the agricultural systems. Thus, from Figure 3.2 and Figure 3.4, it has been observed that the control variables increased the population of prey–I and prey–II and decreased the predator population in the presence of control. The optimal control acted as a stopover of the predator and favorable conditions of prey–I and prey–II. As a result, efficient methods for controlling pests have an important impact on society. We have adopted a balanced control method to effectively control the number of pests. For the fertility of the land, biomass control has been used. This study made a novel contribution to the field of prey–predator studies in agriculture. The results of this ecological paper have great potential in real–life agricultural communities.

Chapter 3

Study of a Prey–Predator Model with Preventing Crop Pest Using Natural Enemies and Control

In this chapter, a mathematical model of an ecological framework of prey, pest, and natural enemy of pest is developed. Different equilibrium points are obtained and their existence and stability of the steady states are evaluated. An optimal control strategy is one that minimizes crop loss while providing the least levels of environmental damage. A variety of chemicals, biological and physical controls, and methods are implemented. Then, using Pontryagin's maximum principle, the existence, characterization, and necessary conditions of the optimal control are evaluated. Finally, numerical simulations are performed to validate the analytical results.

3.1   Introduction

In the last 50 years, the world population has risen at an unprecedented pace. New agricultural technology has increased the production of major crops yet, besides causing deterioration of the climate. However, there is a lack of effective data on food loss or damage caused by such biotic agents, mainly in developing nations. The smal-

I available information demonstrates that an estimated 18-20% of yearly food crops globally may be damaged by pests. Moreover, losses are comparatively higher in the emerging tropics of Asia and Africa, at which population is also projected to grow rapidly over the next 50 years. There is a significant need to accurately measure the level of waste production at various levels from farming to consumer use. It is vital to the advancement of secure, productive, and sustainable methods of pest control and food safety for the long term. More recently, the topic of the management of agricultural insects has received more and more research interest. Unscientific and unjustified application of insecticides has led to catastrophic results. It has been noticed that 10-30% of yield reductions are attributed to pests. The changing agro–climatic factors have contributed significantly to the infestation of several predatory insects in different areas of the world. Approximately 30–35% of the annual agricultural productivity loss in India is attributed to pests, as reported by the Indian Agricultural Research Council. In recent days, nematodes have become a serious risk to crops and lead to the loss of 60 million tons of grains annually worldwide. This has contributed to a detrimental effect on agricultural biosecurity, which is critical to food security. The output of agricultural crops is affected by the occurrence of pests. Numerous methods exist to avoid or reduce these crop losses. The various types of crop waste as well as the various pest control techniques evolved over the last century have been summarized below. An outline of grain declines is provided for wheat, maize, rice, soybeans, potatoes, and cotton for the period 2001-03 on both a local and worldwide basis, despite the current crop protection methods. The cumulative pest loss ranged from around 50% in wheat to 80% in cotton yield. It is expected that yield reduction for wheat, cotton, and soybean is about 26–29%, and 31%, 37%, and 40%, respectively, for rice, maize, and potatoes. Lastly, weeds generated the highest possible liability (34%). Cultivation security in cash crops was much more beneficial than in food crops. While the use of pesticides has helped farmers to increase crop yield, it has also increased susceptibility to the pest's harmful effects. The definition of integrated pest/crops aims to find the optimal standard for the use of pest control methods and to decrease the quantity or frequency of pesticides to an environmentally safe degree. At the global level [51], about one-third of the total grain production has been lost due to insects, viruses, and weeds. Arthropods are killing about 18-20% percent of annual crops, worth more than US$470 billion worldwide. Big problems (13–16%) exist in the areas due to disease,

and the declines in underdeveloped nations are higher. Globally around 27 to 32% of all agricultural food produce in the world are wasted [146]. But these losses did not include the agricultural crop losses in the field. For example Table 3.1 shows the loss of crops attributable to insect plagues in India. The data shown in Table 3.1 taken from first row references.

Table 3.1: Report of crop damage caused by pests (%) in India

Crop	[190]	[192]	[68]	[157]	[72]	[202]	[73]	[75]
Oilseeds	5	5	35	25	25	25	15	20
Cotton	18	18	50	22	50	50	30	30
Pulses	5	5	30	7	15	15	15	15
Rice	10	10	25	18.6	25	25	25	25
Wheat	3	-	5-10	11.4	5	5	5	5
Maize	5	-	25	-	25	25	20	18
Sorghum and millets	3.5	-	35	10	30	30	10	8
Groundnut	5	-	15	-	15	15	15	15
Sugarcane	10	-	20	15	20	20	20	20

Agricultural crop damages caused by pests in India were also reported from periodically [71, 190] and, after the green revolution, the increase in crop losses was higher than that reported at the global stages [71, 190]. The crop wastage rose significantly from 7.2% percent in the 1960s to 23.3% in the early 2000s, but after that, the losses fell to 17.5% [73]. In the pre-green revolution period, it was reported that losses incurred by pest species ranged from 3.5 % in sorghum and millets to 16% in cotton. Vegetable crop damage was estimated to be very massive in India, which was around 30–40 % [8]. In addition to harvest and post-harvest losses, which were reported to be 10–30 % of production, pre–harvest yield reduction of about 40% was unavoidable [134]. As calculated by [73], yield losses declined from 23.3% in the 1990s to 17.5% in 2010 and 15.7% recently [75]. [55] reported a real loss of 39% caused by pests in potatoes globally and without crop security about 71% can be lost to pests. Actual overall losses have been reported to range from 24% in Europe to over 50% in Africa. The yield losses in Indian vegetables due to huge insects are given in Table 3.2 [8, 220].

Table 3.2: Loss of yields in Indian vegetable crops caused by large pest species

Crop	Pest	Yield loss (%)
Chilli Thrips	Chilli Thrips	12–90
	Mites (Polyphagotarsonemus latus)	34
Tomato	Fruit borer (H. armigera)	24–73
Okra	Fruit borer (H. armigera)	22
	Leafhopper (A. biguttula biguttula)	54–66
	Whitefly (B. tabaci)	54
	Shoot and fruit borer (E. vittella)	23–54
Cabbage	Diamondback moth (P. xylostella)	17–99
	Cabbage caterpillar (P. brassicae)	69
	Cabbage leaf webber	28–51
	Cabbage borer (H. undalis)	30–58
Cabbage	Aphid	3–6
	Tobacco caterpillar	4–8
	Potato tuber moth	6–9
	Mite (P. latus)	4–27
Cucurbits	Fruit fly (B. cucurbitae)	20–100
Brinjal	Fruit and shoot borer	11–93

Because of the Animals, pests, diseases, and weeds at least one–third to half of the world crop output is destroyed. Reducing the loss of food would lead to a major increase in the supply of food for use. A precise estimation of these damages is the first important step in reducing these losses. However, it is acknowledged that damage is rising due to different biotic and abiotic stresses in the face of the growing strength of agriculture and the environment on farmland. Thus, there is an urgent need to establish effective pest control techniques and agricultural pests enemy that is at the same time productive, healthy, and persistent. Using pest–resistant cultivars provides so many benefits and can form the center in which to build sustainable farming production. Pest control has appeared recently being one of the most important problems impacting ecologically sustainable due to the growing people communities and increasing food crisis. Hence, there is detailed research of effective pest control strategies. Prey–predation mechanism of prey disease and stage-structured model behaviour are studied by [144, 210, 211]. [172] built up a prey-predator model of the Lokta–volta model kind with irrational impact for integrated pest control. [187] researched a model that consists of predator species, susceptible prey, and infected prey and two pushes for integrated control of the pest. The optimal management technique was explored by [205] using a balanced mix of controls (infection, chemi-

cal, and predation pest control aspects) to avoid the pest population. The [174, 197] suggested a state-dependent dynamic impulsive mechanism by releasing natural enemies and sprinkling pesticides. [243] has mentioned a pest–natural enemy model focused on the application of impulsive pest-specific pesticides. Relevant studies were performed using various kinds of prey–predator models and stage–structured populations. The goal of the present research is to increase crop production and to reduce the pest population. For this, at the higher trophic level of the pest species, we find an appropriate predator(the natural enemy of pest). The study seeks to determine how natural enemy use and balance pesticide can manage the pests. Also, the aim is to illustrate how the monitoring of pest control is greatly influenced by the deletion of the natural enemy due to predation by its predators or the use of dangerous chemical substances.

3.2   Mathematical Model

Many species like spiders, birds, frogs, etc. are recognized as the natural enemy as they feed on agricultural pests. Biological monitoring is the beneficial of predators operation for controlling pests and their serious harm. Through the number of insects and mites, the natural enemies could be used as a biological control for pest management. The use of natural enemies is also useful for the biological management of the land area and wildland weeds. High levels of residues from pesticides can interfere with the reproduction of natural enemies and they are trying to identify and destroy pests. Therefore, the elimination of pests and the protection of the natural enemy from an agriculture sector and ecological viewpoint is very important. By using pesticides, apply them selectively and handle only highly infested areas instead of whole plants. Use more common insecticides in the kinds of invertebrates they destroy, like Bacillus thuringiensis, which only destroys caterpillars that consume treated foliage. Here, we find the prey–predator model [96] since it is renowned for displaying excitable activity and expanding this model by introducing another equation of the prey-treated crop species. In this model, The mathematical model is set up to protect crops from pests through the effective use of natural enemies along with the balanced application of pesticides. To examine the effect of the natural enemy on control of the pest species, we first find a framework of prey–predator in three dimensions. The following is a

purely ecological model:

$$
\begin{cases}
\frac{dP_1}{dt} &= r_1 P_1 \left(1 - \frac{P_1}{K_1}\right) - \alpha_1 P_1 P_2, \\[2mm]
\frac{dP_2}{dt} &= r_2 P_2 \left(1 - \frac{P_2}{K_2}\right) - \frac{m P_3 P_2^2}{\alpha_2^2 + P_2^2} + \alpha_3 P_1 P_2, \\[2mm]
\frac{dP_3}{dt} &= \frac{\gamma P_3 P_2^2}{\alpha_2^2 + P_2^2} - \mu P_3,
\end{cases}
\tag{3.2.1}
$$

with initial data $P_1(0) > 0$, $P_2(0) > 0$ and $P_3(0) > 0$. Context of parameters is shown in the Table 3.3.

Table 3.3: Parameters used in the model

Parameter	Description
$P_1(t)$	Density of crops (prey) at time t
$P_2(t)$	Density of pest at time t
$P_3(t)$	Density of natural enemies of pest at time t
r_1	Intrinsic growth rate of prey
K_1	The carrying capacity of prey
r_2	Intrinsic growth rate of pest
K_2	The carrying capacity of pest
m	Holling type-III functional response with consumption rate
α_1	Predation rate coefficient
α_2	Half saturation constant
α_3	Reproduction rate of pest per prey eaten
γ	Predator conversion rate
μ	The natural mortality rate of the predator

The predation loss term $\frac{m P_3 P_2^2}{\alpha_2^2 + P_2^2}$ has a moving property in the pest equation. We also assumed that the natural enemy is removed from the ecosystem due to predation by its predator apart from natural death. In population ecology, the natural enemies of pest population has different functional responses. We assume that the overall functional response is Holling type III. The carrying capacity K_1 is the number of prey population that can fill a unit area in the absence of pest, K_2 is the population density of pest capable of filling a unit area in the nonexistence of predators and m indicates that the natural enemy may eat the available pest per unit time by converting γ of that quantity into a predator. Also, μ means that through natural death, the predator population dies per unit time. Finally, δ is the rate of natural enemy removal.

3.3 Boundedness of the System

Theorem 3.3.1. The solutions of the system (3.2.1) in the region $\mathbb{R}_+^2$ are bounded.

Proof. We establish the function $w(P_1, P_2, P_3) = P_1 + P_2 + P_3$. The derivative of the $w(P_1, P_2, P_3)$ with respect to time t is

$$
\frac{dw}{dt} = \frac{dP_1}{dt} + \frac{dP_2}{dt} + \frac{dP_3}{dt}
$$

$$
= r_1 P_1 (1 - \frac{P_1}{K_1}) - \alpha_1 P_1 P_2 + r_2 P_2 (1 - \frac{P_2}{K_2}) - \frac{m P_3 P_2^2}{\alpha_2^2 + P_2^2} + \alpha_3 P_1 P_2 + \frac{\gamma P_3 P_2^2}{\alpha_2^2 + P_2^2} - \mu P_3
$$

$$
\leqslant r_1 P_1 (1 - \frac{P_1}{K_1}) + r_2 P_2 (1 - \frac{P_2}{K_2}) - \mu P_3,
$$

$$
\frac{dw}{dt} + \tau w \leqslant r_1 P_1 (1 - \frac{P_1}{K_1}) + r_2 P_2 (1 - \frac{P_2}{K_2}) - \mu P_3 + \tau (P_1 + P_2 + P_3)
$$

$$
\frac{dw}{dt} + \tau w \leqslant r_1 P_1 (1 - \frac{P_1}{K_1}) + r_2 P_2 (1 - \frac{P_2}{K_2}) - \mu P_3 + \tau (P_1 + P_2 + P_3)
$$

$$
= (r_1 + \tau) P_1 + (r_2 + \tau) P_2 - \frac{r_1}{K_1} P_1^2 - \frac{r_2}{K_2} P_2^2 - (\mu - \tau) P_3
$$

$$
\frac{dw}{dt} + \tau w \leqslant \frac{K_1 (r_1 + \tau)^2}{4 r_1} + \frac{K_2 (r_2 + \tau)^2}{4 r_2} = L,
$$

here $0 < \tau < \mu$ and $L = \frac{K_1(r_1+\tau)^2}{4r_1} + \frac{K_2(r_2+\tau)^2}{4r_2}$. Using application of Gronwalls inequality [65], we obtain

$$
0 < w(t) \leqslant e^{-\tau t} (w(0) - \frac{L}{\tau}) + \frac{L}{\tau},
$$

when $t \to \infty$, yields $0 < w(t) < \frac{L}{\tau}$. $\qquad\square$

3.4 Local Stability Analysis

3.4.1 Equilibria of the System

The model (3.2.1) has the following equilibrium points

(i) The trivial equilibrium $E_0(P_1 = 0, P_2 = 0, P_3 = 0)$, which always exists.

(ii) $E_1(P_1 = 0, P_2 = K_2, P_3 = 0)$.

(iii) $E_2(P_1 = K_1, P_2 = 0, P_3 = 0)$.

(iv) $E_3 \left(P_1 = 0, P_2 = -\frac{\sqrt{\mu}\alpha_2}{\sqrt{\gamma - \mu}}, P_3 = \frac{\gamma r_2 \alpha_2^2 \left(\sqrt{\gamma - \mu} K_2 + \sqrt{\mu}\alpha_2 \right)}{m(\gamma - \mu)^{3/2} K_2} \right)$.

(v) $E_4\left(P_1 = 0, P_2 = \frac{\sqrt{\mu}\alpha_2}{\sqrt{\gamma-\mu}}, P_3 = \frac{\gamma r_2 \alpha_2^2\left(\sqrt{\gamma-\mu}K_2 - \sqrt{\mu}\alpha_2\right)}{m(\gamma-\mu)^{3/2}K_2}\right).$

(vi) $E_5\left(P_1 = \frac{K_1 r_2(r_1 - K_2\alpha_1)}{r_1 r_2 + K_1 K_2 \alpha_1 \alpha_3}, P_2 = \frac{K_2 r_1(r_2 + K_1\alpha_3)}{r_1 r_2 + K_1 K_2 \alpha_1 \alpha_3}, P_3 = 0\right).$

(vii) $E_6\left(P_1 = K_1\left(1 + \frac{\sqrt{\mu}\alpha_1\alpha_2}{\sqrt{\gamma-\mu}r_1}\right), P_2 = -\frac{\sqrt{\mu}\alpha_2}{\sqrt{\gamma-\mu}}, P_3 = \frac{\gamma\alpha_2^2\left(\sqrt{\mu}r_1 r_2\alpha_2 + K_2\left(\sqrt{\mu}K_1\alpha_1\alpha_2\alpha_3 + \sqrt{\gamma-\mu}r_1(r_2+K_1\alpha_3)\right)\right)}{m(\gamma-\mu)^{3/2}K_2 r_1}\right).$

(viii) $E_7\left(P_1 = K_1\left(1 - \frac{\sqrt{\mu}\alpha_1\alpha_2}{\sqrt{\gamma-\mu}r_1}\right), P_2 = \frac{\sqrt{\mu}\alpha_2}{\sqrt{\gamma-\mu}}, P_3 = \frac{\gamma\alpha_2^2\left(-\sqrt{\mu}r_1 r_2\alpha_2 + K_2\left(-\sqrt{\mu}K_1\alpha_1\alpha_2\alpha_3 + \sqrt{\gamma-\mu}r_1(r_2+K_1\alpha_3)\right)\right)}{m(\gamma-\mu)^{3/2}K_2 r_1}\right).$

3.4.2   Local Stability

The equilibrium stability of smooth differential equations is evaluated by the sign of a real part of eigenvalues of the Jacobian matrix. An equilibrium is asymptotically stable if all eigenvalues have negative real parts; it is unstable if there is at least one positive real part in eigenvalues of the Jacobian matrix. Moreover, the Routh–Hurwitz stability criterion uses the characteristic polynomial of a Jacobian matrix to provide stability information. Now, to examine the local stability of equilibrium points, the Jacobian matrix $J(P_1, P_2, P_3)$ of the prey–pest–natural enemy of system (3.2.1) at any equilibrium point (P_1, P_2, P_3) is evaluated as

$$J(P_1, P_2, P_3) = \begin{pmatrix} -\frac{P_1 r_1}{K_1} + \left(1 - \frac{P_1}{K_1}\right)r_1 - P_2\alpha_1 & -P_1\alpha_1 & 0 \\ P_2\alpha_3 & M_1 & -\frac{mP_2}{P_2^2 + \alpha_2^2} \\ 0 & M_2 & -\mu + \frac{\gamma P_2^2}{P_2^2 + \alpha_2^2} \end{pmatrix}.$$

where $M_1 = -\frac{P_2 r_2}{K_2} + \left(1 - \frac{P_2}{K_2}\right)r_2 + \frac{2mP_2^2 P_3}{(P_2^2 + \alpha_2^2)^2} - \frac{mP_3}{P_2^2 + \alpha_2^2} + P_1\alpha_3$ and $M_2 = -\frac{2\gamma P_2^3 P_3}{(P_2^2 + \alpha_2^2)^2} + \frac{2\gamma P_2 P_3}{P_2^2 + \alpha_2^2}$

(i)The Jacobian matrix at equilibrium point $E_0(P_1 = 0, P_2 = 0, P_3 = 0)$ is

$$\begin{pmatrix} r_1 & 0 & 0 \\ 0 & r_2 & 0 \\ 0 & 0 & -\mu \end{pmatrix}$$

and the eigen values at the E_0 is r_1, r_2 and $-\mu$. Therefore the equilibrium point is saddle.

(ii) The Jacobian matrix for the equilibrium point $E_1(P_1 = 0, P_2 = K_2, P_3 = 0)$ is

$$\begin{pmatrix} r_1 - K_2\alpha_1 & 0 & 0 \\ K_2\alpha_3 & -r_2 & -\frac{mK_2}{K_2^2+\alpha_2^2} \\ 0 & 0 & -\mu + \frac{\gamma K_2^2}{K_2^2+\alpha_2^2} \end{pmatrix}.$$

The eigenvalues of $J(E_1)$ are $-r_2$, $r_1 - K_2\alpha_1$ and $\frac{\gamma K_2^2 - \mu K_2^2 - \mu\alpha_2^2}{K_2^2+\alpha_2^2}$. Therefore the equilibrium point $E_1(P_1 = 0, P_2 = K_2, P_3 = 0)$, is locally asymptotically stable if $r_1 - K_2\alpha_1 < 0$ and $\frac{\gamma K_2^2 - \mu K_2^2 - \mu\alpha_2^2}{K_2^2+\alpha_2^2} < 0$.

(iii) The Jacobian matrix for the equilibrium point $E_2(P_1 = K_1, P_2 = 0, P_3 = 0)$ is

$$\begin{pmatrix} -r_1 & -K_1\alpha_1 & 0 \\ 0 & r_2 + K_1\alpha_3 & 0 \\ 0 & 0 & -\mu. \end{pmatrix}.$$

The eigenvalues of $J(E_2)$ are $-\mu$, $-r_1$ and $r_2 + K_1\alpha_3$. Since two eigenvalues are negative and other is always positive, therefore the system around the (E_2) point is saddle point.

(iii) The Jacobian matrix for the equilibrium point $E(P_1 = 0, P_2 \neq 0, P_3 \neq 0)$ is

$$\begin{pmatrix} r_1 - P_2\alpha_1 & 0 & 0 \\ P_2\alpha_3 & -\frac{P_2 r_2}{K_2} + \frac{2mP_2^2 P_3}{(P_2^2+\alpha_2^2)^2} - \frac{mP_3}{P_2^2+\alpha_2^2} + \frac{mP_3 P_2}{P_2^2+\alpha_2^2} & -\frac{mP_2}{P_2^2+\alpha_2^2} \\ 0 & -\frac{2\gamma P_2^3 P_3}{(P_2^2+\alpha_2^2)^2} + \frac{2\gamma P_2 P_3}{P_2^2+\alpha_2^2} & 0 \end{pmatrix}.$$

The characteristic polynomial of Jacobian matrix is

$$x^3 + a_1 x^2 + a_2 x + a_3 = 0,$$

where, $a_1 = \left(-r_1 + \frac{P_2 r_2}{K_2} + P_2\alpha_1 - \frac{2mP_2^2 P_3}{(P_2^2+\alpha_2^2)^2} + \frac{mP_3}{P_2^2+\alpha_2^2} - \frac{mP_2 P_3}{P_2^2+\alpha_2^2}\right)$,

$a_2 = -\frac{P_2 r_1 r_2}{K_2} + \frac{P_2^2 r_2 \alpha_1}{K_2} + \frac{2mP_2^2 P_3 r_1}{(P_2^2+\alpha_2^2)^2} - \frac{2mP_2^3 P_3 \alpha_1}{(P_2^2+\alpha_2^2)^2} - \frac{mP_3 r_1}{P_2^2+\alpha_2^2} + \frac{mP_2 P_3 r_1}{P_2^2+\alpha_2^2} + \frac{mP_2 P_3 \alpha_1}{P_2^2+\alpha_2^2} - \frac{mP_2^2 P_3 \alpha_1}{P_2^2+\alpha_2^2}$, $a_3 = 0$.

For the local asymptotically stable of the system, the following Routh-Hurwitz criterion must be satisfied: (1) $a_1 > 0$, $a_2 > 0$, $a_3 > 0$, (2) $a_1 a_2 - a_3 > 0$.

(iv) The Jacobian matrix for the equilibrium point $E(P_1 \neq 0, P_2 = 0, P_3 \neq 0)$ is

$$J = \begin{pmatrix} -\frac{P_1 r_1}{K_1} & -P_1 \alpha_1 & 0 \\ 0 & r_2 - \frac{mP_3}{\alpha_2^2} + P_1 \alpha_3 & 0 \\ 0 & 0 & 0 \end{pmatrix}.$$

The eigenvalues of $J(E)$ are 0, $-\frac{P_1 r_1}{K_1}$ and $r_2 - \frac{mP_3}{\alpha_2^2} + P_1 \alpha_3$. In this case, system is not local asymptotically stable.

(v) The Jacobian matrix for the equilibrium point $E(P_1 \neq 0, P_2 \neq 0, P_3 = 0)$ is

$$\begin{pmatrix} -\frac{P_1 r_1}{K_1} & -P_1 \alpha_1 & 0 \\ P_2 \alpha_3 & -\frac{P_2 r_2}{K_2} + \frac{mP_3 P_2}{P_2^2 + \alpha_2^2} & -\frac{mP_2}{P_2^2 + \alpha_2^2} \\ 0 & 0 & -\mu + \frac{\gamma P_2^2}{P_2^2 + \alpha_2^2} \end{pmatrix}.$$

The characteristic polynomial of the Jacobian matrix is

$$x^3 + a_1 x^2 + a_2 x + a_3 = 0,$$

where $a_1 = \left(\mu + \frac{P_1 r_1}{K_1} + \frac{P_2 r_2}{K_2} - \frac{\gamma P_2^2}{P_2^2 + \alpha_2^2} - \frac{mP_2 P_3}{P_2^2 + \alpha_2^2} \right)$

$a_2 = \left(\frac{\mu P_1 r_1}{K_1} + \frac{\mu P_2 r_2}{K_2} + \frac{P_1 P_2 r_1 r_2}{K_1 K_2} + \frac{m\gamma P_2^3 P_3}{(P_2^2 + \alpha_2^2)^2} - \frac{m\mu P_2 P_3}{P_2^2 + \alpha_2^2} - \frac{\gamma P_1 P_2^2 r_1}{K_1(P_2^2 + \alpha_2^2)} - \frac{mP_1 P_2 P_3 r_1}{K_1(P_2^2 + \alpha_2^2)} - \frac{\gamma P_2^3 r_2}{K_2(P_2^2 + \alpha_2^2)} + P_1 P_2 \alpha_1 \alpha_3 \right)$

$a_3 = \frac{\mu P_1 P_2 r_1 r_2}{K_1 K_2} + \frac{m\gamma P_1 P_2^3 P_3 r_1}{K_1(P_2^2 + \alpha_2^2)^2} - \frac{m\mu P_1 P_2 P_3 r_1}{K_1(P_2^2 + \alpha_2^2)} - \frac{\gamma P_1 P_2^3 r_1 r_2}{K_1 K_2(P_2^2 + \alpha_2^2)} + \mu P_1 P_2 \alpha_1 \alpha_3 - \frac{\gamma P_1 P_2^3 \alpha_1 \alpha_3}{P_2^2 + \alpha_2^2}.$

For the local asymptotically stable of the system, the following Routh–Hurwitz criterion must be satisfied:

(1) $a_1 > 0$, $a_2 > 0$, $a_3 > 0$,

(2) $a_1 a_2 - a_3 > 0$.

(vi) The Jacobian matrix for the equilibrium point $E(P_1 \neq 0, P_2 \neq 0, P_3 \neq 0)$ is

$$\begin{pmatrix} -\frac{P_1 r_1}{K_1} & -P_1 \alpha_1 & 0 \\ P_2 \alpha_3 & -\frac{P_2 r_2}{K_2} + \left(1 - \frac{P_2}{K_2}\right) r_2 + \frac{2mP_2^2 P_3}{(P_2^2 + \alpha_2^2)^2} - \frac{mP_3}{P_2^2 + \alpha_2^2} + P_1 \alpha_3 & -\frac{mP_2}{P_2^2 + \alpha_2^2} \\ 0 & -\frac{2\gamma P_2^3 P_3}{(P_2^2 + \alpha_2^2)^2} + \frac{2\gamma P_2 P_3}{P_2^2 + \alpha_2^2} & 0 \end{pmatrix}.$$

The characteristic equation of system around the equilibrium is

$$x^3 + a_1 x^2 + a_2 x + a_3 = 0,$$

where $a_1 = \left(\frac{P_1 r_1}{K_1} + \left(-1 + \frac{2P_2}{K_2} \right) r_2 - \frac{2mP_2^2 P_3}{(P_2^2 + \alpha_2^2)^2} + \frac{mP_3}{P_2^2 + \alpha_2^2} - P_1 \alpha_3 \right)$

$a_2 = \left(P_1 \left(-1 + \frac{2P_2}{K_2} \right) r_1 \frac{r_2}{K_1} - \frac{2m\gamma P_2^4 P_3}{(P_2^2 + \alpha_2^2)^3} + \frac{2m\gamma P_2^2 P_3}{(P_2^2 + \alpha_2^2)^2} - \frac{2mP_1 P_2^2 P_3 r_1}{K_1 (P_2^2 + \alpha_2^2)^2} + \frac{mP_1 P_3 r_1}{K_1 (P_2^2 + \alpha_2^2)} - \frac{P_1^2 r_1 \alpha_3}{K_1} + P_1 P_2 \alpha_1 \alpha_3 \right)$

$a_3 = \frac{2m\gamma P_1 P_2^4 P_3 r_1}{K_1 (P_2^2 + \alpha_2^2)^3} + \frac{2m\gamma P_1 P_2^2 P_3 r_1}{K_1 (P_2^2 + \alpha_2^2)^2}$.

For the local asymptotically stable of the system, the following Routh–Hurwitz criterion must be satisfied:

(i) $a_1 > 0$, $a_2 > 0$, $a_3 > 0$,

(ii) $a_1 a_2 - a_3 > 0$.

3.5 Mathematical Model in the Presence of Control

Lately, pest-control has become a remarkable issue in ecological field as it can reduce the losses of both food and economy. Recent studies and research has shown that pest population can be decreased by using natural enemy of pest and chemicals like pesticides. It is noticed that spraying of pesticides had reduced the growth of pest population initially but the pest population may revival rapidly after a period of little time or larger than pre treatments level in later stages. Recently, [205] considered the mixture of controls based on prey infection, predation and chemical pesticide application and implemented an optimal plan for monitoring. It is importance that our model can also be modified by using balance pesticides as a control variable when pesticides kill pests. Thus, our new model is

$$\begin{cases} \frac{dP_1}{dt} = r_1 P_1 (1 - \frac{P_1}{K_1}) - \alpha_1 P_1 P_2, \\ \frac{dP_2}{dt} = r_2 P_2 (1 - \frac{P_2}{K_2}) - \frac{mP_3 P_2^2}{\alpha_2^2 + P_2^2} + \alpha_3 P_1 P_2 - ubP_2, \\ \frac{dP_3}{dt} = \frac{\gamma P_3 P_2^2}{\alpha_2^2 + P_2^2} - \mu P_3. \end{cases} \qquad (3.5.1)$$

with initial data $P_1(0) > 0$, $P_2(0) > 0$ and $P_3(0) > 0$. Here, natural enemies of pest P_3 have been used as a biological control strategy for removing harmful organism species. Biological organism control helps to find the natural enemies of a pest and implementing such natural predators into the specific community where the pest has accumulated. The natural enemies must be before release to establish that they do not have a detri-

mental effect on the climate or the economy. Furthermore, many entomopathogens are widely viable in a dosage form that can be treated like a pesticide. Term $\frac{mP_3P_2^2}{\alpha_2^2+P_2^2}$ is negative impact on harmful pests in agriculture. We presume that functional response of type III happens between pest species and their natural enemies, as survival first increases with increasing density of pests, and then decreases. When pest density is controlled by biological control and pesticides, crop density increases. Therefore, P_1 and P_3 are not taken in minimize the objective functional. In addition, pesticide regulation u should concentrate on time and should be used as needed. While our main goal throughout this section is to minimize the number of pests by using pesticide. The aim is to minimize the pest density of P_1. To attain the objective, through this way we construct the functional objective of our optimal control problem as regards:

$$J(u) = \min_{u} \int_{0}^{T_f} (A_1P_2(t) + A_2u(t)^2)dt, \tag{3.5.2}$$

where $A_1 > 0$ and $A_2 > 0$ are weights. A_1 is corresponding to the pest density and A_2 is the parameter of the square of control. The harmful side outcome of the pesticide are remove by the square of the control [79, 217, 218]. The objective functional is subject to (3.5.1). The term A_2u^2 is the cost of control on rate of application of pesticide strategy. We want to find a optimal control such that

$$J(u^*) = \min\{J(u)|u \in U\}, \tag{3.5.3}$$

where U is control set defined by below:

$$U = \{u(t)|u(t) \text{ are lebesgue measurable with } 0 \leqslant t \leqslant 1, \, t \in [0,T].\} \tag{3.5.4}$$

Based on its relative significance, the weight of state variables is typically allocated while many of the control are allocated according to their expense impacts. With the help of Pontryagins maximum principle [122], we obtain the requisite criteria to evaluate the value of the control such that the J is optimized. If this feasible control occurs then this is recognized as optimal control [30, 200]. By establishing the Hamiltonian H and then introducing the maximum Pontryagin principle, We establish the necessary criteria for the existence of optimal control. Adjoint functions also have a common

theme in multivariate calculus as Lagrange multipliers, which add constraints to the function of multiple variables to be optimized. Thus, we consider finding suitable requirements that the adjoint function should fulfill. Then, by separating the diagram from control to functional objective. For minimization, the control variables are strongly convex in the Hamiltonian equation. Let the Hamiltonian H is

$$H(t, P(t), \lambda(t), u(t)) = f(t, P(t), u(t)) + \lambda(t)g(t, P(t), u(t)),$$

where $f(t, P(t), u(t))$ is integrand of the functional $J(u)$ and $g(t, P(t), u(t))$ is right hand side of the equation (3.5.1). If $P_1^*(t)$, $P_2^*(t)$, $P_3^*(t)$ and $u^*(t)$ is an optimal solution, then there is a non–trivial vector function $\lambda(t)$ satisfying the following equations:

$$\begin{cases} \frac{dP}{dt} = \frac{\partial H(t, P^*(t), \lambda(t), u^*(t))}{\partial \lambda}, \\ 0 = \frac{\partial H(t, P^*(t), \lambda(t), u^*(t))}{\partial u}, \\ \lambda'(t) = -\frac{\partial H(t, P^*(t), \lambda(t), u^*(t))}{\partial P}. \end{cases}$$

If the control is bounded, i.e. $a \leqslant u(t) \leqslant b$, then optimal control $u^*(t)$ [200] is given by

$$\begin{cases} u^* = a, & \text{if } \frac{\partial H}{\partial u} < 0, \\ a \leqslant u^* \leqslant b, & \text{if } \frac{\partial H}{\partial u} = 0, \\ u^* = b, & \text{if } \frac{\partial H}{\partial u} > 0. \end{cases}$$

Thus, to find the optimal value of J, we make the Hamiltonian as:
$H = A_1 P_2 + A_2 u^2 + \lambda_1 (r_1 P_1 (1 - \frac{P_1}{K_1}) - \alpha_1 P_1 P_2) + \lambda_2 (r_2 P_2 (1 - \frac{P_2}{K_2}) - \frac{m P_3 P_2^2}{\alpha_2^2 + P_2^2} + \alpha_3 P_1 P_2 - u b P_2) + \lambda_3 (\frac{\gamma P_3 P_2^2}{\alpha_2^2 + P_2^2} - \mu P_3)$
with $\lambda = [\lambda_1, \lambda_2, \lambda_3]^T$, the adjoint vectors linked with the statevariables P_1, P_2, and P_3 associated to the prey-predator model. Pontryagin's maximum principle calculate the exact evolution of the adjoint functions. The optimality scheme of equations can be computed by taking partial derivatives of the Hamiltonian corresponding to the state variable. The optimality technique consists of the state and adjoint systems along with the characterization of the control variables.

Theorem 3.5.1. Given the objective functional $J(u) = \min_u \int_0^{T_f} (A_1 P_2(t) + A_2 u(t)^2) dt$, with initial

data $P_1(0) = P_{10} > 0$, $P_2(0) = P_{20} > 0$, $P_3(0) = P_{30} > 0$, $t \in [0, T_f]$ and $u(t)$ is measurable with $0 \leqslant u(t) \leqslant 1$, then there is an optimal control $u^*(t)$ which minimizes the objective functional $J(u^*)$ such that $J(u^*) = min\{J(u)|0 \leqslant u(t) \leqslant 1\}$.

Proof. To investigate the existence of optimal control, we must first show the following result using the boundedness of the system over a finite given period. The following condition should be fulfilled:

(i) The set of state variables and controls is non–empty.

(ii) The control set U is closed and convex.

(iii) Objective functional (integrand) is convex in U.

(iv) The state system R.H.S is bounded by a linear function in the variables of state and control where coefficients depend on the state and time.

(v) The integrand bounded below by $c_1(|u|^2)^{\frac{\beta}{2}} - c_2$ for $c_1 > 0$, $c_2 > 0$ and $\beta > 1$. We use the results from [200, 233] to check the above conditions. The state and control variables are non–negative values, and in the minimization problem, the convexity of the necessary condition of the objective functional in $u(t)$ is met. The control set is convex and closed by definition and the admissible Lebesgue measurable control variables set $u(t)$ is also convex and closed, integrand $f(t, p, u) = A_1 P_2 + A_2 u^2$ is clearly convex in u.

For the forth condition, the system is linear in the control and can be expressed as $\overrightarrow{g}(t, \overrightarrow{P}, u) = \overrightarrow{\alpha}(t, \overrightarrow{P}) + \overrightarrow{\beta}(t, \overrightarrow{P})u$, where $\overrightarrow{g}(t, \overrightarrow{P}, u)$ is R.H.S of the state equation, $\overrightarrow{P} = (P_1, P_2, P_3)$, $\overrightarrow{\alpha}$ and $\overrightarrow{\beta}$ is a vector valued function of $\overrightarrow{P}$. Using solution of bounded, we see that

$$
\left\| \left[\overrightarrow{g}(t, \overrightarrow{P}, u) \right] \right\| \leqslant \left\| \left[\begin{array}{ccc} r_1 & 0 & 0 \\ \alpha_3 P_2 & r_2 & 0 \\ 0 & 0 & \gamma \end{array} \right] \left[\begin{array}{c} P_1 \\ P_2 \\ P_3 \end{array} \right] \right\| + \left\| \left[\begin{array}{c} 0 \\ -b_2 u P_2 \\ 0 \end{array} \right] \right\|
$$

$$
\leqslant \left\| \left[\begin{array}{ccc} r_1 & 0 & 0 \\ \alpha_3 K_2 & r_2 & 0 \\ 0 & 0 & \gamma \end{array} \right] \left[\begin{array}{c} P_1 \\ P_2 \\ P_3 \end{array} \right] \right\| + \left\| \left[\begin{array}{c} 0 \\ b_2 u K_2 \\ 0 \end{array} \right] \right\|
$$

$$
\leqslant C_1 |\overrightarrow{P}| + C_2 |u|,
$$

where C_1 is dependent on system coefficients and C_2 is maximum norm value.

For the last condition (5),

$$A_1 P_2 + A_2 u^2 \geqslant A_2 (|u|^2)^{\frac{\beta}{2}} \geqslant c_1 (|u|^2)^{\frac{\beta}{2}} - c_2,$$

where c_1 and $c_2 > 0$. Hence, there exists constants c_1, c_2 and $\beta > 1$ such that $A_1 P_2 + A_2 u^2 \geqslant c_1 (|u|^2)^{\frac{\beta}{2}} - c_2$.

The optimal system satisfies all the above conditions and it has been bounded closed, which determines the compactness for the existence of the optimal control. $\qquad\square$

Theorem 3.5.2. If $u^*(t)$ be an optimal control which minimize $J(u)$. Let $P_1^*(t)$, $P_2^*(t)$ and $P_3^*(t)$ are optimal state solutions for the control system (3.5.1), then there exist adjoint variables $\lambda_1(t)$, $\lambda_2(t)$ and $\lambda_3(t)$ such that:

$$
\begin{aligned}
\frac{d\lambda_1}{dt} &= -(\frac{\partial H}{\partial P_1}) = -\frac{(K_1 - 2P_1)\, r_1 \lambda_1}{K_1} + P_2 (\alpha_1 \lambda_1 - \alpha_3 \lambda_2), \\
\frac{d\lambda_2}{dt} &= -(\frac{\partial H}{\partial P_2}) = -A_1 + bu\lambda_2 - r_2 \lambda_2 + \frac{2P_2 r_2 \lambda_2}{K_2} - \frac{2m P_2^2 P_3 \lambda_2}{(P_2^2 + \alpha_2^2)^2} \\
&\quad + \frac{m P_3 \lambda_2}{P_2^2 + \alpha_2^2} + P_1 (\alpha_1 \lambda_1 - \alpha_3 \lambda_2) + \frac{2\gamma P_2^3 P_3 \lambda_3}{(P_2^2 + \alpha_2^2)^2} - \frac{2\gamma P_2 P_3 \lambda_3}{P_2^2 + \alpha_2^2}, \\
\frac{d\lambda_3}{dt} &= -(\frac{\partial H}{\partial P_3}) = \frac{m P_2 \lambda_2 + (-\gamma + \mu) P_2^2 \lambda_3 + \mu \alpha_2^2 \lambda_3}{P_2^2 + \alpha_2^2},
\end{aligned}
\tag{3.5.5}
$$

with the transversality conditions are

$$\lambda_i(T_f) = 0 \text{ for } i = 1,\ 2,\ 3. \tag{3.5.6}$$

Further, the optimal control variable u^* that minimize $J(u)$ is given by

$$u^*(t) = \min\ \{\max\ \{0,\ \frac{\lambda_2 b P_2^*}{2A_2}\},\ 1\}. \tag{3.5.7}$$

Proof. The transversality and adjoint conditions are given result by [122, 200], using the Hamiltonian function H:

$$H(t,\ \overrightarrow{P},\ \overrightarrow{u}) = f(t,\ \overrightarrow{P},\ \overrightarrow{u}) + \sum_{i=1}^{3} \lambda_i g_i(t,\ \overrightarrow{P},\ \overrightarrow{u}),$$

where $f(t,\ \overrightarrow{P},\ \overrightarrow{u})$ is integrand of the functional and $g_i(t,\ \overrightarrow{P},\ \overrightarrow{u})$ are state equations.

$$H = A_1 P_2 + A_2 u^2 + \lambda_1 (r_1 P_1 (1 - \frac{P_1}{K_1}) - \alpha_1 P_1 P_2) + \lambda_2 (r_2 P_2 (1 - \frac{P_2}{K_2}) - \frac{m P_3 P_2^2}{\alpha_2^2 + P_2^2} + \alpha_3 P_1 P_2 - ubP_2) +$$

$\lambda_3 \left(\frac{\gamma P_3 P_2^2}{\alpha_2^2 + P_2^2} - \mu P_3 \right)$

with $\lambda = [\lambda_1, \lambda_2, \lambda_3]^T$, the adjoint vector associated to the state P_1, P_2 and P_3. The Pontryagin's maximum principle [122] provides adjoint system which can be followed as:

$$\frac{d\lambda_1}{dt} = -\left(\frac{\partial H}{\partial P_1} \right) = -\frac{(K_1 - 2P_1) r_1 \lambda_1}{K_1} + P_2 (\alpha_1 \lambda_1 - \alpha_3 \lambda_2),$$

$$\frac{d\lambda_2}{dt} = -\left(\frac{\partial H}{\partial P_2} \right) = -A_1 + bu\lambda_2 - r_2\lambda_2 + \frac{2P_2 r_2 \lambda_2}{K_2} - \frac{2mP_2^2 P_3 \lambda_2}{(P_2^2 + \alpha_2^2)^2} + \frac{mP_3 \lambda_2}{P_2^2 + \alpha_2^2}$$

$$+ P_1 (\alpha_1 \lambda_1 - \alpha_3 \lambda_2) + \frac{2\gamma P_2^3 P_3 \lambda_3}{(P_2^2 + \alpha_2^2)^2} - \frac{2\gamma P_2 P_3 \lambda_3}{P_2^2 + \alpha_2^2},$$

$$\frac{d\lambda_3}{dt} = -\left(\frac{\partial H}{\partial P_3} \right) = \frac{mP_2 \lambda_2 + (-\gamma + \mu) P_2^2 \lambda_3 + \mu \alpha_2^2 \lambda_3}{P_2^2 + \alpha_2^2}.$$

The transversality conditions are

$$\lambda_i(T_f) = 0 \text{ for } i = 1, 2, 3.$$

The optimality condition provides

$$\frac{\partial H}{\partial u} = 2A_2 u - \lambda_2 bP_2 = 0 \text{ at } u = u^*(t)$$

$$\Rightarrow 2A_2 u^* - \lambda_2 bP_2 = 0$$

$$\Rightarrow u^*(t) = \frac{\lambda_2 bP_2^*}{2A_2}.$$

$\square$

3.6 Numerical Simulation

For the simulation objective, we take a simulated set of parameters for minimize pest population and maximize the crop population and we take the initial population for the prey, pest and natural enemies as 2, 1.2, and 0.8 respectively. Figure 3.1 explore the dynamics of the system (3.2.1) by using numerical simulations and computations. Next, we obtain the solution of optimal control problem numerically using fourth order Runge–Kutta procedure [50, 65, 200, 217, 218]. Figure 3.2 shows the solution curves of the state variables crop(prey), pest and natural enemy population in the presence of control and natural enemies versus in the absence of control and natural enemies.

Observation shows that the application of optimal control variables and natural enemy reduce a quite larger number of pest population compared to in the absence of the control and natural enemy. Crop population increases from 2 $gram\ cm^{-3}$ to more than 5.5 $gram\ cm^{-3}$ approximately at $t = 2\ months$. Again from the Figure 3.2, it is easy to observe that pest population increases rapidly in the absence of control and natural enemies and almost constant in the presence of control and natural enemies. Fig. 3.2(c) and Figure 3.2(d) represent the variation of natural enemy and control variables with respect to time respectively. In Figure 3.4, there are some changes in parameters like weight $A_1 = 1$ to 100, $A_2 = 1$ to 50, $r_1 = 0.9\ month^{-1}$ to $0.5\ month^{-1}$, $r_2 = 0.258\ month^{-1}$ to $0.35\ month^{-1}$, $\alpha_2 = 0.25; gram\ cm^{-3}$ to $0.2; gram\ cm^{-3}$, $b = 1$ to 2, $t = 2\ months$ to $0.5\ months$. Figure 3.4(a) shows the crop production increase from 2 $gram\ cm^{-3}$ to 2.25 $gram\ cm^{-3}$ at $t = 0.5$ months, Figure 3.4(b) represent the pest population variation in the presence and absence of natural enemy and pesticide.
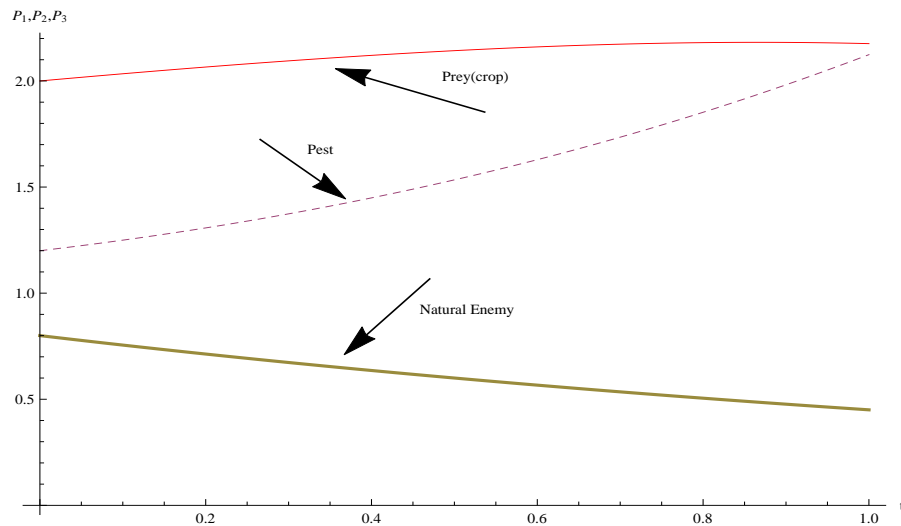
Figure 3.1: The figure illustrates the dynamics of the system between prey, pest, and natural enemy of pest with respect to time, where values of parameters are $r_1 = 0.5\ month^{-1}$, $K_1 = 20$ $gram\ cm^{-3}$, $m = 0.7\ month^{-1}$, $\alpha_1 = 0.23\ gram^{-1}\ cm^3\ month^{-1}$, $r_2 = .35\ month^{-1}$, $K_2 = 15$ $gram\ cm^{-3}$, $\alpha_2 = 0.3\ gram\ cm^{-3}$, $\alpha_3 = .25\ gram^{-1}\ cm^3\ month^{-1}$, $\gamma = 0.026\ month^{-1}$, $\mu = 0.6\ month^{-1}$, $P_{10} = 2\ gram\ cm^{-3}$, $P_{20} = 1.2\ gram\ cm^{-3}$, $P_{30} = 0.9\ gram\ cm^{-3}$ and $t = 2\ months$.
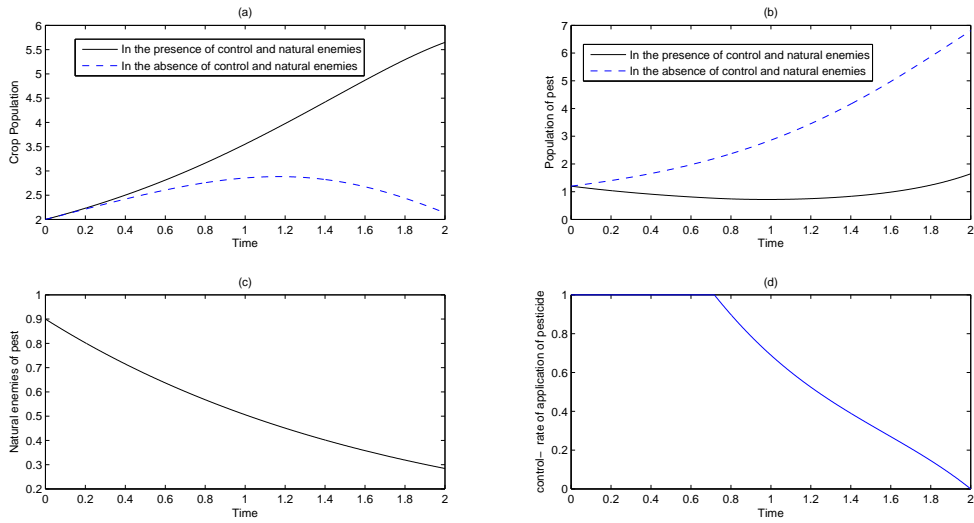
Figure 3.2: The graph depicts the results of the comparison between the curves of prey(crops), pest, and predator individuals in the presence of control and natural enemies versus in the absence of control and natural enemies, natural enemy population, and control variable with respect to the time, where values of parameters are $A_1 = 1$ $month^{-1}$, $A_2 = 1$, $r_1 = 0.9$, $K_1 = 20$ $gram$ cm^{-3}, $\alpha_1 = 0.23$ $gram^{-1}$ cm^3 $month^{-1}$, $r_2 = 0.258$ $month^{-1}$, $K_2 = 15$ $gram$ cm^{-3}, $m = 0.7$ $month^{-1}$, $\alpha_2 = 0.25$ $gram$ cm^{-3}, $\alpha_3 = 0.258$ $gram^{-1}$ cm^3 $month^{-1}$, $b = 1$, $\gamma = 0.0256$ $month^{-1}$, $\mu = 0.6$ $month^{-1}$, $P_{10} = 2$ $gram$ cm^{-3}, $P_{20} = 1.2$ $gram$ cm^{-3}, $P_{30} = 0.9$ $gram$ cm^{-3} and $t = 2$ $months$.
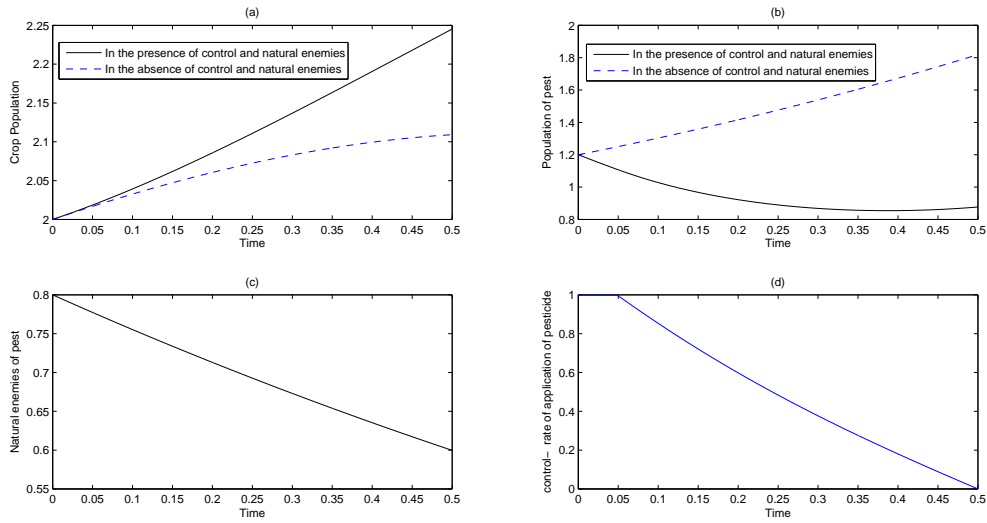
Figure 3.3: The figure depicts the results of the comparison between the curves of prey(crops), pest, and predator population in the presence of control and natural enemies versus in the absence of control and natural enemies, natural enemies population and control variable with respect to the time, where values of parameters are $A_1 = 100$, $A_2 = 50$, $r_1 = 0.5\,month^{-1}$, $K_1 = 20\,gram\,cm^{-3}$, $\alpha_1 = 0.23\ gram^{-1}\,cm^3\,month^{-1}$, $r_2 = 0.35\,month^{-1}$, $K_2 = 15\,gram\,cm^{-3}$, $m = 0.7\,month^{-1}$, $\alpha_2 = 0.2\,gram\,cm^{-3}$, $\alpha_3 = 0.25\ gram^{-1}\,cm^3\,month^{-1}$, $b = 2$, $\gamma = 0.026\,month^{-1}$, $\mu = 0.6\,month^{-1}$, $P_{10} = 2\,gram\,cm^{-3}$, $P_{20} = 1.2\,gram\,cm^{-3}$, $P_{30} = 0.8\,gram\,cm^{-3}$ and $t = 0.5\,months$.
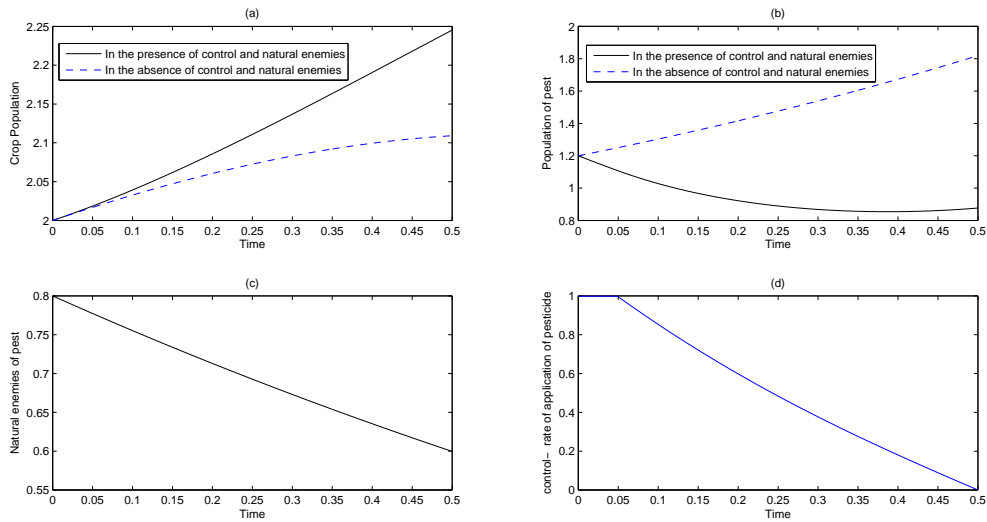
Figure 3.4: The figure depicts the results of the comparison between the curves of prey(crops), pest, and predator.

3.7   Discussion

In this study, we proposed a three-dimensional model of prey (crop), pest (a predator of prey), and natural enemy of pest (a predator of pest), and a systematic approach has been applied to control the pest population using a combination of pesticide and a natural enemy of pest. Studies have shown the system is bound. The existence and stability criteria of the equilibrium point have been established. Further, by applying the Pontryagins maximum principle, we proved the existence and determined the necessary conditions of the optimal control. We have also numerically analyzed the significant effect of the natural enemy on the pest population and crop production in the model. In the presence of the natural enemy and control variables, the pest population has been decreased and crop (prey) production has been increased in the prey–pest–natural enemy of pest model. Thus, our results showed that the natural enemy has a significant role in regulating the pest population.

Chapter 4

Study of Prey Predator System with Additional Food and Effective Pest Control Techniques in Agriculture

In the present chapter, a prey–predator mathematical model describes an ecosystem that includes crops, susceptible pests, infected pests, and the natural enemies of the pests. Further, the dynamic behavior of the framework, the description of steady–state equilibrium behavior, and pest control are discussed. The basic reproduction number and sensitivity analysis are addressed to determine the most influential parameters. Furthermore, a comprehensive analysis of the optimal control strategy is performed. The study discusses the strategic planning of pests, which provides optimal control of pests in contexts of operating cost and ecological harm. Pontryagin's maximum principle is used to develop an optimal strategy for pest control. Finally, numerical simulations are carried out to support the analytical results and to explain various dynamic systems that are used in the model.

4.1 Introduction

Food wastage caused by pests and crop disease has become one of the massive food issues, especially in developing nations. The United Nations has stated that the global population was recorded at 7.2 billion in 2014, an approximate annual growth rate of 82 million, with a quarter of that in low–income nations [226]. This enormous number of people worldwide poses serious problems for food producers and policy experts, particularly in terms of decreasing yield losses caused by pests and crop diseases estimated to be as large as 40% of global output. All kinds of vegetables and crops are our primary source of livelihood, but land resources are limited. However, several tiny insects, weeds, and living organisms are included to contribute to the loss of these essential crops. There are so many bacteria, fungi, viruses, etc. that cause damage by infecting crops. Managing theses are one of the world's biggest challenges [188]. Table 4.1 demonstrates the overall worldwide output of grain from 2010–11 to 2016–17 and the prediction for the 2017–18 and 2018–19 [245].

Table 4.1: Total world grain production 2010–11 to 2018–19

Years	Production in million metric tons
2010–11	2200.9
2011–12	2314.4
2012–13	2266.2
2013–14	2474.7
2014–15	2532.0
2015–16	2058.0
2016–17	2186.0
2017–18	2142.0
2018–19	2121.0

Here, an overview is presented on various kinds of crop damage. For the duration 2001–03, among crops, the total worldwide massive loss due to pests varied from nearly 50% in wheat to more than 80% in cotton yield. Actions are recorded as falls off 26–29% for soybean, wheat, and cotton, and 31, 37, and 40% for maize, potatoes, and rice, respectively. Overall, seeds recorded the largest potential damage (34%), with animal pests and pathogens being less significant (losses of 18 and 16%) [51]. As per a study by US Agriculture and Natural Resources scientists and other representatives of the International Society for Plant Pathology, organizations recognize that they

are losing agricultural productivity for 5 major food crops by 10% to 40% due to pests. The factors that work against growers include viruses, bacteria, fungi, oomycetes, nematodes, arthropods, mollusks, vertebrates, and parasitic plants [175, 212]. Consequently, the issue of pest control must inevitably be approached comprehensively, which has contributed to the growth of numerous innovative solutions, like integrated pest management (IPM). The primary principle of IPM is the appropriate and systematic application of various pest management strategies to keep pest risk to a minimum while reducing hazards to humans, livestock, plants, and the ecosystem. Integrated pest control research is extensive and should serve as an inspiration for the mathematical explanation of pest control strategies. An important motivating factor in the implementation of IPM programs provides a clear understanding of the relationship between the various aspects of the related agricultural systems, such as plants, pests, natural predators, and bio–pesticides. The mathematical study of ecological processes is one of the main research topics in the field of agricultural modeling, which could be regarded as a nonlinear science to a significant extent because of almost all ecological interactions. One of the key challenges and issues includes developing computational models that include accurate recommendations and knowledge of field studies in real environments so that these models could be used as tools to help for removing the pest. Our factory farming system is highly dependent on chemicals that regulate weeds, pests and quell fungi. The U.S. Environmental Protection Agency's new study on the selling and usage of pesticides places in the U.S. at 1.1 billion pounds in both 2011 and 2012, which is 23% of the approximately six billion pounds consumed globally [48]. In recent years, using pesticides has become a public health threat, an ecological tragedy, and has even triggered the creation of superweeds that must destroy increasingly dangerous pesticide formulations. In addition to serious agricultural chemical poisoning, pesticides may have extremely long health consequences for staff and customers, as well as for people living along with crops where they are used. For example, chlorpyrifos and other organophosphates are hazardous to brain activity and are linked with genital infections and neurodegenerative problems between farmworkers and people residing in agricultural fields [11]. Research has found in utero, the pesticide is extremely harmful to infants [24]. There is a chance of glyphosate and cancer [90, 227]. If we consider for thousands of years, it is projected that only 4 million square kilometers below 4 percent of the globe's ice–free and

non–barren surface area has been used for agriculture. 10% of the earths surface is covered by ice, and 19% is a wasteland deserts, hot salt pans, seas, dunes, and exposed rocks. This leaves behind what we call a 'habitable area'. According to the UN Food and Agriculture Agency, half of all habitable area is used for farming. The land area of the globe is 13,003 million hectares. 4,889 million hectares are known as 'farmland area' [87]. Losses caused by pests: crop loss from all factors - 500 billion US $ annually worldwide, insect pests - 15.6% loss of production, plant pathogens - 13.3%, weeds - 13.2%. Statistics show the amounts of pesticides used throughout the farming production for crops and seeds. Table 4.2 demonstrates the agricultural use of pesticides in the world between 2013 and 2017 [222].

Table 4.2: Agricultural use pesticides in the world from 2013 to 2017

Year	2013	2014	2015	2016	2017
Value(megatonnes)	4.05	4.11	4.06	4.09	4.11

Many of the latest pest control approaches have concentrated on organic insecticides. As stated by [58], the use of chemical insecticides is an effort to control the pest directly at a minimal price. However, these chemicals have been identified to have a variety of negative effects on the environment, including chemical residues in crops and agricultural habitats. Efficient management of these pests can be achieved using living organisms, reducing their abundance. There are many species and birds whose feed is these insects, but they cannot affect farming. Thus, such inhabitants could be used by some of the insect biological controls. Usage of predator species to kill pests can be seen in the research work [10, 196, 208, 217]. Therefore, the pest may be an infection with certain bacterial or viral diseases. For example, baculovirus normally develops in plants, so these viruses do not have any direct impact on crop yield, but they can be used to decrease the pest population [128]. In the specific field of agricultural pest control, the challenge is to develop reliable mathematical models capable of at least describing different techniques of pest control qualitatively. As from roots of the idea of integrated pest control models in the late 1950s, the study has provided a valuable selection of mathematical models that focuses on the different characteristics of application–based pest-integrated management models [236]. [29] considered appropriate biological and chemical pest control combinations to be used

in specific ecosystems of plants, pests, and parasites. Parasites can manage the pest population on their own accord to some extent, but this effect is negatively affected by the use of pesticides, as [29] has also found that the chemicals harm the parasites. [22] explained pest control by adding an infected insect. Thus, infection with the insect population has also become one of the ways in which they can be effectively eliminated from farm crops. The impetuous pest control model has been chosen and reformed as a hybrid dynamic system [171], enabling the parametric analysis of the system's response periodically via numerical continuation methods [22]. In this way, it has been possible to address concerns such as increasing the effectiveness of impetuous pest control while minimizing production costs and environmental damages. In the southern part of India, two of the most commercially valuable crops are coconut and oil palm trees. However, the insect Oryctes rhinoceros is seriously affecting both trees. Central Plantation Crops Research Institute (CPCRI) has identified a Baculovirus Oryctes (BVO) virus, which could be used to kill such species of pests [138]. Therefore, this Baculovirus Oryctes can be considered one of the natural pesticides of the Oryctes rhinoceros pest. Thus, it can be stated that the use of pesticide monitoring in parallel, pest infection, and the use of biological predator populations would, for the most part, be appropriate pest control strategies. However, it is obvious that the infection that spreads occurring inside the pest can also be transmitted between predators. On the other side, where the pest species is the only food supply for the predator, the effect of pests will diminish the predator and even then the predator species could die out. To preserve the predator population, there should be an additional source of food. A significant role plays an alternative food supply for predator species [170, 225]. Although to control the pest, the consequence of alternative food attracts more attention than the usual predator–prey dynamics in the framework of biological preservation. Alternative food sources should be provided to the natural enemies of the pest for both predator protection and reduction of pests.

In this work, we develop a four–dimensional dynamical system modeling consists of a crop, susceptible pest, infected pest, and natural enemy of the pest. We take an interest in knowing the pest's effect on crops and the impact of natural enemies of pests on pest populations. Further, alternative food is used as a simultaneous food source for predators (the natural enemy of the pest). Two mathematical models are presented in this study, one in the absence of control and the other in the presence

of control. A prey–predator system is established consisting of four species, namely, the crop (prey), the susceptible pest, the infected pest, and the natural enemies of the pest. We discuss the basic reproduction numbers at disease–free equilibrium points and sensitivity analysis in the presence of prey. The coexistence of equilibrium systems under various conditions is examined. We present numerical reports to address certain important biological cases that our model illustrates. Further, an optimal control problem is constructed and solved analytically. Here, two types of control variables are used; first, the rate of application of pesticide, and second, the rate of application of biomass organic fertilizer. The goals of these controls are to eliminate pest density and increase crop density as well as land fertility. This work is described as follows: In Section 4.2, the prey–predator model is developed in the presence of crop (prey), susceptible–infected pest, and natural enemies of pests. Section 4.3 describes the boundedness of the system, equilibria of the system, local stability, and sensitivity analysis of the basic reproduction number. The existence and global stability analysis of the endemic equilibrium are discussed in Section 4.4. Section 4.5 illustrate the dynamical behavior and biological interpretation of the model and its discussion through the numerical simulation. Formulation and application of optimal control problem, cost–effectiveness analysis, the existence of controls, characterization of the optimal control pair, and the optimality system are performed in Section 4.5. Section 4.7 demonstrates numerical simulations for validation of the theoretical results of the optimal control problem through different parameters. Finally, a brief discussion and future scope are shown in Section 4.8.

4.2   Mathematical Model

System dynamics modeling is a way of explaining and simulating dynamically complex problems through system behavior. Since the creation of the modeling process, the approach itself has been used for a wide variety of applications, along with the modeling of a complex ecosystem. Given its demonstrated ability to incorporate the complex interactions between influencing factors in an interconnected system, a system dynamics modeling technique is selected for this analysis. The method for designing system dynamic structures usually involves iterative progress that starts with a clear demonstration of the modeling goal. It continues with the integrative approaches

94

and their interactions via dynamic casting and outline hypotheses, accompanied by model simulation and explanation. A notable limitation in the modeling of system dynamics is the complexity, if not meaninglessness, of model validation, focused on how model outputs and actions accurately reflect the real world. All mathematical models, however complex, are subjective approximations of truth intended to describe the observable facts. It appears that the model's observations must be balanced by the unpredictability of the input information that it attempts to explain and the validity of the concepts used to construct its equations. A good example of this is the active discussion on the inability of current models to forecast or remove the factors for agricultural production details. The deficient focus has been reported between crop, pest, and natural enemies. This study would apply new behavioral equations to existing mathematical models. It will also include changing the existing models to connect them to new equations modeling in the agriculture sector. The true test of the improved model would be its ability to continuously incorporate one more equation that needs a preventive remedy. No mathematical model could be an ideal representation of reality. However, the process of developing, evaluating, and updating models forces scientists and researchers to strengthen their viewpoints about how a mathematical model operates. This enhances the scientific discussion of what influences mathematical model behavior and what should be done to handle model losses. A prey–predator model for prey, predator, and additional food in an ecosystem has been studied in [43, 205, 218, 219].

In this work, a variable P_1 representing crop density has been introduced to study the effect of crop production in agriculture. We build a mathematical model according to the following hypothesis:

(A_1) Let the population density of the crops biomass (roots, stem, leaf, flower, and so on.) be P_1 at the time t. $P_1(t)$ can only reproduce the logistic law of growth with an inherent growth rate r_1 and ecosystem carrying capacity K_1. In addition, it is supposed that there is a negative impact of λP_1, ρP_1 on crop biomass density due to susceptible pest and infected pest, where λ and ρ are predation rate coefficients with Holling type I functional response. Consequently, the rate of change of the biomass crop can be as follows

$$\frac{dP_1}{dt} = r_1 P_1 \left(1 - \frac{P_1}{K_1} \right) - \lambda P_1 P_2 - \rho P_1 P_3,$$

(A_2) At any given time t, the pest population is divided into two classes, namely the susceptible pest $P_2(t)$ and the infected pest $P_3(t)$. Thus, $P_2(t) + P_3(t)$ is the total pest population density.

(A_3) Between the two categories of pest, the susceptible pest population $P_2(t)$ can only grow with an intrinsic growth rate of r_2 and an environmental carrying capacity of K_2 according to logistic law of growth. Thus the rate of change of susceptible pest $P_2(t)$ can be presented as the differential equation below

$$\frac{dP_2}{dt} = r_2 P_2 \left(1 - \frac{P_2 + \eta P_3}{K_2} \right),$$

here, η is the effect of an individual predator on a pest per unit growth rate compared to an individual's influence on its own per unit growth rate [166]. Because of their direct interaction with the infected pest, disease spread within the susceptible crop, and let α be the infection power. The predators consume both susceptible and infected insects, but infected pests are often more easily obtainable to the predator as they are fragile and easy to capture, while it takes some time to predate the susceptible pests [217]. Thus, we suppose that the predator P_4 predates susceptible pests βP_2 at a rate of linear response where β is the maximum rate of capture and infected pests with Holling type–I functional response γP_3 where γ is the maximum rate of capture. Further, we suppose that the rate of death of the infected pest is ω. Accordingly, the rate of conversion for susceptible and infected pests can be isolated as follows

$$\frac{dP_2}{dt} = \gamma P_1 P_2 - \sigma P_2 + r_2 P_2 \left(1 - \frac{P_2 + \eta P_3}{K_2} \right) - \alpha P_2 P_3 - \beta P_2 P_4,$$

$$\frac{dP_3}{dt} = \alpha P_2 P_3 + \rho P_1 P_3 - \gamma P_3 P_4 - \omega P_3,$$

(A_4) [179, 201] studied the interplay of pests (susceptible and infected) with their predators and found that infectious illness among animal and plant communities may influence the system. [207] proposed an ecoepidemic model with infectious illness in pest and predator consuming diseased preys for meals. In this situation, infected pests are more accessible to predators since they are easier to trap than healthier pests. Infected pests are weaker and simpler to trap, according to [97, 164]. Furthermore, under the current framework, it is considered that the infected pest has less strength than the susceptible pests. As a result, the predator's capturing capacity is

greater for infected pest. The predator population P_3 can catch infected pests easily at a rate of n_1, whereas the capturing rate of susceptible populations P_2 is assumed to be l. According to [150], digestion of infected pests contributes to negative increase in the predator population. There is a negative effect parameters n_2 to the biomass of predator populations due to the infection from the infected pests. Furthermore, we suppose that $n_2\gamma P_3$ has a detrimental impact on the biomass of predator species due to contamination from infected pests. The predator's natural mortality rate is μ and it has density–dependent mortality rate δ. Additional food is provided to predator P_4. Some alternative food sources are always accessible in consistent quantities that are unaffected by consumption. Many arthropod predators can depend on plan–provided alternative food sources like pollen or nectar, which is relatively unaffected by the predator's usage [137]. For both the conservation of the predator and the elimination of the pest, an alternative supply of food is provided to the natural enemy of the pest [23]. [170] explored the use of alternative food as a supplement to the predator's diet. When the desired prey density falls low, predators consume additional food. The growth rate due to additional food is d [225]. The predator's capability to recognize additional food is characterised by the proportionality constant. Hence, the rate of change for the predator population is as described in the following

$$\frac{dP_4}{dt} = l\beta P_2 P_4 + (n_1 - n_2)\gamma P_3 P_4 + d(1 - \frac{P_2 + \eta P_3}{K_2})P_4 - \mu P_4 - \delta P_4^2.$$

Here, the growth of predator by providing the additional food is considered as a logistic growth at the rate d i.e. $\left(d(1 - \frac{P_2+\eta P_3}{K_2})P_4\right)$ while the growth of the predator by consuming infected and susceptible pest is considered bilinear growth, i.e. $(l\beta P_2 P_4 + (n_1 - n_2)\gamma P_3 P_4)$ at the same time, respectively. Thus, we develop four dimensions models consisting of the crop (prey), susceptible pest, infected pest, and natural enemies of the pest as predator. Moreover, this study examines the application of optimal control to the system in the presence of two control variables: first, the rate of application of pesticide, and second, the rate of application of biomass organic fertilizer. Integrating all the above hypotheses, we describe eco–epidemic structure in

the following ways:

$$
\begin{cases}
\frac{dP_1}{dt} = r_1 P_1 \left(1 - \frac{P_1}{K_1}\right) - \lambda P_1 P_2 - \rho P_1 P_3, \\
\frac{dP_2}{dt} = \lambda P_1 P_2 - \sigma P_2 + r_2 P_2 \left(1 - \frac{P_2 + \eta P_3}{K_2}\right) - \alpha P_2 P_3 - \beta P_2 P_4, \\
\frac{dP_3}{dt} = \alpha P_2 P_3 + \rho P_1 P_3 - \gamma P_3 P_4 - \omega P_3, \\
\frac{dP_4}{dt} = l\beta P_2 P_4 + (n_1 - n_2)\gamma P_3 P_4 + d\left(1 - \frac{P_2 + \eta P_3}{K_2}\right) P_4 - \mu P_4 - \delta (P_4)^2.
\end{cases}
\tag{4.2.1}
$$

with initial conditions $P_1(0) = P_{10} \geqslant 0$, $P_2(0) = P_{20} \geqslant 0$, $P_3(0) = P_{30} \geqslant 0$, and $P_4(0) = P_{40} \geqslant 0$.

Table 4.3: Description of the parameters

Parameters	Description
r_1	Net growth rate of crop
K_1	Carrying capacity of crop
ρ	Predation rate coefficients
λ	Predation rate of susceptible pest
σ	Natural mortality rate of susceptible pest
K_2	Environmental carrying capacity
r_2	Intrinsic growth rate of susceptible pest
η	Influence of individual predators on the pest growth rate per capita
α	Force of infection
β	Maximum capturing rate of susceptible pests
γ	Maximum capturing rate of infected pests
ω	Death rate of the infected pest
l	Predator species contributions from susceptible pests
n_1	Predator species contributions from infected pest.
n_2	Negative effect to the biomass of predator species from infected pests.
d	Growth rate due to the food
μ	Natural death rate of natural enemy of the pest
δ	Density dependent mortality rate

4.3 Dynamical Behavior of the System

4.3.1 Boundedness of the System

First, let us define a function, $X = P_1 + P_2 + P_3 + \frac{1}{l}P_4$. The time derivative of X is

$$\frac{dX}{dt} = \frac{dP_1}{dt} + \frac{dP_2}{dt} + \frac{dP_3}{dt} + \frac{1}{l}\frac{dP_4}{dt},$$

from the equation (4.2.1), we can obtain

$$\frac{dX}{dt} = r_1 P_1\left(1 - \frac{P_1}{K_1}\right) - \lambda P_1 P_2 - \rho P_1 P_3 + \lambda P_1 P_2 - \sigma P_2 + r_2 P_2\left(1 - \frac{P_2 + \eta P_3}{K_2}\right) - \alpha P_2 P_3 - \beta P_2 P_4$$

$$+ \alpha P_2 P_3 + \rho P_1 P_3 - \gamma P_3 P_4 - \omega P_3 + \beta P_2 P_4 + \frac{1}{l}(n_1 - n_2)\gamma P_3 P_4$$

$$+ \frac{d}{l}\left(1 - \frac{P_2 + \eta P_3}{K_2}\right)P_4 - \frac{\mu}{l}P_4 - \frac{\delta}{l}(P_4)^2,$$

$$= r_1 P_1\left(1 - \frac{P_1}{K_1}\right) - \sigma P_2 + r_2 P_2\left(1 - \frac{P_2 + \eta P_3}{K_2}\right) - \gamma P_3 P_4 - \omega P_3 + \frac{1}{l}(n_1 - n_2)\gamma P_3 P_4$$

$$+ \frac{d}{l}\left(1 - \frac{P_2 + \eta P_3}{K_2}\right)P_4 - \frac{\mu}{l}P_4 - \frac{\delta}{l}(P_4)^2.$$

Let $(n_1 - n_2) < l$, we have

$$\frac{dX}{dt} + \omega X \leqslant r_1 P_1\left(1 - \frac{P_1}{K_1}\right) + \omega P_1 + r_2 P_2\left(1 - \frac{P_2}{K_2}\right) + \omega P_2 + \frac{1}{l}P_4(d + \omega - \delta P_4),$$

$$= -\frac{r_1 P_1^2}{K_1} + (r_1 + \omega)P_1 - \frac{r_1 P_2^2}{K_1} + (r_1 + \omega)P_2 + \frac{(d + \omega)P_4}{l} - \frac{\delta}{l}P_4^2 \qquad (4.3.1)$$

Here, let $f(P_1) = -\frac{r_1 P_1^2}{K_1} + (r_1 + \omega)P_1 \Rightarrow f'(P_1) = r_1 + \omega - \frac{2r_1 P_1}{K_1}$, for max/min $f'(P_1) = 0$
$\Rightarrow r_1 + \omega - \frac{2r_1 P_1}{K_1} = 0 \Rightarrow P_1 = \frac{(r_1 + \omega)K_1}{2r_1}$, and $f''(P_1) = \frac{-2r_1}{K_1}$, which shows that $f''(P_1) < 0$.
Thus maximum value of $f(P_1) = (r_1 + \omega)\frac{(r_1 + \omega)K_1}{2r_1} - \frac{r_1}{K_1}\left(\frac{(r_1 + \omega)K_1}{2r_1}\right)^2 = \frac{K_1(r_1 + \omega)^2}{4r_1}$. Similarly,
$r_2 P_2\left(1 - \frac{P_2}{K_2}\right) + \omega P_2 \leqslant \frac{K_2(r_2 + \omega)^2}{4r_2}$. For the term $\frac{(d + \omega)P_4}{l} - \frac{\delta}{l}P_4^2$, let $f(P_4) = \frac{(d + \omega)P_4}{l} - \frac{\delta}{l}P_4^2 \Rightarrow$
$f'(P_4) = \frac{(d + \omega)}{l} - \frac{2\delta P_4}{l}$. For max/min $f'(P_4) = 0$, which implies $P_4 = \frac{d + \omega}{2\delta}$. And $f''(P_4) = \frac{-2\delta}{l}$.
Thus $f(P_4) = \frac{(d + \omega)P_4}{l} - \frac{\delta}{l}P_4^2 = \frac{(d + \omega)^2}{4l\delta}$ at $P_4 = \frac{d + \omega}{2\delta}$. Thus, $\frac{1}{l}P_4(d + \omega - \delta P_4) \leqslant \frac{(d + \omega)^2}{4l\delta}$. As
a result, the inequality (4.3.1) may be represented as

$$\frac{dX}{dt} + \omega X \leqslant \frac{K_1(r_1 + \omega)^2}{4r_1} + \frac{K_2(r_2 + \omega)^2}{4r_2} + \frac{(d + \omega)^2}{4l\delta}.$$

Thus, we have a constant $L = \frac{K_1(r_1+\omega)^2}{4r_1} + \frac{K_2(r_2+\omega)^2}{4r_2} + \frac{(d+\omega)^2}{4l\delta}$, such that

$$\Rightarrow \frac{dX}{dt} + \omega X \leqslant L,$$

applying the theorem of differential inequality [65], we obtain

$$0 < X(P_1, P_2, P_3, P_4) \leqslant \frac{L}{\omega}(1 - e^{-\omega t}) + X(P_1(0), P_2(0), P_3(0), P_4(0))e^{-\omega t}.$$

As $t \to \infty$, we have $0 < X \leqslant \frac{L}{\omega}$, since $\sup_{t \to \infty} X(t) = \frac{L}{\omega}$. Hence, all the solutions of (4.2.1) are confined in the region

$$S = \left\{ (P_1, P_2, P_3, P_4) \in R_4^+ : 0 < X < \frac{L}{\omega} + \varepsilon \right\},$$

for any $\varepsilon > 0$ and for $t \to \infty$. Thus, the system (4.2.1) is always uniformly bounded.

4.3.2 Equilibria of the System

The system has the following equilibrium points:

(1) The trivial equilibrium $E_0 (P_1^*, P_2^*, P_3^*, P_4^*) = (0, 0, 0, 0)$.

(2) The pest and natural enemy free equilibrium $E_1 (P_1^*, P_2^*, P_3^*, P_4^*)$, where

$$P_1^* = K_1, \ P_2^* = 0, \ P_3^* = 0, \ P_4^* = 0,$$

this equilibrium is feasible.

(3) The crop, infected pest, and natural enemy free equilibrium point $E_2 (P_1^*, P_2^*, P_3^*, P_4^*)$, where

$$P_1^* = 0, \ P_2^* = \frac{-\sigma K_2 + K_2 r_2}{r_2}, \ P_3^* = 0, \ P_4^* = 0,$$

which is biologically feasible if $r_2 > \sigma$.

(4) The crop and pest free equilibrium $E_3 (P_1^*, P_2^*, P_3^*, P_4^*)$, where

$$P_1^* = 0, \ P_2^* = 0, \ P_3^* = 0, \ P_4^* = \frac{d - \mu}{\delta},$$

which is acceptable biologically if $d > \mu$.

(5) The infected pest and natural enemy free equilibrium point $E_4 (P_1^*, P_2^*, P_3^*, P_4^*)$,

where,

$$P_1^* = \frac{\sigma\lambda K_1 K_2 - \lambda K_1 K_2 r_2 + K_1 r_1 r_2}{\lambda^2 K_1 K_2 + r_1 r_2}, \; P_2^* = \frac{r_1(-\sigma K_2 + \lambda K_1 K_2 + K_2 r_2)}{\lambda^2 K_1 K_2 + r_1 r_2}, \; P_3^* = 0, \; P_4^* = 0,$$

which is biologically feasible if $(\sigma\lambda K_2 + r_1 r_2) > (\lambda K_2 r_2)$ and $(\lambda K_1 + r_2) > \sigma$.

(6) The crop and natural enemy of pest free equilibrium point E_5 $(P_1^*, P_2^*, P_3^*, P_4^*)$, where

$$P_1^* = 0, \; P_2^* = \frac{\omega}{\alpha}, \; P_3^* = -\frac{\sigma\alpha K_2 + \omega r_2 - \alpha K_2 r_2}{\alpha(\alpha K_2 + \eta r_2)}, \; P_4^* = 0,$$

which is biologically feasible if $\sigma\alpha K_2 + \omega r_2 < \alpha K_2 r_2$.

(7) The crop and susceptible pest free equilibrium point E_6 $(P_1^*, P_2^*, P_3^*, P_4^*)$, where

$$P_1^* = 0, \; P_2^* = 0, \; P_3^* = -\frac{d\gamma K_2 - \gamma\mu K_2 + \delta\omega K_2}{\gamma(-d\eta + \gamma K_2 n_1 - \gamma K_2 n_2)}, \; P_4^* = -\frac{\omega}{\gamma},$$

that is not acceptable biologically as P_4^* is always negative due to ω and γ are always positive.

(8) The pest free equilibrium E_7 $(P_1^*, P_2^*, P_3^*, P_4^*)$, where

$$P_1^* = K_1, \; P_2^* = 0, \; P_3^* = 0, \; P_4^* = \frac{d - \mu}{\delta},$$

this equilibrium is feasible if $d > \mu$.

(9) The susceptible pest and natural enemy of pest free equilibrium point E_8 $(P_1^*, P_2^*, P_3^*, P_4^*)$, where

$$P_1^* = \frac{\omega}{\rho}, \; P_2^* = 0, \; P_3^* = \frac{(-\omega + \rho K_1) r_1}{\rho^2 K_1}, \; P_4^* = 0,$$

which is biologically feasible if $\rho K_1 > \omega$.

(10) The crop and infected pest free equilibrium point E_9 $(P_1^*, P_2^*, P_3^*, P_4^*)$, where

$$P_1^* = 0, \; P_2^* = \frac{K_2(\sigma\beta + d\delta - \beta\mu - \delta r_2)}{d\beta - l\beta^2 K_2 - \delta r_2}, \; P_3^* = 0, \; P_4^* = \frac{\sigma l\beta K_2 + \mu r_2 - l\beta K_2 r_2 - d\sigma}{d\beta - l\beta^2 K_2 - \delta r_2},$$

which is biologically feasible if the following conditions are satisfy (i) $d\beta + \sigma\delta > \beta\mu + \delta r$ and $d\beta > l\beta^2 K_2 + \delta r_2$ or $d\beta + \sigma\delta < \beta\mu + \delta r$ and $d\beta < l\beta^2 K_2 + \delta r_2$, (ii) $\sigma l\beta K_2 + \mu r_2 > l\beta K_2 r_2 + d\sigma$ and $d\beta > l\beta^2 K_2 + \delta r_2$ or $\sigma l\beta K_2 + \mu r_2 < l\beta K_2 r_2 + d\sigma$ and $d\beta < l\beta^2 K_2 + \delta r_2$.

(11) The crop free equilibrium point $E_{10}(P_1^*, P_2^*, P_3^*, P_4^*)$, where

$$P_1^* = \frac{m_3 - m_4}{m_1 - m_2}, \ P_2^* = \frac{m_5 - m_6}{m_1 - m_2}, \ P_3^* = \frac{m_7 - m_8}{m_1 - m_2}, \ P_4^* = 0,$$

where $m_1 = \eta \lambda \rho K_1 r_2$, $m_2 = \rho^2 K_1 r_2 + \alpha \eta r_1 r_2 + \alpha^2 K_2 r_1$, $m_3 = \sigma \alpha \rho K_1 K_2 + \alpha^2 K_1 K_2 r_1 + \alpha \eta K_1 r_1 r_2 + \rho \omega K_1 r_2$, $m_4 = \eta \lambda \omega K_1 r_2 + \alpha \rho K_1 K_2 r_2 + \alpha \lambda \omega K_1 K_2$, $m_5 = \lambda \rho \omega K_1 K_2 + \alpha \omega K_2 r_1 + \rho^2 K_1 K_2 r_2 + \eta \omega r_1 r_2$, $m_6 = \alpha \rho K_1 K_2 r_1 + \eta \rho K_1 r_1 r_2 + \sigma \rho^2 K_1 K_2$, $m_7 = \sigma \lambda \rho K_1 K_2 + \rho K_1 r_1 r_2 + \alpha K_2 r_1 r_2 + \alpha \lambda K_1 K_2 r_1$, $m_8 = \lambda^2 \omega K_1 K_2 + d \alpha K_2 r_1 + \lambda \rho K_1 K_2 r_2 + \omega r_1 r_2$, which is biologically feasible if the following conditions are satisfy (i) $m_3 > m_4$ and $m_1 > m_2$ or $m_3 < m_4$ and $m_1 < m_2$, (ii) $m_5 > m_6$ and $m_1 > m_2$ or $m_5 < m_6$ and $m_1 < m_2$, (iii) $m_7 > m_8$ and $m_1 > m_2$ or $m_7 < m_8$ and $m_1 < m_2$.

(12) $E_{11} (P_1^*, P_2^*, P_3^*, P_4^*)$, where

$$P_1^* = K_1 + \frac{f_1 - f_2}{r_1 (f_3 - d\beta r_1)}, \ P_2^* = \frac{f_4 - f_5}{f_3 - d\beta r_1}, \ P_3^* = 0, \ P_4^* = \frac{f_6 - f_7}{f_3 - d\beta r_1},$$

where

$f_1 = \lambda K_1 K_2 d\beta r_1 + \lambda K_1 K_2 \sigma \delta r_1$, $f_2 = \lambda K_1 K_2 \beta \mu r_1 + \lambda K_1 K_2 \delta \lambda K_1 r_1 + \lambda K_1 K_2 \delta r_1 r_2$, $f_3 = \delta \lambda^2 K_1 K_2 + l\beta^2 K_2 r_1 + \delta r_1 r_2$, $f_4 = K_2 \beta \mu r_1 + K_2 \delta \lambda K_1 r_1 + K_2 \delta r_1 r_2$, $f_5 = K_2 d\beta r_1 + K_2 \sigma \delta r_1$, $f_6 = d\lambda^2 K_1 K_2 + d\sigma r_1 + l\beta \lambda K_1 K_2 r_1 + l\beta K_2 r_1 r_2$, $f_7 = \lambda^2 \mu K_1 K_2 + d\lambda K_1 r_1 + \sigma l\beta K_2 r_1 + \mu r_1 r_2$, which is biologically feasible if the following conditions are satisfy (i) $f_1 > f_2$ and $f_3 > d\beta r_1$, or $f_1 < f_2$ and $f_3 < d\beta r_1$, (ii) $f_4 > f_5$ and $f_3 > d\beta r_1$, or $f_4 < f_5$ and $f_3 < d\beta r_1$, (iii) $f_6 > f_7$ and $f_3 > d\beta r_1$, or $f_6 < f_7$ and $f_3 < d\beta r_1$.

(13) The susceptible pest and natural enemy of pest free equilibrium point $E_{12} (P_1^*, P_2^*, P_3^*, P_4^*)$, where

$$P_1^* = K_1 + \frac{\rho K_1 (h_1 - h_2)}{r_1 (h_3 - h_4)}, \ P_2^* = 0, \ P_3^* = \frac{h_2 - h_1}{h_3 - h_4}, \ P_4^* = \frac{-\omega + \rho K_1}{\gamma} + \frac{\rho^2 K_1 (h_1 - h_2)}{\gamma r_1 (h_3 - h_4)},$$

where

$h_1 = \gamma \mu K_2 r_1 + \delta \rho K_1 K_2 r_1$, $h_2 = \delta \omega K_2 r_1 + d\gamma K_2 r_1$, $h_3 = d\gamma \eta r_1 + \gamma^2 K_2 n_2 r_1$, $h_4 = \gamma^2 K_2 n_1 r_1 + \delta \rho^2 K_1 K_2$, which is biologically feasible if the following conditions are satisfy (i)P_1^* will be biologically if $r_1 h_3 + \rho h_1 > r h_4 + \rho h_2$ and $h_3 > h_4$, (ii)P_3^* will be biologically if $h_2 > h_1$ and $h_3 > h_4$ or $h_2 < h_1$ and $h_3 < h_4$, (iii)P_4^* will be biologically if $\omega < \rho K_1$, $h_1 > h_2$ and $h_3 > h_4$ or $\omega < \rho K_1$, $h_1 < h_2$ and $h_3 < h_4$.

(14) The crop free equilibrium point $E_{13} (P_1^*, P_2^*, P_3^*, P_4^*)$, where

$$P_1^* = 0, \ P_2^* = \frac{g_1 - g_2}{g_3 - g_4}, \ P_3^* = \frac{g_5 - g_6}{g_7 - g_8}, \ P_4^* = \frac{g_9 - g_{10}}{g_{11} - g_{12}},$$

where

$g_1 = d\sigma\gamma\eta + d\alpha\gamma K_2 + \alpha\delta\omega K_2 + \beta\gamma\omega K_2 n_1 + \sigma\gamma^2 K_2 n_2 + \delta\eta\omega r_2 + \gamma^2 K_2 n_1 r_2, \ g_2 = d\beta\eta\omega + \alpha\gamma\mu K_2 + \sigma\gamma^2 K_2 n_1 + \beta\gamma\omega K_2 n_2 + \gamma\eta\mu r_2 + \gamma^2 K_2 n_2 r_2, g_3 = d\alpha\gamma + \alpha^2\delta K_2 + \alpha\beta\gamma K_2 n_1 + \alpha\delta\eta r_2 + \gamma^2 n_1 r_2, \ g_4 = d\alpha\beta\eta + l\alpha\beta\gamma K_2 + \alpha\beta\gamma K_2 n_2 + l\beta\gamma\eta r_2 + \gamma^2 n_2 r_2, \ g_5 = d\beta\omega + \alpha\delta K_2 r_2 + \sigma l\beta\gamma K_2 + \alpha\beta\mu K_2 + \gamma\mu r_2, \ g_6 = d\alpha\beta K_2 + \sigma\alpha\delta K_2 + l\beta^2\omega K_2 + \delta\omega r_2 + d\sigma\gamma + l\beta\gamma K_2 r_2, \ g_7 = d\alpha\gamma + \alpha^2\delta K_2 + \alpha\beta\gamma K_2 n_1 + \alpha\delta\eta r_2 + \gamma^2 n_1 r_2, g_8 = d\alpha\beta\eta + l\alpha\beta\gamma K_2 + \alpha\beta\gamma K_2 n_2 + l\beta\gamma\eta r_2 + \gamma^2 n_2 r_2,$

$g_9 = d\sigma\alpha\eta + d\alpha^2 K_2 + l\alpha\beta\omega K_2 + \sigma\alpha\gamma K_2 n_2 + l\beta\eta\omega r_2 + \alpha\gamma K_2 n_1 r_2 + \gamma\omega n_2 r_2, \ g_{10} = d\alpha\omega + \alpha^2\mu K_2 + \sigma\alpha\gamma K_2 n_1 + \alpha\eta\mu r_2 + \gamma\omega n_1 r_2 + \alpha\gamma K_2 n_2 r_2, g_{11} = d\alpha\gamma + \alpha^2\delta K_2 + \alpha\beta\gamma K_2 n_1 + \alpha\delta\eta r_2 + \gamma^2 n_1 r_2, \ g_{12} = d\alpha\beta\eta + l\alpha\beta\gamma K_2 + \alpha\beta\gamma K_2 n_2 + l\beta\gamma\eta r_2 + \gamma^2 n_2 r_2,$

which is biologically feasible if the following conditions are satisfy (i) $g_1 > g_2$ and $g_3 > g_4$, or $g_1 < g_2$ and $g_3 < g_4$, (ii) $g_5 > g_6$ and $g_7 > g_8$ or $g_5 < g_6$ and $g_7 < g_8$, (iii) $g_9 > g_{10}$ and $g_{11} > g_{12}$ or $g_9 < g_{10}$ and $g_{11} < g_{12}$.

(15) The crop, pest and natural enemy of pest coexistence equilibrium point E_{14} $(P_1^*, \ P_2^*, \ P_3^*, \ P_4^*)$. Where, the interior equilibrium whose feasibility criterion is given in Section 4.4.

4.3.3 Basic Reproduction Number

We introduce the basic reproduction number during the entire period. This is characterised as the number of secondary infected individuals caused by a single infected individual. The approach developed by [110, 158] can be used to obtain the expression for the basic reproduction number. The basic reproduction number is determined using the next–generation matrix procedure [156, 158, 159, 167]. Let G be the next generation matrix, which includes $f_i(t)$, $v_i^+(t)$, and $v_i^-(t)$, $i = 1, 2, 3, ...,n \in N$; where $f_i(t)$ is the rate of presence of new infections in the compartment i, $v_i^+(t)$ is the rate of immigration of individuals into the compartment i, and $v_i^-(t)$ is the rate at which new individuals are transferred from compartment i.

Theorem 4.3.1. The basic reproduction numbers for infected pest at disease–free equilibrium

point E_4, E_5, E_6, and E_{11} in the presence of prey (crop) are

$$R_{01} = \frac{\delta K_1 \rho}{-\gamma\mu + \gamma d + \delta\omega}, \quad R_{02} = \frac{K_1 \rho}{\omega},$$

$$R_{03} = \frac{K_1 \left(\lambda K_2 \left(d\rho + \alpha r_1 - \rho r_2\right) + \rho r_1 r_2\right) + \alpha K_2 r_1 \left(r_2 - d\right)}{\omega \left(\lambda^2 K_1 K_2 + r_1 r_2\right)}, \quad \text{and}$$

$$R_{04} = \frac{\alpha K_2 r_1 \left(\beta\mu - d(\beta + \delta) + \delta r_2\right) + K_1 Q_1}{\lambda K_1 Q_2 + Q_3 r_1},$$

respectively. Where $Q_1 = K_2 \left(\lambda\rho\left(-\beta\mu + d(\beta + \delta) - \delta r_2\right) + r_1 \left(\alpha\delta\lambda + \beta^2 l\rho\right)\right) + \rho r_1 \left(\delta r_2 - \beta d\right)$,
$Q_2 = K_2 \left(\lambda(-\gamma\mu + \gamma d + \delta\omega) + \beta\gamma l r_1\right) - \gamma d r_1$, and
$Q_3 = d(\gamma d - \beta\omega) + \beta K_2 l \left(\beta\omega + \gamma(-d) + \gamma r_2\right) + r_2(\delta\omega - \gamma\mu)$.

Proof. It is clearly, P_3 is the only relevant class of infection. The class $P_3(t)$ from our model (4.2.1) can be expressed as follows:

$$\frac{dP_3}{dt} = \alpha P_2 P_3 + \rho P_1 P_3 - \gamma P_3 P_4 - \omega P_3,$$

In this process, the matrices $f(t)$ and $v(t) = v^-(t) - v^+(t)$, corresponding to the gain and loss components of equation (4.2.1) can be defined as $f(t) = \alpha P_2 P_3 + \rho P_1 P_3$, $v(t) = \gamma P_3 P_4 + \omega P_3$. The Jacobian matrices of $f(t)$ and $v(t)$ are, at disease–free equilibrium point with prey, E_4, respectively, given by

$$F_1 = \rho K_1, \quad V_1 = \omega - \frac{\gamma(\mu - d)}{\delta}.$$

Now the next generation matrix is defined as $G_1 = F_1 V_1^{-1}$ and the basic reproduction number R_{01} of the system is defined by the spectral radius of the matrix $F_1 V_1^{-1}$. Thus,

$$R_{01} = \frac{\delta K_1 \rho}{-\gamma\mu + \gamma d + \delta\omega}.$$

Similarly, the Jacobian matrices of $f(t)$ and $v(t)$ are, at disease–free equilibrium point, E_5, respectively, given by

$$F_2 = \rho K_1, \quad V_2 = \omega.$$

Now the next generation matrix is defined as $G_2 = F_2 V_2^{-1}$ and the basic reproduction number R_{02} of the system is defined by the spectral radius of the matrix $F_2 V_2^{-1}$. Thus,

$$R_{02} = \frac{K_1 \rho}{\omega}.$$

Similarly, the Jacobian matrices of $f(t)$ and $v(t)$ are, at disease–free equilibrium point, E_6, respectively, given by

$$F_3 = \frac{\alpha r_1 \left(-dK_2 + \lambda K_1 K_2 + K_2 r_2 \right)}{\lambda^2 K_1 K_2 + r_1 r_2} - \frac{\rho \left(-d\lambda K_1 K_2 + \lambda K_1 K_2 r_2 - K_1 r_1 r_2 \right)}{\lambda^2 K_1 K_2 + r_1 r_2}, \quad V_3 = \omega.$$

Now the next generation matrix is defined as $G_3 = F_3 V_3^{-1}$ and the basic reproduction number R_{03} of the system is defined by the spectral radius of the matrix $F_3 V_3^{-1}$. Thus,

$$R_{03} = \frac{K_1 \left(\lambda K_2 \left(d\rho + \alpha r_1 - \rho r_2 \right) + \rho r_1 r_2 \right) + \alpha K_2 r_1 \left(r_2 - d \right)}{\omega \left(\lambda^2 K_1 K_2 + r_1 r_2 \right)}.$$

Similarly, the Jacobian matrices of $f(t)$ and $v(t)$ are, at disease–free equilibrium point, E_{11}, respectively, given by

$$F_4 = \rho \left(K_1 - \frac{\lambda K_1 K_2 \left(\beta(-d)r_1 - d\delta r_1 + \delta \lambda K_1 r_1 + \beta \mu r_1 + \delta r_2 r_1 \right)}{r_1 \left(-\beta dr_1 + \delta \lambda^2 K_1 K_2 + \beta^2 K_2 l r_1 + \delta r_1 r_2 \right)} \right)$$
$$- \frac{\alpha K_2 \left(\beta dr_1 + d\delta r_1 - \delta \lambda K_1 r_1 - \beta \mu r_1 - \delta r_2 r_1 \right)}{-\beta dr_1 + \delta \lambda^2 K_1 K_2 + \beta^2 K_2 l r_1 + \delta r_1 r_2},$$

$$V_4 = \omega - \frac{\gamma \left(d^2 \left(-r_1 \right) - d\lambda^2 K_1 K_2 + \beta dK_2 l r_1 + d\lambda K_1 r_1 + \lambda^2 K_1 K_2 \mu - \beta \lambda K_1 K_2 l r_1 - \beta K_2 l r_1 r_2 + \mu r_1 r_2 \right)}{-\beta dr_1 + \delta \lambda^2 K_1 K_2 + \beta^2 K_2 l r_1 + \delta r_1 r_2}.$$

Now the next generation matrix is defined as $G_4 = F_4 V_4^{-1}$ and the basic reproduction number R_{04} of the system is defined by the spectral radius of the matrix $F_4 V_4^{-1}$. Thus,

$$R_{04} = \frac{\alpha K_2 r_1 \left(\beta \mu - d(\beta + \delta) + \delta r_2 \right) + K_1 Q_1}{\lambda K_1 Q_2 + Q_3 r_1},$$

where, $Q_1 = K_2 \left(\lambda \rho \left(-\beta \mu + d(\beta + \delta) - \delta r_2 \right) + r_1 \left(\alpha \delta \lambda + \beta^2 l\rho \right) \right) + \rho r_1 \left(\delta r_2 - \beta d \right)$,
$Q_2 = K_2 \left(\lambda \left(-\gamma \mu + \gamma d + \delta \omega \right) + \beta \gamma l r_1 \right) - \gamma dr_1$, and
$Q_3 = d(\gamma d - \beta \omega) + \beta K_2 l \left(\beta \omega + \gamma(-d) + \gamma r_2 \right) + r_2(\delta \omega - \gamma \mu)$. $\qquad\square$

With respect to disease–free equilibrium in the presence of prey, if $R_{01} > 1$, $R_{02} > 1$, $R_{03} > 1$, and $R_{04} > 1$, then the disease is endemic and infected individual generates more than one new infection on average, the infection has the potential to expand across a population in the species. If $R_{01} = 1$, $R_{02} = 1$, $R_{03} = 1$, and $R_{04} = 1$, then the disease is stable, and if $R_{01} < 1$, $R_{02} < 1$, $R_{03} < 1$, and $R_{04} < 1$, then the infection may die out in the long run. When there is no infection at the disease-free equilibrium state. As a result, all infected categories will be zero.

4.3.4 Local Stability

We draw conclusions in the following theorem concerning the asymptotic behavior of trajectories system (4.2.1).

Theorem 4.3.2. At different equilibria, the system (4.2.1) has the following behavior

(1) The trivial equilibrium E_0 is unstable since one of the eigenvalues is always positive $r_1 > 0$.

(2) The pest and natural pest of pest free equilibrium point E_1 is locally asymptotically stable if $\mu > d$, $\omega > \rho K_1$, $-r_1$, and $d > \lambda K_1 + r_2$.

(3) The crop, infected pest and natural enemy free equilibrium point E_2 is locally asymptotically stable if $\omega > \alpha P_2^*$, $\mu K_2 + \sigma P_2^* > l \beta K_2 P_2^* + \sigma K_2$, and $\lambda P_2^* > r_1$.

(4) The crop and pest free equilibrium E_3 is unstable since one of the eigenvalues $r_1 > 0$ is always positive.

(5) The infected pest and natural enemy free equilibrium point E_4 is locally asymptotically stable if $d_5 > 0$, $d_6 > 0$, $d_7 > 0$, $d_8 > 0$, $d_5 d_6 - d_7 > 0$, and $(d_5 d_6 - d_7)d_7 - d_5^2 d_8 > 0$.

(6) The crop and natural enemy of pest free equilibrium point E_5 is locally asymptotically stable if $s_1 > 0$, $s_2 > 0$, $s_3 > 0$, $s_4 > 0$, $s_4 s_3 - s_2 > 0$, and $(s_4 s_3 - s_2)s_2 - s_4^2 s_1 > 0$.

(7) The crop and susceptible pest free equilibrium point E_6 is not biologically feasible. Since the population size P_4 is always a non–negative variable, the local stability study has not been performed.

(8) The pest free equilibrium point E_7 is locally asymptotically stable if $\omega + \gamma P_4^* > \rho K_1$, $\mu + 2\delta P_4^* > d$, and $d + \beta P_4^* > r_2 + \lambda K_1$.

(9) The susceptible pest and natural enemy of pest free equilibrium point E_8 is locally asymptotically stable if $d_9 > 0$, $d_{10} > 0$, $d_{11} > 0$, $d_{12} > 0$, $d_9 d_{10} - d_{11} > 0$, and $(d_9 d_{10} - d_{11})d_{11} - d_9^2 d_{12} > 0$.

(10) The crop and infected pest free equilibrium point E_9 is locally asymptotically stable if the equilibrium point E_9 is locally asymptotically stable if $\omega + \gamma P_4^* > \alpha P_2^*$, $\lambda P_2^* > r_1$, and $d_{13} > \sqrt{d_{14} - d_{15}}$.

(11) The natural enemy of pest equilibrium point E_{10}, is locally asymptotically stable if $d_{42} > 0$, $d_{43} > 0$, $d_{44} > 0$, $d_{41} > 0$, $d_{42} d_{43} - d_{44} > 0$, and $(d_{42} d_{43} - d_{44})d_{44} - d_{42}^2 d_{41} > 0$.

(12) The infected pest free equilibrium point E_{11} is locally asymptotically stable if $d_{36} > 0$, $d_{37} > 0$, $d_{38} > 0$, $d_{35} > 0$, $d_{36} d_{37} - d_{38} > 0$, and $(d_{36} d_{37} - d_{38})d_{38} - d_{36}^2 d_{35} > 0$.

(13) The susceptible pest free equilibrium point E_{12} is locally asymptotically stable if $d_{21} > 0$, $d_{20} > 0$, $d_{19} > 0$, $d_{22} > 0$, $d_{21} d_{20} - d_{19} > 0$, and $(d_{21} d_{20} - d_{19})d_{19} - d_{21}^2 d_{22} > 0$.

(14)The crop free equilibrium point E_{13} is locally asymptotically stable if $d_{32} > 0$, $d_{33} > 0$, $d_{31} > 0$, $d_{34} > 0$, $d_{32}d_{33} - d_{34} > 0$, and $(d_{32}d_{33} - d_{34})d_{34} - d_{32}^2 d_{31} > 0$.

(15) The crop, pest and natural enemy of pest coexistence equilibrium E_{14}, is locally asymptotically stable if $a_1 > 0$, $a_2 > 0$, $a_3 > 0$, $a_4 > 0$, $a_1 a_2 - a_3 > 0$, and $(a_1 a_2 - a_3)a_3 - a_1^2 a_4 > 0$. The proof of theorem provides details of the parameters used in this theorem.

Proof. The stability analysis of the system (4.2.1) is governed by the Jacobian matrix

$$J = \begin{pmatrix} R & -\lambda P_1 & -\rho P_1 & 0 \\ \lambda P_2 & Q & -\alpha P_2 - \frac{\eta P_2 r_2}{K_2} & -\beta P_2 \\ \rho P_3 & \alpha P_3 & -\omega + \rho P_1 + \alpha P_2 - \gamma P_4 & -\gamma P_3 \\ 0 & l\beta P_4 - \frac{dP_4}{K_2} & -\frac{d\eta P_4}{K_2} + \gamma(n_1 - n_2)P_4 & P \end{pmatrix},$$

where,

$$R = -\lambda P_2 - \rho P_3 - \frac{P_1 r_1}{K_1} + \left(1 - \frac{P_1}{K_1}\right) r_1,$$

$$P = -\mu + l\beta P_2 + \gamma(n_1 - n_2)P_3 + d\left(1 - \frac{P_2 + \eta P_3}{K_2}\right) - 2\delta P_4,$$

$$Q = -\sigma + \lambda P_1 - \alpha P_3 - \beta P_4 - \frac{P_2 r_2}{K_2} + \left(1 - \frac{P_2 + \eta P_3}{K_2}\right) r_2.$$

(1) The Jacobian matrix of system (4.2.1) at equilibrium point $E_0 = (0, 0, 0, 0)$ is

$$J(E_0) = \begin{pmatrix} r_1 & 0 & 0 & 0 \\ 0 & -\sigma + r_2 & 0 & 0 \\ 0 & 0 & -\omega & 0 \\ 0 & 0 & 0 & d - \mu \end{pmatrix},$$

the eigenvalues of $J(E_0)$ are $\lambda_1 = d - \mu$, $\lambda_2 = -\omega$, $\lambda_3 = r_1$ and $\lambda = -\sigma + r_2$. Hence, the trivial steady state E_0 is unstable since one of the eigenvalues is always positive $r_1 > 0$. The $P_1 - P_2 - P_4$ plane space acts like a stable space if $d < \mu$, and $r_2 < \sigma$ while the P_3 axis behaves as a unstable. Ecologically, the equilibrium point E_0 is not stable due to growth rate of prey (crop) $r_1 > 0$.

(2) The Jacobian matrix of system (4.2.1) at equilibrium point $E_1 = (K_1, 0, 0, 0)$ is

$$J(E_1) = \begin{pmatrix} -r_1 & -\lambda K_1 & -\rho K_1 & 0 \\ 0 & -d + \lambda K_1 + r_2 & 0 & 0 \\ 0 & 0 & -\omega + \rho K_1 & 0 \\ 0 & 0 & 0 & d - \mu \end{pmatrix},$$

the eigenvalues of $J(E_1)$ are $d - \mu, -\omega + \rho K_1, -r_1, -d + \lambda K_1 + r_2$. The equilibrium point E_1 is locally asymptotically stable if

$$\mu > d, \ \omega > \rho K_1, \ -r_1, \text{ and } d > \lambda K_1 + r_2. \tag{4.3.2}$$

(3) The Jacobian matrix of system (4.2.1) at equilibrium point $E_2 = (0, P_2^*, 0, 0)$ is

$$J(E_2) = \begin{pmatrix} -\lambda P_2^* + r_1 & 0 & 0 & 0 \\ \lambda P_2^* & -\frac{P_2^* r_2}{K_2} & -\alpha P_2^* - \frac{\eta P_2^* r_2}{K_2} & -\beta P_2^* \\ 0 & 0 & -\omega + \alpha P_2^* & 0 \\ 0 & 0 & 0 & -\mu + l\beta P_2^* + \sigma \left(1 - \frac{P_2^*}{K_2}\right) \end{pmatrix}$$

the eigenvalues of $J(E_2)$ are $-\omega + \alpha P_2^*$, $\frac{dK_2 - \mu K_2 - \sigma P_2^* + l\beta K_2 P_2^*}{K_2}, -\lambda P_2^* + r_1, -\frac{P_2^* r_2}{K_2}$. The equilibrium point E_2 is locally asymptotically stable if

$$\omega > \alpha P_2^*, \ \mu K_2 + \sigma P_2^* > l\beta K_2 P_2^* + \sigma K_2, \text{ and } \lambda P_2^* > r_1. \tag{4.3.3}$$

(4) The Jacobian matrix of system (4.2.1) at equilibrium point $E_3 = (0, 0, 0, P_4^*)$ is

$$J(E_3) = \begin{pmatrix} r_1 & 0 & 0 & 0 \\ 0 & -d - \beta P_4^* + r_2 & 0 & 0 \\ 0 & 0 & -\omega - \gamma P_4^* & 0 \\ 0 & l\beta P_4^* - \frac{dP_4^*}{K_2} & -\frac{d\eta P_4^*}{K_2} + \gamma(n_1 - n_2)P_4^* & d - \mu - 2\delta P_4^* \end{pmatrix},$$

the eigenvalues of $J(E_3)$ are $-\omega - \gamma P_4^*$, $d - \mu - 2\delta P_4^*$, r_1, $-d - \beta P_4^* + r_2$. Hence, steady state (E_3) is unstable since one of the eigenvalues is always positive $r_1 > 0$.

(5) The Jacobian matrix of system (4.2.1) at equilibrium point $E_4 = (P_1^*,\ P_2^*,\ 0,\ 0)$ is

$$J(E_4) = \begin{pmatrix} -\frac{P_1^* r_1}{K_1} & -\lambda P_1^* & -\rho P_1^* & 0 \\ \lambda P_2^* & -\frac{P_2^* r_2}{K_2} & f_3 & -\beta P_2^* \\ 0 & 0 & f_2 & 0 \\ 0 & 0 & 0 & f_1 \end{pmatrix},$$

where $f_1 = -\mu + l\beta P_2^* + \sigma\left(1 - \frac{P_2^*}{K_2}\right)$, $f_2 = -\omega + \rho P_1^* + \alpha P_2^*$, $f_3 = -\alpha P_2^* - \frac{\eta P_2^* r_2}{K_2}$,

Then the characteristic equation of the $J(E_4)$ is given by $x^4 + d_5 x^3 + d_6 x^2 + d_7 x + d_8 = 0$, where

$d_5 = \left(-f_1 - f_2 + \frac{P_1 r_1}{K_1} + \frac{P_2 r_2}{K_2}\right)$, $d_6 = \left(f_1 f_2 + \lambda^2 P_1^* P_2 - \frac{f_1 P_1^* r_1}{K_1} - \frac{f_2 P_1^* r_1}{K_1} - \frac{f_1 P_2^* r_2}{K_2} - \frac{f_2 P_2^* r_2}{K_2} + \frac{P_1^* P_2^* r_1 r_2}{K_1 K_2}\right)$

$d_7 = \left(-\lambda^2 f_1 P_1^* P_2^* - \lambda^2 f_2 P_1^* P_2^* + \frac{f_1 f_2 P_1^* r_1}{K_1} + \frac{f_1 f_2 P_2^* r_2}{K_2} - \frac{f_1 P_1^* P_2^* r_1 r_2}{K_1 K_2} - \frac{f_2 P_1^* P_2^* r_1 r_2}{K_1 K_2}\right)$,

and $d_8 = \lambda^2 f_1 f_2 P_1^* P_2^* + \frac{f_1 f_2 P_1^* P_2^* r_1 r_2}{K_1 K_2}$. Using the Routh-Hurwitz conditions [95, 126, 136], the equilibrium point, $E_4 = (P_1^*,\ P_2^*,\ 0,\ 0)$, is locally asymptotically stable if

$$d_5 > 0,\ d_7 > 0,\ d_8 > 0,\ \text{and}\ (d_5 d_6 - d_7)d_7 - d_5^2 d_8 > 0. \tag{4.3.4}$$

(6) The Jacobian matrix of system (4.2.1) at equilibrium point $E_5 = (0,\ P_2^*,\ P_3^*,\ 0)$ is

$$J(E_5) = \begin{pmatrix} d_1 & 0 & 0 & 0 \\ \lambda P_2^* & -\frac{P_2 r_2}{K_2} & d_2 & -\beta P_2^* \\ \rho P_3^* & \alpha P_3^* & 0 & -\gamma P_3^* \\ 0 & 0 & 0 & d_3 \end{pmatrix},$$

where

$d_1 = -\lambda P_2^* - \rho P_3^* + r_1$, $d_2 = -\alpha P_2^* - \frac{\eta P_2^* r_2}{K_2}$, $d_3 = -\mu + l\beta P_2^* + \gamma(n_1 - n_2)P_3^* + d\left(1 - \frac{P_2^* + \eta P_3^*}{K_2}\right)$.

Then the characteristic equation of the $J(E_5)$ is given by $x^4 + s_4 x^3 + s_3 x^2 + s_2 x + s_1 = 0$, where

$s_1 = -\alpha d_1 d_2 d_3 P_3$, $s_2 = \left(\alpha d_1 d_2 P_3 + \alpha d_2 d_3 P_3^* + \frac{d_1 d_3 P_2^* r_2}{K_2}\right)$,

$s_3 = \left(d_1 d_3 - \alpha d_2 P_3^* - \frac{d_1 P_2^* r_2}{K_2} - \frac{d_3 P_2^* r_2}{K_2}\right)$, $s_4 = \left(-d_1 - d_3 + \frac{P_2^* r_2}{K_2}\right)$, using the Routh-Hurwitz

conditions [95, 126, 136], the equilibrium point E_5, is locally asymptotically stable if

$$s_1 > 0,\ s_2 > 0,\ s_3 > 0,\ \text{and}\ (s_4 s_3 - s_2)s_2 - s_4^2 s_1 > 0. \tag{4.3.5}$$

(7) The value of P_4^* is always negative at equilibrium point E_6. Therefore, the local stability study has not been performed.

(8) The Jacobian matrix of system (4.2.1) at equilibrium point $E_7 = (K_1, 0, 0, P_4^*)$ is

$$J(E_7) = \begin{pmatrix} -r_1 & -\lambda K_1 & -\rho K_1 & 0 \\ 0 & -d + \lambda K_1 - \beta P_4^* + r_2 & 0 & 0 \\ 0 & 0 & -\omega + \rho K_1 - \gamma P_4^* & 0 \\ 0 & l\beta P_4^* - \frac{dP_4^*}{K_2} & -\frac{d\eta P_4^*}{K_2} + \gamma(n_1 - n_2)P_4^* & d - \mu - 2\delta P_4^* \end{pmatrix},$$

the eigenvalues of $J(E_7)$ are $-\omega + \rho K_1 - \gamma P_4^*$, $d - \mu - 2\delta P_4^*$, $-r_1$, $-d + \lambda K_1 - \beta P_4^* + r_2$. The equilibrium point E_7 is locally asymptotically stable if

$$\omega + \gamma P_4^* > \rho K_1, \ \mu + 2\delta P_4^* > d, \ \text{and} \ d + \beta P_4^* > r_2 + \lambda K_1. \tag{4.3.6}$$

(9) The Jacobian matrix of system (4.2.1) at equilibrium point $E_8 = (P_1^*, 0, P_3^*, 0)$ is

$$J(E_8) = \begin{pmatrix} -\frac{P_1 r_1}{K_1} & -\lambda P_1^* & -\rho P_1^* & 0 \\ 0 & f_4 & 0 & 0 \\ \rho P_3^* & \alpha P_3^* & 0 & -\gamma P_3^* \\ 0 & 0 & 0 & f_5 \end{pmatrix},$$

where $f_4 = -d + \lambda P_1^* - \alpha P_3^* + \left(1 - \frac{\eta P_3^*}{K_2}\right)r_2$, $f_5 = -\mu + \gamma(n_1 - n_2)P_3^* + d\left(1 - \frac{\eta P_3^*}{K_2}\right)$. Then the characteristic equation of the $J(E_8)$ is given by $x^4 + d_9 x^3 + d_{10} x^2 + d_{11} x + d_{12}$, where $d_9 = \left(-f_4 - f_5 + \frac{P_1^* r_1}{K_1}\right)$, $d_{10} = \left(f_4 f_5 + \rho^2 P_1^* P_3^* - \frac{f_4 P_1^* r_1}{K_1} - \frac{f_5 P_1^* r_1}{K_1}\right)$, $d_{11} = \left(-\rho^2 f_4 P_1^* P_3^* - \rho^2 f_5 P_1^* P_3^* + \frac{f_4 f_5 P_1^* r_1}{K_1}\right)$, $d_{12} = \rho^2 f_4 f_5 P_1^* P_3^*$. using the Routh-Hurwitz conditions [95, 126, 136], the equilibrium point E_8 is locally asymptotically stable if

$$d_9 > 0, \ d_{11} > 0, \ d_{12} > 0, \ \text{and} \ (d_9 d_{10} - d_{11})d_{11} - d_9^2 d_{12} > 0. \tag{4.3.7}$$

(10) The Jacobian matrix of system (4.2.1) at equilibrium point $E_9 = (0, P_2^*, 0, P_4^*)$ is

$$J(E_9) = \begin{pmatrix} -\lambda P_2^* + r_1 & 0 & 0 & 0 \\ \lambda P_2^* & -\frac{P_2^* r_2}{K_2} & -\alpha P_2^* - \frac{\eta P_2^* r_2}{K_2} & -\beta P_2^* \\ 0 & 0 & -\omega + \alpha P_2^* - \gamma P_4^* & 0 \\ 0 & l\beta P_4^* - \frac{dP_4^*}{K_2} & -\frac{d\eta P_4^*}{K_2} + \gamma(n_1 - n_2)P_4^* & -\delta P_4^* \end{pmatrix},$$

the eigenvalues of $J(E_9)$ are $-\omega + \alpha P_2^* - \gamma P_4^*$, $-\lambda P_2^* + r_1$, and

$\frac{d_{13}-\sqrt{d_{14}-d_{15}}}{2K_2}$, $\frac{d_{13}+\sqrt{d_{14}-d_{15}}}{2K_2}$, where $d_{13} = -\delta K_2 P_4^* - P_2^* r_2$, $d_{14} = (\delta K_2 P_4^* + P_2^* r_2)^2$, and $d_{15} = 4\left(-d\beta K_2 P_2^* P_4^* + l\beta^2 K_2^2 P_2^* P_4^* + \delta K_2 P_2^* P_4^* r_2\right)$. The equilibrium point E_9 is locally asymptotically stable if

$$\omega + \gamma P_4^* > \alpha P_2^*, \ \lambda P_2^* > r_1, \text{ and } d_{13} > \sqrt{d_{14} - d_{15}}. \qquad (4.3.8)$$

(11) The Jacobian matrix of system (4.2.1) at equilibrium point $E_{10} = (P_1^*, P_2^*, P_3^*, 0)$ can be written

$$J(E_{10}) = \begin{pmatrix} -\frac{P_1^* r_1}{K_1} & -\lambda P_1^* & -\rho P_1^* & 0 \\ \lambda P_2^* & -\frac{P_2^* r_2}{K_2} & d_{40} & -\beta P_2^* \\ \rho P_3^* & \alpha P_3^* & 0 & -\gamma P_3^* \\ 0 & 0 & 0 & d_{39} \end{pmatrix}$$

where $d_{39} = -\mu + l\beta P_2^* + \gamma(n_1 - n_2) P_3^* + d\left(1 - \frac{P_2^* + \eta P_3^*}{K_2}\right)$,

$d_{40} = -\alpha P_2^* - \frac{\eta P_2^* r_2}{K_2}$,

then the characteristic equation of the $J(E_{10})$ is given by $x^4 + d_{42}x^3 + d_{43}x^2 + d_{44}x + d_{41} = 0$, where $d_{41} = -\lambda \rho d_{39} d_{40} P_1^* P_3^* - \alpha \lambda \rho d_{39} P_1^* P_2^* P_3^* + \frac{\alpha d_{39} d_{40} P_1^* P_3^* r_1}{K_1} - \frac{\rho^2 d_{39} P_1^* P_2^* P_3^* r_2}{K_2}$,

$d_{42} = \left(-d_{39} + \frac{P_1^* r_1}{K_1} + \frac{P_2^* r_2}{K_2}\right)$,

$d_{43} = \left(\lambda^2 P_1^* P_2^* - \alpha d_{40} P_3^* + \rho^2 P_1^* P_3^* - \frac{d_{39} P_1^* r_1}{K_1} - \frac{d_{39} P_2^* r_2}{K_2} + \frac{P_1^* P_2^* r_1 r_2}{K_1 K_2}\right)$,

$d_{44} = -\lambda^2 d_{39} P_1^* P_2^* + \alpha d_{39} d_{40} P_3^* - \rho^2 d_{39} P_1^* P_3^* + \lambda \rho d_{40} P_1 P_3 + \alpha \lambda \rho P_1 P_2 P_3 - \frac{\alpha d_{40} P_1 P_3 r_1}{K_1}$
$+ \frac{\rho^2 P_1^* P_2^* P_3^* r_2}{K_2} - \frac{d_{39} P_1^* P_2^* r_1 r_2}{K_1 K_2}$,

using the Routh-Hurwitz conditions [95,126,136], the equilibrium point, E_{10}, is locally asymptotically stable if

$$d_{42} > 0, \ d_{44} > 0, \ d_{41} > 0, \text{ and } (d_{42}d_{43} - d_{44})d_{44} - d_{42}^2 d_{41} > 0. \qquad (4.3.9)$$

(12) The Jacobian matrix of system (4.2.1) at equilibrium point $E_{11} = (P_1^*, P_2^*, 0, P_4^*)$ is

$$J(E_{11}) = \begin{pmatrix} -\frac{P_1^* r_1}{K_1} & -\lambda P_1^* & -\rho P_1^* & 0 \\ \lambda P_2^* & -\frac{P_2^* r_2}{K_2} & d_{23} & -\beta P_2^* \\ 0 & 0 & d_{24} & 0 \\ 0 & d_{26} & d_{25} & -\delta P_4^* \end{pmatrix},$$

where $d_{23} = -\alpha P_2^* - \frac{\eta P_2^* r_2}{K_2}$, $d_{24} = -\omega + \rho P_1^* + \alpha P_2^* - \gamma P_4^*$, $d_{25} = -\frac{d\eta P_4^*}{K_2} + \gamma(n_1 - n_2) P_4^*$, $d_{26} = l\beta P_4^* - \frac{dP_4^*}{K_2}$,

111

then the characteristic equation of the $J(E_{11})$ is given by

$$x^4 + d_{36}x^3 + d_{37}x^2 + d_{38}x + d_{35} = 0,$$

where $d_{35} = -\delta\lambda^2 d_{24}P_1^*P_2^*P_4^* - \frac{\beta d_{24}d_{26}P_1^*P_2^*r_1}{K_1} - \frac{\delta d_{24}P_1^*P_2^*P_4^*r_1r_2}{K_1K_2}$, $d_{36} = \left(-d_{24} + \delta P_4^* + \frac{P_1^*r_1}{K_1} + \frac{P_2^*r_2}{K_2}\right)$,

$d_{37} = \left(\beta d_{26}P_2^* + \lambda^2 P_1^*P_2^* - \delta d_{24}P_4^* - \frac{d_{24}P_1^*r_1}{K_1} + \frac{\delta P_1^*P_4^*r_1}{K_1} - \frac{d_{24}P_2^*r_2}{K_2} + \frac{\delta P_2^*P_4^*r_2}{K_2} + \frac{P_1^*P_2^*r_1r_2}{K_1K_2}\right)$

$d_{38} = -\beta d_{24}d_{26}P_2^* - \lambda^2 d_{24}P_1^*P_2^* + \delta\lambda^2 P_1^*P_2^*P_4^* + \frac{\beta d_{26}P_1^*P_2^*r_1}{K_1} - \frac{\delta d_{24}P_1^*P_4^*r_1}{K_1} - \frac{\delta d_{24}P_2^*P_4^*r_2}{K_2}$

$- \frac{d_{24}P_1^*P_2^*r_1r_2}{K_1K_2} + \frac{\delta P_1^*P_2^*P_4^*r_1r_2}{K_1K_2},$

using the Routh-Hurwitz conditions [95,126,136], the equilibrium point, $E_{11} = (P_1^*, P_2^*, 0, P_4^*)$, is locally asymptotically stable if

$$d_{36} > 0, \ d_{38} > 0, \ d_{35} > 0, \ \text{and} \ (d_{36}d_{37} - d_{38})d_{38} - d_{36}^2 d_{35} > 0. \tag{4.3.10}$$

(13) The Jacobian matrix of system (4.2.1) at equilibrium point $E_{12} = (P_1^*, 0, P_3^*, P_4^*)$ can be written

$$J(E_{12}) = \begin{pmatrix} -\frac{P_1^*r_1}{K_1} & -\lambda P_1^* & -\rho P_1^* & 0 \\ 0 & d_{16} & 0 & 0 \\ \rho P_3^* & \alpha P_3^* & 0 & -\gamma P_3^* \\ 0 & d_{18} & d_{17} & -\delta P_4^* \end{pmatrix},$$

where $d_{16} = -d + \lambda P_1^* - \alpha P_3^* - \beta P_4^* + \left(1 - \frac{\eta P_3^*}{K_2}\right)r_2$, $d_{17} = -\frac{d\eta P_4^*}{K_2} + \gamma(n_1 - n_2)P_4^*$, $d_{18} = l\beta P_4^* - \frac{dP_4^*}{K_2}$,

Then the characteristic equation of the $J(E_{12})$ is given by $x^4 + d_{21}x^3 + d_{20}x^2 + d_{19}x + d_{22} = 0$,

where $d_{19} = \left(-\gamma d_{16}d_{17}P_3^* - \rho^2 d_{16}P_1^*P_3^* + \delta\rho^2 P_1^*P_3^*P_4^* + \frac{\gamma d_{17}P_1^*P_3^*r_1}{K_1} - \frac{\delta d_{16}P_1^*P_4^*r_1}{K_1}\right)$,

$d_{20} = \left(\gamma d_{17}P_3^* + \rho^2 P_1^*P_3^* - \delta d_{16}P_4^* - \frac{d_{16}P_1^*r_1}{K_1} + \frac{\delta P_1^*P_4^*r_1}{K_1}\right)$, $d_{21} = \left(-d_{16} + \delta P_4^* + \frac{P_1^*r_1}{K_1}\right)$,

$d_{22} = -\delta\rho^2 d_{16}P_1^*P_3^*P_4^* - \frac{\gamma d_{16}d_{17}P_1^*P_3^*r_1}{K_1}$, using the Routh-Hurwitz conditions [95,126,136], the equilibrium point E_{12} is locally asymptotically stable if

$$d_{20} > 0, \ d_{19} > 0, \ d_{22} > 0, \ \text{and} \ (d_{21}d_{20} - d_{19})d_{19} - d_{21}^2 d_{22} > 0. \tag{4.3.11}$$

(14) The Jacobian matrix of system (4.2.1) at equilibrium point $E_{13} = (0, P_2^*, P_3^*, P_4^*)$ is

$$J(E_{13}) = \begin{pmatrix} d_{27} & 0 & 0 & 0 \\ \lambda P_2^* & -\frac{P_2^* r_2}{K_2} & d_{28} & -\beta P_2^* \\ \rho P_3^* & \alpha P_3^* & 0 & -\gamma P_3 \\ 0 & d_{30} & d_{29} & -\delta P_4^* \end{pmatrix}$$

where $d_{27} = -\lambda P_2^* - \rho P_3^* + r_1, d_{28} = -\alpha P_2^* - \frac{\eta P_2^* r_2}{K_2}, d_{29} = -\frac{d\eta P_4^*}{K_2} + \gamma(n_1 - n_2) P_4^*$, $d_{30} = l\beta P_4^* - \frac{dP_4^*}{K_2}$,

then the characteristic equation of the $J(E_{13})$ is given by $x^4 + d_{32}x^3 + d_{33}x^2 + d_{34}x + d_{31} = 0$, where $d_{31} = -\gamma d_{27}d_{28}d_{30}P_3^* - \alpha\beta d_{27}d_{29}P_2^*P_3^* + \alpha\delta d_{27}d_{28}P_3^*P_4^* - \frac{\gamma d_{27}d_{29}P_2^*P_3^* r_2}{K_2}$,

$d_{32} = \left(-d_{27} + \delta P_4^* + \frac{P_2^* r_2}{K_2}\right)$,

$d_{33} = \left(\beta d_{30}P_2^* - \alpha d_{28}P_3^* + \gamma d_{29}P_3^* - \delta d_{27}P_4^* - \frac{d_{27}P_2^* r_2}{K_2} + \frac{\delta P_2^* P_4 r_2}{K_2}\right)$,

$d_{34} = -\beta d_{27}d_{30}P_2 + \alpha d_{27}d_{28}P_3^* - \gamma d_{27}d_{29}P_3^* + \gamma d_{28}d_{30}P_3^* + \alpha\beta d_{29}P_2^*P_3 - \alpha\delta d_{28}P_3^*P_4^*$
$+ \frac{\gamma d_{29}P_2^*P_3^* r_2}{K_2} - \frac{\delta d_{27}P_2^*P_4^* r_2}{K_2}$.

Using the Routh-Hurwitz conditions [95, 126, 136], the equilibrium point E_{13} is locally asymptotically stable if

$$d_{32} > 0, \ d_{31} > 0, \ d_{34} > 0, \text{ and } (d_{32}d_{33} - d_{34})d_{34} - d_{32}^2 d_{31} > 0. \tag{4.3.12}$$

(15) The Jacobian matrix of system (4.2.1) at equilibrium point $E_{14} = (P_1^*, P_2^*, P_3^*, P_4^*)$ is

$$J(E_{14}) = \begin{pmatrix} -\lambda P_2^* - \frac{P_1^* r_1}{K_1} + \left(1 - \frac{P_1^*}{K_1}\right)r_1 & -\lambda P_1^* & 0 & 0 \\ m\lambda P_2^* & P & -\alpha P_2^* - \frac{\eta P_2^* r_2}{K_2} & -\beta P_2^* \\ 0 & \alpha P_3^* & -\omega + \alpha P_2^* - \gamma P_4^* & -\gamma P_3^* \\ 0 & l\beta P_4^* - \frac{dP_4^*}{K_2} & -\frac{d\eta P_4^*}{K_2} + \gamma(n_1 - n_2)P_4^* & Q \end{pmatrix},$$

where

$$P = -\sigma + m\lambda P_1^* - \alpha P_3^* - \beta P_4^* - \frac{P_2^* r_2}{K_2} + \left(1 - \frac{P_2^* + \eta P_3^*}{K_2}\right)r_2,$$

$$Q = -\mu + l\beta P_2^* + \gamma(n_1 - n_2)P_3^* + d\left(1 - \frac{P_2^* + \eta P_3^*}{K_2}\right) - 2\delta P_4^*,$$

113

after simplification of jacobian matrix,

$$
J(E_{14}) = \begin{pmatrix}
-\frac{P_1^* r_1}{K_1} & -\lambda P_1^* & 0 & 0 \\
m\lambda P_2^* & -\frac{P_2^* r_2}{K_2} & -\alpha P_2^* - \frac{\eta P_2^* r_2}{K_2} & -\beta P_2^* \\
0 & \alpha P_3^* & 0 & -\gamma P_3^* \\
0 & l\beta P_4^* - \frac{dP_4^*}{K_2} & -\frac{d\eta P_4^*}{K_2} + \gamma(n_1 - n_2) P_4^* & 0
\end{pmatrix},
$$

then the characteristic equation of the $J(E_{14})$ is given by

$$
x^4 + a_1 x^3 + a_2 x^2 + a_3 x + a_4 = 0,
$$

where

$$
a_4 = -\frac{P_1^* P_2^* P_3^* P_4^* \left(m\gamma\lambda^2 K_1 \left(d\eta + \gamma K_2 (-n_1 + n_2) \right) \right)}{K_1 K_2}
$$
$$
+ \frac{P_1^* 1 P_2^* P_3^* P_4^* r_1 \left(d\alpha(-\gamma + \beta\eta) + \alpha\beta\gamma K_2 (l - n_1 + n_2) + \gamma(l\beta\eta - \gamma n_1 + \gamma n_2) r_2 \right)}{K_1 K_2},
$$

$$
a_3 = \frac{K_1 P_2^* P_3^* P_4^* \left(d\alpha(\gamma - \beta\eta) - \alpha\beta\gamma K_2 (l - n_1 + n_2) + \gamma(-l\beta\eta + \gamma n_1 - \gamma n_2) r_2 \right)}{K_1 K_2}
$$
$$
+ \frac{P_1 r_1 \left(-d\gamma\eta P_3^* P_4^* + K_2 \left(\gamma^2 (n_1 - n_2) P_3^* P_4^* + P_2^* \left(\alpha^2 P_3^* + l\beta^2 P_4^* \right) \right) + P_2^* \left(-d\beta P_4 + \alpha\eta P_3 r_2 \right) \right)}{K_1 K_2},
$$

$$
a_1 = \frac{P_1^* r_1}{K_1} + \frac{P_2^* r_2}{K_2},
$$

$$
a_2 = m\lambda^2 P_1^* P_2^* + \alpha^2 P_2^* P_3^* + l\beta^2 P_2^* P_4^* - \frac{d\beta P_2^* P_4^*}{K_2} - \frac{d\gamma\eta P_3^* P_4^*}{K_2}
$$
$$
+ \gamma^2 n_1 P_3^* P_4^* - \gamma^2 n_2 P_3^* P_4^* + \frac{\alpha\eta P_2^* P_3^* r_2}{K_2} + \frac{P_1^* P_2^* r_1 r_2}{K_1 K_2},
$$

using the Routh-Hurwitz conditions [95, 126, 136], the coexistence equilibrium point E_{14} is locally asymptotically stable if

$$
a_1 > 0, \ a_3 > 0, \ a_4 > 0, \ \text{and} \ (a_1 a_2 - a_3)a_3 - a_1^2 a_4 > 0. \tag{4.3.13}
$$

$\square$

114

4.3.5 Sensitivity Analysis

Sensitivity analysis may reveal important details about how biological behaviors are changing with respect to the parameters. We determine the sensitivity indices of the basic reproduction number to the parameters as mentioned in Table 4.6. These indices indicate how important each parameter is for disease spread and distribution. We investigate the effect of the basic reproduction number R_{01}, R_{02}, R_{03}, and R_{04} for certain key parameters to conduct a sensitivity analysis of the model. Following [34, 155], we calculate the normalized forward sensitivity index of the reproduction number, which estimates the relative change in a variable with respect to the relative change in its parameter. The normalized forward sensitivity index of a variable, h, that depend differentially on a parameter, l, is defined as: $\Gamma_l^h = \frac{1}{h} \times \frac{\partial h}{\partial l}$.

Table 4.4: Sensitivity indices of R_{01}, R_{02}, and R_{03} corresponding to all parameters

Parameters	Sensitivity index(R_{01})	Sensitivity index (R_{02})	Sensitivity index (R_{03})
K_1	1	1	0.0449
ρ	1	1	0.0625
ω	-0.8148	-1	-1
δ	0.1852	-	-
γ	-0.1852	-	-
μ	1.2963	-	-
K_2	-	-	-0.0175
r_1	-	-	0.9550
d	-	-	0.1038
r_2	-	-	-0.0862
λ	-	-	-0.9774
α	-	-	0.9375

Table 4.5: Sensitivity indices of R_{04} corresponding to all parameters

Parameters	Sensitivity index	Parameters	Sensitivity index
r_1	0.5802	K_1	0.1458
λ	-0.6967	d	-0.5723
ρ	0.2624	r_2	-0.1329
K_2	-0.1413	α	0.7375
β	-0.2040	γ	-0.3797
ω	-0.6202	l	-0.2987
μ	0.7406	δ	0.2850

Mathematically, the sensitivity of the system is characterized by sensitivity indices. Table 4.4 and Table 4.5 display the sensitivity indices of R_{01}, R_{02}, R_{03}, and R_{04}. In Table 4.4, we observe that the sensitivity indices of R_{01} has positive value with respect to parameters, namely, K_1, ρ, δ, and μ. Similarly, the sensitivity indices of R_{02} and R_{03} have positive values with respect to parameters, namely, K_1, ρ and K_1, ρ, r_1, d, α, respectively. Further, the parameters, namely, r_1, ρ, μ, K_1, α, and δ are positively sensitive and remaining are the negative sensitive parameters in Table 4.5. We can see from Table 4.4 and Table 4.5 that the parameters, which show the most sensitivity is the adequate contact rate among prey, susceptible, and infectious individuals. These indices suggest that if we can increase crop density while decreasing the sufficient contact rate of infected individuals, the value of basic reproduction numbers decrease.

4.4   Global Stability Analysis

Here, we discuss the existence and global asymptotic stability of an interior equilibrium of model (4.2.1). The interior equilibrium $E^*(P_1^*, P_2^*, P_3^*, P_4^*)$ is the point of intersection of the following equations

$$r_1\left(1 - \frac{P_1}{K_1}\right) - \lambda P_2 - \rho P_3 = 0, \tag{4.4.1}$$

$$\lambda P_1 - \sigma + r_2\left(1 - \frac{P_2 + \eta P_3}{K_2}\right) - \alpha P_3 - \beta P_4 = 0, \tag{4.4.2}$$

$$\alpha P_2 + \rho P_1 - \gamma P_4 - \omega = 0, \tag{4.4.3}$$

$$l\beta P_2 + (n_1 - n_2)\gamma P_3 + d\left(1 - \frac{P_2 + \eta P_3}{K_2}\right) - \mu - \delta P_4 = 0, \tag{4.4.4}$$

from equation (4.4.1)

$$P_1 = -\frac{K_1(\lambda P_2 + \rho P_3 - r_1)}{r_1}, \tag{4.4.5}$$

from equation (4.4.3)

$$P_4 = \frac{-\omega + \rho P_1 + \alpha P_2}{\gamma}, \tag{4.4.6}$$

from the equations (4.4.5), (4.4.6) and (4.4.2)

$$\delta_3 P_3 + P_2 \delta_2 + \delta_1 = 0, \tag{4.4.7}$$

116

where, $\delta_1 = \frac{\beta\omega}{\gamma} + \lambda K_1 + r_2 - \sigma$, $\delta_2 = -\frac{\alpha\beta}{\gamma} - \frac{\lambda^2 K_1}{r_1} - \frac{r_2}{K_2}$, $\delta_3 = -\alpha - \frac{\lambda\rho K_1}{r_1} - \frac{\eta r_2}{K_2}$, from the equations (4.4.5), (4.4.6) and (4.4.4)

$$\delta_6 P_3 + P_2 \delta_5 + \delta_4 = 0, \tag{4.4.8}$$

where, $\delta_4 = d + \frac{\delta\omega}{\gamma} - \mu - \frac{\delta\rho K_1}{\gamma}$, $\delta_5 = l\beta + \frac{\delta\lambda\rho K_1}{\gamma r_1} - \frac{\alpha\delta}{\gamma} - \frac{d}{K_2}$, $\delta_6 = \gamma n_1 + \frac{\delta\rho^2 K_1}{\gamma r_1} - \gamma n_2 - \frac{d\eta}{K_2}$.
from the equations (4.4.7) and (4.4.8), we can obtain equilibrium points,

$$P_2^* = \frac{-\delta_3\delta_4 + \delta_1\delta_6}{\delta_3\delta_5 - \delta_2\delta_6}, P_3^* = \frac{-\delta_2\delta_4 + \delta_1\delta_5}{-\delta_3\delta_5 + \delta_2\delta_6},$$

further, from the equations (4.4.5) and (4.4.6), we can obtain

$$P_1^* = K_1 - \frac{\lambda K_1 P_2^*}{r_1} - \frac{K_1 P_3^* \rho}{r_1}, \ P_4^* = -\frac{\omega}{\gamma} + \frac{\alpha P_2^*}{\gamma} + \frac{P_1^* \rho}{\gamma}$$

The equilibrium points P_1^*, P_2^*, P_3^*, and P_4^* are positive if the following conditions are satisfied,

(1) $P_3^* > 0$ if $\delta_2\delta_4 > \delta_1\delta_5$ and $\delta_3\delta_5 > \delta_2\delta_6$ or $\delta_2\delta_4 < \delta_1\delta_5$ and $\delta_3\delta_5 < \delta_2\delta_6$,

(2) $P_2^* > 0$ if $\delta_3\delta_4 > \delta_1\delta_6$ and $\delta_3\delta_5 < \delta_2\delta_6$ or $\delta_3\delta_4 < \delta_1\delta_6$ and $\delta_3\delta_5 > \delta_2\delta_6$,

(3) $P_1^* > 0$ if $K_1 > \frac{\lambda K_1 P_2^*}{r_1} + \frac{K_1 P_3^* \rho}{r_1}$, $P_2^* > 0$, and $P_3^* > 0$,

(4) $P_4^* > 0$ if $\frac{\omega}{\gamma} < \frac{\alpha P_2^*}{\gamma} + \frac{P_1^* \rho}{\gamma}$, $P_2^* > 0$, and $P_3^* > 0$,

(5) $\delta_1 > 0$ if $\frac{\beta\omega}{\gamma} + \lambda K_1 + r_2 > \frac{\beta\rho K_1}{\gamma} + d, \delta_2 > 0$ if $\frac{\beta\lambda\rho K_1}{\gamma r_1} > \frac{\alpha\beta}{\gamma} + \frac{\lambda^2 K_1}{r_1} + \frac{r_2}{K_2}, \delta_3 > 0$ if $\frac{\beta\rho^2 K_1}{\gamma r_1} > \alpha + \frac{\lambda\rho K_1}{r_1} + \frac{\eta r_2}{K_2}$,

$\delta_4 > 0$ if $d + \frac{\delta\omega}{\gamma} > \mu + \frac{\delta\rho K_1}{\gamma}, \delta_5 > 0$ if $l\beta + \frac{\delta\lambda\rho K_1}{\gamma r_1} > \frac{\alpha\delta}{\gamma} + \frac{d}{K_2}, \delta_6 > 0$ if $\gamma n_1 + \frac{\delta\rho^2 K_1}{\gamma r_1} > \gamma n_2 + \frac{d\eta}{K_2}$.
In this section the global stability of equilibrium point $E_{14}(P_1^*, P_2^*, P_3^*, P_4^*)$ is determined with the help of Lyapunov method as shown in the following theorem.

Theorem 4.4.1. The positive interior equilibrium $E_{14}^*(P_1^*, P_2^*, P_3^*, P_4^*)$ is globally asymptotically stable if

$$\frac{c_1 r}{K_1} > 0, \ c_1 = c_3, \ c_1 > c_2, \ \frac{r_2 c_2}{K_2} > 0, \ \text{and} \ \frac{c_1 r}{K_1}\frac{r_2 c_2}{K_2} > (\lambda\frac{(c_1 - c_2)}{2})^2.$$

Where, $c_1 = \frac{d}{\beta K_2} - l$, $c_2 = \frac{d}{\beta K_2} - l$, and $c_3 = (n_1 - n_2)\gamma - \frac{d\eta}{K_2}$.

117

Proof. Firstly, we define a Lyapunov function

$$V(P_1, P_2, , P_3) = c_1 \left(P_1 - P_1^* - P_1^* \ln \frac{P_1}{P_1^*} \right) + c_2 \left(P_2 - P_2^* - P_2^* \ln \frac{P_2}{P_2^*} \right)$$
$$+ c_3 \left(P_3 - P_3^* - P_3^* \ln \frac{P_3}{P_3^*} \right) + c_4 \left(P_4 - P_4^* - P_4^* \ln \frac{P_4}{P_4^*} \right),$$

where $c_j; j = 1, 2, 3, 4$ are positive constants to be determined later. V is continuously differentiable, positive definite, real valued function with $V(P_1^*, P_2^*, P_3^*, P_4^*) = 0$ and $V(P_1, P_2, P_3, P_4) > 0$ for all $(P_1, P_2, P_3, P_4) \neq (P_1^*, P_2^*, P_3^*, P_4^*)$ in the R_+^4. So by differentiate V with respect to the time and then simplifying the resulting terms we obtain,

$$\frac{dV}{dt} = c_1 \left(1 - \frac{P_1^*}{P_1} \right) \frac{dP_1}{dt} + c_2 \left(1 - \frac{P_2^*}{P_2} \right) \frac{dP_2}{dt} + c_3 \left(1 - \frac{P_3^*}{P_3} \right) \frac{dP_3}{dt} + c_4 \left(1 - \frac{P_4^*}{P_4} \right) \frac{dP_4}{dt},$$

putting the values of $\frac{dP_1}{dt}$, $\frac{dP_2}{dt}$ and $\frac{dP_3}{dt}$ from the equation (4.2.1), we have

$$\frac{dV}{dt} = c_1 \left(1 - \frac{P_1^*}{P_1} \right) \left(r_1 P_1 \left(1 - \frac{P_1}{K_1} \right) - \lambda P_1 P_2 - \rho P_1 P_3 \right)$$
$$+ c_2 \left(1 - \frac{P_2^*}{P_2} \right) \left(\lambda P_1 P_2 - \sigma P_2 + r_2 P_2 \left(1 - \frac{P_2 + \eta P_3}{K_2} \right) - \alpha P_2 P_3 - \beta P_2 P_4 \right)$$
$$+ c_3 \left(1 - \frac{P_3^*}{P_3} \right) (\alpha P_2 P_3 + \rho P_1 P_3 - \gamma P_3 P_4 - \omega P_3)$$
$$+ c_4 \left(1 - \frac{P_4^*}{P_4} \right) \left(l\beta P_2 P_4 + (n_1 - n_2) \gamma P_3 P_4 + d \left(1 - \frac{P_2 + \eta P_3}{K_2} \right) P_4 - \mu P_4 - \delta (P_4)^2 \right),$$

$$\frac{dV}{dt} = c_1 (P_1 - P_1^*) \left(r_1 \left(1 - \frac{P_1}{K_1} \right) - \lambda P_2 - \rho P_3 - \left(r_1 \left(1 - \frac{P_1^*}{K_1} \right) - \lambda P_2^* - \rho P_3^* \right) \right)$$
$$+ c_2 (P_2 - P_2^*) \left(\lambda P_1 - \sigma + r_2 \left(1 - \frac{P_2 + \eta P_3}{K_2} \right) - \alpha P_3 - \beta P_4 \right)$$
$$+ c_2 (P_2 - P_2^*) \left((-m\lambda P_1^* + \sigma - r_2 \left(1 - \frac{P_2^* + \eta P_3^*}{K_2} \right) + \alpha P_3^* + \beta P_4^*) \right)$$
$$+ c_3 (P_3 - P_3^*) (\alpha P_2 + \rho P_1 - \gamma P_4 - \omega - (\alpha P_2^* + \rho P_1^* - \gamma P_4^* - \omega))$$
$$+ c_4 (P_4 - P_4^*) l\beta P_2 + (n_1 - n_2) \gamma P_3 + d \left(1 - \frac{P_2 + \eta P_3}{K_2} \right) - \mu - \delta P_4$$
$$- \left(l\beta P_2^* + (n_1 - n_2) \gamma P_3^* + d \left(1 - \frac{P_2^* + \eta P_3^*}{K_2} \right) - \mu - \delta P_4^* \right),$$

$$\frac{dV}{dt} = -\frac{c_1 r_1}{K_1}(P_1 - P_1^*)^2 - \lambda c_1(P_2 - P_2^*)(P_1 - P_1^*) + \rho(c_3 - c_1)(P_1 - P_1^*)(P_3 - P_3^*)$$

$$+ c_2\lambda(P_1 - P_1^*)(P_2 - P_2^*) - \frac{r_2 c_2}{K_2}(P_2 - P_2^*)^2 - c_2\left(\frac{r_2\eta}{K_2} + \alpha\right)(P_3 - P_3^*)(P_2 - P_2^*)$$

$$- \beta c_2(P_2 - P_2^*)(P_4 - P_4^*) + c_3\alpha(P_2 - P_2^*)(P_3 - P_3^*) - c_3\gamma(P_3 - P_3^*)(P_4 - P_4^*)$$

$$+ c_4\left(l\beta - \frac{d}{K_2}\right)(P_2 - P_2^*)(P_4 - P_4^*) + c_4\left((n_1 - n_2)\gamma - \frac{d\eta}{K_2}\right)(P_4 - P_4^*)(P_3 - P_3^*),$$

$$\frac{dV}{dt} = -\frac{c_1 r_1}{K_1}(P_1 - P_1^*)^2 - \frac{r_2 c_2}{K_2}(P_2 - P_2^*)^2 - \lambda(c_1 - c_2)(P_1 - P_1^*)(P_2 - P_2^*)$$

$$+ \rho(c_3 - c_1)(P_1 - P_1^*)(P_3 - P_3^*) - \left(\frac{c_2 r_2\eta}{K_2} + c_2\alpha - c_3\alpha\right)(P_3 - P_3^*)(P_2 - P_2^*)$$

$$- \left(\beta c_2 + c_4\left(l\beta - \frac{d}{K_2}\right)\right)(P_2 - P_2^*)(P_4 - P_4^*)$$

$$- \left(c_3\gamma - c_4(n_1 - n_2)\gamma + \frac{c_4 d\eta}{K_2}\right)(P_4 - P_4^*)(P_3 - P_3^*).$$

Choosing $c_1 = \frac{d}{\beta K_2} - l$, $c_2 = \frac{d}{\beta K_2} - l$, $c_3 = (n_1 - n_2) - \frac{d\eta}{\gamma K_2}$, $c_4 = 1$.

Using the value of c_1, c_2, c_3 and c_4, we obtain

$$\frac{dV}{dt} = -\frac{c_1 r_1}{K_1}(P_1 - P_1^*)^2 - \frac{r_2 c_2}{K_2}(P_2 - P_2^*)^2 - \lambda(c_1 - c_2)(P_1 - P_1^*)(P_2 - P_2^*)$$

$$- \rho(c_1 - c_3)(P_1 - P_1^*)(P_3 - P_3^*) - \left(\frac{c_2 r_2\eta}{K_2} + c_2\alpha - c_3\alpha\right)(P_3 - P_3^*)(P_2 - P_2^*).$$

Thus, $\frac{dV}{dt}$ is a quadratic form which can be expressed as $\frac{dV}{dt} = -Z^T A Z$, where $Z^T = (P_1 - P_1^*, P_2 - P_2^*, P_3 - P_3^*)$ and the symmetric matrix is given by

$$A = \begin{pmatrix} c_{11} & c_{12} & c_{13} \\ c_{12} & c_{22} & c_{23} \\ c_{13} & c_{23} & c_{33} \end{pmatrix},$$

where $c_{11} = \frac{c_1 r_1}{K_1}$, $c_{12} = \lambda\frac{(c_1 - c_2)}{2}$, $c_{13} = \rho\frac{(c_1 - c_3)}{2}$, $c_{23} = \frac{(\frac{c_2 r_2\eta}{K_2} + c_2\alpha - c_3\alpha)}{2}$, $c_{22} = \frac{r_2 c_2}{K_2}$, and $c_{33} = 0$.
The point $(P_1^*, P_2^*, P_3^*, P_4^*)$ is globally asymptotically stable if $\frac{dV}{dt} < 0$; that is the matrix A is positive definite [216]. Now the matrix A is positive if $c_{11} > 0$, $c_{13} = 0$, $c_{12} > 0$, $c_{22} > 0$, $c_{23} = 0$, and $c_{11}c_{22} - c_{12}^2 > 0$. $c_{11} > 0$, gives $\frac{c_1 r}{K_1} > 0$, $c_{13} = 0$ gives $c_1 = c_3$, $c_{12} > 0$ gives $c_1 > c_2$, $c_{22} > 0$ gives $\frac{r_2 c_2}{K_2} > 0$, and $c_{11}c_{22} - c_{12}^2 > 0$ gives $\frac{c_1 r}{K_1}\frac{r_2 c_2}{K_2} > \left(\lambda\frac{(c_1 - c_2)}{2}\right)^2$. Also, $\frac{dV}{dt} = 0$

at E_{14}. Then, we define the invariant set as

$$\Omega = \{(P_1, P_2, P_3, P_4) \in R_4^+ : \frac{dV}{dt} = 0\}.$$

Hence, by LaSalles Invariance Principle [92], it follows that the E_{14} is said to be globally asymptotically stable. This completes the proof. □

4.5 Numerical Simulation and Its Discussion

For simulation purposes, we perform numerical simulations to analyze the dynamic behavior of the system (4.2.1). The mathematical parameters of the models representing a certain pattern can be modified to achieve a stronger agreement between the performance of the model and the observations. Because these parameters are experimentally determined, the computational parameters used throughout models to explain actual processes might be ambiguous. Additionally, the initial conditions of the model may not be well recognized. Despite these limitations, models are effective tools for representing natural processes. Models are also the only way of extrapolating to broad spatial scales or forecasting the future. Because of their significance in ecology, we are trying to determine precision by validating models. For the same, the land area of the globe is 13,003 million hectares and 4,889 million hectares are classified as agricultural area according to the Food and Agriculture Organization (FAO). The estimation of crop growth rate is proportional to crop production and can be derived using Table 4.1. The growth rate can be estimated by taking the average annual production between 2010–11 and 2018–19. Thus, the average annual production is 2255.02 million metric tonnes over 4,889 million hectares. Therefore, growth rate $= \frac{2255.02 \text{ million metric tonnes}}{4,889 \text{ million ha}}$ per year i.e., $r_1 = 0.53$ centigram meter^{-2} hour^{-1} (cg m^{-2} hours^{-1}). Thus, $r_1 = 0.53$ hours^{-1}. In this part, we provide some simulation work to validate our analytical results. We consider for this objective $r_1 = 0.53$(estimated). Further, due to the limitations of the availability of data, in this study, we take the parameters by numerically experimental values to meet the requirement of the proposed model.

Table 4.6: Parameter value used in simulation.

Parameters	Value	Parameters	Value
r_1	0.53[estimated]	K_2	10
K_1	5	α	0.40
λ	0.30	β	0.20
σ	0.20	γ	0.20
d	0.40	ω	0.4
ρ	0.20	n_1	0.30
r_2	0.40	n_2	0.15
η	1	μ	0.35
δ	0.11	l	0.50

By this dataset of parameters, we justify our theoretical results, which reflect the effectiveness of our proposed study. In this work, to observe how the proposed models react to changes in model data. Understanding the extent of the change in model results to changes in model data or parameters is often referring to as susceptibility tests. Identifying model parameters that have a significant impact on model performance is helpful since these parameters can be regulated as effectively as possible. Figure 4.1 illustrates the graph of population density between prey (crop), susceptible pest, infected pest and natural enemy of pest with respect to different parameters and times t. Figure 4.1a shows that the crop density decreases rapidly when P_2, P_3, and P_4 increase. For Figure 4.1b, we use a simulated set of parameters from Table 4.6. In Figure 4.1b, population density P_3 increases while population density P_2 and P_4 decrease compared to Figure 4.1a when some parameters change, i.e., $r_1 = 0.53$, $\lambda = 0.3$, $\sigma = 0.2$, $\rho = 0.2$, $r_2 = 0.4$ $\alpha = 0.4$, $\omega = 0.4$, $l = 0.5$, $\mu = 0.35$. Thus, Figure 4.1 shows that susceptible pests, infected pests and natural enemies of pest are growing in size, implying that predation happens on crops, resulting in a gradual decrease in the number of prey density. Figure 4.2 illustrates the graph of population density between prey (crop), susceptible pest, infected pest and natural enemy of pest with respect to different parameters and times t. Further, Figure 4.2 signifies the case when the significance of diseased pest predator species contributions n_1 is greater than the negative influence parameters n_2 on the biomass of predator species caused by pest infection. Figure 4.2a demonstrates that crop density P_1 falls as P_2 and P_3 grow, although natural enemies of pests P_4 remain constant. Figure 4.2b shows that when P_2 and P_3 grow, crop den-

sity P_1 declines fast while P_4 increases slowly. In Figure 4.2b, population density P_2 and P_3 increases more compared to Figure 4.2a when some parameters change, i.e., $r_1 = 0.6$, $\lambda = 0.4$, $\sigma = 0.4$, $\rho = 0.3$, $r_2 = 0.7$, $\alpha = 0.2$, $\omega = 0.3$, $l = 0.5$, $\mu = 0.3$. to $r_1 = 0.53$, $\lambda = 0.3$, $\sigma = 0.2$, $\rho = 0.2$, $r_2 = 0.4$ $\alpha = 0.4$, $\omega = 0.4$, $l = 0.5$, $\mu = 0.35$ and remaining parameters are same. Thus, Figure 4.1 depicts the dynamic behaviour of the system when $n_1 > n_2$, whereas Figure 4.2 depicts the dynamic behaviour of the system when $n_1 < n_2$. For the same set of numerical parameters, it is observed that the population of the P_4 increases in the case $n_1 > n_2$, but remains almost constant in the case $n_1 < n_2$.

(a) $r_1 = 0.6$, $\lambda = 0.4$, $\sigma = 0.4$, $\rho = 0.3$, $r_2 = 0.7$, $\alpha = 0.2$, $\omega = 0.3$, $l = 0.5$, $\mu = 0.3$.

(b) $r_1 = 0.53$, $\lambda = 0.3$, $\sigma = 0.2$, $\rho = 0.2$, $r_2 = 0.4$ $\alpha = 0.4$, $\omega = 0.4$, $l = 0.5$, $\mu = 0.35$.

Figure 4.1: Time series diagrams between crop, susceptible pest, infected pest and natural enemies of pest population of the system for the parameter values $K_1 = 5$, $d = 0.4$, $\eta = 1$, $K_2 = 10$, $\beta = 0.2$, $\gamma = 0.2$, $n_1 = 0.3$, $n_2 = 0.15$, and $\delta = 0.11$.

(a) $r_1 = 0.53$, $\lambda = 0.30$, $\sigma = 0.20$, $\rho = 0.20$, $r_2 = 0.40$, $\alpha = 0.40$, $\omega = 0.40$, $n_1 = 0.10$, $n_2 = 0.20$, $\mu = 0.35$.

(b) $r_1 = 0.60$, $\lambda = 0.40$, $\sigma = 0.40$, $\rho = 0.30$, $r_2 = 0.70$ $\alpha = 0.20$, $\omega = 0.3$, $n_1 = 0.15$, $n_2 = 0.30$, $\mu = 0.30$.
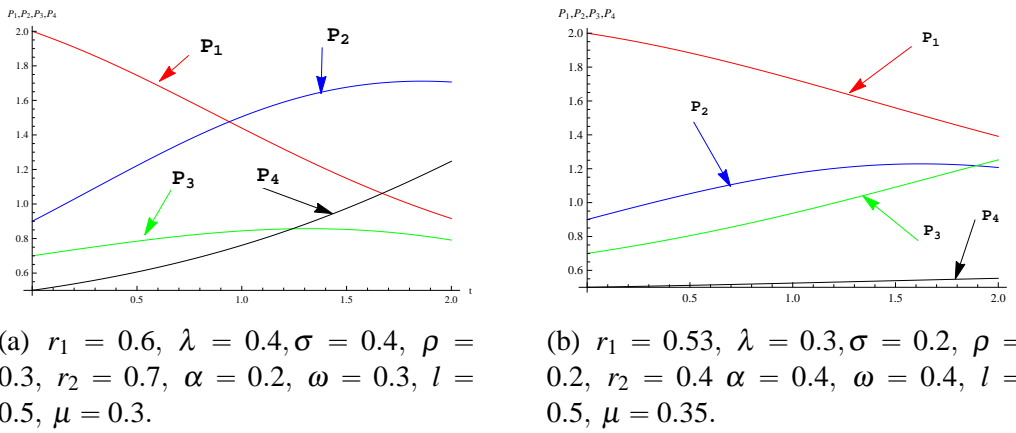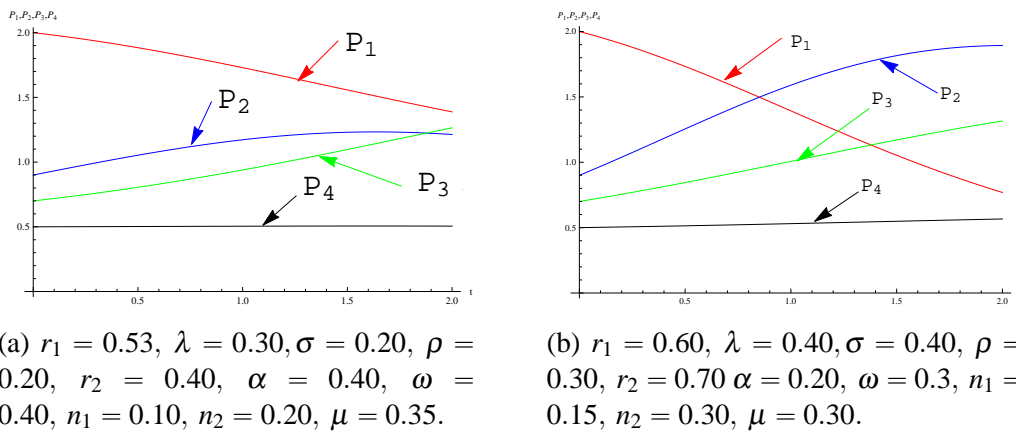
Figure 4.2: Time series diagrams between crop, susceptible pest, infected pest and natural enemies of pest population of the system for the parameter values $K_1 = 5$, $d = 0.4$, $\eta = 1$, $K_2 = 10$, $\beta = 0.2$, $\gamma = 0.2$, $l = 0.50$ and $\delta = 0.11$.

4.5.1 Numerical Simulation of Local Stability at the Coexistence Equilibrium Point

It is difficult to interpret the theoretical results due to complicated equilibrium points. To visualize the theoretical and stability results obtained in Section 4.3.4, we use numerical simulation to validate the theoretical aspects. For this, we consider the set of parametric values given in Table 4.6. For this collection of parametric values, all four species survive and have a stable population density, as shown in Figure 4.3. Further, for the set of parametric values given in Table 4.6 and (4.5.1), the stability condition (4.3.13) is well satisfied. The equilibrium point $(1.1273, 0.8652, 0.7545, 0.8579)$ and $(0.8337, 0.1760, 1.2080, 0.4407)$ are stable, as illustrated in Figure 4.3a and Figure 4.3b, respectively. Figure 4.3a shows that initially the susceptible pest, infected pest, and natural enemy of pest species increase while crop density decreases. Later, crop density rises, and all four living things gradually reach their steady states and become asymptotically stable. Similarly, consider the different parameters described by (4.5.1). Figure 4.3b depicts that initially P_2, P_3, and P_4 increase while P_1 falls. Further, the density of infected pests is more compared to the other three living organisms. Later, all four eventually attain their steady states and achieve asymptotically stability. Since these groups share the same ecosystem, they can be cooperative or compete with one another depending on the situation. Figure 4.4 shows phase portrait of the model system (4.2.1) with different initial conditions and the set of parametric values are taken from Table 4.6. Thus, all solutions approach toward the point $(1.1273, 0.8652, 0.7545, 0.8579)$.

$$r_1 = 0.53, \ K_1 = 5, \ \lambda = 0.45, \ \sigma = 0.2, \ d = 0.4, \ \rho = 0.3, \ r_2 = 0.6, \ \eta = 1, \ K_2 = 10, \ \alpha = 0.5,$$
$$\beta = 0.2, \ \gamma = 0.2, \ \omega = 0.25, \ l = 0.5, \ n_1 = 0.3, \ n_2 = 0.15, \ \mu = 0.35, \ \delta = 0.11. \quad (4.5.1)$$
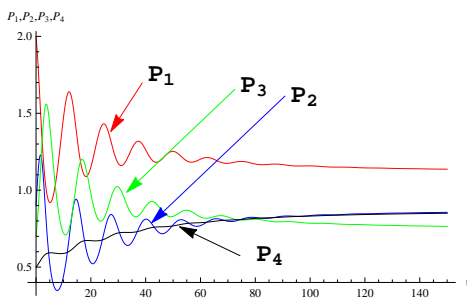
(a) Equilibrium point$(1.1273, 0.8652,$
$0.7545, 0.8579)$
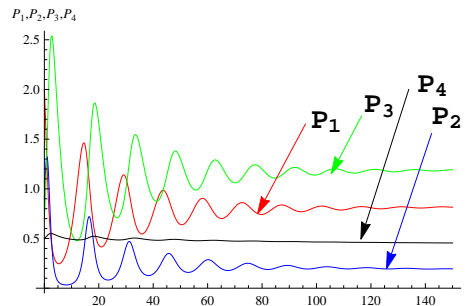
(b) Equilibrium point$(0.8337, 0.1760,$
$1.208, 0.4407)$

Figure 4.3: Solution curves coverage to the endemic equilibrium for the model system (4.2.1), showing that all species survive and ultimately evolve to their steady states, the parametric values are outlined for (a) in Table 4.6, and (b) in equation (4.5.1).
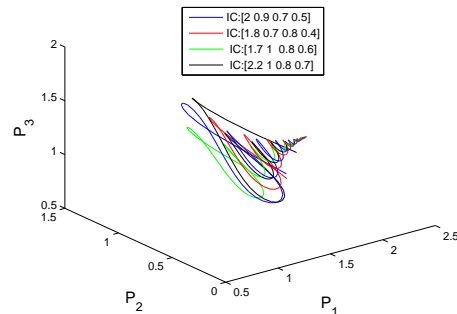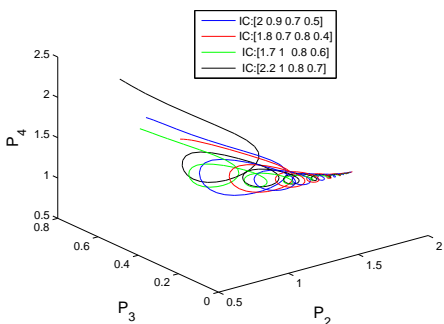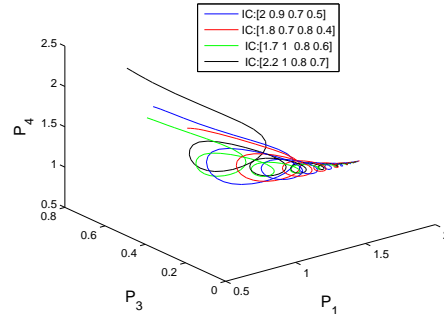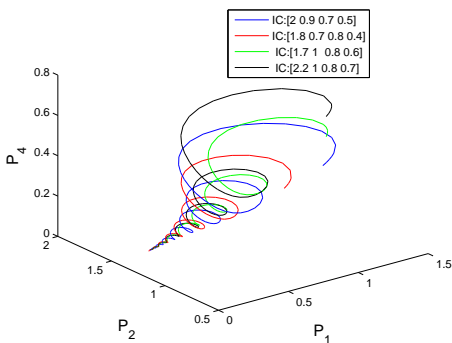
Figure 4.4: Phase portrait of model system (4.2.1) and equilibrium point
$(1.1273, 0.8652, 0.7545, 0.8579)$

.

4.5.2 Biological Interpretation of the Parameters Using Sensitivity Analysis

A mathematical model includes the parameters that increase the complexity of the model and make it more complicated to analyze the parameters that occur in the

model. Therefore, parameter sensitivity helps us determine theimportance of the parameter. Several factors influence the basic reproduction number, including the period of infectivity of affected individuals, the infectiousness of the pest, and the number of susceptible pests in the population that the infected pest contacts. The sensitivity index assesses the relative change in a state variable P_1, P_2, P_3, and P_4, which results from a relative change in the parameters. The basic reproduction number is more sensitive to the parameterwith the highest sensitivity index value (ρ, μ, α, δ, r_1, and K_1) and least sensitive to parameter with the lowest sensitive index value in the Table 4.4 and Table 4.5. Figure 4.5 and Figure 4.6 represent the dynamic behavior of P_1, P_2, P_3, and P_4 of the system (4.2.1), when the value of one parameter varies and the other parameters remain constant. We consider the only parameters ρ, μ, α, δ, r_1, and K_1 as these parameters have a positive sensitivity index value. In Figure 4.5a, Figure 4.5b and Figure 4.5d, we see that population density P_1, P_2, and P_4 decrease when the value of ρ increases. Further, the infected pest population P_3 increases, the value of ρ increases in Figure 4.5c. In Figure 4.5f–4.5h, the value of μ increases, the population density of P_2 and P_3 increases but the population density of P_4 decreases. Figure 4.5i–4.5l shows that the population density of P_1, P_2, P_3, and P_4 approximately does not change when the value of α changes. In Figure 4.6a–4.6d, the population density of P_1, P_2, and P_3, approximately does not change when the value of δ increases but P_4 decreases. If the value of r_1 increases, we see a rise in the population density of P_1, P_2, and P_3 while the population density of P_4 approximately has same value in Figure 4.6e–4.6h. In Figure 4.6i–4.6l, the population density of P_1, P_2, and P_3 increases when the value of K_1 increases while the population density of P_4 decreases. In Figure 4.5c, Figure 4.5g, Figure 4.6c and Figure 4.6k, the population density of infected pest population P_3 decreases when parameter values decrease. This is because, the basic reproduction number R_{01}, is less than unity at $\rho = 0.09$ and $\mu = 0.34$. Similarly, R_{03} is less than unity at $\alpha = 0.23$ and R_{04} is less than unity at $\delta = 0.06$, $r_1 = 0.39$, and $K_1 = 2.2$.
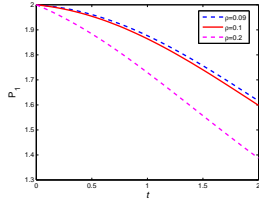
(a) Variation of P_1 when ρ varies
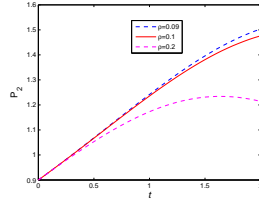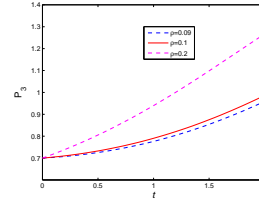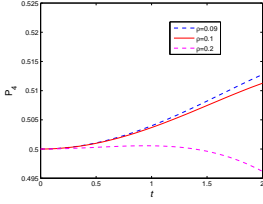
(b) Variation of P_2 when ρ varies

(c) Variation of P_3 when ρ varies

(d) Variation of P_4 when ρ varies
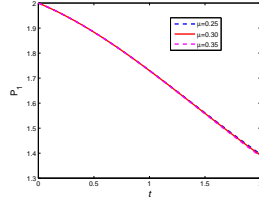
(e) Variation of P_1 when μ varies
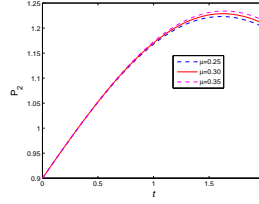
(f) Variation of P_2 when μ varies
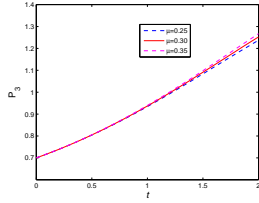
(g) Variation of P_3 when μ varies
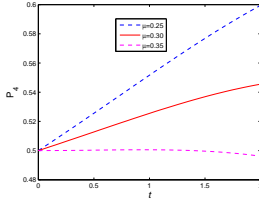
(h) Variation of P_4 when μ varies
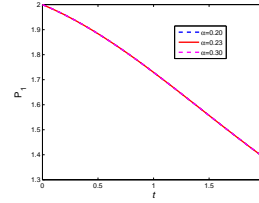
(i) Variation of P_1 when α varies
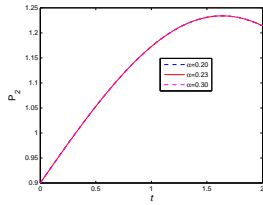
(j) Variation of P_2 when α varies
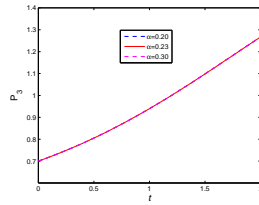
(k) Variation of P_3 when α varies
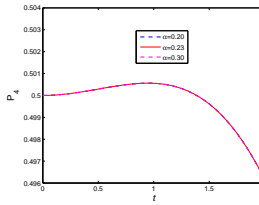
(l) Variation of P_4 when α varies

Figure 4.5: Dynamical behavior of the P_1, P_2, P_3, and P_4 of the system (4.2.1) and parameter values are taken from Table 4.6.
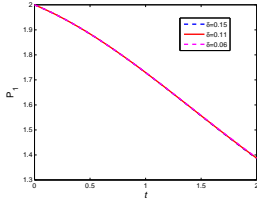
(a) Variation of P_1 when δ varies
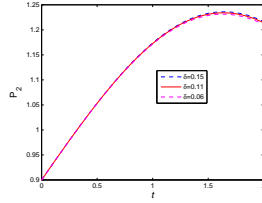
(b) Variation of P_2 when δ varies
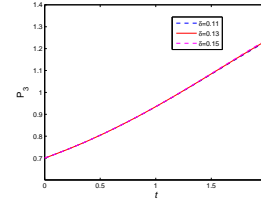
(c) Variation of P_3 when δ varies
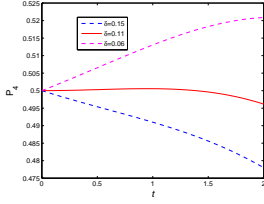
(d) Variation of P_4 when δ varies
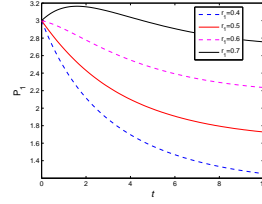
(e) Variation of P_1 when r_1 varies
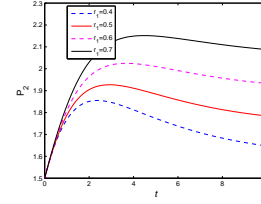
(f) Variation of P_2 when r_1 varies
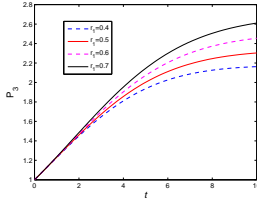
(g) Variation of P_3 when r_1 varies
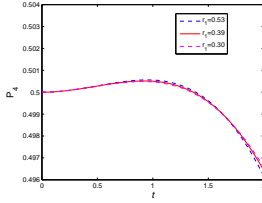
(h) Variation of P_4 when r_1 varies
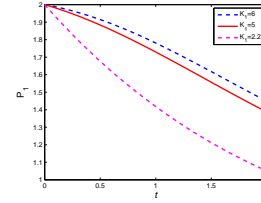
(i) Variation of P_1 when K_1 varies
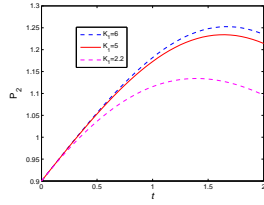
(j) Variation of P_2 when K_1 varies
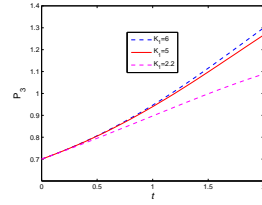
(k) Variation of P_3 when K_1 varies
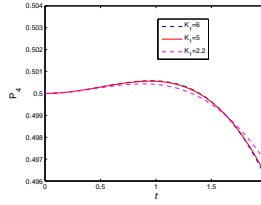
(l) Variation of P_4 when K_1 varies

Figure 4.6: Dynamical behavior of the P_1, P_2, P_3, and P_4 of the system (4.2.1) and parameter values are taken from Table 4.6.

4.6 Formulation and Application of Optimal Control Problem

Despite a marked rise in pesticide consumption, yield loss has not decreased dramatically over the last 40 years. However, pesticide usage has enabled farmers to change output strategies to boost crop yield without facing higher losses due to increased pests [51]. The definition of crop management involves a threshold concept

for the implementation of pest control measures and a decline in the pesticide quantity implemented to an economically and environmentally appropriate standard. Biological management assistance may be obtained from a natural enemy of the predator, a pest of the pest. These may be parasitic insects that eat the other pest. Organic species are used since not all pesticides are chemicals, such as biological pesticides, botanical pesticides, and bio–engineered species. Pyrethrum, distilled with chrysanthemums, is an example of a botanical pesticide. We have presented the system's dynamic behaviors across the preceding section using the natural enemies of the pest, namely the predator. But control of the pest may not always be feasible by using only such types of controls. So we need to take some more control measures. Usage of pesticides is very helpful for this circumstance. Other side, pesticides used extensively in crop development can degrade and harm the ecosystem of microorganisms in the soil. Several pesticides are persistent soil pollutants, whose effects may decades and have a negative influence on soil conservation [141]. Many research focuses on acute effects, failing to consider the chronic impacts of pesticides on soil quality [36]. Biomass is animal manure and a plant substance used for fertilizing the land. For instance, woods or forest leftovers, garbage from crop production (bagasse, straw), horticulture, food manufacturing, animal farming (nitrogen and phosphorus–rich manure), or human excrement from sewage treatment plants [25]. Despite the fact that burning plant–based biomass emits CO_2, it is still considered a renewable energy source since photosynthesis recycles CO_2 into new crops. Because a considerable amount of CO_2 is transported to the soil during each cycle, the efficient emission of CO_2 into the atmosphere can turn negative in certain instances [244]. The microbial biomass decomposes biotic and abiotic residues to release CO_2 and existing plant nutrients. Microbial biomass tends to rise in agricultural systems that yield plant wastes. The size of the microbial biomass is influenced by soil parameters such as pH, clay, and the accessibility of organic carbon. Bacteria and fungus make up the majority of the microbial biomass, which decompose agricultural wastes and organic materials in the soil. This process makes nutrients like nitrogen (N) accessible for plant absorption in the soil. Approximately half of a soils profile's microbial biomass is found in the top 10 cm [239]. [203, 217] used pesticide controls in their works to decrease the cost of pests. Furthermore, since the pesticide is generally some type of poison, it more or less affects all the system's creatures and therefore also affects the predator popula-

tion that is not taken into consideration in [217]. In this context, the control $u_1(t)$ and $u_2(t)$ represent the rate of application of pesticide and rate of application of biomass, respectively. The control $u_1(t)$ and $u_2(t)$ are the effort aimed at preventing pest density and increasing the crop density as well as the fertility of the land, respectively. The density of the plant is increased by $a_1 u_1 P_1$. Further, the susceptible, infected pests, and predator population are minimized by $b_1 u_2 P_2$, $b_2 u_2 P_3$, and $b_3 u_2 P_4$, respectively. We consider that the control of pesticides is more efficient for the infected than the susceptible one, so we take distinct death rates, namely, b_1 and b_2. We assume that the density of the predator population reduces at a rate of b_3 because of the pesticide control u_1. Therefore the model (4.2.1) is modified as follows

$$
\begin{cases}
\frac{dP_1}{dt} = r_1 P_1 \left(1 - \frac{P_1}{K_1}\right) - \lambda P_1 P_2 - \rho P_1 P_3 + a_1 u_1 P_1, \\
\frac{dP_2}{dt} = \lambda P_1 P_2 - \sigma P_2 + r_2 P_2 \left(1 - \frac{P_2 + \eta P_3}{K_2}\right) - \alpha P_2 P_3 - \beta P_2 P_4 - b_1 u_2 P_2, \\
\frac{dP_3}{dt} = \alpha P_2 P_3 + \rho P_1 P_3 - \gamma P_3 P_4 - \omega P_3 - b_2 u_2 P_3, \\
\frac{dP_4}{dt} = l\beta P_2 P_4 + (n_1 - n_2) \gamma P_3 P_4 + d \left(1 - \frac{P_2 + \eta P_3}{K_2}\right) P_4 - \mu P_4 - \delta (P_4)^2 - b_3 u_2 P_4,
\end{cases}
\tag{4.6.1}
$$

subject to the initial conditions

$$
P_1(0) = P_{10} \geqslant 0, \ P_2(0) = P_{20} \geqslant 0, \ P_3(0) = P_{30} \geqslant 0 \text{ and } P_4(0) = P_{40} \geqslant 0.
\tag{4.6.2}
$$

Additionally, these pesticide controls u_1 and u_2 should be time–dependent because it is used based on needs. Since our main objective in this section is to decrease the number of pests as well as increase the fertility of the land, we must bear in mind both its negative impact on the environment and its costs. Unless more is used, the crops may become hazardous. Thus, the objective is to minimize the population density of pests at the final time of controls while increasing the population density as well as minimizing the cost. The control strategies are applied to costs such as the cost of application of pesticide and cost of biomass. For the achievement of goals, we minimize the following objective functional over the time over time–dependent controls $u_1(t)$ and $u_2(t)$:

$$
J(u_1, u_2) = \min_{(u_1, u_2)} \int_0^{t_f} (A_1 P_2(t) + A_2 P_3(t) - B_1 P_1(t) + A_3 u_1^2(t) + A_4 u_2^2(t)) dt,
\tag{4.6.3}
$$

subject to the system of differential equations (4.6.1) along with the initial conditions (4.6.2). The weight constants B_1, A_1, A_2, A_3, and A_4 are non–negative constants that balance the relative importance of terms in $J(u_1, u_2)$ [54]. The terms $A_1 P_2(t) + A_2 P_3(t)$ and $B_1 P_1(t))$ in the objective functional give the respective the density of pests and the density of plant over the time period t_f being modeled. The term $A_3 u_1^2(t)$ represents the cost for application of biomass and $A_4 u_2^2(t)$ represents the cost for application of pesticides. Moreover, A_3 and A_4 are associated with the square of the pesticide control and square of the biomass control. The square of the control parameters are used to eliminate the bad side effects of the control variables [80, 218, 219]. The objective functional $J(u_1, u_2)$ is a continuously differentiable function of state variables P_1, P_2, P_3, P_4, and control variable u_1 and u_2. With the help of Pontryagins maximum principle [122], we obtain the necessary criteria for evaluating a positive control value for which the J is optimized. It is regarded to be the optimal control if this feasible control happens [30, 200]. Now we need to determine a control u_1^* and u_{2*} such that

$$J(u_1^*, \, u_2^*) = \min_{u_1, \, u_2 \in U} J(u_1, \, u_2), \tag{4.6.4}$$

where $U = \{(u_1(t), \, u_2(t)) : \text{is measurable and } 0 \leqslant u_1(t) \leqslant 1 \, , \, 0 \leqslant u_2(t) \leqslant 1 \text{ for } t \in [0, t_f]\}$ is the set for the controls. In order to demonstrate the existence of an optimal control problem, the state functions of the eco–epidemiological model must be bounded. The results of positivity and boundedness are based on the structure of the system. To use Pontryagins maximum principle [122] on the time–dependent controls, we first need existence of optimal controls, characterize the time–dependent controls, and adjoint equations for system (4.6.1). Now using the results in [41, 240], we state and prove the following theorem.

Theorem 4.6.1. There exist optimal controls $(u_1^*, u_2^*) \in U$, which minimize the objective functional, $J(u_1, u_2)$, subject to the state system (4.6.1).

Proof. To determine the existence of optimal control to the system, we take a result from [41, 240]. To demonstrate the existence of optimum control, the following requirements must be met:

(i) The set of controls and associated state variables is not empty.

(ii) The control set is convex and closed.

(iii) The right–hand side of the state system (4.6.1) is bounded by a linear function in the state

and control variables (u_1, u_2).

(iv) The integrand of the objective functional is convex on U.

(v) There exist constants c_1, $c_2 > 0$ and $n > 1$ such that the integrand of the objective functional fulfills

$$A_1 P_2 + A_2 P_3 - B_1 P_1 + A_3 u_1^2 + A_4 u_2^2 \geqslant c_1 (|u_1|^2 + |u_2|^2)^{\frac{n}{2}} - c_2.$$

To verify the first and second conditions, the state and control variables are non–empty and non–negative. The control variables u_1 and u_2 are also convex and closed by the given definition, which gives the condition (ii). For the condition (iii), the control model system can be expressed as a linear function of control variables υ with the coefficients as functions of time and state variables $f(t, P, \upsilon) = \gamma(t, P) + \xi(t, P)\upsilon$, where, $\upsilon = (u_1, u_2) \in U$, $P = (P_1, P_2, P_3, P_4)$, $f(t, P, \upsilon)$ be the right–hand of (4.6.1),

$$\gamma(t,P) = \begin{pmatrix} r_1 P_1 \left(1 - \frac{P_1}{K_1}\right) - \lambda P_1 P_2 - \rho P_1 P_3 \\ \lambda P_1 P_2 - \sigma P_2 + r_2 P_2 \left(1 - \frac{P_2 + \eta P_3}{K_2}\right) - \alpha P_2 P_3 - \beta P_2 P_4 \\ \alpha P_2 P_3 + \rho P_1 P_3 - \gamma P_3 P_4 - \omega P_3 \\ l\beta P_2 P_4 + (n_1 - n_2)\gamma P_3 P_4 + d\left(1 - \frac{P_2 + \eta P_3}{K_2}\right)P_4 - \mu P_4 - \delta (P_4)^2 \end{pmatrix}, \quad \xi(t, P) = \begin{pmatrix} a_1 P_1 & 0 \\ 0 & -b_1 P_2 \\ 0 & -b_2 P_3 \\ 0 & -b_3 P_4 \end{pmatrix},$$

$$|f(t,P,\upsilon)| \leqslant \left\| \begin{pmatrix} r_1 & 0 & 0 & 0 \\ 0 & \lambda P_1 + r_2 & 0 & 0 \\ 0 & 0 & \alpha P_2 + \rho P_1 & 0 \\ 0 & 0 & 0 & l\beta P_2 + (n_1 - n_2)\gamma P_3 + d \end{pmatrix} \begin{pmatrix} P_1 \\ P_2 \\ P_3 \\ P_4 \end{pmatrix} \right\|$$
$$+ \left\| \begin{pmatrix} a_1 P_1 & 0 \\ 0 & -b_1 P_2 \\ 0 & -b_2 P_3 \\ 0 & -b_3 P_4 \end{pmatrix} \begin{pmatrix} u_1 \\ u_2 \end{pmatrix} \right\|.$$

Using Boundedness of the system in Section 4.3, there exist constants $C_1 > 0, C_2 > 0, C_3 > 0$, and $C_4 > 0$ such that $0 < P_1 \leqslant C_1, 0 < P_2 \leqslant C_2, 0 < P_3 \leqslant C_3$ and $0 < P_4 \leqslant C_4$, for all $t \in [0, t_f]$.

Therefore,

$$|f(t,P,\upsilon)| \leqslant \left| \begin{pmatrix} r_1 & 0 & 0 & 0 \\ 0 & \lambda C_1 + r_2 & 0 & 0 \\ 0 & 0 & \alpha C_2 + \rho P_1 & 0 \\ 0 & 0 & 0 & l\beta C_2 + (n_1 - n_2)\gamma C_3 + d \end{pmatrix} \begin{pmatrix} P_1 \\ P_2 \\ P_3 \\ P_4 \end{pmatrix} \right|$$

$$+ \left| \begin{pmatrix} a_1 C_1 & 0 \\ 0 & -b_1 C_2 \\ 0 & -b_2 C_3 \\ 0 & -b_3 C_4 \end{pmatrix} \begin{pmatrix} u_1 \\ u_2 \end{pmatrix} \right|$$

$$\leqslant K_1 |P| + K_2 |\upsilon|,$$

where K_1 and K_2 are the upper bound of the matrices. Hence, we see that the right–hand side is bounded by a sum of the state and the control variables. Therefore, condition (iii) is satisfied. The integrand in the objective functional, $A_1 P_2 + A_2 P_3 - B_1 P_1 A_3 u_1^2 + A_3 u_2^2$, is clearly convex on u_1 and u_2, which gives the condition (iv). For the last condition (v),

$$A_1 P_2 + A_2 P_3 - B_1 P_1 + A_3 u_1^2 + A_4 u_2^2 \geqslant A_3 u_1^2 + A_4 u_2^2 - B_1 P_1,$$

$$\geqslant min(A_3, A_4)(u_1^2 + u_2^2) - B_1 P_1,$$

$$\geqslant c_1(u_1^2 + u_2^2) - c_2.$$

Hence, $A_1 P_2 + A_2 P_3 - B_1 P_1 + A_3 u_1^2 + A_4 u_2^2 \geqslant c_1(|u_1|^2 + |u_2|^2)^{\frac{n}{2}} - c_2$, where, $c_1 = min(A_3, A_4)$, $c_2 = B_3 |P_1|$, and $n = 2 > 1$.

Using all conditions we can conclude that there exists an optimal control (u_1^*, u_1^*) such that

$$J(u_1^*, u_2^*) = \min_{u_1, u_2 \in \Omega} J(u_1, u_2),$$

$\square$

4.6.1 Characterization of the Optimal Control

The time–dependent controls and adjoint equations are characterised. [122] is used to obtain the necessary conditions for the optimal control pair based on Pontryagin's

132

maximum principle. The following is an expression of the Hamiltonian:

$$
\begin{aligned}
H = \; & A_1 P_2 + A_2 P_3 - B_1 P_1 + A_3 u_1^2 + A_3 u_2^2 \\
& + \lambda_1 \left(P_1 r_1 \left(1 - \frac{P_1}{K_1} \right) - \lambda P_1 P_2 - P_1 P_3 \rho + a_1 u_1 P_1 \right) \\
& + \lambda_2 \left(-dP_2 + P_2 r_2 \left(1 - \frac{\eta P_3 + P_2}{K_2} \right) - \alpha P_3 P_2 - \beta P_4 P_2 + \lambda P_1 P_2 - b_1 P_2 u_2 \right) \\
& + \lambda_3 \left(\alpha P_2 P_3 - \gamma P_4 P_3 + P_1 P_3 \rho + P_3 (-\omega) - b_2 P_3 u_2 \right) \\
& + \lambda_4 \left(dP_4 \left(1 - \frac{\eta P_3 + P_2}{K_2} \right) + \beta l P_2 P_4 + \gamma (n_1 - n_2) P_3 P_4 - \delta P_4^2 - \mu P_4 - b_3 P_4 u_2 \right),
\end{aligned}
$$

where λ_1, λ_2, λ_3, and λ_4 are adjoint functions associated with the state functions P_1, P_2, P_3, and P_4, respectively.

Theorem 4.6.2. If u_1^* and u_2^* be an optimal control which minimize $J(u_1, u_2)$. Let $P_1^*(t)$, $P_2^*(t)$, $P_3^*(t)$, and $P_4^*(t)$ are optimal state solutions for the control system (4.6.1), then there exist adjoint variables $\lambda_1(t), \lambda_2(t), \lambda_3(t)$, and $\lambda_4(t)$ satisfying the following

$$
\left\{
\begin{aligned}
\frac{d\lambda_1}{dt} =\; & -\lambda_1 \left(a_1 u_1 + r_1 \left(1 - \frac{P_1}{K_1} \right) - \frac{P_1 r_1}{K_1} - \lambda P_2 - P_3 \rho \right) + B_1 - \lambda_3 P_3 \rho - \lambda \lambda_2 P_2, \\
\frac{d\lambda_2}{dt} =\; & -A_1 - \lambda_2 \left(-b_1 u_2 - d + r_2 \left(1 - \frac{\eta P_3 + P_2}{K_2} \right) - \frac{P_2 r_2}{K_2} - \alpha P_3 - \beta P_4 + \lambda P_1 \right) + \lambda \lambda_1 P_1 \\
& - \lambda_4 \left(\beta l P_4 - \frac{dP_4}{K_2} \right) - \alpha \lambda_3 P_3 \\
\frac{d\lambda_3}{dt} =\; & -A_2 + \lambda_3 \left(b_2 u_2 - \alpha P_2 + \gamma P_4 - P_1 \rho + \omega \right) + \lambda_2 \left(\frac{\eta P_2 r_2}{K_2} + \alpha P_2 \right) + \lambda_1 P_1 \rho \\
& \lambda_4 + \left(\frac{d\eta P_4}{K_2} - \gamma (n_1 - n_2) P_4 \right) \\
\frac{d\lambda_4}{dt} =\; & -\lambda_4 \left(-b_3 u_2 + d \left(1 - \frac{\eta P_3 + P_2}{K_2} \right) + \beta l P_2 - \mu + \gamma (n_1 - n_2) P_3 - 2\delta P_4 \right) + \beta \lambda_2 P_2 + \gamma \lambda_3 P_3.
\end{aligned}
\right.
$$

$$(4.6.5)$$

with transversality conditions are

$$
\lambda_i(T_f) = 0, \; i = 1, 2, 3, 4.
$$

Further, the optimal control variable $u_1^*(t)$ and $u_2^*(t)$ that minimize $J(u_1, u_2)$ are given by

$$
u_1^*(t) = \min \left\{ \max \left\{ 0, \; -\frac{a_1 \lambda_1 P_1}{2A_3} \right\}, 1 \right\},
$$

$$
\text{and } u_2^*(t) = \min \left\{ \max \left\{ 0, \; \frac{b_1 \lambda_2 P_2 + b_2 \lambda_3 P_3 + b_3 \lambda_4 P_4}{2A_4} \right\}, 1 \right\}.
$$

Proof. The partial derivatives of the Hamiltonian, H, with respect to each state variable are

133

used to evaluate the adjoint equations. That is,

$$\lambda_1'(t) = -\frac{\partial H}{\partial P_1}, \ \lambda_2'(t) = -\frac{\partial H}{\partial P_2}, \ \lambda_3'(t) = -\frac{\partial H}{\partial P_3}, \ \lambda_4'(t) = -\frac{\partial H}{\partial P_4}.$$

Differentiating the Hamiltonian, H, with respect to the controls (u_1, u_2) at t can be used to predict how the control would behave. Where, $0 < u_j < 1$ for all $(j = 1, 2)$

$\frac{\partial H}{\partial u_1} = 0 = a_1 \lambda_1 P_1 + 2A_3 u_1^*$ at $u_1 = u_1^*(t) \Rightarrow u_1^* = -\frac{a_1 \lambda_1 P_1}{2A_3}$,

$\frac{\partial H}{\partial u_2} = 0 = 2A_4 u_2^* - b_1 \lambda_2 P_2 - b_2 \lambda_3 P_3 - b_3 \lambda_4 P_4$, at $u_2 = u_2^*(t) \Rightarrow u_2^* = \frac{b_1 \lambda_2 P_2 + b_2 \lambda_3 P_3 + b_3 \lambda_4 P_4}{2A_4}$. There-

fore, by using the bounds for the control [200], $u_1(t)$ and $u_2(t)$, we get

$$u_1^* = min\left\{max\left\{0, -\frac{a_1 \lambda_1 P_1}{2A_3}\right\}, 1\right\}, \ u_2^* = min\left\{max\left\{0, \frac{b_1 \lambda_2 P_2 + b_2 \lambda_3 P_3 + b_3 \lambda_4 P_4}{2A_4}\right\}, 1\right\}.$$

$\square$

4.6.2 Optimality System

The optimality system consists of the state system and adjoint system with initial and transversal conditions with the characterization of optimal control. The following optimality system characterizes the optimal control.

$$\frac{dP_1}{dt} = r_1 P_1 \left(1 - \frac{P_1}{K_1}\right) - \lambda P_1 P_2 - \rho P_1 P_3 + a_1 P_1 min\left\{max\left\{0, -\frac{a_1 \lambda_1 P_1}{2A_3}\right\}, 1\right\},$$

$$\frac{dP_2}{dt} = \lambda P_1 P_2 - \sigma P_2 + r_2 P_2 \left(1 - \frac{P_2 + \eta * P_3}{K_2}\right) - \alpha P_2 P_3 - \beta P_2 P_4$$

$$- b_1 P_2 min\left\{max\left\{0, \frac{b_1 \lambda_2 P_2 + b_2 \lambda_3 P_3 + b_3 \lambda_4 P_4}{2A_4}\right\}, 1\right\},$$

$$\frac{dP_3}{dt} = \alpha P_2 P_3 + \rho P_1 P_3 - \gamma P_3 P_4 - \omega P_3 - b_2 P_3 min\left\{max\left\{0, \frac{b_1 \lambda_2 P_2 + b_2 \lambda_3 P_3 + b_3 \lambda_4 P_4}{2A_4}\right\}, 1\right\},$$

$$\frac{dP_4}{dt} = l\beta P_2 P_4 + (n_1 - n_2)\gamma P_3 P_4 + d\left(1 - \frac{P_2 + \eta P_3}{K_2}\right)P_4 - \mu P_4 - \delta(P_4)^2$$

$$- b_3 P_4 min\left\{max\left\{0, \frac{b_1 \lambda_2 P_2 + b_2 \lambda_3 P_3 + b_3 \lambda_4 P_4}{2A_4}\right\}, 1\right\},$$

$$\frac{d\lambda_1}{dt} = -\lambda_1 \left(a_1 min \left\{ max \left\{ 0, -\frac{a_1 \lambda_1 P_1}{2A_3} \right\}, 1 \right\} + r_1 \left(1 - \frac{P_1}{K_1} \right) - \frac{P_1 r_1}{K_1} - \lambda P_2 - P_3 \rho \right)$$

$$+ B_1 - \lambda_3 P_3 \rho - \lambda \lambda_2 P_2,$$

$$\frac{d\lambda_2}{dt} = -A_1 - \lambda_2 \left(-d + r_2 \left(1 - \frac{\eta P_3 + P_2}{K_2} \right) - \frac{P_2 r_2}{K_2} - \alpha P_3 - \beta P_4 + \lambda P_1 \right) + \lambda \lambda_1 P_1$$

$$- \lambda_4 \left(\beta l P_4 - \frac{dP_4}{K_2} \right) - \alpha \lambda_3 P_3 + \lambda_2 b_1 \, min \left\{ max \left\{ 0, \frac{b_1 \lambda_2 P_2 + b_2 \lambda_3 P_3 + b_3 \lambda_4 P_4}{2A_4} \right\}, 1 \right\},$$

$$\frac{d\lambda_3}{dt} = -A_2 + \lambda_3 \left(b_2 u_2 - \alpha P_2 + \gamma P_4 - P_1 \rho + \omega \right) + \lambda_2 \left(\frac{\eta P_2 r_2}{K_2} + \alpha P_2 \right) + \lambda_1 P_1 \rho$$

$$\lambda_4 + \left(\frac{d \eta P_4}{K_2} - \gamma (n_1 - n_2) P_4 \right) + \lambda_3 b_2 \, min \left\{ max \left\{ 0, \frac{b_1 \lambda_2 P_2 + b_2 \lambda_3 P_3 + b_3 \lambda_4 P_4}{2A_4} \right\}, 1 \right\},$$

$$\frac{d\lambda_4}{dt} = -\lambda_4 \left(d \left(1 - \frac{\eta P_3 + P_2}{K_2} \right) + \beta l P_2 - \mu + \gamma (n_1 - n_2) P_3 - 2\delta P_4 \right) + \beta \lambda_2 P_2 + \gamma \lambda_3 P_3$$

$$+ \lambda_4 b_3 \, min \left\{ max \left\{ 0, \frac{b_1 \lambda_2 P_2 + b_2 \lambda_3 P_3 + b_3 \lambda_4 P_4}{2A_4} \right\}, 1 \right\},$$

with initial conditions

$$P_1(0) = P_{10} \geqslant 0, \ P_2(0) = P_{20} \geqslant 0, \ P_3(0) = P_{30} \geqslant 0 \text{ and } P_4(0) = P_{40} \geqslant 0,$$

and transversality equations

$$\lambda_i(T_f) = 0, \ i = 1, 2, 3, 4.$$

4.7 Numerical Simulations for Optimal Control Problem

Because this study is qualitative, and it is not based on any survey and census. We consider taking a simulated set of parameters for the objective of computation. This is one of the limitations of our model and the same is persistent in the huge published literature. Therefore, because our aim in this issue is to reduce pests and save crops, we consider the value of $A_1 = 1$, $A_2 = 1$, $A_3 = 1$, and $B_1 = 1$. We use this control within 2 unit time, which could be in hours, days, weeks, or even months. Next, we assume that the initial values for the crop, susceptible pest, infected pest, and natural enemy of the pest are $P_1(0) = 2$, $P_2(0) = 1.5$, $P_3(0) = 0.7$, and $P_4(0) = 0.5$ with appropriate u-nits, respectively. We use Runge-Kutta fourth–order iterative method to numerically solve the optimality system. The forward–backward sweep method for the iterative

procedure of the optimality system is given in [200, 218, 219]. The forward–backward sweep method convergence is based on the study done by [234]. In Figure 4.7, we describe the solution curves for the four–state variables, both in appearance and non–appearance of the control. Figure 4.7(a) indicates that the population density of crops is approximately 6 and 1.8 unit at 2 unit time in the presence of control and the absence of control, respectively. Similarly, Figure 4.7(b), Figure 4.7(c) and Figure 4.7(d) show that the population density of P_1, P_2, and P_3 is approximately 0.85, 0, 0.1 units in the presence of control and 1.2, 1.2, 0.6 units in the absence of control, respectively. We observe that the population density P_3 decreases in the presence of control. In Figure 4.7(d), the population density P_4 tends to zero in the presence of control as there are two factors; first, the P_4 primarily depends on the P_3 population density and P_3 population density decreases with respect to time in the presence of control, second, control is applied on P_4. Thus, the usage of optimal control is found to eliminate a much greater number of pests than in the absence of control. We choose some different parameters to see the variation in performance of a population density of P_1, P_2, P_3, and P_4. In comparison to parameters of Figure 4.7, we use the parameters, i.e., $A_1 = 2$, $A_2 = 2$ $\alpha = 0.2$, $\sigma = 0.3$, $\beta = 0.3$, $\omega = 0.3$, $\mu = 0.25$, $r_2 = 0.5$, $l = 1$, $b_1 = 1$, $b_2 = 1$, and $b_3 = 1$ in Figure 4.8 and the rest of the parameters are the same. Figure 4.8(a) shows that the population density of P_1 is approximately 3.9 units in the presence of control and 1.2 units in the absence of control at 2 unit time compared to the Figure 4.7(a). Further, Figure 4.8(b), Figure 4.8(c), and Figure 4.8(d) show that the population density is approximately 1, 0.25, 0.2 unit in the presence of control and 1.8, 0.7, 1.2 unit in the absence of control at time 2 unit, respectively. In Figure 4.8, the control parameters of pesticides, i.e., $b_1 = 1$, $b_2 = 1$, and $b_3 = 1$, are used. Thus, pesticides are applied two times, three times, and two times less than on P_2, P_3, and P_4, respectively, compared to Figure 4.7. This is also evident from Figure 4.7(d) that the natural enemy of pests suffers much due to the use of pesticide control. It happens because the implementation of pesticide control dramatically reduces the pest population and the natural enemy of the pest population is primarily dependent on pests for their meals. Thus, we can conclude that applying the optimal control of pesticides not only minimizes the pest population but also decreases the natural enemy of the pest populations. Figure 4.7(e) and Figure 4.7(f) represent the variation of optimal control variables u_1 and u_2. Figure 4.7(g), Figure 4.7(h), Figure 4.7(i) and

Figure 4.7(j) represent the variation of adjoint variables in the presence control. Figure 4.8(e) and Figure 4.8(f) show the variation of control variables with respect to time t. From Figure 4.7(e) and Figure 4.7(f), we observe that the control variables; the rate of application of biomass u_1 and rate of application of pesticide u_2 are maximum at approximately 1.4 and 0.7 unit time, respectively. Similarly, in Figure 4.8(e) and Figure 4.8(f), u_1 and u_2 are maximum at approximately 1.7 and 1.1 unit time, respectively. Thus, according to the need for pesticide decreases after some time within 2 unit time. Figure 4.8(g), Figure 4.8(h), Figure 4.8(i), and Figure 4.8(j) show the variation of adjoint variables. We see that a comparison of the control strategy with and without is examined. Control criteria have a significant impact on reducing pest individuals and controlling disease dynamics. Further, if there is a high incidence, the controls would be sufficient for a longer time. Optimal control is more efficient in terms of reducing the number of pests and decrease the cost of the two control strategies. Based on the simulation work, we observe that the optimal control variables are essential for pest elimination. Thus, the application of control variables is useful to reduce the pest population as well as increasing crop production.
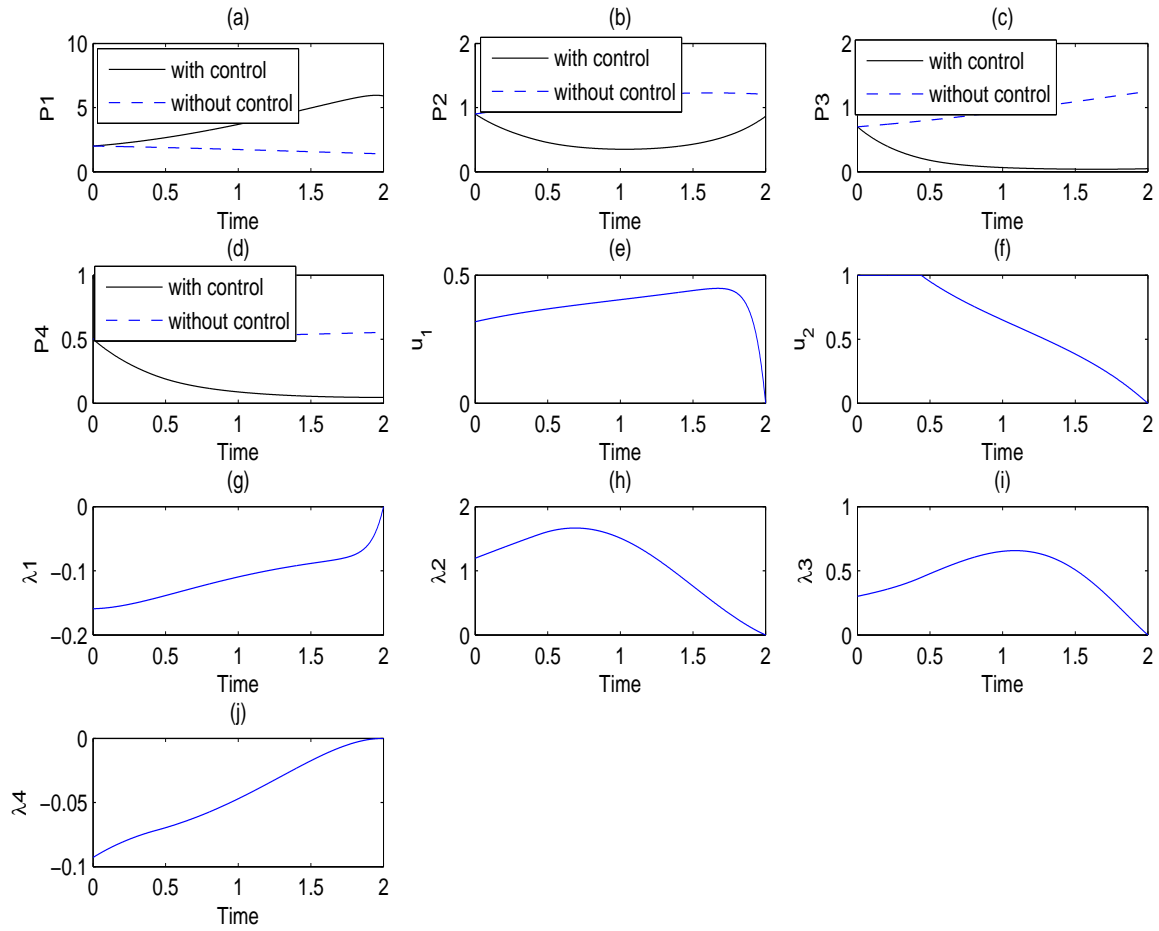
Figure 4.7: Comparison between the figures of individuals with control versus without control, which represent the results for prey, susceptible pest, infected pest and natural enemy of pest, control and adjoint variables with respect to time, where the values of parameters are $A_1 = 1$, $A_2 = 1$, $A_3 = 1$, $B_1 = 1$, $r_1 = 0.53$, $K_1 = 5$, $\lambda = 0.3$, $\rho = 0.2$, $\sigma = 0.2$, $d = 0.4$, $r_2 = 0.4$, $K_2 = 10$, $\eta = 1$, $\alpha = 0.4$, $\beta = 0.2$, $\mu = 0.35$, $\delta = 0.11$, $\omega = 0.4$, $\gamma = 0.2$, $l = 0.5$, $a_1 = 2$, $b_1 = 2$, $b_2 = 3$, $b_3 = 2$, $n_1 = 0.3$, $n_2 = 0.15$, $P_{10} = 2$, $P_{20} = 0.9$, $P_{30} = 0.7$, $P_{40} = 0.5$, and $t = 2$.
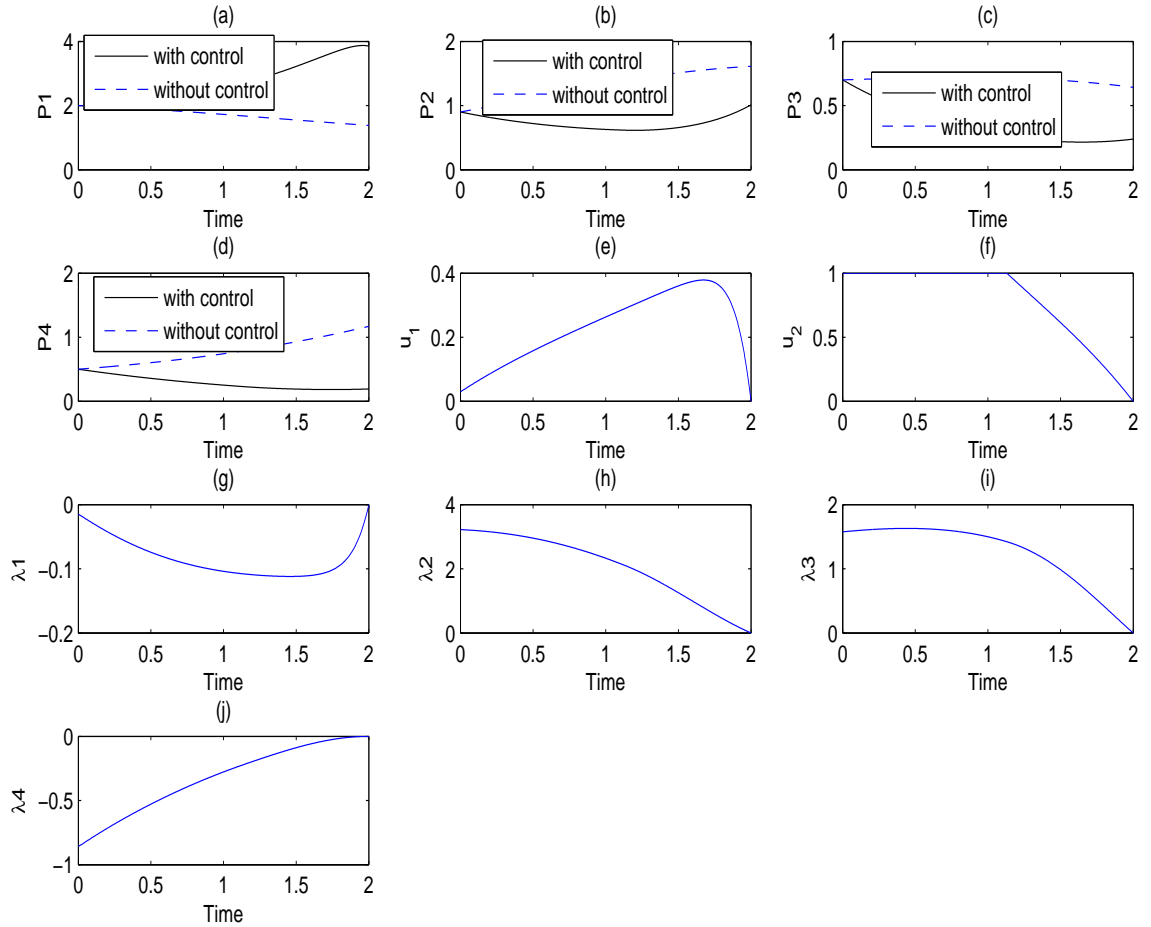
Figure 4.8: Comparison between the figures of individuals with control versus without control, which represent the results for prey, susceptible pest, infected pest and natural enemy of pest, control and adjoint variables with respect to time, where the values of parameters are $A_1 = 2$, $A_2 = 2$, $A_3 = 1$, $B_1 = 1$, $r_1 = 0.53$, $K_1 = 5$, $\lambda = 0.3$, $\rho = 0.2$, $\sigma = 0.25$, $d = 0.4$, $r_2 = 0.5$, $K_2 = 10$, $\eta = 1$, $\alpha = 0.2$, $\beta = 0.3$, $\mu = 0.25$, $\delta = 0.11$, $\omega = 0.3$, $\gamma = 0.45$, $l = 1$, $a_1 = 2$, $b_1 = 1$, $b_2 = 1$, $b_3 = 1$, $n_1 = 0.3$, $n_2 = 0.15$, $P_{10} = 2$, $P_{20} = 0.9$, $P_{30} = 0.7$, $P_{40} = 0.5$, and $t = 2$.

4.8 Discussion and Future Scope

This chapter has shown improvements in modeling agricultural processes by using dynamic simulation modeling. The model allowed three separate systems to explore user interactions; integrated crops, pests, and natural enemies of the pest. Input data on sustainability indices have been evaluated for the relative influence of modeling. This study uses a systemic approach to managing the pest population by combining

four possible methods: the productive use of predators, (ii) the spread of infectious diseases among the pest population, and (iii) utilization of chemical pesticides, and (iv) to provide additional food to the natural enemy of the pest. Our mathematical model is a prey-predator system with four state variables, namely, plant biomass P_1, susceptible pest P_2, infected pest P_3 and biological predator P_4. Additionally, we assumed that the predator species had an additional source of food to prevent themselves when there would be quite a small or negligible availability of the pest population. In terms of pest–related control, the importance of additional food is very important, because it helps protect predators (natural enemies of pests) when the number of pests is insufficient. It has been shown that the model $(4.2.1)$ is uniformly bounded and that all solutions are completely defined in the positive region. We perform a thorough analysis of the behavior of the system by examining the structure of the system through all its equilibria. The point of equilibrium, depending on various circumstances, is asymptotically stable locally. Also, it has been observed that all equilibrium points are conditionally feasible and locally asymptotically stable except the crop and susceptible pest-free equilibrium point that is unacceptable biologically. The coexistence of equilibrium solutions under various conditions has been examined. The effect of susceptible–infected pest in the presence of natural enemy has been studied as well various dynamical behaviour. The phase portrait of model system $(4.2.1)$ has been studied at coexistence equilibrium point. Moreover, all four species, i.e., P_1, P_2, P_2, and P_4 finally got their steady states at equilibrium point E_{14} under certain condition. The reproduction numbers, i.e., R_{01}, R_{02}, R_{03}, and R_{04} have been calculated at disease–free equilibrium in the presence of prey using the next–generation matrix approach. The parameters that have a significant influence on the basic reproduction number have been recognized. Further, the sensitivity indices of basic reproduction number, i.e., R_{01}, R_{02}, R_{03}, and R_{04} have been performed with respect to all the parameters using the numerical values of the parameters. It has been shown that the disease propagation dynamics are characterized by the basic reproduction number. In Section 4.5.2, the influence of one parameter changing its value, while the other remains the same has been studied in the model. Further, a mathematical model of prey–predator in the presence and absence of the control variables has been discussed. In order to minimize susceptible pest, the infected pest, and treatment expense, an optimal control strategy is developed and solved analytically. The control techniques that included

two control variables, the rate of organic biomass application and the rate of pesticide application, produced better outcomes, implying that both control factors are effective. Control u_1 enhanced soil fertility as well as crop output, whereas control u_2 reduced pest density. The simulation work is carried out to investigate the effect of combining both controls. Our numerical results showed that the application of control variables and pesticide has a big impact on the control system in agriculture. In Figure 4.7 and Figure 4.8, it has been observed that the optimal control acted as a stopover of the pest population and favorable conditions of crops. The main objective of this study is to know the impact of pest control on crops. Mathematical models are very important for understanding and providing useful abstract concepts of potential biological phenomena and ecological interactions that occur in pest control applications. The argument presented here has been led by two criteria: mathematical modeling, and a useful approach to control the pest. Besides, the types of pest control approaches discussed in our study can be briefly summarized as follows: chemical pesticides and biological (natural pest enemy) that are properly combined in the farming systems. Although there are a large number of effective mathematical model studies on the modeling of crop pest control strategies in the literature, the numerical studies are mainly carried out at the computational level. This is motivated by the key contribution of this research, which involves the use of appropriate numerical methods for managing pests. For this reason, the pest control model was chosen and reformulated in the sense of dynamical systems. Future development in this area would involve a multidisciplinary collaboration between epidemiologists, modelers, mathematical experts, and computational specialists to devise mathematical models that provide accurate prediction and explaining of field observations in actual ecosystems, with a view to developing mathematical models that focus on providing an accurate estimation between crops, pests and the natural enemy of agricultural pests. Future research may improve the practicality and relevance of the model by modifying a set of parameters, soil fertility variability, and ground use parameter values. Also, potential modeling efforts could have a useful effect by analyzing productivity for other regions of the world, comparing and contrasting the relative economic, ecological potential impact of strategic planning and the degree of incorporation on the viability of the manufacturing process. We expect that the decision–makers and farmers to consider the use of various modeling activities in the future. Researchers will give a more overview

of the essential elements of farming system productivity and ecology and economic sustainability and will establish more flexible management practices and development strategies for truly sustainable agriculture.

Chapter 5

A Prey Predator Model and Control of a Nematodes Pest Using Control in Banana: Mathematical Modelling and Qualitative Analysis

In the present chapter, this work provides a mathematical model for understanding the dynamics of banana–nematodes and its pest detection mechanisms to assist banana growers. Two factors are discussed: the mathematical model and the type of nematode pest management technique. The sensitivity analysis, local stability, global stability, and the dynamic behavior of the mathematical model are performed. The optimal control mathematical model for controlling nematode infestations is addressed. This mathematical model depicts several management strategies, such as the initial release of infected predators and the destruction of nematodes. Numerical simulations are used to demonstrate and validate the theoretical results.

5.1 Introduction

Banana is a globally important fruit crop. In 2011, 107 million tons of bananas were obtained in more than 130 countries, and the total trade value of 9 billion dollars out of 0.1% of the globe's farming fields [172]. According to [61], the global banana production increased at an annual growth rate of 3.2% between 2000 and 2017, achieving a record 114 million tons in 2017, up from approximately 67 million tons in 2000. The major sources are India, which produced an average of 29 million tons per annum between 2010 and 2017, and 11 million tons of China. As per the latest available data from 2017, approximately 5.6 million hectares of land are dedicated to banana global production [246]. In 2016, the global production of bananas and plantains was 148 million tonnes, India and China led by a combined total (for bananas alone) of 28% of worldwide [246]. The Philippines, Ecuador, Indonesia, and Brazil were also the leading producers, representing 20% of the world's total bananas and plants [247, 248]. In India, small–scale farmers are mainly grown for domestic consumption and income generation in the regions. Bananas play an essential role in reducing food crisis, as they are becoming a common staple food for most Indians. They have become more popular due to their adaptability to various climates, ease of manufacturing, and a ready market. Banana is mainly grown for food and the manufacture of fibers used in textiles. Banana soil is expected to be well–drained, with appropriate fertility and humidity levels. High, rich, pH–rich, loamy soil between 6–7.5 is most favorable for crop production. This poor productivity of bananas can be influenced by several causes such as unpredictable climatic conditions, lack of availability of reliability–planting material, poor farming techniques, and the pervasiveness of pests and diseases. Bananas are grown in India under different environmental conditions and systems of production. Tree–parasitic nematodes are a major issue of bananas globally. The plant–parasitic nematodes happen in banana roots or root areas and are associated with three or more species infestations. Therefore, quantifying the harm per individual species is dangerous. The ground signs of banana, nematode infection may be disturbed with those linked with root systems that have been weakened or diseased. Severely infected plants are scrubby with thin pseudo roots, whereas leaf is yellow or show discolored, greenish–yellow bands around the blades of the vine. Since the presence of root node nematodes is in almost all banana plantations, monitoring their

current population in young crops is especially important. The general view is that such pests can cause serious damage to young age trees, leading to sub–optimal growth performance. While plant–parasitic nematodes are not a key factor in the production of bananas, they can still cause serious crop losses and significantly reduce the production [145]. Nematodes are soil pathogen invading the plant's roots, and blocking its vascular network. Efficient banana planting promotes the infestation of pests and diseases along with banana parasitic nematodes. A serious banana issue globally is plant–parasitic nematodes. A large percentage of pest species and nematodes are infesting banana crops and reducing production, efficiency, and quality. The attack of nematode results in developmental problems, dried leaves, roots cut, bright red black infections of the roots of the banana, and their splitting. The infestation of nematode is one of the big main drawbacks of banana growth. The massive nematodes linked with nematode infestation are root–lesion nematode, the root–knot nematode, spiral nematode, and burrowing nematode, being one of the major limitations in banana cultivation. The root–knot nematodes are worldwide threats to plant growth among the plant–parasitic nematodes. Out of these, M.arenaria, Meloidogyne incognita, and M.javanica has been observed to harm bananas and plantains [45,152]. Plant–parasitic nematodes generally appear in banana roots or root areas and describe a co–occurence infestations of three or more organisms. Consequently, the measurement of damage by specific organisms is problematic. The over–ground signs of nematode infection on bananas could be inaccurate with those related to dead or damaged plant roots. Generally, the root–knot nematodes are root parasites or under the surface of the stem on the plant. Many places in a field may be heavily infected, while plants in other regions may present with no symptoms of the disease. The root–knot nematode organisms usually noted in contact with regional banana plantations are found in bananas [178]. The root-knot nematodes were the most extensive along with spiral nematodes set at 72% of the overall plant–parasitic nematode community [117]. The general opinion is that such nematode pests can cause significant harm to new plants, leading to suboptimal growth performance. The Radopholus similis, nematode burrowing is a highly damaging banana cultivation pest around the globe. Infection with R.Similis creates massive degradation of crucial roots and weak banana plant. The nematode can be present all over plant roots as well as the rhizome [53]. The root–knot nematodes are among the top five plant pathogens

145

that damage crop yields worldwide and are one of the main harmful crop diseases. The crop infestation has a major impact on their health, production, and efficacy. They are adapted to parasitize a wide range of plants and have been recorded to have an impact on more than 3000 cultivated and wild plant species [184]. They are spread globally over a broad range of tropical, subtropical, and temperate areas of the earth's geographical and climatic conditions. So many roots of plants (226 species from 43 families) are globally known to play as habitats of the root–knot nematodes [99]. It is very difficult to remove nematodes. In several situations, nematode harm causes other accompanying pathogenic issues and may improve a complex syndrome. Infection of the root–node banana nematodes induce galls on the root as well as generate most of the above–ground symptoms such as yellowing, negatively impacting, mid-day withering, and huge nematode banana pests prematurely shedding leaves. The All India Coordinated Research Project (AICRP) on Plant Parasitic Nematodes with an integrated strategy for control has provided adequate information about the various plant-parasitic nematodes, which include root node nematodes. Eatable yield loss due to nematodes in bananas could be up to 12% [185]. [93] reported the plant's parasitic nematodes are causing worldwide annual production losses of 12.3%. Consequently, an integrated study was adopted to control the banana nematode infections complex by biological control agent and chemical nematicide in nematodes. Mathematics is becoming a big tool to research plant outbreaks and disease growth [154]. Various mathematical and computational frameworks for plant disease pests have been developed in the soil. Several multiple rotational planting models have been developed to handle root–node nematode dynamics. Meloidogyne arenaria, Meloidogyne incognita and root lesion nematode Pratylenchus penetrans [32, 237]. Several responses–diffusion models have been formulated to connect the spatial and temporal dynamics of soil pathogens. Several responses–diffusion and dynamics of a prey–predator models have been formulated to connect the spatial and temporal dynamics of soil infectious diseases [31, 37, 208]. To our awareness, however, there is one model introduced for Radopholus similis [168]. Nematicides can be added to contain this disease. Its effectiveness is sometimes restricted. Also, in some nations, the ecological footprint of nematicides and their general perniciousness have resulted in their restriction [194]. Nonetheless, they are still sometimes used, because they are very cost-effective and easy to apply [33]. It is necessary to build more effi-

cient and environmentally friendly banana plant frameworks. In his study of R. simile survival, [35] observed that nematode populations suffer rapid decline when hosts are missing. [191] have worked on plant epidemics. The models of bananas for controlling the R. similis are based on semi–discrete formalism. Of that kind, the methodology is a model of consistent hypotheses that are discreetly perturbed. In the biological sciences, some investigators have applied this type of scheme [127]. Banana fruits are typically seedless and procreate asexual reproduction by the development of suckers that are the outgrowths of vegetative stems. Throughout their initial development, the suckers start sharing the rhizome of their parent [118]. Therefore, if the maternal plants are infested, the suckers are like that [118, 125]. Normally, one sucker is picked in commercial cultivation growing and reproduce the plant [100]. The tree of bananas continually creates roots before fruiting; then the development of the plant focuses on the roots and fruits [131]. The banana bunch is cultivated when the rising season ends, and the plant is either reduced or naturally dies [100]. The roots, which are not participating in the sucker's growth easily destroy their freshness [17]. Like other family Pratylenchidae nematodes, Radopholus similis is a mandatory parasite that could only exist in fresh roots and that cause root gangrene [180]. This is found primarily in roots of plants, and occasionally in land; the density proportion in soils and roots is probably much less $\frac{1}{100}$ [135]. If the functioning organ is infected, it is Radopholus similis that burrows the tissue while feeding. The chemicals applied for regulation of root–knot nematodes in early tests involved halogenated hydrocarbon fumigants such as DD, EDB, etc. Methyl bromide has been applied for experimental land sterilization to regulate root-knot checked details on the chemical regulation of root node nematodes in India [42]. These chemicals have been tested for soil use with granular nematicides [162].

5.2   Mathematical Models

Here, we build and apply a mathematical model that enables us to study the banana root as a sustainable resource for agriculture in the control of pests. Our present study aimed to investigate which are the best spatial structures for nematode regulation in plant field agricultural scenarios. This research assumes that nematodes are homogeneously distributed in the roots. Therefore, we are developing a multi-periodic

compartmental framework that predicts root development, insect dynamics, and root ability to interact. Two types, growing, and reproduction of bananas are recognized. During the first case, a parent plant sucker is chosen to build a new plant. Within our model, the old root pool is applied to the parent plant's dying roots. For the second scenario, after the parent plant's uproot a new nematode–free vitroplant is started planting. Several root tips are still found in the ground, and the uprooting being only flawless. In this work, we develop and modify the framework of a mathematical model on previous work [59,91]. A framework of the study of the development and protection of a soilborne banana problem is analyzed and controlled by using control variables as pesticides. Further, we assume that crops are grown in non-arid warmer areas, which ensure that crops are not adversely affected by climates such as autumn or extreme temperatures, and can be grown anytime throughout the year. Furthermore, the control techniques are described throughout this study Radopholus similis and its interactions with bananas and plantains are implemented. The following additional modeling assumptions are considered:

(i) The nematode population is categorized into four components: functional biomass root of banana P_1, free soil nematodes P_2, infesting plant roots nematodes P_3, infesting old root pool nematodes P_4.

(ii) The functional root density of banana biomass P_1 is one compartment.

(iii) Banana root systems logistically expand throughout a cropping period during a cultivation period until the flowering prevents the root growth [169]. The length of the growing cycle, i.e., the time between the beginning of the growing seasons and the flowering of the plant is marked as d; the total crop period time is considered as D. We represent the starting point for the $(n+1)^{th}$ season by t_n, and in the first season, we assign $t_0 = 0$ to starting point. Consequently, the logistic growth of root during a cropping season is presented by

$$\frac{dP_1}{dt} = r(t)P_1(1 - \frac{P_1}{K}),$$

$$r(t) = \begin{cases} r, \ for \ t \in (t_n, t_n + d], \\ 0, \ t \in (t_n + d, t_n + D], \end{cases}$$

where K is environmental carrying capacity $K > 0$.

(iv) The term $\phi(P)$ is the direct transmission rate from free pests nematode predator

148

P_2 to infesting predator nematodes, that could be density dependent with $\phi(P) = \beta P$.

(v) Infesting pests nematode P_3 survive on banana roots a functional response of Holling type II that is ideal for invertebrate species [28]. They are subject to natural mortality $\mu + m$. Let infesting pests nematode is suffering from additional illnesses per capita mortality μ. This mortality rate tends to vary with the mortality rate of soils, since different conditions exist.

(vi) The consumed root biomass is sometimes used to develop and reproduce, while feeding nematodes. Regrowth takes place indoors (proportion γ) or outdoors (proportion $1 - \gamma$). The conversion rate for ingested biomass to pests is α.

(vii) The old root pool tends to lose its freshness easily and it diminishes in the soil. Then the infestation pests are free in the ground. They suffer natural mortality δ_1 as well.

(viii) We consider the per capita rate of control $h(t) \geqslant 0$. Thus, control function, $h(t)$, is working to remove the infesting pests nematode and free nematode from the soil and banana roots.

Under the aforementioned hypotheses, this model includes four state variables, namely: functional root density biomass, free nematodes pest population density, infesting nematodes pest population density in the banana root, and infecting nematodes in an existing old root pool P_4 connect with the functional root of banana P_1 in the season of cropping for $t \in [t_n, t_n + D]$.

$$
\begin{cases}
\frac{dP_1}{dt} = r(t)P_1(t)\left(1 - \frac{P_1(t)}{K}\right) - \frac{aP_1(t)P_3(t)}{P_1(t)+\delta}, \\
\frac{dP_2}{dt} = \alpha a(1-\gamma)\frac{P_1(t)P_3(t)}{P_1(t)+\delta} - \frac{\phi(P(t))P_2(t)P_3(t)}{P(t)} - (m+h(t))P_2(t) + \delta_1 P_4, \\
\frac{dP_3}{dt} = \alpha a \gamma \frac{P_1(t)P_3(t)}{P_1(t)+\delta} + \frac{\phi(P(t))P_2(t)P_3(t)}{P(t)} - (m+h(t)+\mu)P_3, \\
\frac{dP_4}{dt} = -(\delta_1 + \mu)P_4(t),
\end{cases}
\tag{5.2.1}
$$

with initial conditions

$$
P_1(0^+) = P_{10}, \ P_2(0^+) = P_{20}, \ P_3(0^+) = P_{30}, \ P_4(0^+) = P_{40}, \tag{5.2.2}
$$

where 0^+ refers for an instant that immediately tends to follow the starting time of 0. If the rate is too high for δ_1 the P_4 population will be moved to P_2 very easily, along with the former root pool. Therefore, we suppose that moving from P_4 to P_2 is immediate,

and rewrite (5.2.1) the following

$$
\begin{cases}
\frac{dP_1}{dt} = r(t)P_1(t)(1 - \frac{P_1(t)}{K}) - \frac{aP_1(t)P_3(t)}{P_1(t)+\delta}, \\
\frac{dP_2}{dt} = \alpha a(1-\gamma)\frac{P_1(t)P_3(t)}{P_1(t)+\delta} - \frac{\phi(P(t))P_2(t)P_3(t)}{P(t)} - (m+h(t))P_2(t), \\
\frac{dP_3}{dt} = \alpha a\gamma\frac{P_1(t)P_3(t)}{P_1(t)+\delta} + \frac{\phi(P(t))P_2(t)P_3(t)}{P(t)} - (m+h(t)+\mu)P_3,
\end{cases}
\tag{5.2.3}
$$

with initial conditions

$$
P_1(0) = P_{10}, \ P_2(0) = P_{20}, \ P_3(0) = P_{30}. \tag{5.2.4}
$$

It is assumed that in the non–appearance of predators P_3, the prey population P_1 keeps growing logistically with an inherent per capita rate of growth of $r > 0$ and an ecosystem carrying capacity of $K > 0$. A summary of the system parameters is given in Table 5.1.

Table 5.1: Parameters of the model

Parameters	Description
d	Duration of the roots growth
D	Duration of the cropping season
β	Infestation rate
K	Maximum roots biomass
r	Roots growth rate
m	Mortality rate of pests
μ	Additional mortality rate of infesting pests
a	Consumption rate
α	Conversion rate of banana roots
δ	Half-saturation constant
γ	Proportion of pests laid inside
P_{10}	Initial biomass of the functional root density
P_{20}	initial free nematodes pest population density
P_{30}	Initial infesting nematodes pest population density
P_{40}	Initial biomass of the functional old root density

For the first situation, there is the growth of a seedling in the banana tree and a new sucker grows from the old roots. Pesticide nematicides are used to manage the insect at the start of each growing season. The second situation, it is planting a pest-free vitro. $P(t) = P_2(t) + P_3(t)$ is the total population of predators (nematodes) at time t. In this study, the structure of (5.2.3) in the interval $(t_n, t_n + d]$ will be called

the first subsystem of (5.2.3), while the second subsystem of (5.2.3) will fall in the interval $(t_n + d, t_n + D]$ with $r = 0$. Figure 5.1 displays a schematic diagram illustrating the procedures of parasitism within the cropping period.
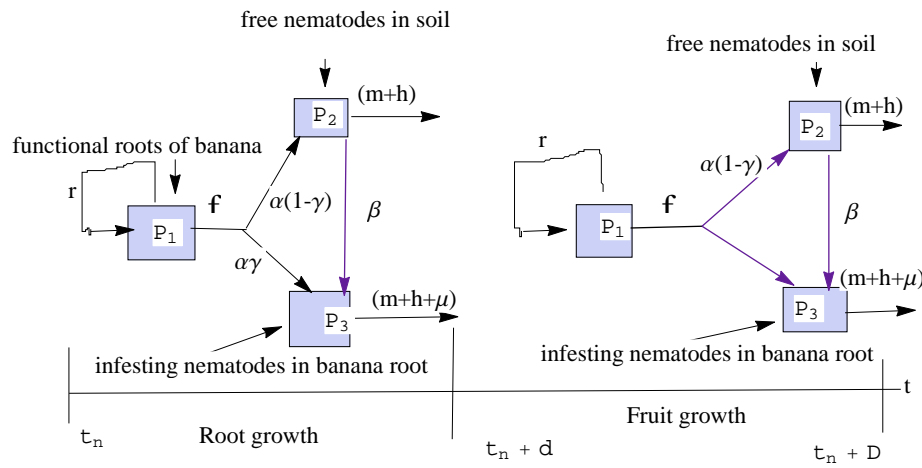
Figure 5.1: Schematic representation of the core model (5.2.3).

5.3   Chemical Control Model

In this situation, there is a vegetative growth in the banana plant, and a new sucker grows from the old roots. Chemical nematicides are used to manage the pest at the starting of the growing season. The pest–free vitroplant is cultivated. In order to monitor the nematodes, a fallow is added in two crop seasons. Nematicides can control nematodes. They have two types of nematode action: the touch effect and the systemic effect. Each season is quickly followed by the coming season, so $t_n = nD$. Contact nematicides destroy nematodes immediately after target, whereas systemic nematicides are collected from the plant's roots and distributed through the organs where they operate in opposition to pests. Most nematicides can have adverse effects. The nematicide is used at the start of each season and has systemic as well as interaction effects. At the end of this period, a ratio of q_1 of the total root biomass refers to the sucker that will develop during the next season. Supposing that nematodes spread homogeneously in the soil, the sucker brings the q_2 ratio of plaguing nematodes. Residual roots of the existing original tree are transmitted to the former root pool as the sucker is the new parent tree. So, the original root pool holds $(1 - q_2)$ of infested pests. The results are shown in the following swapping principle at the

151

beginning of the new season

$$
\begin{cases}
P_1(t_n^+) = q_1 P_1(t_n), \\
P_2(t_n^+) = P_2(t_n), \\
P_3(t_n^+) = q_2 P_3(t_n), \\
P_4(t_n^+) = (1 - q_2) P_3(t_n), n \in \mathbb{N}^+
\end{cases}
\tag{5.3.1}
$$

As we have presumed, the infesting pests in the old root pool P_4 instantly transform into free pests, the previous switching rule (5.3.1) can be written as described in the following

$$
\begin{cases}
P_1(t_n^+) = q_1 P_1(t_n), \\
P_2(t_n^+) = P_2(t_n) + (1 - q_2) P_3(t_n), \\
P_3(t_n^+) = q_2 P_3(t_n),
\end{cases}
\tag{5.3.2}
$$

We make the following assumptions for including the nematicide action:

(i) We presume the actual removal of the nematicide is extremely quick, thus nematicide's effect on the nematode is immediate [66, 204]. The nematicide interaction behavior on a free pest is therefore provided for a certain period of time by

$$
P_2(t_n^+) = \eta \left(P_2(t_n) + (1 - q_2) P_3(t_n) \right),
\tag{5.3.3}
$$

with $0 \leqslant \eta < 1$, the nematode survival rate with nematicide use.

(ii) Further, we assume that efficiency is the same for both free pests and infecting pests, so we get

$$
P_3(t_n^+) = \eta q_2 P_3(t_n),
\tag{5.3.4}
$$

from the (5.3.3) and (5.3.4), the seasonal switching rule is given by

$$
\begin{cases}
P_1(t_n^+) = q_1 P_1(t_n), \\
P_2(t_n^+) = \eta \left(P_2(t_n) + (1 - q_2) P_3(t_n) \right), \\
P_3(t_n^+) = \eta q_2 P_3(t_n),
\end{cases}
\tag{5.3.5}
$$

systems (5.2.3) and (5.3.5) with $t_n = nD$ form our multi–seasonal model using nematicide. Figure 5.2 provides a diagram.

152
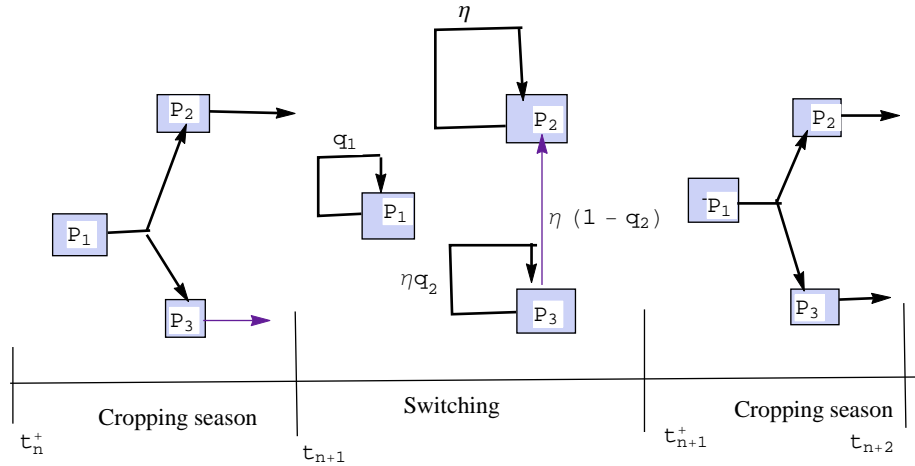
Figure 5.2: Schematic description of the plant–pest dynamics path for model (5.2.3) and (5.3.5) during two growing season.

In Figure 5.2, on the time axis, line between t_n^+, t_{n+1} and t_{n+1}^+, t_{n+2} illustrates the continuous timing, while the line t_{n+1} and t_{n+1}^+ between line indicates a discrete timing when flipping. The core system is based on communication during continuous periods in Figure 5.1. Fresh root biomass of bananas P_1 is initialized at swapping as q portion of the biomass obtained from the previous season, the free nematode sample size of P_2 is assigned as a population of free nematodes collected from the previous season plus a portion of $(1 - q_2)$ of the previous season's infestation nematodes received, all with an instantaneous work of the nematicide survival rate η. The population infected with nematode P_3 is computed as part of the portion q_2 of the infecting nematode population received from the prior season, with a life expectancy rate η to the nematicide's instant operation.

5.4 Analysis of the System

In this section, we investigate the positivity and boundedness of the system, followed by a discussion of the basic reproduction number, equilibria and their stability, sensitivity, and so on. Let, we study the model when $h(t) = h > 0$ (due to sustainability

153

of the pest). Thus, system (5.2.3) can be written as:

$$
\begin{cases}
\frac{dP_1}{dt} = r(t)P_1(t)(1 - \frac{P_1(t)}{K}) - \frac{aP_1(t)P_3(t)}{P_1(t)+\delta}, \\
\frac{dP_2}{dt} = \alpha a(1-\gamma)\frac{P_1(t)P_3(t)}{P_1(t)+\delta} - \beta P_2(t)P_3(t) - (m+h)P_2(t), \\
\frac{dP_3}{dt} = \alpha a\gamma\frac{P_1(t)P_3(t)}{P_1(t)+\delta} + \beta P_2(t)P_3(t) - (m+h+\mu)P_3.
\end{cases}
\tag{5.4.1}
$$

5.4.1 Positivity

It is important to demonstrate that all the solutions of the system with positive initial data will remain positive for model (5.4.1). The following theorem will demonstrate this.

Theorem 5.4.1. Let the initial data $P_1(0) > 0$, $P_2(0) > 0$, and $P_3(0) > 0$. Then the solutions of $(P_1(t),\ P_2(t),\ P_3(t))$ of the system (5.4.1) are positive.

Proof. (i) Positivity of $P_1(t)$: from the model (5.4.1)

$$
\frac{dP_1}{dt} = r(t)P_1(t)(1 - \frac{P_1(t)}{K}) - \frac{aP_1(t)P_3(t)}{P_1(t)+\delta},
\tag{5.4.2}
$$

without loss of generality and removing all the positive terms from the right–hand side of the differential equation (5.4.2), the differential inequality is as follows:

$$
\frac{dP_1}{dt} \geqslant \frac{-rP_1^2}{K} - \frac{aP_1P_3}{P_1+\delta} \geqslant \frac{-rP_1^2}{K} - \frac{aP_1P_3}{\delta},,
$$

Assume that $\frac{KaP_3}{r(\delta)} = C$, then the differential inequality is reduced to

$$
\frac{dP_1}{dt} \geqslant -\frac{r}{K}P_1(P_1 + C).
$$

This inequality can be organised for integration by using a partial fraction and then integrating the integral inequality,

$$
\frac{1}{C}\ln|(\frac{P_1}{P_1+C})| \geqslant -\frac{r}{K}t + C_1,
$$

where C_1 is integration constant. Finally, solving for P_1 will give us

$$
P_1(t) \geqslant \frac{ACe^{\frac{-rC}{K}t}}{1 - Ae^{\frac{-rC}{K}t}},
$$

154

where $A = e^{CC_1}$. Therefore $P_1(t) > 0$ for $1 - Ae^{\frac{-rC}{K}t} > 0$. That is, $P_1(t)$ is nonnegative for $t > \frac{K}{Cr}\ln A$.

(ii) Positivity of $P_2(t)$: from the model (5.4.1),

$$\frac{dP_2}{dt} = \alpha a(1-\gamma)\frac{P_1(t)P_3(t)}{P_1(t)+\delta} - \beta P_2(t)P_3(t) - (m+h)P_2(t) \geqslant -P_2(\beta P_3 + m + h). \quad (5.4.3)$$

We assume that $\beta P_3 + m + h = A_2$, then the differential inequality is reduced to $\frac{dP_2}{dt} \geqslant -P_2 A_2$. Applying integration by separation of variable method yields $\ln|P_2| \geqslant e^{-A_2 t} + Q_1$, where Q_1 is integration constant by separation of variable method. Then, solving for P_2 will result in $P_2(t) \geqslant e^{-ct+Q_1}$ which is the exponential function that is positive at all time. Hence, $P_2(t)$ is positive.

(iii) Positivity of $P_3(t)$: from the model (5.4.1),

$$\frac{dP_3}{dt} = \alpha a\gamma\frac{P_1(t)P_3(t)}{P_1(t)+\delta} + \beta P_2(t)P_3(t) - (m+h+\mu)P_3 \geqslant -(m+h+\mu)P_3. \quad (5.4.4)$$

Applying integration by separation of variable method yields $\ln|P_3| \geqslant e^{-(m+h+\mu)t} + Q_2$, where Q_2 is integration constant by separation of variable method. Then, solving for P_3 will result in $P_3(t) \geqslant e^{-(m+h+\mu)t+Q_2}$ which is the exponential function that is positive at all time. Hence, $P_3(t)$ is positive. $\qquad\square$

5.4.2 Boundedness of the System

To study the boundedness criteria of the system (5.4.1), we state the following result.

Theorem 5.4.2. All solutions of the model (5.4.1) are uniformly bounded.

Proof. First, let us define a function, $X = \alpha P_1 + P_2 + P_3$. The time derivative of X is

$$\frac{dX}{dt} = \alpha\frac{dP_1}{dt} + \frac{dP_2}{dt} + \frac{dP_3}{dt}$$

155

from the equation (5.4.1), we can obtain,

$$\frac{dX}{dt} = \alpha r P_1 (1 - \frac{P_1}{K}) - \alpha \frac{a P_1 P_3}{P_1 + \delta} + \alpha a (1 - \gamma) \frac{P_1 P_3}{P_1 + \delta} - \beta P_2 P_3$$

$$- (m+h)P_2 + \alpha a \gamma \frac{P_1 P_3}{P_1 + \delta} + \beta P_2 P_3 - (m+h+\mu)P_3,$$

$$\Rightarrow \frac{dX}{dt} = \alpha r P_1 (1 - \frac{P_1}{K}) - (m+h)P_2 - (m+h+\mu)P_3,$$

$$\Rightarrow \frac{dX}{dt} + (m+h)X = \alpha r P_1 (1 - \frac{P_1}{K}) - (m+h)P_2 - (m+h+\mu)P_3 + (m+h)(\alpha P_1 + P_2 + P_3),$$

$$\Rightarrow \frac{dX}{dt} + (m+h)X \leqslant \alpha r P_1 (1 - \frac{P_1}{K}) + \alpha(m+h)P_1,$$

$$\Rightarrow \frac{dX}{dt} + (m+h)X \leqslant \frac{K\alpha(r+m+h)^2}{4r}.$$

Thus, we have a constant $L = \frac{K\alpha(r+m+h)^2}{4r}$, such that

$$\Rightarrow \frac{dX}{dt} + (m+h)X \leqslant L,$$

applying the theorem of differential inequality [65], we obtain

$$0 < X(P_1, P_2, P_3) \leqslant \frac{L}{(m+h)}(1 - e^{-(m+h)t}) + X(P_1(0), P_2(0), P_3(0))e^{-(m+h)t}.$$

As $t \to \infty$, we have $0 < X \leqslant \frac{L}{(m+h)}$, since $\sup_{t \to \infty} X(t) = \frac{L}{(m+h)}$. Hence all the solutions of (5.4.1) are confined in the region

$$S = \{(P_1, P_2, P_3) \in R_3^+ : 0 < X \leqslant \frac{L}{(m+h)} + \varepsilon\},$$

for any $\varepsilon > 0$ and for $t \to \infty$. Hence the theorem. $\qquad \square$

Remark 1 (Equilibrium points). *System* (5.4.1) *has following possible equilibria points*

(i) The trivial equilibrium point $E_0(P_1^*, P_2^*, P_3^*)$, where

$$P_1^* = 0, P_2^* = 0, P_3^* = 0.$$

(ii) The functional root biomass of banana free equilibrium point $E_1(P_1^*, P_2^*, P_3^*)$, where

$$P_1^* = 0, P_2^* = \frac{h + m + \mu}{\beta}, P_3^* = \frac{-h - m}{\beta},$$

which is not biologically feasible because P_3^* is always negative.

(iii) The nematodes pest free equilibrium point $E_2(P_1^*, P_2^*, P_3^*)$, where

$$P_1^* = K, P_2^* = 0, P_3^* = 0,$$

which is biologically feasible.

(iv) The functional roots of banana, free nematodes in soil and infesting nematodes in root coexistence equilibrium $E_4(P_1^*, P_2^*, P_3^*)$, where the interior equilibrium point $E^*(P_1^*, P_2^*, P_3^*)$ is the point of intersection of the following equations:

$$r(1 - \frac{P_1}{K}) - \frac{aP_3}{P_1 + \delta} = 0, \tag{5.4.5}$$

$$\alpha a(1 - \gamma)\frac{P_1 P_3}{P_1 + \delta} - \beta P_2 P_3 - (m + h)P_2 = 0, \tag{5.4.6}$$

$$\alpha a \gamma \frac{P_1}{P_1 + \delta} + \beta P_2 - (m + h + \mu) = 0. \tag{5.4.7}$$

from (5.4.5) equation,

$$P_3 = \frac{r(K - P_1)(\delta + P_1)}{aK}, \tag{5.4.8}$$

from (5.4.7) equation,

$$P_2 = \frac{1}{\beta}(h + \mu + m - \frac{a\alpha\gamma P_1}{\delta + P_1}), \tag{5.4.9}$$

Putting the value of P_2 and P_3 from (5.4.8) and (5.4.9), in the equation of (5.4.6), we can observe that P_1 satisfy the following equation:

$$\frac{r\alpha(1 - \gamma)(K - P_1)P_1}{K} - \frac{1}{\beta}\left((h + m)\left(h + m + \mu - \frac{a\alpha\gamma P_1}{\delta + P_1}\right)\right) \tag{5.4.10}$$
$$- \frac{1}{aK}\left(r(K - P_1)(\delta + P_1)\left(h + m + \mu - \frac{a\alpha\gamma P_1}{\delta + P_1}\right)\right) = 0.$$

Equation (5.4.10) can be rewritten as

$$\delta_4 P_1^3 + \delta_3 P_1^2 + \delta_2 P_1 + \delta_1 = 0. \tag{5.4.11}$$

Where
$\delta_1 = \frac{(-h-m)\delta(h+m+\mu)}{\beta} - \frac{r\delta^2(h+m+\mu)}{a}$, $\delta_2 = \frac{a(h+m)\alpha\gamma}{\beta} + r\alpha(1-\gamma)\delta + r\alpha\gamma\delta + \frac{(-h-m)(h+m+\mu)}{\beta} - \frac{2r\delta(h+m+\mu)}{a} + \frac{r\delta^2(h+m+\mu)}{aK}$, $\delta_3 = r\alpha(1-\gamma) + r\alpha\gamma - \frac{r\alpha(1-\gamma)\delta}{K} - \frac{r\alpha\gamma\delta}{K} - \frac{r(h+m+\mu)}{a} + \frac{2r\delta(h+m+\mu)}{aK}$,
$\delta_4 = -\frac{r\alpha(1-\gamma)}{K} - \frac{r\alpha\gamma}{K} + \frac{r(h+m+\mu)}{aK}$.

Since $\delta_1 < 0$, and if $\delta_4 > 0$, then the Descartess rule of sign gives that the equation (5.4.11) has a positive root P_1^* (say). The values of P_2 and P_3 can be obtained from (5.4.9) and (5.4.8). Moreover, in both cases, either $\delta_3 > 0$ and $\delta_2 > 0$ or $\delta_3 < 0$ and $\delta_2 < 0$, equation (5.4.11) possess exactly one positive root. This proves the uniqueness of E_4. P_2^* and P_3^* are positive if $h + m + \mu > \frac{a\alpha\gamma P_1^*}{\delta + P_1^*}$ and $K > P_1^*$.

5.4.3   Basic Reproduction Number

We observe that the system (5.4.1) has a nematodes pest–free equilibrium point $E_2(P_1^* = K, P_2^* = 0, P_3^* = 0)$ and it always exits. Now we introduce the basic reproduction number R_0, during the entire period, this is characterized as the number of secondary infected individuals caused by a single infected individual. Furthermore, the approach developed by [110, 158, 167] can be used to obtain the expression for the basic reproduction number. The basic replication number is determined using the next–generation matrix procedure. These matrices are determined at the disease–free equilibrium point E_2, the associated non–negative matrix, F, of the new infection terms, and the non–singular matrix, V, for the remaining transfer terms, are given, respectively, by

$$F = \begin{pmatrix} 0 & \frac{aK\alpha(1-\gamma)}{K+\delta} \\ 0 & \frac{aK\alpha\gamma}{K+\delta} \end{pmatrix}, \quad V = \begin{pmatrix} h+m & 0 \\ 0 & h+m+\mu \end{pmatrix},$$

and

$$FV^{-1} = \begin{pmatrix} 0 & \frac{aK\alpha(1-\gamma)}{(K+\delta)(h+m+\mu)} \\ 0 & \frac{aK\alpha\gamma}{(K+\delta)(h+m+\mu)} \end{pmatrix}$$

158

Eigenvalues of $FV^{-1} = 0$ and $\frac{a\alpha\gamma K}{(\delta+K)(h+\mu+m)}$. The basic reproduction number R_0 of the system is defined by the spectral radius of the matrix FV^{-1}. Thus, $R_0 = \frac{a\alpha\gamma K}{(\delta+K)(h+\mu+m)}$. When it comes to $R_0 < 1$, each infected individual creates on average less than one new infected person, implying that the disease will eventually die out. If $R_0 > 1$, each individual makes more than one new infected individual, meaning that the disease will continue to spread throughout the population.

5.4.4 Local Stability

We draw conclusions in the following theorem concerning the asymptotic behavior of system (5.4.1).

Theorem 5.4.3. At different equilibria, the system (5.4.1) has the following behavior:

(1)The trivial equilibrium point E_0 is not stable, since one eigenvalues r is always positive, therefore E_0 is saddle point which is unstable.

(2) The functional root biomass of banana free equilibrium point E_1 is not stable, since two eigenvalues $\frac{ah+am+r\beta\delta}{\beta\delta}$ and $\sqrt{h+m}\sqrt{h+m+\mu}$ are always positive and one is negative, therefore E_1 is saddle point which is unstable.

(3) The nematodes pest free equilibrium point E_2 is locally asymptotically stable if $R_0 < 1$.

(4) The functional roots of banana, free nematodes in soil and infesting nematodes in root coexistence equilibrium E_3 is locally asymptotically stable if $A_1 > 0$, $A_3 > 0$ and $A_1A_2 > A_3$. Where $A_1 = -c_{11} - c_{22} - c_{33}$, $A_2 = -c_{12}c_{21} + c_{11}c_{22} - c_{13}c_{31} - c_{23}c_{32} + c_{11}c_{33} + c_{22}c_{33}$, $A_3 = c_{13}c_{22}c_{31} - c_{12}c_{23}c_{31} - c_{13}c_{21}c_{32} + c_{11}c_{23}c_{32} + c_{12}c_{21}c_{33} - c_{11}c_{22}c_{33}$, and further, $c_{11} = -\frac{rP_1^*}{K} + r\left(1 - \frac{P_1^*}{K}\right) + \frac{aP_1^*P_3^*}{(\delta+P_1^*)^2} - \frac{aP_3^*}{\delta+P_1^*}$, $c_{12} = 0$, $c_{13} = -\frac{aP_1^*}{\delta+P_1^*}$, $c_{21} = -\frac{a\alpha(1-\gamma)P_1^*P_3^*}{(\delta+P_1^*)^2} + \frac{a\alpha(1-\gamma)P_3^*}{\delta+P_1^*}$, $c_{22} = -h - m - \beta P_3^*$, $c_{23} = \frac{a\alpha(1-\gamma)P_1^*}{\delta+P_1^*} - \beta P_2^*$, $c_{31} = -\frac{a\alpha\gamma P_1^*P_3^*}{(\delta+P_1^*)^2} + \frac{a\alpha\gamma P_3^*}{\delta+P_1^*}$, $c_{32} = \beta P_3^*$, $c_{33} = -h - m - \mu + \frac{a\alpha\gamma P_1^*}{\delta+P_1^*} + \beta P_2^*$.

5.4.5 Global Stability Analysis

Here, we discuss the global asymptotic stability of an interior equilibrium of model (5.4.1).

Theorem 5.4.4. The positive interior equilibrium $E_4(P_1^*, P_2^*, P_3^*)$ is globally asymptotically

stable if all the conditions are simultaneously hold:

$$(1)\frac{r}{K} > \frac{aP_3^*}{(P_1 + \delta)(P_1^* + \delta)},$$

$$(2)\frac{P_1^* P_3^*}{P_1^* + \delta} > \frac{P_1 P_3}{P_1 + \delta},$$

and

$$(3)P_2 > P_2^*.$$

Proof. Firstly, we define a Lyapunov function

$$V(P_1, P_2, , P_3) = c_1(P_1 - P_1^* - P_1^* \ln \frac{P_1}{P_1^*}) + c_2(P_2 - P_2^* - P_2^* \ln \frac{P_2}{P_2^*}) + c_3(P_3 - P_3^* - P_3^* \ln \frac{P_3}{P_3^*}),$$

where c_1, c_2 and c_3 are positive constants to be determined later. It can be easily see that the function V is zero at the equilibrium point $(P_1^*, P_2^*, , P_3^*)$ and is positive for all other values of P_1, P_2, and P_3. The derivative of Lyapunov function V is

$$\frac{dV}{dt} = c_1(1 - \frac{P_1^*}{P_1})\frac{dP_1}{dt} + c_2(1 - \frac{P_2^*}{P_2})\frac{dP_2}{dt} + c_3(1 - \frac{P_3^*}{P_3})\frac{dP_3}{dt},$$

putting the values of $\frac{dP_1}{dt}$, $\frac{dP_2}{dt}$, and $\frac{dP_3}{dt}$ from the equation (5.4.1), we have

$$\frac{dV}{dt} = c_1(1 - \frac{P_1^*}{P_1})\left(rP_1(1 - \frac{P_1}{K}) - \frac{aP_1 P_3}{P_1 + \delta}\right) + c_2(1 - \frac{P_2^*}{P_2})\left(\alpha a(1 - \gamma)\frac{P_1 P_3}{P_1 + \delta} - \beta P_2 P_3 - (m + h)P_2\right)$$

$$+ c_3(1 - \frac{P_3^*}{P_3})\left(\alpha a \gamma \frac{P_1 P_3}{P_1 + \delta} + \beta P_2 P_3 - (m + h + \mu)P_3\right),$$

$$\frac{dV}{dt} = c_1(P_1 - P_1^*)\left(r(1 - \frac{P_1}{K}) - \frac{aP_3}{P_1 + \delta} - (r(1 - \frac{P_1^*}{K}) - \frac{aP_3^*}{P_1^* + \delta})\right)$$

$$+ c_2\frac{(P_2 - P_2^*)}{P_2}\left(\alpha a(1 - \gamma)\frac{P_1 P_3}{P_1 + \delta} - \beta P_2 P_3 - (m + h)P_2 - (\alpha a(1 - \gamma)\frac{P_1^* P_3^*}{P_1^* + \delta} - \beta P_2^* P_3^* - (m + h)P_2^*)\right)$$

$$+ c_3(P_3 - P_3^*)\left(\alpha a \gamma \frac{P_1}{P_1 + \delta} + \beta P_2 - (m + h + \mu) - (\alpha a \gamma \frac{P_1^*}{P_1^* + \delta} + \beta P_2^* - (m + h + \mu))\right),$$

$$\frac{dV}{dt} = -c_1\left(\frac{r}{K} - \frac{aP_3^*}{(P_1 + \delta)(P_1^* + \delta)}\right)(P_1 - P_1^*)^2 - c_1\left(\frac{\delta a + aP_1^*)}{(P_1 + \delta)(P_1^* + \delta)}\right)(P_1 - P_1^*)(P_3 - P_3^*)$$

160

$$+c_2\frac{\alpha a(1-\gamma)}{P_2}\left(\frac{P_1P_3}{P_1+\delta}-\frac{P_1^*P_3^*}{P_1^*+\delta}\right)(P_2-P_2^*)$$

$$-c_2\beta(P_2-P_2^*)(P_3-P_3^*)-c_2(\beta P_3^*+(m+h))\frac{(P_2-P_2^*)^2}{P_2}$$

$$+\frac{c_3\alpha a\gamma\delta}{(P_1+\delta)(P_1^*+\delta)}(P_3-P_3^*)(P_1-P_1^*)+c_3\beta(P_2-P_2^*)(P_3-P_3^*),$$

$$\frac{dV}{dt}=-c_1\left(\frac{r}{K}-\frac{aP_3^*}{(P_1+\delta)(P_1^*+\delta)}\right)(P_1-P_1^*)^2+\left(\frac{-c_1(a\delta+aP_1^*)+c_3\alpha a\gamma\delta}{(P_1+\delta)(P_1^*+\delta)}\right)(P_1-P_1^*)(P_3-P_3^*)$$

$$+c_2\frac{\alpha a(1-\gamma)}{P_2}\left(\frac{P_1P_3}{P_1+\delta}-\frac{P_1^*P_3^*}{P_1^*+\delta}\right)(P_2-P_2^*)$$

$$-c_2\beta(P_2-P_2^*)(P_3-P_3^*)-c_2(\beta P_3^*+(m+h))\frac{(P_2-P_2^*)^2}{P_2}$$

$$+c_3\beta(P_2-P_2^*)(P_3-P_3^*),$$

Choosing $c_1=\frac{\alpha\gamma\delta}{\delta+P_1^*}$, $c_2=1$, and $c_3=1$.

$$\frac{dV}{dt}\leqslant-\frac{\alpha\gamma\delta}{\delta+P_1^*}\left(\frac{r}{K}-\frac{aP_3^*}{(P_1+\delta)(P_1^*+\delta)}\right)(P_1-P_1^*)^2-(\beta P_3^*+(m+h))\frac{(P_2-P_2^*)^2}{P_2}$$

$$-\frac{\alpha a(1-\gamma)}{P_2}\left(\frac{P_1^*P_3^*}{P_1^*+\delta}-\frac{P_1P_3}{P_1+\delta}\right)(P_2-P_2^*)$$

It then follows that, $\frac{dV}{dt}<0$ if $\frac{r}{K}>\frac{aP_3^*}{(P_1+\delta)(P_1^*+\delta)}$, $\frac{P_1^*P_3^*}{P_1^*+\delta}>\frac{P_1P_3}{P_1+\delta}$, and $P_2>P_2^*$. Also,$\frac{dV}{dt}=0$ at $E_4(P_1^*,P_2^*,P_3^*)$. We then define the invariant set as

$$\Omega=\{(P_1,P_2,P_3)\in R_3^+:\frac{dV}{dt}=0\}.$$

Hence, by LaSalles Invariance Principle [6, 92], it follows that the $E_4(P_1^*,P_2^*,P_3^*)$ is said to be globally asymptotically stable. $\qquad\square$

5.4.6 Sensitivity Analysis

Sensitivity analysis may reveal important details about how biological behaviors are changing with respect to the parameters. We determine the sensitivity indices of the basic reproduction number to the parameters as mentioned in Table 5.2. These indices indicate how important each parameter is for disease spread and distribution. We ivestigate the effect of the basic reproduction number R_0 for certain key parame-

ters in order to do a sensitivity analysis of the model. Following [34, 155], we calculate the normalized forward sensitivity index of the reproduction number, which estimates the relative change in a variable with respect to the relative change in its parameter.

Definition. The normalized forward sensitivity index of a variable, h , that depend differentially on a parameter, l, is defined as: $\Gamma_l^h = \frac{1}{h} \times \frac{\partial h}{\partial l}$.

Table 5.2: Sensitivity indices of model parameters

Serial	Parameters	Description	Sensitivity index
1	α	Conversion rate of banana roots	1
2	a	Consumption rate	1
3	γ	Proportion of pests laid inside	1
4	h	Proportion of pests laid inside	-0.2500
5	m	Mortality rate of pests	-0.5208
6	μ	Additional mortality rate of infesting pests	-0.2292
7	δ	Half–saturation constant	-0.3333

Mathematically, the sensitivity of the system is characterized. To study the sensitivity of R_0 , we choose a set of parameters α, a, γ, h, μ, m, δ. The sensitivity index of R_0 with respect to α is given by $\Gamma_\alpha^{R_0} = \frac{\alpha}{R_0} \times \frac{\partial R_0}{\partial \alpha} = 1$. The sensitivity indices of R_0 with respect to the other parameters of the model are given by $\Gamma_a^{R_0} = \frac{a}{R_0} \times \frac{\partial R_0}{\partial a} = 1$, $\Gamma_\gamma^{R_0} = \frac{\gamma}{R_0} \times \frac{\partial R_0}{\partial \gamma} = 1$, $\Gamma_h^{R_0} = \frac{h}{R_0} \times \frac{\partial R_0}{\partial h} = -\frac{h}{h+\mu+m}$, $\Gamma_\mu^{R_0} = \frac{\mu}{R_0} \times \frac{\partial R_0}{\partial \mu} = -\frac{\mu}{h+\mu+m}$, $\Gamma_m^{R_0} = \frac{m}{R_0} \times \frac{\partial R_0}{\partial m} = -\frac{m}{h+\mu+m}$, $\Gamma_\delta^{R_0} = \frac{\delta}{R_0} \times \frac{\partial R_0}{\partial \delta} = -\frac{\delta}{\delta+K}$.

Some numerical simulations are performed based on our analytical results. For simulation works, the parameter set is chosen as feasible value $S = \{a, \alpha, \gamma, K, h, \mu, \delta, m\} = \{0.4, 3.5, 0.6, 4, 0.12, 0.11, 2, 0.25\}$. Table 5.2 represents the sensitivity indices of R_0. In Table 5.2, we observe that the parameters namely α, a and γ are the positively sensitive and h, m, μ and δ are the negative sensitive parameters.

5.5   Numerical Simulation and Its Discussion

For the simulation purposes, we perform numerical simulations to analyze the dynamical behavior of the system (5.4.1). The mathematical parameters of the models representing a certain pattern can be modified to achieve a stronger agreement between the performance of the model and the observations. Table 5.3 describes the numerical values of the parameters that have been used in computational models.

Parameters used in this model are taken assumed feasible values which are shown in Table 5.3.

Table 5.3: Parameters used for simulation purpose.

Parameters	Values	Units	Parameters	Values	Units
β	0.3	$gram^{-1}\,day^{-1}$	δ	2	$gram$
K	4	$gram$	h	0.12	day^{-1}
r	0.4	day^{-1}	γ	0.6	–
m	0.25	day^{-1}	P_{10}	2	$gram/cm^3$
μ	0.11	day^{-1}	P_{20}	1	$gram/cm^3$
a	0.4	$gram\,day^{-1}$	P_{30}	0.9	$gram/cm^3$
α	3.5	$gram^{-1}$			

Figure 5.3 shows, the graph between functional root of biomass (P_1), free nematodes in soil (P_2), and infecting nematodes (P_3) population density with respect to time t (days). Figure 5.3(a) describes that the population density of P_1 initially increases but after some time P_1 decreases as P_3 population increases for the parameters $r = 0.4, K = 4, a = 0.4,\ \delta = 2,\ \beta = 0.2,\ \alpha = 3.5, \gamma = 0.4,\ h = 0.12,\ \mu = 0.02,\ m = 0.25$. In Fig. 5.3(b), there are several parameter changes compared to Fig. 5.3(a) as a from 0.4 to 0.6, β from 0.2 to 0.3, γ from 0.4 to 0.6, and μ from 0.02 to 0.11, h from 0.12 to 0.3, m from 0.25 to 0.30. Figure 5.3(b) shows that the P_3 population increases while P_2 decreases. Thus, in Fig. 5.3(b), P_1 decreases more compared to Fig. 5.3(a). Figure 5.4 and Figure 5.5 show the interaction between functional root biomass of banana P_1, free nematodes in soil P_2, and infesting nematodes in roots P_3 at $t = 2$ (days) and $t = 100$ (days), respectively. Phase space trajectories of the model are shown in Fig. 5.6.

(a)   (b)
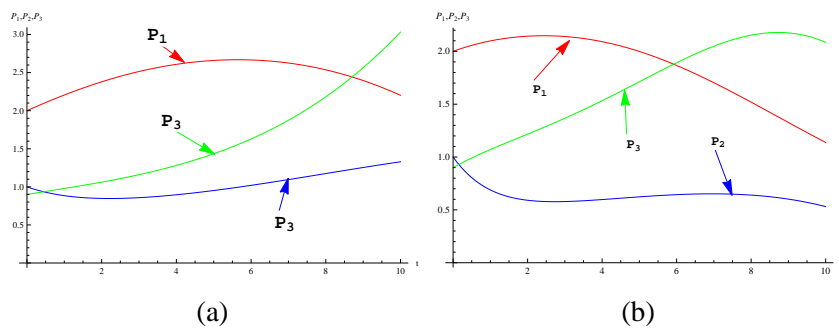
Figure 5.3: Time series diagrams between P_1, P_2 and P_3 in roots population density of the system for the parameter values $r = 0.4$, $K = 4$, $a = 0.4, 0.6$, $\delta = 2$, $\beta = 0.2, 0.3$, $\alpha = 3.5$, $\gamma = 0.4, 0.6$, $h = 0.12, 0.3$, $\mu = 0.02, 0.11$, and $m = 0.25, 0.3$.

Figure 5.4: The interaction between functional root biomass of banana, free nematodes in soil, and infesting nematodes in roots of the system for the parameter values $r = 0.4$, $k = 4$, $a = 0.4$, $\delta = 2$, $\alpha = 3.5$, $\gamma = 0.4$, $\beta = 0.2$, $h = 0.12$, $m = 0.25$, $\mu = 0.02$, $P_{10} = 2$, $P_{20} = 1$, $P_{30} = 0.8$ and $t = 2$.

Figure 5.5: The interaction between P_1, P_2 and P_3 for the parameter values $r = 0.4$, $k = 4$, $a = 0.4$, $\delta = 2$, $\alpha = 3.5$, $\gamma = 0.4$, $\beta = 0.2$, $h = 0.12$, $m = 0.25$, $\mu = 0.02$, $P_{10} = 2$, $P_{20} = 1$, $P_{30} = 0.8$ and $t = 100$.
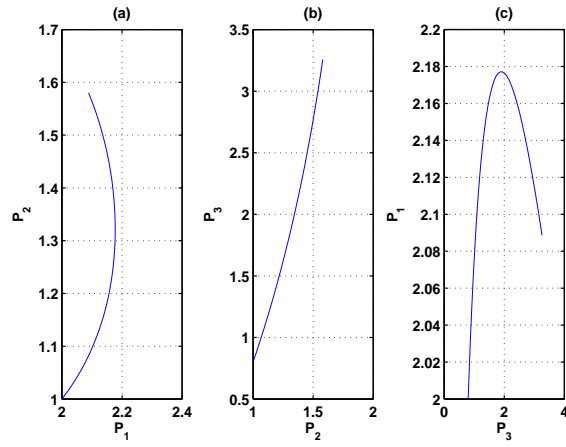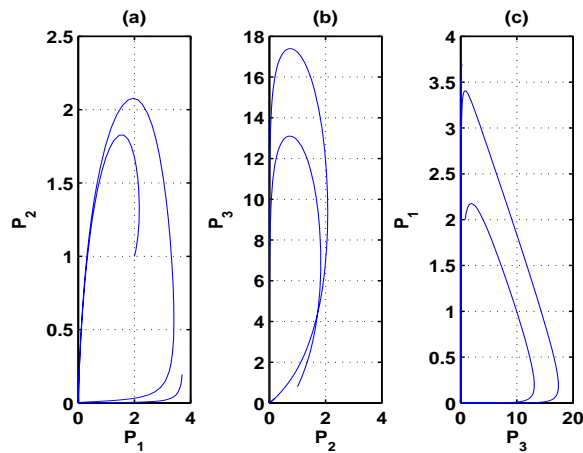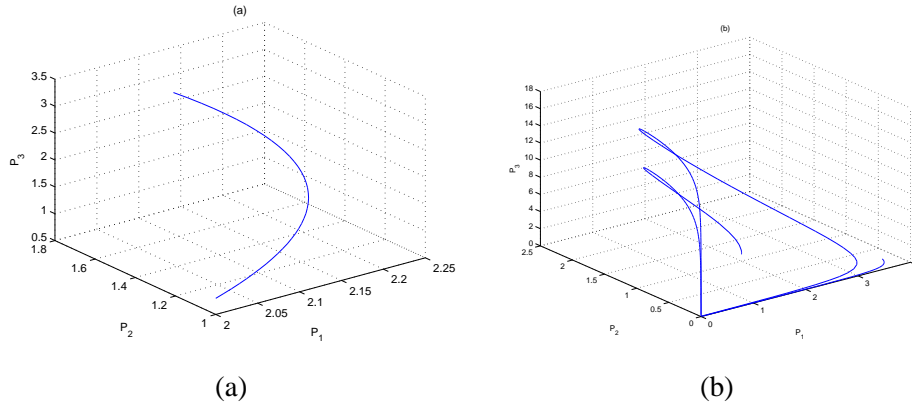
(a)   (b)

Figure 5.6: Phase space trajectories of functional root biomass of banana, free nematodes in soil, and infesting nematodes in roots of the system for the parameter values $r = 0.4$, $k = 4$, $a = 0.4$, $\delta = 2$, $\alpha = 3.5$, $\gamma = 0.4$, $\beta = 0.2$, $h = 0.12$, $m = 0.25$, $\mu = 0.02$, $P_{10} = 2$, $P_{20} = 1$, $P_{30} = 0.8$ and $t = 2$, 100.

5.6   Optimal Control Formulation and Analysis

In the present circumstances, nematologists around the world are faced with the lack of availability of effective chemical nematicides coupled with their unaffordable costs and environmental risks; the focus these days is on the biological means of nematode control. The use of control agents for efficient nematode managemen-t provides long–term economical and eco–friendly management choices. The ideal biocontrol system must be robust and self–sustaining. Plant–parasitic nematodes be-longing to various communities, including India, are being investigated globally. Con-trol of plant–parasitic nematodes requires an inundation of bio–formulations in the soil to achieve satisfactory control over the season. The objective of the optimal is (i) to use a variety of compatible control strategies, (ii) Maximizing natural environmental tolerance to plant–parasitic nematodes, (iii) To apply strict and severe control mea-sures only when essential, and (iv) Optimize the profits of the farmer with a particular destination and material suggestions. Time–varying controls, $h(t)$, is to be chosen. Therefore, using system (5.2.3), we minimize the objective functional

$$J(h) = \int_{o}^{t_f} (A_1(P_2(t) + P_3(t)) - A_2P_1(t))dt + \int_{o}^{t_f} (ch(t)(P_2(t) + P_3(t)) + \varepsilon h(t)^2)dt, \quad (5.6.1)$$

over time–dependent controls $h(t)$, weight constants, A_1, A_2, c, and ε are nonnegative constants that balance the relative importance of terms in J. The terms $\int_{o}^{t_f} (A_1(P_2(t) +$

$P_3(t))dt$ and $\int_o^{t_f} A_2 P_1(t))dt$ determine the corresponding number of nematodes and the functional root biomass across time t_f being modeled. The term $h(P_2 + P_3)$, represents the total number of nematodes culled, where h represents the per capita rate of application of insecticide on nematodes, and c is the cost per nematodes killed. Thus, $\int_o^{t_f}(ch(t)(P_2(t) + P_3(t)) + \varepsilon h(t)^2)dt$ gives the cost of killing nematodes from the population. As the costs in an objective functional are frequently nonlinear functions of the control actions [84, 200]. We find h^* such that

$$J(h^*) = \inf_h (J(h) \tag{5.6.2}$$

subject to the state system defined in (5.2.3), where objective function is given by equation (5.6.1), and the set of feasible control is

$$U = \{J(h) \in (L^\infty([0, t_f]))|h : [0, t_f] \to [0, 1]\},$$

to show the occurrence of an optimal problem of control, we need to bound the state functions of the eco–epidemiological model. The effects of the positivity and boundedness results below drive from the system.

Theorem 5.6.1. Given the state equations for P_1, P_2, and P_3, defined in equation (5.2.3) with initial conditions (5.2.4), and $P_{10} \geqslant 0$, $P_{20} \geqslant 0$, $P_{30} \geqslant 0$, there exist constants C_1, C_2, $C_3 > 0$ such that $0 < P_1 \leqslant C_1$, $0 < P_2 \leqslant C_2$ and $0 < P_3 \leqslant C_3$, for all $t \in [0, t_f]$.

To use Pontryagins maximum principle [122] on the time–dependent controls, we first need existence of optimal controls, characterize the time–dependent controls, and adjoint equations for system (5.2.3).

Theorem 5.6.2. There exist optimal controls $h^* \in U$ which minimize the objective functional, J, subject to the state system (5.2.3).

Proof. The infimum is finite by the uniform boundedness of states and controls, and therefore, sequence minimization occurs $\{h^n\}$

$$\lim_{n \to \infty} J(h_n) = \inf_{(h) \in U} J(h).$$

Since the corresponding states P_{1_n}, P_{2_n}, and P_{3_n} is bound uniformly for all n over the range $[0, t_f]$ and from the structure of the model (5.2.3), it implies that its derivatives are always

bounded uniformly. Thus, P_{1_n}, P_{2_n}, and P_{3_n} are Lipschitz continuous with the same Lipschitz constant. Therefore, the sequence $\{P_{1_n}, P_{2_n}, P_{3_n}\}$ is equicontinuous, and therefore, by Arzela-laAscoli theorem, it does exist (P_1^*, P_2^*, P_3^*) such that on a subsequence,

$$(P_{1_n}, P_{2_n}, P_{3_n}) \rightarrow (P_1^*, P_2^*, P_3^*) \text{ uniformly on } [0, t_f].$$

Also, control sequences, h_n, are bounded to any n and t, so there is a subsequence. h_{n_k}, and controls $(h^*) \in U$ such that $h_{n_k} \rightarrow h^*$ weakly in $L^1([0, t_f])$. Using the lower–semicontinuity of L^1 norms with respect to weak convergence, we have

$$J(h^*) \leqslant \liminf_{n \to \infty} \int_o^{t_f} (A_1(P_{2_n}(t) + P_{3_n}(t)) - A_2 P_{1_n}(t)) dt$$
$$+ \liminf_{n \to \infty} \int_o^{t_f} (ch_n(t)(P_{2_n}(t) + P_{3_n}(t)) + \varepsilon h_n(t)^2) dt$$
$$= \inf_{(h) \in U} J(h).$$

Using the convergence of the state sequences and passing to the limit in the ordinary differential equations system, we have that P_1^*, P_2^*, and P_3^* are the states corresponding to the control h^*. Note that the uniform convergence of states and the weak convergence of controls are important for the convergence terms such as $h_n P_{2_n}$. Thus, we conclude that h^* is optimal control. $\qquad \square$

We characterize the time–dependent control and the corresponding adjoint equations, when density and frequency–dependent transmission rates are studied. We apply Pontryagins maximum principle to our problem [122]. The Hamiltonian is defined as follows:

$$H = A_1(P_2 + P_3) - A_2 P_1 + ch(P_2 + P_3) + \varepsilon h^2 + \lambda_1 \left(rP_1 \left(1 - \frac{P_1}{K}\right) - \frac{aP_1 P_3}{P_1 + \delta} \right)$$
$$+ \lambda_2 \left(\alpha a(1 - \gamma) \frac{P_1 P_3}{P_1 + \delta} - \beta P_2 P_3 - (m+h)P_2 \right) + \lambda_3 \left(\alpha a\gamma \frac{P_1 P_3}{P_1 + \delta} + \beta P_2 P_3 - (m+h+\mu)P_3 \right),$$

where λ_1, λ_2 and λ_3 are adjoint variables associated with the state variables P_1, P_2, and P_3, respectively. The following theorem characterizes optimality.

Theorem 5.6.3. There exists an optimal control h^*, corresponding states P_1^*, P_2^*, and P_3^*, there

exist adjoint variables λ_1, λ_2, and λ_2 satisfying the equations

$$
\begin{cases}
\lambda_1'(t) &= A_2 + \left(\frac{rP_1}{K} - r\left(1 - \frac{P_1}{K}\right) - \frac{aP_1P_3}{(\delta+P_1)^2} + \frac{aP_3}{\delta+P_1}\right)\lambda_1 \\
& \quad + \left(\frac{a\alpha(1-\gamma)P_1P_3}{(\delta+P_1)^2} - \frac{a\alpha(1-\gamma)P_3}{\delta+P_1}\right)\lambda_2 + \left(\frac{a\alpha\gamma P_1P_3}{(\delta+P_1)^2} - \frac{a\alpha\gamma P_3}{\delta+P_1}\right)\lambda_3, \\
\lambda_2'(t) &= -ch - A_1 - (-h - m - \beta P_3)\lambda_2 - \beta P_3\lambda_3, \\
\lambda_3'(t) &= -ch - A_1 + \frac{aP_1\lambda_1}{\delta+P_1} + \left(-\frac{a\alpha(1-\gamma)P_1}{\delta+P_1} + \beta P_2\right)\lambda_2 + \left(h + m + \mu - \frac{a\alpha\gamma P_1}{\delta+P_1} - \beta P_2\right)\lambda_3,
\end{cases}
$$
(5.6.3)

with final time conditions

$$\lambda_1(t_f) = \lambda_2(t_f) = \lambda_3(t_f) = 0. \tag{5.6.4}$$

In addition, optimal characterisation for the time–dependent control $h^*(t)$ is

$$h^*(t) = min\left\{1, max\left\{0, \frac{-cP_2^*(t) - cP_3^*(t) + P_2^*(t)\lambda_2(t) + P_3^*(t)\lambda_3(t)}{2\varepsilon}\right\}\right\}. \tag{5.6.5}$$

Proof. The following equations are derived from the partial derivatives of the Hamiltonian, H, with respect to each state variable. That is,

$$\lambda_1'(t) = -\frac{\partial H}{\partial P_1}, \quad \lambda_2'(t) = -\frac{\partial H}{\partial P_2}, \quad \lambda_3'(t) = -\frac{\partial H}{\partial P_3}.$$

The behaviour of the control can be determined by differentiating the Hamiltonian, H, with respect to the control h. Thus,

$$
\begin{aligned}
\frac{\partial H}{\partial h} &= 2h\varepsilon + c(P_2 + P_3) - P_2\lambda_2 - P_3\lambda_3 = 0 \text{ at } h = h^*(t), \\
\Rightarrow h^* &= \frac{-cP_2^* - cP_3^* + P_2^*\lambda_2 + P_3^*\lambda_3}{2\varepsilon}.
\end{aligned}
$$

Therefore, the following is obtained by using the bound for the control $h(t)$ [200].

$$h^*(t) = min\left\{1, max\left\{0, \frac{-cP_2^*(t) - cP_3^*(t) + P_2^*(t)\lambda_2(t) + P_3^*(t)\lambda_3(t)}{2\varepsilon}\right\}\right\}.$$

□

5.6.1 Optimality System

The optimality system consists of the state system and adjoint system with initial and transversal conditions together with characterization of optimal control. The following

optimality system characterizes the optimal control:

$$\frac{dP_1}{dt} = r(t)P_1(t)\left(1 - \frac{P_1(t)}{K}\right) - \frac{aP_1(t)P_3(t)}{P_1(t) + \delta},$$

$$\frac{dP_2}{dt} = \alpha a(1-\gamma)\frac{P_1(t)P_3(t)}{P_1(t)+\delta} - \beta P_2(t)P_3(t)$$
$$- \left(m + \min\left\{1, \max\left\{0, \frac{-cP_2^*(t) - cP_3^*(t) + P_2^*(t)\lambda_2(t) + P_3^*(t)\lambda_3(t)}{2\varepsilon}\right\}\right\}\right)P_2(t),$$

$$\frac{dP_3}{dt} = \alpha a\gamma\frac{P_1(t)P_3(t)}{P_1(t)+\delta} + \beta P_2(t)P_3(t)$$
$$- \left(m + \min\left\{1, \max\left\{0, \frac{-cP_2^*(t) - cP_3^*(t) + P_2^*(t)\lambda_2(t) + P_3^*(t)\lambda_3(t)}{2\varepsilon}\right\}\right\} + \mu\right)P_3,$$

$$\lambda_1'(t) = A_2 + \left(\frac{rP_1}{K} - r\left(1 - \frac{P_1}{K}\right) - \frac{aP_1P_3}{(\delta + P_1)^2} + \frac{aP_3}{\delta + P_1}\right)\lambda_1$$
$$+ \left(\frac{a\alpha(1-\gamma)P_1P_3}{(\delta + P_1)^2} - \frac{a\alpha(1-\gamma)P_3}{\delta + P_1}\right)\lambda_2 + \left(\frac{a\alpha\gamma P_1P_3}{(\delta + P_1)^2} - \frac{a\alpha\gamma P_3}{\delta + P_1}\right)\lambda_3,$$

$$\lambda_2'(t) = -c\min\left\{1, \max\left\{0, \frac{-cP_2^*(t) - cP_3^*(t) + P_2^*(t)\lambda_2(t) + P_3^*(t)\lambda_3(t)}{2\varepsilon}\right\}\right\} - A_1$$
$$- \left(-\min\left\{1, \max\left\{0, \frac{-cP_2^*(t) - cP_3^*(t) + P_2^*(t)\lambda_2(t) + P_3^*(t)\lambda_3(t)}{2\varepsilon}\right\}\right\} - m - \beta P_3\right)\lambda_2 - \beta P_3\lambda_3,$$

$$\lambda_3'(t) = -c\min\left\{1, \max\left\{0, \frac{-cP_2^*(t) - cP_3^*(t) + P_2^*(t)\lambda_2(t) + P_3^*(t)\lambda_3(t)}{2\varepsilon}\right\}\right\} - A_1$$
$$+ \frac{aP_1\lambda_1}{\delta + P_1} + \left(-\frac{a\alpha(1-\gamma)P_1}{\delta + P_1} + \beta P_2\right)\lambda_2$$
$$+ \left(\min\left\{1, \max\left\{0, \frac{-cP_2^*(t) - cP_3^*(t) + P_2^*(t)\lambda_2(t) + P_3^*(t)\lambda_3(t)}{2\varepsilon}\right\}\right\} + m + \mu - \frac{a\alpha\gamma P_1}{\delta + P_1} - \beta P_2\right)\lambda_3,$$

and subject to the following conditions

$$P_1(0) = P_{10}, \ P_2(0) = P_{20}, \ P_3(0) = P_{30}, \ \lambda_1(t_f) = 0, \ \lambda_2(t_f) = 0 \text{ and } \lambda_3(t_f) = 0.$$

5.7 Numerical Simulations for Optimal Control Problem

In this section, we analyze various control techniques in numerical simulations for the model. We begin by looking at three comparison contexts, consisting of functional biomass P_1, free nematodes in soil P_2 population, and infesting nematodes P_3 dynamics in the absence and presence of control variables. When analyzing control approaches, we find the impact of numerous factors when evaluating the control methods, the period in which regulation can be applied, and various price parameterizations. The numerical simulation is described the features before doing so. An iterative scheme is used to solve the optimality system. Now we numerically solve the optimal control problem using Runge–Kutta's iterative process of fourth–order. The procedure of solution of the system (5.2.3) and (5.6.3) are given in [50, 200, 218, 219]. The convergence of the forward–backward sweeping method is based on work by [234]. Thus, we consider taking a set of simulated parameters for the calculation. Therefore, because this issue is about reducing pests and also saving crops, we consider both A_1 and A_2 weights to be 1. Also, we take $\varepsilon = 0.1$ unit in Fig. 5.7 and 0.01 unit in Fig. 5.8 as it is related to the cost of killing. We utilize this control within 2 (days), which could be in weeks or even months. So we set the time as 2 (days). Let, we take initial population density of P_1, P_2 and P_3 are 2, 1, and 0.9 units respectively. Figure 5.7 describes the solution curves for the three state variables, both in appearance and non–appearance of the control. The use of optimal control is found to remove a considerably higher number of nematode pests than without the control. Figure 5.7(a) indicates that in the presence of control and the absence of control, the population density of functional root plant biomass P_1 is approximately 2.35 and 1.8 units at 2 (days), respectively. Similarly, Figure 5.7(b) and Figure 5.7(c) show that the population density of P_2 and P_3 is approximately 0.50 and 0.85 units in the presence of control and 0.90, 2.80 units in the absence of control, respectively. In Fig. 5.8, we choose different parameters in comparison to Fig. 5.7, i.e., $A_1 = 100$, $A_2 = 50$, $r = 0.4$, $k = 4$, $a = 0.6$, $\gamma = 0.6$, $\beta = 0.3$, $m = 0.25$, $\varepsilon = 0.01$. Figure 5.8(a) shows that the population density of P_1 is 2.55 units in the presence of control and 1.9 units in the absence of control which is more population density compared to the Fig. 5.7(a). Similarly, Figure 5.8(b) and Figure 5.8(c) show that the population density is approximately 0.25, 0.50 units in the presence of control and 0.70,

3.25 in the absence of control at time 2 (days), respectively. This is also evident from Fig. 5.7(b) and Fig. 5.7(c) that the nematode pest has suffered much due to the application of pesticide control. This is because applying pesticide control significantly decreases the population of nematode pests. Thus, we can conclude that applying the optimal control of pesticides not only minimizes the pest population but also decreases the natural enemy of the pest populations. Figure 5.7(d) represents the variation of optimal control and Figure 5.7(e), Figure 5.7(f) and Figure 5.7(g) describe the variation of adjoint variables in the presence control. From Fig. 5.7(e), it is observed that the control would be best if this is to be used for about 1 (days) of time at its maximum level. Figure 5.8(e) shows the control variation with respect to time t and Figure 5.8(e), 5.8(f) and 5.8(g) show the adjoint variables variation.

Figure 5.7: Comparison between the figures of individuals with control versus without control, which represent the results for prey, predator, control and adjoint variables with respect to time, where value of parameters are $A_1 = 1$, $A_2 = 1$, $c = 1$, $r = 0.4$, $k = 4$, $a = 0.6$, $\delta = 2$, $\alpha = 3.5$, $\gamma = 0.6$, $\beta = 0.3$, $m = 0.25$, $\mu = 0.11$, $\varepsilon = 0.1$, $P_{10} = 2$, $P_{20} = 1$, $P_{30} = 0.9$ and $t = 2\,days$.
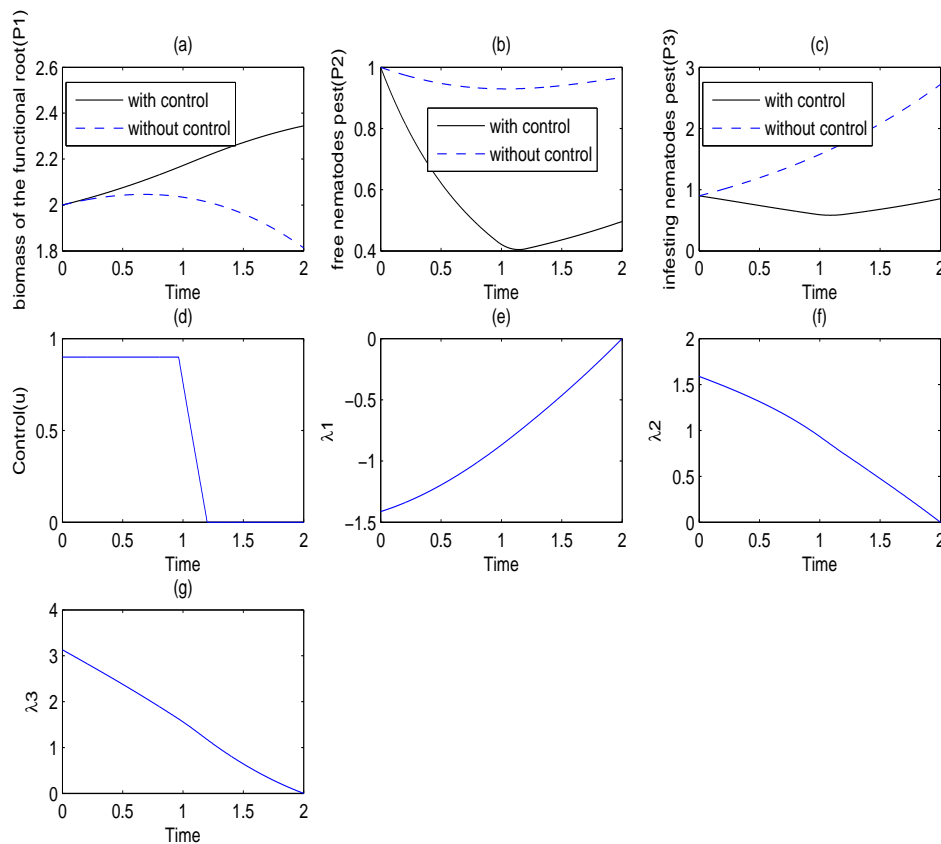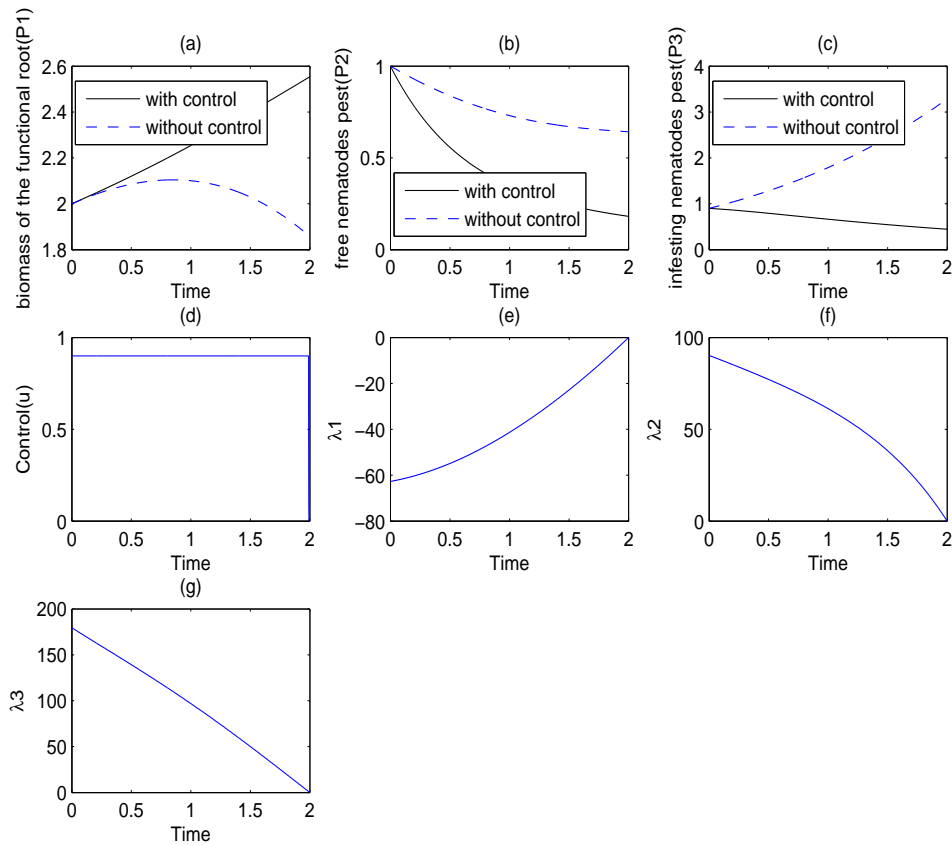
Figure 5.8: Comparison between the figures of individuals with control versus without control, which represent the results for prey, predator, control and adjoint variables with respect to time, where the value of parameters are $A_1 = 100$, $A_2 = 50$, $c = 1$, $r = 0.5$, $k = 4$, $a = 0.6$, $\delta = 2$, $\alpha = 3.5$, $\gamma = 0.7$, $\beta = 0.4$, $m = 0.3$, $\mu = 0.10$, $\varepsilon = 0.01$, $P_{10} = 2$, $P_{20} = 1$, $P_{30} = 0.9$ and $t = 2\ days$.

5.8 Discussion and Future Scope

In this research, the core idea is that the control of nematode pests is a dynamic process. Mathematical models are significant to understand and provide useful corresponding biological abstractions mechanisms and environmentally friendly interactions occurring in applications for pest control. The work has suggested a multi–seasonal structure explaining the infestation of banana roots by the nematodes. The mathematical model is a prey–predator scheme with three variables of the state, namely functional biomass of banana P_1, free nematodes pest in soil P_2, and infecting nematodes in roots P_3. Additionally, the types of approaches to pest control discussed

in our analysis can be briefly classified as follows: chemical pesticides and replanting properly mixed in the context. The study found that bananas are affected by various illnesses. Nematodes are the most destructive banana pests, which cause a loss of crops. A broad variety of variables tend to affect the results. In addition, there are eco–epidemiological criteria based on monitoring costs, their weighting in the objective framework, the useful technique of the control process, and the initial state. The model (5.2.3) is uniformly bounded, and all solutions are completely defined in the positive region. We performed the behavior of the system by analyzing the system's structure through all its equilibriums. Depending on various conditions, the point of equilibrium is locally asymptotically stable. It has also been observed that all points of equilibrium are conditionally feasible and locally asymptotically stable, except for the trivial equilibrium point E_0 and the functional root biomass of banana–free equilibrium point E_1. We have performed the resulting model with a more depth qualitative optimal control study and determine the circumstances in which this is optimal. In Figure 5.7 and Figure 5.8, it has been observed that the optimal control worked as a break of the nematodes population and favorable conditions of the functional root of banana. Thus, Nematode population density has declined, while functional root biomass population density has increased. Our study found an effective strategy for banana pest identification and diseases. It relies on a rise in the amount of pesticide. Future research in the field would involve a multidisciplinary interaction between agronomists, environmental modelers, and mathematical researchers, and computational experts, aimed at building Mathematical models, which offer reliable outcomes and recognizing field findings in actual environments so that all the models can be regarded as development tools. Finally, to apply optimal control techniques, the parameters need to be well known and this may increase the performance of our future optimal control systems.

Chapter 6

Preventing the Spread of Locust Swarm and Pest in Agriculture: Mathematical Modeling and Qualitative Analysis

In the present chapter, we present an interaction between the prey and predator model consisting of three species: crops, pests, and locust swarms. Under specific circumstances, all possible existences of the biological equilibrium points of the systems are described. The local asymptotic stability of various equilibrium points is demonstrated to analyse the dynamics of the system. This study investigates the appropriate use of management measures to prevent the expansion of the swarm through optimal control techniques. There are two kinds of control variables utilised: first, the application of pesticide, and second, the application of creating awareness. We determine the existence and Pontryagins maximum principle is utilised to characterise optimal controls. Finally, the theoretical analysis is validated by numerical simulations.

6.1 Motivation and Biological Background

The global agricultural production is undergoing significant changes because consumers' needs, input prices, food security and environmental concerns are rapidly changing. Agricultural production systems are undergoing fast changes in response to shifts in manufacturing costs, customer expectations and growing food safety, security and environmental concerns. A key challenge is the necessity, while retaining the economically viable production system of farmers, to establish sustainable production systems addressing social concerns for impacts on the environment and for nutritional content. A locust is a big, mostly tropical, grasshopper with great flying skills that migrate in massive swarms that harm the crop tremendously. However, the current number of swarm volumes would rise exponentially if these attacks are not halted and humanity would have to handle up to 80 million locusts per km^2. They feed, raise, with extremely high fertility. The heathen grow their numbers by 16,000 times in only three breeding periods [250]. They do not harm animals or people, but can ruin plants and other vegetative areas. But $1km^2$ swarm has over 40 million locusts, and they consume roughly 35,000 humans, twenty camels or six elephants in the same quantity of food in a single day [251]. In the last two years, several nations have seen a rise in locust swarms. The main reason is the cyclonic storms in Mekunu and Luban that occurred in Oman and Yemen from May and October 2018. The locusts are currently active in the state of India such as Rajasthan, Gujarat, Maharashtra, Uttar Pradesh, and Madhya Pradesh. Although there were no cycles of locusts until 1962, however, major upsurges occurred between 1978 and 1993 [252]. They consume millet, rice, maize, sorghum, sugarcane, barley, cotton, fruit trees, date palm, vegetables, rangeland grasses, acacia, pines, and bananas [250]. Because of its tremendous population density, it is often difficult to control a locust swarm. Even a insignificant $1km^2$ swarm has around 1–1.5 billion insects and any prevention action against such a massive population are considered as futility [251, 252]. [251, 252] was concerned about the control of locust swarms, such as spraying insects on aircraft and helicopters, thin dust impregnated with insecticide, pumping insecticides, protection in the usage and storage of pesticide products, and environmental issues. An efficient food and fiber strategy utilizes farm resources to avoid harmful environmental and human consequences, maintains the quality and natural productivity of land,

and supports dynamic rural communities. Accordingly, the five overall objectives for sustainable production systems are to meet human requirements, strengthen the environment and natural resource base, increase resource efficiency, boost the financial viability of farming and enhance the quality of life for farmers and society. [29, 236] presented systematically integrated pest management models. Further, interactions between crop, pest, diseases, and pest predators and successive studies of mathematical models for pest control have been carried out by [22, 171]. Many models are available to facilitate decision-making on crops and animal production, such as management of agricultural resources [119]. Although these models often represent biophysical processes in great detail, the necessity for vast volumes of input data and the need for rigorous calibration and validation in the running of each application can restrict their use. Although [206] provided a mathematical model for the usage in agricultural decision–making systems to be used in dynamic systems, its models have not even been used in real agricultural systems. One of the main aims of ecology was to understand the relationships among prey and predator [1, 3, 228]. The functional response is also important in defining the relationships between individuals, other animals and their environments [85]. Several elements, directly and indirectly, influence predator eating rates and thus functional response, such as accessible food items, prey–predator structure, predator density, the effectiveness of search, prey escape capacity, predator's hunting capacity, and encounter rate, etc. There are several extensive analyzes of the aspects that affect predatory use rates of resources [70, 102]. The modified Leslie predator–prey system has been designed to take account of global dynamics and co–existence between the system, motivated by the above existing theoretical works [83, 176] and experimental evidence relating to environmental disturbances and their impact on the associated ecosystem [13, 101].

In this work, we develop a three–dimensional dynamical system modeling consists of crops, pests, and locust swarms. We take an interest in knowing the pest's effect on crops and the impact of the locust swarm. This paper presents two mathematical models, one in the absence of control and the other in the presence of control. The coexistence of equilibrium systems under various conditions is examined. To address some important biological instances, we give numerical reports that our model shows. Further, an optimal control problem is developed and evaluated analytically. Here, two types of control variables are used; first, the rate of application of pesti-

cide, and second, application of awareness to promote the necessary steps. The paper is described as follows: in Section 6.2, the formation of the prey–predator model is developed in the presence of crop (prey), pest (predator–I), and locust swarms (predator–II). Section 6.4 describes the positivity and boundedness of the system, equilibria of the system, and local stability. The existence and global stability analysis of the endemic equilibrium are discussed in Section 6.5. Section 6.6 illustrates the dynamical behavior and biological interpretation of the model and its discussion through the numerical simulation. Formulation and application of optimal control problem, cost–effectiveness analysis, the existence of controls, characterization of the optimal control pair, and the optimality system are performed in Section 6.7. Section 6.8 demonstrates numerical simulations for the validation of the theoretical results of the optimal control problem through different parameters. Finally, Section 6.9 summarizes our study with various biological consequences and future research relevant to our results.

6.2 Formulation of Prey–Predator Mathematical Model

In studying agricultural issues, mathematical modeling is an important technical method. Mathematical ecology demands the study of pesticides and their effects on crop populations in the study of the dynamics of a plant population. Different species interactions have a harmful effect on one species or both. Crops and pests are interactions where one species get nourishment, while the other is damaged. Prey–predator behavior is a highly prevalent kind of natural biological interaction. Many mathematical models are available to simulate prey–predator, such as Lotka–Volterra system, Chemostat–type system, Kolmogorov systems, etc. Considering that the predator function differs from the predator growth function, the renowned system Leslie type prey–predator system [161]. A functional choice of reactions strongly affects the dynamic interaction between the interacting population [47, 150, 161]. [139] proposed the prey–predator model with Holling type II and modified Leslie–Gower functional response. The many changed versions can be seen by interested readers [56, 103, 129]. In this paper, a mathematical formulation of a prey–predator system with one prey species and two predator species is considered. Here, prey species is density of crops, predator–I means a destructive insect that attacks crops, food, livestock, etc.,

predator–II means locust swarmsthat damage numerous acres of agriculture in a short period of time, destroying farmer livelihoods and affecting a community's food production. Further, we consider the modified Leslie–Gower type prey–predator system in prey and predator-II. Based on the above formulations and assumptions, the one prey and two predator modelisgiven by the following system of deterministic differential equations:

$$
\begin{cases}
\frac{dP_1(t)}{dt} = r_1P_1(t) - i_1P_1^2(t) - c_1(1-m_1)P_2(t)P_1(t) - \frac{cP_1P_3}{b+c_3P_1(t)+dP_3(t)}, \\
\frac{dP_2(t)}{dt} = r_2P_2(t) - i_2P_2^2(t) + c_2(1-m_1)P_1(t)P_2(t), \\
\frac{dP_3(t)}{dt} = r_3P_3(t) - \frac{eP_3^2(t)}{P_1(t)+K},
\end{cases}
\tag{6.2.1}
$$

with initial data $P_1(0) > 0$, $P_2(0) > 0$, and $P_3(0) > 0$, where P_1, P_2, and P_3 represent the population densities of crop, pest and locust swarm at time t, respectively. r_1, i_1, c_1, m_1, c, b, c_3, d, r_2, i_2, c_2, r_3, e, and K are model parameters assuming only positive values. K measures the extent to which environment provides protection to locust swarm. These parameters are defined in Table 6.1.

Table 6.1: Description of variables and parameters

Variables and Parameters	Meaning
$P_1(t)$	Density of crops (prey) at time t
$P_2(t)$	Density of predators-I at time t
$P_3(t)$	Densities of predator-II at t
i_1	Competition among preys
i_2	Competition among predators-I
c_1	Response of prey to predators-I
c_2	Response of predators-I to prey
r_1	Growth rate of prey
r_2	Growth of predator-I
m_1	Special threshold value of prey
r_3	Growth rate of predator-II
c	Maximum value which per capita reduction rate of prey can attain
b	Measures the half saturation of prey species,
e	Maximum value which per capita reduction rate of predator-II can attain
c_3	Measures the handling time on the feeding rate
d	Coefficient of interference among predator-II
b	Measures the half saturation of prey species

179

6.3 Positiveness and Boundedness of the System

It is essential to show that for model (6.2.1), the solutionsof the system with positive initial data will remain positive. This is demonstrated by the theorem below.

Theorem 6.3.1. The solutions of $(P_1(t),\ P_2(t),\ P_3(t))$ of the system (6.2.1) with the initial data $P_1(0) > 0$, $P_2(0) > 0$, and $P_3(0) > 0$ are positive.

Proof. Since all of the parameters used in the system are positive. Thus, we can establish lower bounds on each of the model's equations (6.2.1). (i) Positivity of $P_1(t)$: from the model (6.2.1)

$$\frac{dP_1}{dt} = r_1 P_1(t) - i_1 P_1^2(t) - c_1(1 - m_1)P_2(t)P_1(t) - \frac{cP_1(t)P_3(t)}{b + c_3 P_1(t) + dP_3(t)}. \tag{6.3.1}$$

Without loss of generality and from (6.3.1), we obtain the differential inequality

$$\frac{dP_1}{dt} \geqslant -i_1 P_1^2(t) - c_1 P_2(t)P_1(t) - \frac{cP_1(t)P_3(t)}{b + c_3 P_1(t) + dP_3(t)}.$$

We can eliminate inequalities and obtain the results:

$$P_1(t) \geqslant P_1(0)e^{-\int_0^t \left(i_1 P_1(s) + c_1 P_2(s) + \frac{cP_3(s)}{b + c_3 P_1(s) + dP_3(s)} \right)ds}$$

Clearly $P_1(0) > 0$ implies $P_1(t) > 0\ \forall\, t > 0$.
(ii) Positivity of $P_2(t)$: from the model (6.2.1),

$$\frac{dP_2}{dt} = r_2 P_2 - i_2 P_2^2 + c_2(1 - m_1)P_1 P_2 \geqslant -i_2 P_2^2(t) - c_2 m_1 P_1(t)P_2(t). \tag{6.3.2}$$

We can eliminate inequalities and obtain the results:

$$P_2(t) \geqslant P_2(0)e^{-\int_0^t (i_2 P_2(s) + c_2 m_1 P_1(s))ds}$$

Clearly $P_2(0) > 0$ implies $P_2(t) > 0\ \forall\, t > 0$.
(iii) Positivity of $P_3(t)$: from the model (6.2.1),

$$\frac{dP_3}{dt} = r_3 P_3(t) - \frac{eP_3^2(t)}{P_1(t) + K} \geqslant -\frac{eP_3^2(t)}{P_1(t) + K}. \tag{6.3.3}$$

We can eliminate inequalities and obtain the results:

$$P_3(t) \geqslant P_3(0)e^{-\int_0^t \left(\frac{eP_3(s)}{P_1(s)+K} \right) ds}$$

Clearly $P_3(0) > 0$ implies $P_3(t) > 0 \; \forall \, t > 0$. $\qquad\qquad\qquad\qquad\qquad\qquad\square$

Theorem 6.3.2. All solutions of the model system (6.2.1) that initiate in R_+^3 are uniformly bounded.

Proof. We define the function $w(P_1, P_2, P_3) = P_1 + P_2 + P_3$. For $\eta > 0$, adding ηw and derivative of $w(P_1, P_2, P_3)$ with respect to t is

$$\frac{dw}{dt} + \eta w = \frac{dP_1}{dt} + \frac{dP_2}{dt} + \frac{dP_3}{dt} + \eta(P_1 + P_2 + P_3),$$

$$= r_1 P_1 - i_1 P_1^2 - c_1(1-m_1)P_2 P_1 - \frac{cP_1 P_3}{b + c_3 P_1(t) + dP_3}$$

$$+ r_2 P_2 - i_2 P_2^2 + c_2(1-m_1)P_1 P_2 + r_3 P_3 - \frac{eP_3^2(t)}{P_1 + K} + \eta(P_1 + P_2 + P_3),$$

$$\Rightarrow \frac{dw}{dt} + \eta w = (r_1 + \eta - i_1 P_1)P_1 + (r_2 + \eta - i_2 P_2)P_2 + (r_3 + \eta)P_3,$$

holds for all P_1, P_2, and P_3 nonnegative and assuming $c_1 > c_2$. Moreover, it can be easily verified that max of $(r_1 + \eta - i_1 P_1)P_1 = \frac{(r_1+\eta)^2}{4i_1}$ and max of $(r_2 + \eta - i_2 P_2)P_2 = \frac{(r_2+\eta)^2}{4i_2}$. Further, $\frac{dP_3}{dt} \leqslant r_3 P_3 \Rightarrow P_3(t) \leqslant Q_4 e^{r_3}$, where Q_4 is integration constant.

$\Rightarrow \frac{dw}{dt} + \eta w \leqslant \frac{(r_1+\eta)^2}{4i_1} + \frac{(r_2+\eta)^2}{4i_2} + (r_3 + \eta)Q_4 e^{r_3}$, thus, we select a value $k > 0$ such that $k = \frac{(r_1+\eta)^2}{4i_1} + \frac{(r_2+\eta)^2}{4i_2} + (r_3 + \eta)Q_4 e^{r_3}$. Then, $\frac{dw}{dt} + \eta w \leqslant k$.

Applying the theory of differential inequality [65],

$$0 < w(P_1, P_2, P_3) \leqslant \frac{k}{\eta}(1 - e^{-\eta t}) + \frac{w(P_1(0), P_2(0), P_3(0))}{e^{\eta t}},$$

for $t \to \infty$, we have, $0 < w(P_1, P_2, P_3) \leqslant \frac{k}{\eta}$. Hence, all the solution of system (6.2.1) are

$$\Theta = \{(P_1, P_2, P_3) \in R_+^3 : 0 < w \leqslant \frac{k}{\eta}\}.$$

$\qquad\qquad\qquad\qquad\qquad\qquad\qquad\qquad\qquad\qquad\qquad\qquad\qquad\qquad\square$

6.4   Steady States and Stability Analysis

System (6.2.1) has following possible equilibria points:

(i) The trivial equilibrium point $E_0(P_1^*, P_2^*, P_3^*)$, where

$$P_1^* = 0, \; P_2^* = 0, \; P_3^* = 0.$$

(ii) The crop and pest free equilibrium point $E_1(P_1^*, P_2^*, P_3^*)$, where

$$P_1^* = 0, \; P_2^* = 0, \; P_3^* = \frac{Kr_3}{e},$$

which is biologically feasible.

(iii) The pest and locust swarm free equilibrium point $E_2(P_1^*, P_2^*, P_3^*)$, where

$$P_1^* = \frac{r_1}{i_1}, \; P_2^* = 0, \; P_3^* = 0,$$

which is biologically feasible.

(iv) The crop and locust swarm free equilibrium point $E_3(P_1^*, P_2^*, P_3^*)$, where

$$P_1^* = 0, \; P_2^* = \frac{r_2}{i_2}, \; P_3^* = 0,$$

which is biologically feasible.

(v) The pest and locust swarm free equilibrium point $E_4(P_1^*, P_2^*, P_3^*)$, where

$$P_1^* = -\frac{b}{c_3}, \; P_2^* = 0, \; P_3^* = 0,$$

which is not biologically feasible since $P_1^* < 0$.

(vi) The crop free equilibrium point $E_5(P_1^*, P_2^*, P_3^*)$, where

$$P_1^* = 0, \; P_2^* = \frac{r_2}{i_2}, \; P_3^* = \frac{Kr_3}{e},$$

which is biologically feasible.

(vii) The locust swarm free equilibrium point $E_6(P_1^*, P_2^*, P_3^*)$, where

$$P_1^* = -\frac{b}{c_3}, \; P_2^* = \frac{bc_2m_1 - bc_2 + c_3r_2}{c_3i_2}, \; P_3^* = 0,$$

which is not biologically feasible since $P_1^* < 0$.

(viii) The locust swarm free equilibrium point $E_7(P_1^*, P_2^*, P_3^*)$, where

$$P_1^* = \frac{i_2 r_1 + c_1 m_1 r_2 - c_1 r_2}{c_1 c_2 + i_1 i_2 + c_1 c_2 m_1^2 - 2 c_1 c_2 m_1}, P_2^* = \frac{c_2 r_1 + i_1 r_2 - c_2 m_1 r_1}{c_1 c_2 + i_1 i_2 + c_1 c_2 m_1^2 - 2 c_1 c_2 m_1}, P_3^* = 0,$$

which is biologically feasible if $i_2 r_1 + c_1 m_1 r_2 > c_1 r_2, c_1 c_2 + i_1 i_2 + c_1 c_2 m_1^2 > 2 c_1 c_2 m_1$ or $i_2 r_1 + c_1 m_1 r_2 < c_1 r_2, c_1 c_2 + i_1 i_2 + c_1 c_2 m_1^2 < 2 c_1 c_2 m_1$, and $c_2 r_1 + i_1 r_2 > c_2 m_1 r_1, c_1 c_2 + i_1 i_2 + c_1 c_2 m_1^2 > 2 c_1 c_2 m_1$ or $c_2 r_1 + i_1 r_2 < c_2 m_1 r_1, c_1 c_2 + i_1 i_2 + c_1 c_2 m_1^2 < 2 c_1 c_2 m_1$.

(ix) The pest free equilibrium point $E_8(P_1^*, P_2^*, P_3^*)$, where

$$P_1^* = \frac{d_1 + \sqrt{d_2}}{2 i_1 (c_3 e + d r_3)}, \ P_2^* = 0, \ P_3^* = \frac{r_3 (d_1 + \sqrt{d_2})}{2 i_1 (c_3 e + d r_3)},$$

and $d_1 = -b e i_1 + c_3 e r_1 - c r_3 - d i_1 K r_3 + d r_1 r_3$,

$d_2 = (i_1 (b e + d K r_3) + r_3 (c - d r_1) + c_3 (-e) r_1)^2 + 4 i_1 (c_3 e + d r_3) (r_1 (b e + d K r_3) - c K r_3)$,

$d_3 = 2 i_1 (c_3 e + d r_3)$, which is biologically feasible if $d_1 > 0$ and $d_2 > 0$.

(x) The crop, pest, and locust swarm coexistence equilibrium point $E_9(P_1^*, P_2^*, P_3^*)$, where the interior equilibrium point $E^*(P_1^*, P_2^*, P_3^*)$ is the point of intersection of the following equations:

$$-\frac{c P_3}{b + c_3 P_1 + d P_3} - c_1 (1 - m_1) P_2 - i_1 P_1 + r_1 = 0, \tag{6.4.1}$$

$$c_2 (1 - m_1) P_1 - i_2 P_2 + r_2 = 0, \tag{6.4.2}$$

$$r_3 - \frac{e P_3}{K + P_1} = 0, \tag{6.4.3}$$

from (6.4.1) and (6.4.2)

$$P_2 = \frac{P_1 (c_2 - c_2 m_1) + r_2}{i_2}, \ P_3 = \frac{r_3 (K + P_1)}{e}, \tag{6.4.4}$$

using the value of P_2 and P_3 from equation (6.4.4), then, P_1 satisfies the following equation:

$$P_1^2 Q + P_1 R + P = 0, \tag{6.4.5}$$

where, $Q = d r_3 \left(-\frac{c_1 c_2 m_1^2}{i_2} + \frac{2 c_1 c_2 m_1}{i_2} - \frac{c_1 c_2}{i_2} - i_1 \right) + c_3 e \left(-\frac{c_1 c_2 m_1^2}{i_2} + \frac{2 c_1 c_2 m_1}{i_2} - \frac{c_1 c_2}{i_2} - i_1 \right)$

$P = b e \left(\frac{c_1 m_1 r_2}{i_2} - \frac{c_1 r_2}{i_2} + r_1 \right) - c K r_3 + d K r_3$

183

$R = be\left(-\frac{c_1c_2m_1^2}{i_2} + \frac{2c_1c_2m_1}{i_2} - \frac{c_1c_2}{i_2} - i_1\right) + dKr_3\left(-\frac{c_1c_2m_1^2}{i_2} + \frac{2c_1c_2m_1}{i_2} - \frac{c_1c_2}{i_2} - i_1\right) + c_3e - cr_3 + dr_3,$

If $Q > 0$ and $R^2 - 4PQ > 0$, then (6.4.5) has a positive root P_1^*(say). For the value of P_1^*, values of P_2^* and P_3^* can be obtained from equation (6.4.4). P_2^* is positive if $c_2 > c_2m$ and P_3^* is positive as P_1^* is positive.

6.4.1 Local Stability

The stability analysis of the model (6.2.1) is governed by the Jacobian matrix

$$J = \begin{pmatrix} Q_5 & Q_6 & -\frac{cP_1}{b+c_3P_1+dP_2} \\ c_2(1-m_1)P_2 & Q_7 & 0 \\ Q_8 & 0 & -\frac{2eP_3}{K+P_1} + r_3 \end{pmatrix}, \quad (6.4.6)$$

where, $Q_5 = -2i_1P_1 - c_1(1-m_1)P_2 + \frac{cc_3P_1P_3}{(b+c_3P_1+dP_2)^2} - \frac{cP_3}{b+c_3P_1+dP_2} + r_1$, $Q_6 = -c_1(1-m_1)P_1 + \frac{cdP_1P_3}{(b+c_3P_1+dP_2)^2}$, $Q_7 = c_2(1-m_1)P_1 - 2i_2P_2 + r_2$, and $Q_8 = \frac{eP_3^2}{(K+P_1)^2}$.

Theorem 6.4.1. At different equilibria, the system (6.2.1) has the following behavior:

(i) The trivial equilibrium E_0 is unstable since all eigenvalues of (6.4.6) at E_0 are always positive.

(ii) The equilibrium E_1 is unstable, since one of the eigenvalues of (6.4.6) at E_1 is always positive, i.e., $r_2 > 0$.

(iii) The equilibrium E_2 is unstable, since one of the eigenvalues of (6.4.6) at E_2 is always positive, i.e., $r_3 > 0$.

(iv) The equilibrium E_3 is unstable, since one of the eigenvalues of (6.4.6) at E_3 is always positive, i.e., $r_3 > 0$.

(v) The equilibrium point E_5 is locally asymptotically stable if $bei_2^2r_1 + dec_1m_1r_2^2 + bec_1i_2m_1r_2 + dei_2r_1r_2 > bec_1i_2r_2 - dec_1r_2^2 - cKi_2^2r_3$.

(vi) The equilibrium E_7 is locally asymptotically stable if $s_1 > 0$, $s_2 > 0$, $s_3 > 0$, and $s_1s_2 - s_3 > 0$.

(vii) The equilibrium point E_8 is locally asymptotically stable if $d_{14} < 0$, $d_{11} + d_{16} - \sqrt{d_{11}^2 - 2d_{16}d_{11} + d_{16}^2 + 4d_{13}d_{15}} < 0$, and $d_{11} + d_{16} + \sqrt{d_{11}^2 - 2d_{16}d_{11} + d_{16}^2 + 4d_{13}d_{15}} < 0$.

(viii) The equilibrium point E_{10} is locally asymptotically stable if $g_1 > 0$, $g_2 > 0$, $g_3 > 0$, and $g_1g_2 - g_3 > 0$, where all parameters are mentioned in the proof.

Proof. (1) The Jacobian matrix at E_0 is $J(E_0) = \begin{pmatrix} r_1 & 0 & 0 \\ 0 & r_2 & 0 \\ 0 & 0 & r_3 \end{pmatrix}$. The eigenvalues of $J(E_0)$

are r_1, r_2, and r_3. Hence, E_0 is unstable since all eigenvalues are always positive.

(2) The Jacobian matrix at E_1 is

$$J(E_1) = \begin{pmatrix} r_1 - \frac{cKr_3}{be} & 0 & 0 \\ 0 & r_2 & 0 \\ \frac{r_3^2}{e} & 0 & -r_3 \end{pmatrix}.$$

The eigenvalues of $J(E_1)$ are $r_2, -r_3, \frac{ber_1 - cKr_3}{be}$. Hence, E_1 is unstable since r_2 is always positive.

(3) The Jacobian matrix at E_2 is

$$J(E_2) = \begin{pmatrix} -r_1 & -\frac{c_1(1-m_1)r_1}{i_1} & -\frac{cr_1}{i_1\left(b+\frac{c_3r_1}{i_1}\right)} \\ 0 & \frac{c_2(1-m_1)r_1}{i_1} + r_2 & 0 \\ 0 & 0 & r_3 \end{pmatrix}.$$

The eigenvalues of $J(E_2)$ are $-r_1$, $\frac{c_2r_1 - c_2m_1r_1 + i_1r_2}{i_1}$, r_3. Hence, E_2 is unstable since eigenvalue r_3 are always positive.

(4) The Jacobian matrix at E_3 is

$$J(E_3) = \begin{pmatrix} r_1 - \frac{c_1(1-m_1)r_2}{i_2} & 0 & 0 \\ \frac{c_2(1-m_1)r_2}{i_2} & -r_2 & 0 \\ 0 & 0 & r_3 \end{pmatrix}.$$

The eigenvalues of $J(E_3)$ are $-r_2$, $\frac{i_2r_1 - c_1r_2 + c_1m_1r_2}{i_2}$, r_3. Hence, E_3 is unstable since eigenvalue r_3 is always positive.

(5) The Jacobian matrix at E_5 is

$$J(E_5) = \begin{pmatrix} r_1 - \frac{c_1(1-m_1)r_2}{i_2} - \frac{cKr_3}{e\left(b+\frac{dr_2}{i_2}\right)} & 0 & 0 \\ \frac{c_2(1-m_1)r_2}{i_2} & -r_2 & 0 \\ \frac{r_3^2}{e} & 0 & -r_3 \end{pmatrix}.$$

185

The eigenvalues of $J(E_5)$ are $-r_2$, $-r_3$, and $\frac{bei_2^2 r_1 + dec_1 m_1 r_2^2 + bec_1 i_2 m_1 r_2 + dei_2 r_1 r_2 - bec_1 i_2 r_2 - dec_1 r_2^2 - cKi_2^2 r_3}{ei_2(bi_2 + dr_2)}$.

The equilibrium point E_5 is locally asymptotically stable if

$$bei_2^2 r_1 + dec_1 m_1 r_2^2 + bec_1 i_2 m_1 r_2 + dei_2 r_1 r_2 > bec_1 i_2 r_2 - dec_1 r_2^2 - cKi_2^2 r_3. \qquad (6.4.7)$$

(6) The Jacobian matrix at E_7 is

$$J(E_7) = \begin{pmatrix} d_6 & d_{67} & d_8 \\ d_9 & d_{10} & 0 \\ 0 & 0 & r_3 \end{pmatrix}$$

where, $d_6 = -c_1(1-m_1)P_2^* - 2i_1 P_1^* + r_1$, $d_7 = -c_1(1-m_1)P_1^*$, $d_8 = -\frac{cP_1^*}{b+c_3 P_1^* + dP_2^*}$, $d_9 = c_2(1-m_1)P_2^*$, and $d_{10} = c_2(1-m_1)P_1^* - 2i_2 P_2^* + r_2$.

The eigenvalues of $J(E_7)$ are $\frac{1}{2}\left(d_6 + d_{10} - \sqrt{d_6^2 - 2d_{10}d_6 + d_{10}^2 + 4d_9 d_{67}}\right)$,
$\frac{1}{2}\left(d_6 + d_{10} + \sqrt{d_6^2 - 2d_{10}d_6 + d_{10}^2 + 4d_9 d_{67}}\right)$, and r_3.

Then, the characteristic equation of the $J(E_7)$ is given by

$$s_1 x^2 + s_2 x + s_3 + x^3 = 0,$$

where, $s_1 = -d_6 - d_{10} - r_3$, $s_2 = d_6 r_3 + d_{10} r_3 - d_7 d_9 + d_6 d_{10}$, $s_3 = d_7 d_9 r_3 - d_6 d_{10} r_3$. Using the Routh-Hurwitz conditions [95, 126, 136], the equilibrium point E_7 is locally asymptotically stable if

$$s_1 > 0, \ s_2 > 0, \ s_3 > 0, \ \text{and } s_1 s_2 - s_3 > 0. \qquad (6.4.8)$$

(7) The jacobian matrix at E_8 is

$$J(E_8) = \begin{pmatrix} d_{11} & d_{12} & d_{13} \\ 0 & d_{14} & 0 \\ d_{15} & 0 & d_{16} \end{pmatrix},$$

where, $d_{11} = \frac{cc_3 P_3^* P_1^*}{(b+c_3 P_1^*)^2} - \frac{cP_3^*}{b+c_3 P_1^*} - 2i_1 P_1^* + r_1$, $d_{12} = \frac{cdP_1^* P_3^*}{(b+c_3 P_1^*)^2} - c_1(1-m_1)P_1^*$, $d_{13} = -\frac{cP_1^*}{b+c_3 P_1^*}$,
$d_{14} = c_2(1-m_1)P_1^* + r_2$, $d_{15} = \frac{eP_3^{*2}}{(K+P_1^*)^2}$, and $d_{16} = r_3 - \frac{2eP_3^*}{K+P_1^*}$.

The eigenvalues of the Jacobian matrix $J(E_8)$ are d_{14}, $\frac{1}{2}\left(d_{11} + d_{16} - \sqrt{d_{11}^2 - 2d_{16}d_{11} + d_{16}^2 + 4d_{13}d_{15}}\right)$,

186

and $\frac{1}{2}\left(d_{11} + d_{16} + \sqrt{d_{11}^2 - 2d_{16}d_{11} + d_{16}^2 + 4d_{13}d_{15}}\right)$.

The equilibrium point E_8 is locally asymptotically stable if

$$d_{14} < 0, \; d_{11} + d_{16} - \sqrt{d_{11}^2 - 2d_{16}d_{11} + d_{16}^2 + 4d_{13}d_{15}} < 0, \text{ and}$$

$$d_{11} + d_{16} + \sqrt{d_{11}^2 - 2d_{16}d_{11} + d_{16}^2 + 4d_{13}d_{15}} < 0. \tag{6.4.9}$$

(8) The Jacobian matrix at E_{10} is

$$J(E_10) = \begin{pmatrix} d_{17} & d_{18} & d_{19} \\ d_{20} & d_{21} & 0 \\ d_{22} & 0 & d_{23} \end{pmatrix},$$

where, $d_{17} = \frac{cc_3 P_3^* P_1^*}{(b+c_3 P_1^* + dP_2^*)^2} - \frac{cP_3^*}{b+c_3 P_1^* + dP_2^*} - c_1 (1 - m_1) P_2^* - 2i_1 P_1^* + r_1, d_{18} = \frac{cdP_1^* P_3^*}{(b+c_3 P_1^* + dP_2^*)^2} - c_1 (1 - m_1) P_1^*, d_{19} = -\frac{cP_1^*}{b+c_3 P_1^* + dP_2^*}, d_{20} = c_2 (1 - m_1) P_2^*, d_{21} = c_2 (1 - m_1) P_1^* - 2i_2 P_2^* + r_2, d_{22} = \frac{eP_3^{*2}}{(K+P_1^*)^2}$, and $d_{23} = r_3 - \frac{2eP_3^*}{K+P_1^*}$. Then the characteristic equation of the $J(E_{10})$ is given by

$$x^3 + g_1 x^2 + g_2 x + g_3 = 0,$$

where $g_1 = -d_{17} - d_{21} - d_{23}$, $g_2 = -d_{18}d_{20} + d_{17}d_{21} - d_{19}d_{21} + d_{17}d_{23} + d_{21}d_{23}$, and $g_3 = d_{19}d_{21}^2 - d_{17}d_{23}d_{21} + d_{18}d_{20}d_{23}$, using the Routh-Hurwitz conditions [95, 126, 136], the equilibrium point E_{10} is locally asymptotically stable if

$$g_1 > 0, \; g_2 > 0, \; g_3 > 0, \text{ and } g_1 g_2 - g_3 > 0. \tag{6.4.10}$$

$\square$

6.5 Global Stability

Theorem 6.5.1. The coexistence equilibrium point $E(P_1^*, P_2^*, P_3^*)$ is globally asymptotically stable if (i) $i > \frac{cc_3 P_3^*}{bd}$ and (ii) $cP_1^* > b$.

Proof. Firstly, we define a Lyapunov function

$$V(P_1, P_2, ,P_3) = (P_1 - P_1^* - P_1^* \ln \frac{P_1}{P_1^*}) + h_1(P_2 - P_2^* - P_2^* \ln \frac{P_2}{P_2^*}) + h_2(P_3 - P_3^* - P_3^* \ln \frac{P_3}{P_3^*}),$$

187

where h_1 and h_2 are positive constants to be determined later. It can be easily seen that the function V is zero at the equilibrium point $(P_1^*, P_2^*, , P_3^*)$ and is positive for all other values of P_1, P_2, and P_3. The derivative of Lyapunov function V is

$$\frac{dV}{dt} = (1 - \frac{P_1^*}{P_1})\frac{dP_1}{dt} + h_1(1 - \frac{P_2^*}{P_2})\frac{dP_2}{dt} + h_2(1 - \frac{P_3^*}{P_3})\frac{dP_3}{dt},$$

putting the values of $\frac{dP_1}{dt}$, $\frac{dP_2}{dt}$ and $\frac{dP_3}{dt}$ from (6.2.1), we have

$$\frac{dV}{dt} = (1 - \frac{P_1^*}{P_1})(r_1 P_1 - i_1 P_1^2 - c_1(1 - m_1)P_2 P_1 - \frac{cP_1 P_3}{b + c_3 P_1 + dP_3})$$
$$+ h_1(1 - \frac{P_2^*}{P_2})(r_2 P_2 - i_2 P_2^2 + c_2(1 - m_1)P_1 P_2)$$
$$+ h_2(1 - \frac{P_3^*}{P_3})(r_3 P_3 - \frac{eP_3^2}{P_1 + K}),$$
$$= (P_1 - P_1^*)\left(r_1 - i_1 P_1 - c_1(1 - m_1)P_2 - \frac{cP_3}{b + c_3 P_1 + dP_3} - \right.$$
$$\left. r_1 + i_1 P_1^* + c_1(1 - m_1)P_2^* + \frac{cP_3^*}{b + c_3 P_1^* + dP_3^*} \right)$$
$$+ h_1(P_2 - P_2^*)\left(r_2 - i_2 P_2 + c_2(1 - m_1)P_1 - r_2 + i_2 P_2^* - c_2(1 - m_1)P_1^* \right)$$
$$+ h_2(P_3 - P_3^*)\left(r_3 - \frac{eP_3}{P_1 + K} - r_3 + \frac{eP_3^*}{P_1^* + K} \right),$$

Define $r_1(P_1, P_2) = (b + c_3 P_1^* + dP_3^*)(b + c_3 P_1 + dP_3)$, $r_2(P_1) = (P_1 + K)(P_1^* + K)$

$$\frac{dV}{dt} = (-i + \frac{cc_3 P_3^*}{r_1(P_1, P_2)})(P_1 - P_1^*)^2 - i_2 h_1(P_2 - P_2^*)^2 - h_2\frac{eP_1^* + eK}{r_2(P_1)}(P_3 - P_3^*)^2$$
$$\left(-c_1(1 - m_1) + c_2(1 - m_2)h_1 \right)(P_1 - P_1^*)(P_2 - P_2^*) + \left(\frac{bc}{r_1} - \frac{cc_3 P_1^*}{r_1} + \frac{eP_3^*}{r_2}h_2 \right)(P_3 - P_3^*)(P_1 - P_1^*),$$

choosing $h_1 = \frac{c_1(1 - m_1)}{c_2(1 - m_2)}$, $h_2 = \frac{cr_2(cP_1^* - b)}{r_1 eP_3^*}$, then we obtain

$$\frac{dV}{dt} \leqslant -(i - \frac{cc_3}{bd})(P_1 - P_1^*)^2 - i_2\frac{c_1(1 - m_1)}{c_2(1 - m_2)}(P_2 - P_2^*)^2 - \frac{cr_2(cP_1^* - b)}{r_1 eP_3^*}\frac{e}{K}(P_3 - P_3^*)^2,$$

without loss of generality, we obtain

$$\frac{dV}{dt} < 0 \text{ if } (i)\, i > \frac{cc_3 P_3^*}{bd}, \text{ and } (ii)\, cP_1^* > b.$$

188

Consequently, V is a Lyapunov function. We then define the invariant set as

$$\Omega = \{(P_1, P_2, P_3) \in R_3^+ : \frac{dV}{dt} = 0\}.$$

Hence, by LaSalles invariance principle [6, 92], it follows that the $E_{10}(P_1^*, P_2^*, P_3^*)$ is globally asymptotically stable. $\qquad\square$

6.6 Numerical Simulation and its Discussion

For simulation purposes, we perform numerical simulations to analyze the dynamic behavior of the system (6.2.1). In order to establish a stronger concurrence between the model performance and the observations the mathematical parameters can be significantly changed of the model representing a given model. Some of our analysis conclusions are validated in this section using numerical simulations, which are obviously quite interesting and have the benefit that the interaction effects between distinct classes can easily be identified. However, several scenarios have been carried out addressing the biologically viable parameter and the results have shown the variety of dynamic outcomes obtained in all the examined circumstances. As this problem is not a case study for a particular species, experimental hypothetical values are taken in Table 6.2 with the aim of presenting the preceding analytical results of the previous sections. Furthermore, we take a qualitative rather than a quantitative approach to this.

Table 6.2: Parameter value used in simulation.

Parameter	Value	Parameter	Value
r_1	0.6	d	0.1
i_1	0.15	r_2	0.5
c_1	0.2	i_2	0.4
m_1	0.6	c_2	0.3
c	0.5	r_3	0.35
b	10	e	1
c_3	0.001	K	5

Figures 6.1a and Figures 6.2a are plotted using Table 6.2 for the time t=5 and t=100 units, respectively. Figures 6.1b and Figures 6.2b are plotted using $r_1 = 0.7$, $i_1 = 0.2$, $c_1 = 0.35$, $m_1 = 0.6$, $c = 2$, $b = 10$, $c_3 = 0.001$, $d = 0.1$, $r_2 = 0.5$, $i_2 = 0.35$, $c_2 =$

189

0.25, $r_3 = 0.35$, $e = 1$, $K = 5$. Figures 6.1a represent that the density of crop decreases, when the population density of pest and locust swarm increase. However, Figures 6.1b shows that the population density of P_1 decreases more compared to Figures 6.1a. Becausethe competition among prey, response of predators-I to prey, and maximum value , which per capitareduction rate of prey are $i_1 = 0.2, c_2 = 0.4$, and $c = 2$,, respectively. Further, Figures 6.2a and Figures 6.2b coverage to the endemic equilibrium for the model system (6.2.1).

(a)   (b)
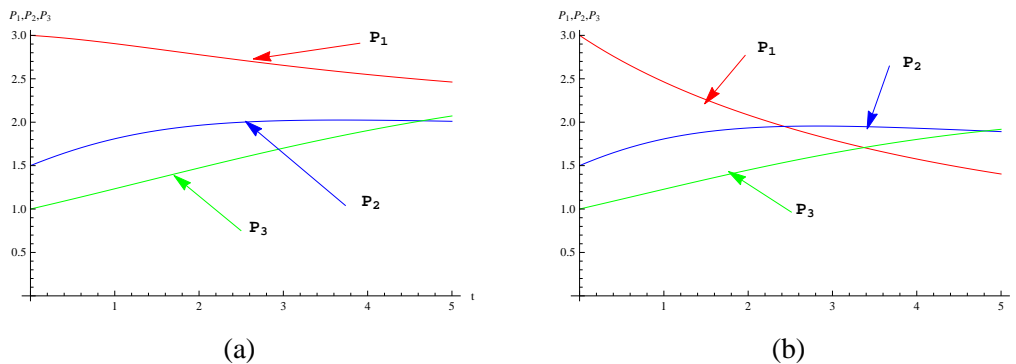
Figure 6.1: Time series diagrams between population density of crop, pest, and locust swarm of the system for $t = 5$ units.

(a) Equilibrium point$(2.17022, 1.90107, 2.50958)$ (b) Equilibrium point$(0.8328, 1.6665, 2.0415)$
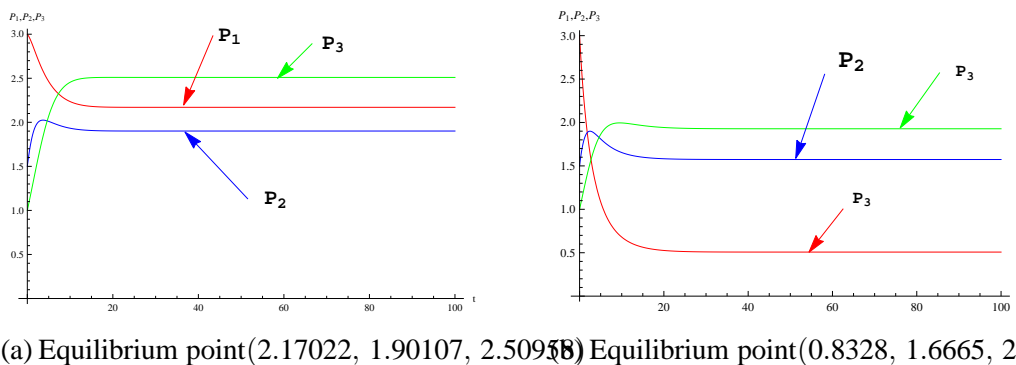
Figure 6.2: Solution curves coverage to the endemic equilibrium for the model system (6.2.1), showing that all species survive and ultimately evolve to their steady states.

6.6.1   Numerical Simulation of Local Stability

The equilibrium points, corresponding eigenvalues and the nature of the equilibrium points of the model are presented in Section 6.4. It is difficult to interpret the theoretical results due to complicated equilibrium points. To visualize the theoretical and stability results obtained in Section 6.4, we use numerical simulation to validate the

theoretical aspects. In this section, we discuss only those equilibrium points , which have biological feasible and asymptotically stable.

For the set of parametric values given in (6.6.1), the stability condition (6.4.7) is fulfilled and the equilibrium point $E_5(0, 1.4814, 2.7132)$ is stable. Figure 6.3b shows that for parametric values given in (6.6.1), the crop P_1 decreases rapidly while P_2 and P_3 increase. Finally, all three species eventually get their steady states $E_5(0, 1.4814, 2.7132)$. Eventually, the density of crop is cleared out from the system. The pest and locust swarms grow well and lead to stability in the prey–predator system. Moreover, Figure 6.4a represent phase portrait of the model system (6.2.1) with parametric values given in (6.6.1). Starting from various initial conditions, all the solution approach toward $E_5(0, 1.4814, 2.7132)$. The different initial conditions are shown in Figure 6.4a.

$$r_1 = 0.45,\ i_1 = 1,\ c_1 = 0.25,\ m_1 = 0.5,\ c = 2,\ b = 10,\ c_3 = 0.001,\ d = 0.1,$$

$$r_2 = 0.4,\ i_2 = 0.27,\ c_2 = 0.125,\ r_3 = 0.35,\ e = 0.258,\ K = 2. \qquad (6.6.1)$$

For the set of parametric values given in (6.6.2), the stability condition (6.4.8) is fulfilled and the equilibrium point $E_7(1.2808, 0.7882, 0)$ is stable. Figure 6.3b shows that for parametric values given in (6.6.1), the crop P_1, pest P_2, and P_3 decrease.Finally, all three species finally get their steady states $E_7(1.2808, 0.7882, 0)$. Eventually, the density of crop is cleared out from the system. Figure 6.3b represent phase portrait of model system. It is clear from Figure 6.3b, using different initial population densities of the species the trajectories for the species indicate that the nontrivial equilibrium point $E_7(1.2808, 0.7882, 0)$ is stable asymptotically stable. The different initial population density is shown in Figure 6.3b.

$$r_1 = 0.4,\ i_1 = 0.3,\ c_1 = 0.1,\ m_1 = 0.8,\ c = 2,\ b = 10,\ c_3 = 0.001,\ d = 0.1,$$

$$r_2 = 0.2,\ i_2 = 0.27,\ c_2 = 0.05,\ r_3 = 0.05,\ e = 2.7,\ K = 0.9. \qquad (6.6.2)$$

For the set of parametric values given in (6.6.3), the stability condition (6.4.1) is satisfied and the equilibrium point $E_8(1.3371, 0, .6674)$ is stable. Figure 6.3c shows that for parametric values given in (6.6.3), the crop P_1 decreases rapidly, after some time approach to stable. Similarly, P_2 and P_3 decrease and P_2 approaches zero. Thus, all three species finally get their steady states $E_8(1.3371, 0, .6674)$. Eventually, the density

of pest is died out from the system. Moreover, Figure 6.4c represent phase portrait of the model system (6.2.1) with parametric values given in (6.6.3). Starting from various initial conditions, all the solution approach toward $E_8(1.3371, 0, .6674)$. The different initial conditions are shown in Figure 6.4c.

$$r_1 = 0.4,\ i_1 = 0.2,\ c_1 = 0.1,\ m_1 = 0.9,\ c = 2,\ b = 10,\ c_3 = 0.001,\ d = 0.1,$$
$$r_2 = 0.05,\ i_2 = 1.7,\ c_2 = 0.1,\ r_3 = 0.2,\ e = 1,\ K = 2. \tag{6.6.3}$$

Figure 6.4d represent phase portrait of the model system (6.2.1) with parametric values given in Table 6.2. Starting from various initial conditions, all the solution approach toward $E_9(2.1702, 1.9011, 2.5096)$. The different initial conditions are shown in Figure 6.4c. Thus, all three ultimately attain their steady states and achieve asymptotically stability. Since these groups share the same ecosystem, they can be cooperative or compete with one another depending on the situation.

(a)   Equilibrium   point
$(0, 1.4814, 2.7132)$

(b)   Equilibrium   point
$(1.2808, 0.7882, 0)$

(c)   Equilibrium   point
$(1.3371, 0, 0.6674)$
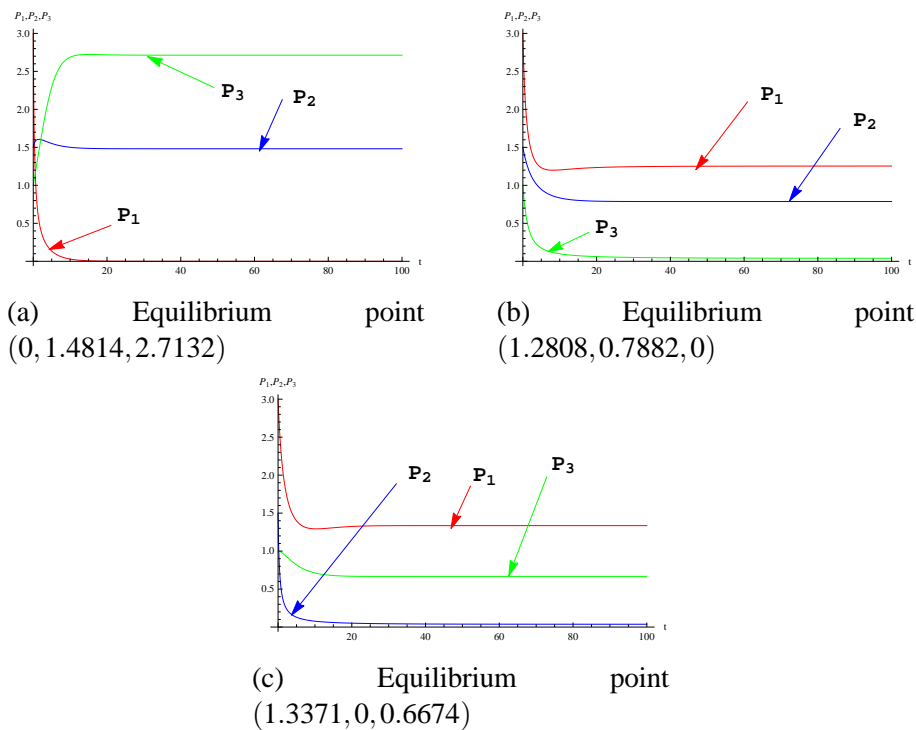
Figure 6.3: Asymptotic stable solution at equilibrium points for the model system (6.2.1).

(a) Stable point(0,1.4814,2.7132)

(b) Stable point(1.2808,0.7882,0)

(c) Stable point(1.3371,0,0.6674)

(d) Stable point(2.1702,1.9011,2.5096)
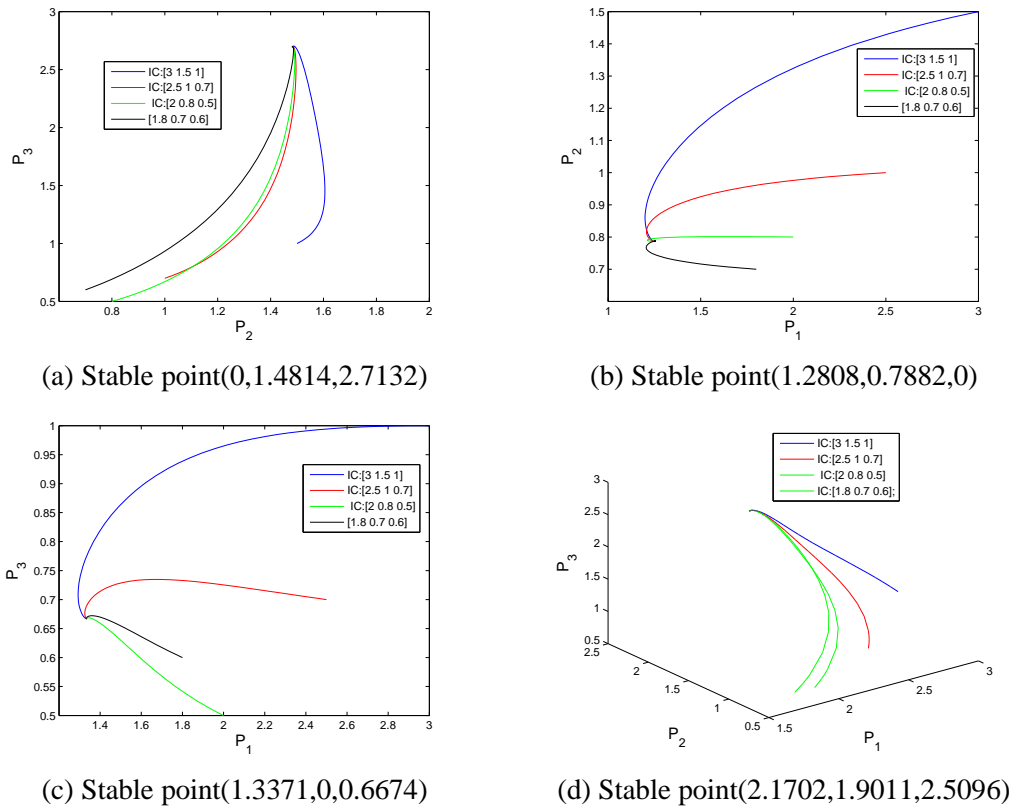
Figure 6.4: Phase portrait of model system (6.2.1).

6.6.2 Biological Interpretation of the Parameters

A mathematical model includes the parameters that increase the complexity of the model and make it more complicated to analyze the parameters that occur in the model. Therefore, we analyze the variation of population density when one parameter varies and keeping the rest of the parameters unchanged. Figure 6.5a–Figure 6.5b, we see that the density of crop P_1 increases while the population density of P_2 and P_3 species are almost the same when d increases and while leaving the rest of the parameters same in Table 6.2. Similarly, Figure 6.5e–Figure 6.5f represent the density of crop P_1 increases while the population density of P_2 and P_3 species is almost the same when c_3 increases and keeping the rest of the parameters unchanged in Table 6.2. Figure 6.5g–Figure 6.6c represent the density of P_1, P_2, and P_3 decrease when c and i_1 increase and keeping the rest of the parameters unchanged in Table 6.2. Figure 6.6d–Figure 6.6f, we see that the density of crop P_1 and P_2 increase while the population density of P_3 species decreases when e increases and keeping the rest of the parameters unchanged in Table 6.2. Figure 6.6g–Figure 6.6i represent the density

of crop P_1 and P_2 increase while the population density of P_2 is almost the same when b increases and keeping the rest of the parameters unchanged in Table 6.2. Figure 6.7a–Figure 6.7c represent the density P_1, P_2, and P_3 increases when r_1 increases and keeping the rest of the parameters unchanged in Table 6.2. We observe from Figure 6.7d–Figure 6.7f that P_1 decreases when r_2 increases and locust swarm P_3 decrease while pest density P_2 increases. Similarly, Figure 6.7g–Figure 6.7o show the variation of population density P_1, P_2, and P_3 when one parameter varies and keeping the rest of the parameters unchanged. Further, Figure 6.6j–Figure 6.6r show the variation of population density P_1, P_2, and P_3 when m_1, K, and i_2 varies and keeping the rest of the parameters unchanged.
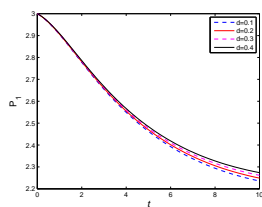
(a) Variation of P_1 when d varies (b) Variation of P_2 when d varies (c) Variation of P_3 when d varies
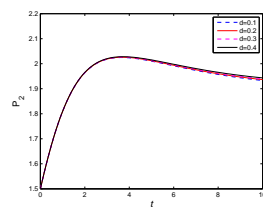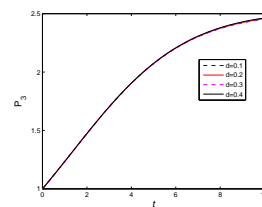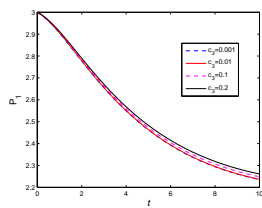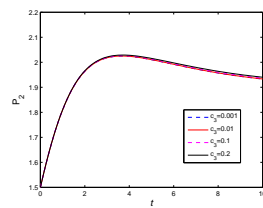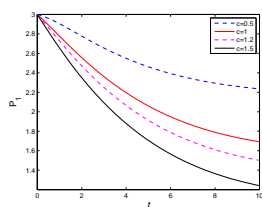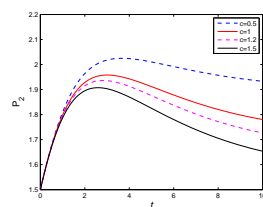
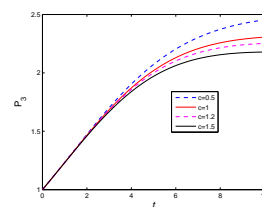(d) Variation of P_1 when c_3 varies (e) Variation of P_2 when c_3 varies (f) Variation of P_3 when c_3 varies
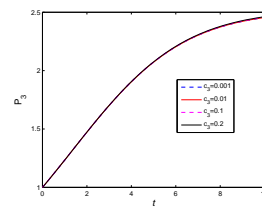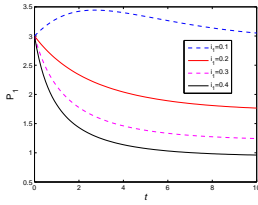
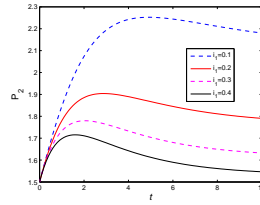(g) Variation of P_1 when c varies (h) Variation of P_2 when c varies (i) Variation of P_3 when c varies
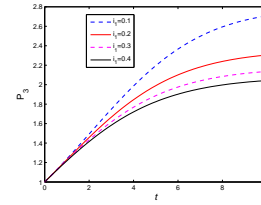
Figure 6.5: Dynamical behavior of the P_1, P_2, and P_3 of the system (6.2.1) and parameter values are taken from Table 6.2.
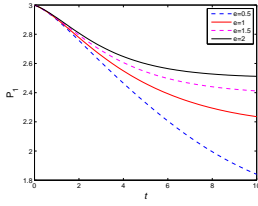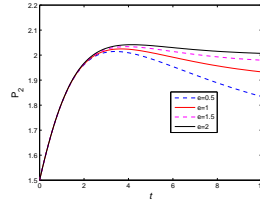
(a) Variation of P_1 when i_1 varies

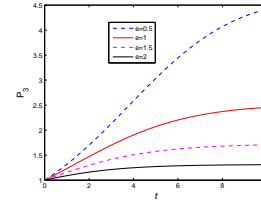(b) Variation of P_2 when i_1 varies
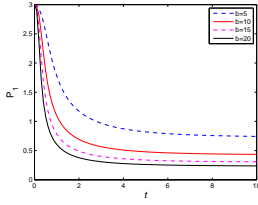
(c) Variation of P_3 when i_1 varies
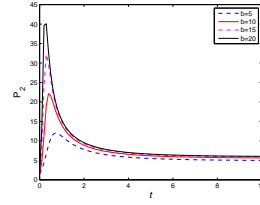
(d) Variation of P_1 when e varies

(e) Variation of P_2 when e varies

(f) Variation of P_3 when e varies

(g) Variation of P_1 when b varies

(h) Variation of P_2 when b varies

(i) Variation of P_3 when b varies

(j) Variation of P_1 when m_1 varies

(k) Variation of P_1 when m_1 varies

(l) Variation of P_1 when m_1 varies

(m) Variation of P_1 when K varies

(n) Variation of P_2 when K varies

(o) Variation of P_3 when K varies

(p) Variation of P_1 when i_2 varies

(q) Variation of P_2 when i_2 varies

(r) Variation of P_3 when i_2 varies

Figure 6.6: Dynamical behavior of the P_1, P_2, and P_3 of the system (6.2.1) and parameter values are taken from Table 6.2.

(a) Variation of P_1 when r_1 varies (b) Variation of P_2 when r_1 varies (c) Variation of P_3 when r_1 varies
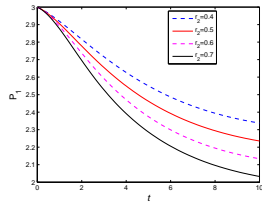
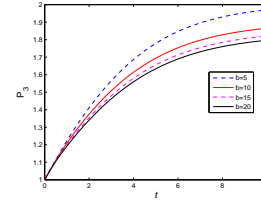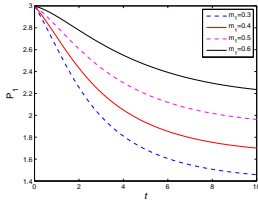(d) Variation of P_1 when r_2 varies (e) Variation of P_2 when r_2 varies (f) Variation of P_3 when r_2 varies
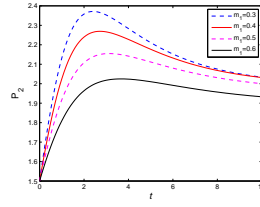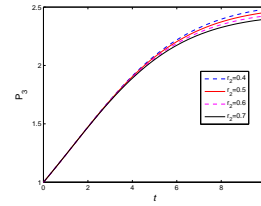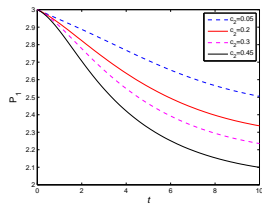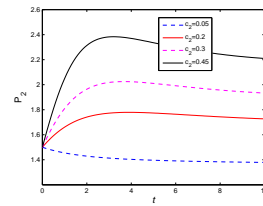
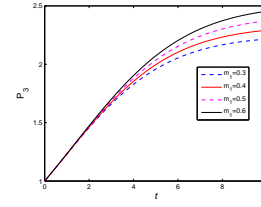(g) Variation of P_1 when c_2 varies (h) Variation of P_2 when c_2 varies (i) Variation of P_3 when c_2 varies
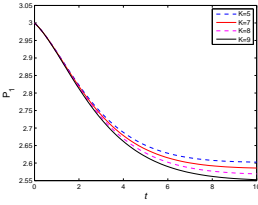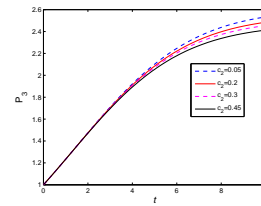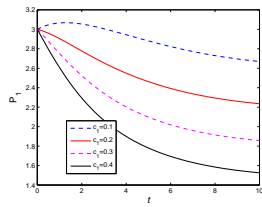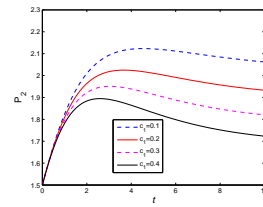
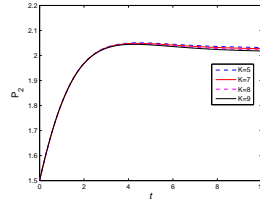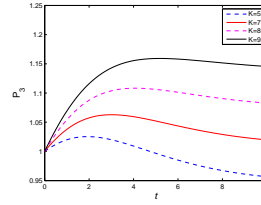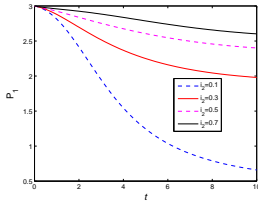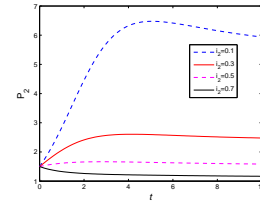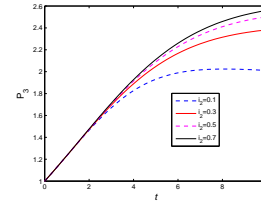(j) Variation of P_1 when c_1 varies (k) Variation of P_2 when c_1 varies (l) Variation of P_3 when c_1 varies
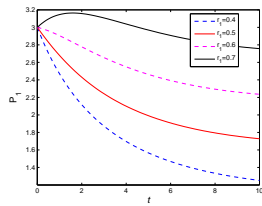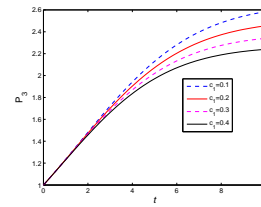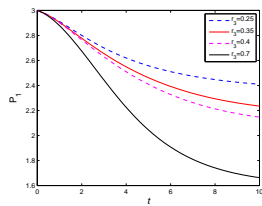
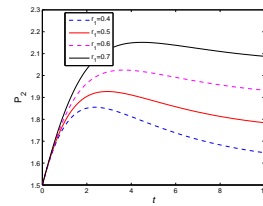(m) Variation of P_1 when r_3 varies (n) Variation of P_2 when r_3 varies (o) Variation of P_3 when r_3 varies
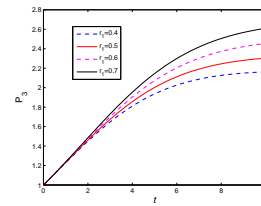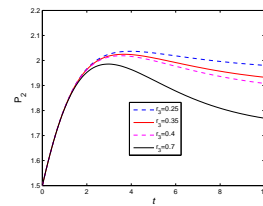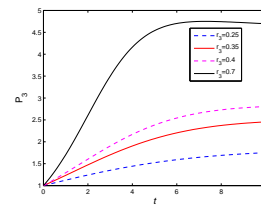
Figure 6.7: Dynamical behavior of the P_1, P_2, and P_3, of the system (6.2.1) and parameter values are taken from Table 6.2.
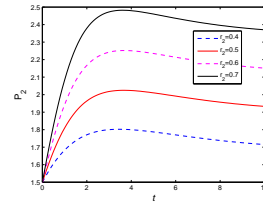
6.7 Formulation and Application of Optimal Control Problem

Optimal control techniques develop optimal strategies to control the various factors that affect the systems. In this section, we develop a prey–predator model using control variables and we verify how effective controls in a prey–predator model work. Pontryagins maximum technique is used to find the necessary condition for the principle of optimal control system [122]. Our first aim is to increase the amount of crop and reduce predator populations, which damage the crop. Here, two control variables are used: the first is applied to the pest, which kills the insect, and the second is applied to the locust swarm, which measures the effort required to raise awareness, leading to a drop in the transmission rate. The second variable of control means awareness-raising of aircraft for the locust control (sprinkling kits are to be provided for dessert craft control purposes), local warning routine activities, advanced planning, and preparation of aircraft (screening schedule prepared, emergency plan update, testing of the contingency plan), actions made during everyday control operations before the high alert. Let $u_1(t)$ measures the rate of application of pesticide to reduce pest individuals and $u_2(t)$ represents the effort required to raise awareness, which reduces the transmission rate. Further, $u_1(t)$ is the percentage of predator individuals because the amount of pesticide in use depends on the predator populations. The control functions, $u_1(t)$ and $u_2(t)$ are bounded, Lebesgue integrable functions. Now, the model with two control strategies is given below:

$$
\begin{cases}
\frac{dP_1(t)}{dt} = r_1P_1(t) - i_1P_1^2(t) - c_1(1-m_1)P_2(t)P_1(t) - \frac{cP_1P_3}{b+c_3P_1(t)+dP_3(t)}, \\
\frac{dP_2(t)}{dt} = r_2P_2(t) - i_2P_2^2(t) + c_2(1-m_1)P_1(t)P_2(t) - b_1u_1P_2, \\
\frac{dP_3(t)}{dt} = r_3P_3(t) - \frac{eP_3^2(t)}{P_1(t)+K} - b_2u_2P_3,
\end{cases}
\tag{6.7.1}
$$

with initial conditions,

$$
P_1(0) = P_{10} \geqslant 0, \ P_2(0) = P_{20} \geqslant 0, \ P_3(0) = P_{30} \geqslant 0.
\tag{6.7.2}
$$

Our primary goal is to reduce the overall number of pests while also reducing locust swarm individuals, as well as the expense of raising awareness and treating them at

regular intervals. For fulfilling our purpose, the following is the goal function with which we perform:

$$\text{Minimize } J(u_1(t), u_2(t)) = \int_0^T (A_1P_2 + A_2P_3 + \frac{1}{2}(B_1u_1^2 + B_2u_2^2))dt, \qquad (6.7.3)$$

where, B_1 and B_2 are weight parameters that help to balance the corresponding costs. In the objective function, A_1P_2 represents the total pest density, A_2P_3 represents the locust swarm density, $B_1\frac{u_1^2}{2}$ represents the cost for pesticide, and $B_2\frac{u_2^2}{2}$ represents the cost for creating awareness. The square of the control parameters is used to eliminate the bad side effects of the control variables [80, 218, 219]. We define the control set as follows:

$$U = \{(u_1(t), u_2(t)) : 0 \leqslant u_1(t) \leqslant 1, \ 0 \leqslant u_2(t) \leqslant 1,, \ t \in [0, T]\}$$

6.7.1 Existence of Optimal Control

To use Pontryagins maximum principle [122] on the time–dependent controls, we first need the existence of optimal controls, characterize the time–dependent controls, and adjoint equations for system (6.7.1). Now, using the results in [41, 148, 240], the following theorem is stated.

Theorem 6.7.1. Given the objective functional J, defined on the control set U, and subject to the state system with non–negative initial conditions at $t = 0$, then there exists an optimal control $u = (u_1, u_2)$ such that $J(u) = \min \{J(u_1, u_2)|u_1, u_2 \in U\}$.

Proof. To prove the existence of optimal control using the result from [41, 148, 240], if the following conditions are hold

(i) The set of controls and corresponding state variables are nonempty.

(ii) The control set is convex and closed.

(iii) The right–hand side of the state system (6.7.1) is bounded by a linear function in the state and control variables (u_1, u_2).

(iv) The integrand of the objective functional is convex on U.

(v) There exist constants $c_1, c_2 > 0$ and $n > 1$ such that the integrand of the objective functional

satisfies

$$A_1 P_2 + A_2 P_3 + \frac{1}{2}(B_1 u_2^2 + B_2 u_3^2) \geqslant c_1(|u_1|^2 + |u_2|^2)^{\frac{n}{2}} - c_2.$$

To verify the first and second conditions, the state and control variables are non–empty and non–negative. The control variables u_1 and u_2 are also convex and closed by the given definition, which gives the condition (ii). For the condition (iii), the control model system can be expressed as a linear function of control variables υ with the coefficients as functions of time and state variables

$$f(t, P, \upsilon) = \gamma(t, P) + \xi(t, P)\upsilon,$$

where, $\upsilon = (u_1, u_2) \in U$, $P = (P_1, P_2, P_3)$, $f(t, P, \upsilon)$ be the right–hand of (6.7.1),

$$\gamma(t,P) = \begin{pmatrix} r_1 P_1(t) - i_1 P_1^2(t) - c_1(1-m_1)P_2(t)P_1(t) - \frac{cP_1 P_3}{b+c_3 P_1(t)+dP_3(t)}, \\ r_2 P_2(t) - i_2 P_2^2(t) + c_2(1-m_1)P_1(t)P_2(t), \\ r_3 P_3(t) - \frac{eP_3^2(t)}{P_1(t)+K} \end{pmatrix}, \quad \xi(t, P) = \begin{pmatrix} 0 & 0 \\ -b_1 P_2 & 0 \\ 0 & -b_2 P_2 \end{pmatrix},$$

$$|f(t,P,\upsilon)| \leqslant \left| \begin{pmatrix} r_1 & 0 & 0 \\ 0 & r_2 + c_2(1-m_1)P_1 & 0 \\ 0 & 0 & r_3 \end{pmatrix} \begin{pmatrix} P_1 \\ P_2 \\ P_3 \end{pmatrix} + \begin{pmatrix} 0 & 0 \\ -b_1 P_2 & 0 \\ 0 & -b_2 P_3 \end{pmatrix} \begin{pmatrix} u_1 \\ u_2 \end{pmatrix} \right|.$$

Using Boundedness of the system (6.2.1), there exist constants $C_1 > 0$, $C_2 > 0$, and $C_3 > 0$, such that $0 < P_1 \leqslant C_1$, $0 < P_2 \leqslant C_2$, and $0 < P_3 \leqslant C_3$ for all $t \in [0, t_f]$. Therefore,

$$|f(t,P,\upsilon)| \leqslant \left| \begin{pmatrix} r_1 & 0 & 0 \\ 0 & r_2 + c_2(1-m_1)C_1 & 0 \\ 0 & 0 & r_3 \end{pmatrix} \begin{pmatrix} P_1 \\ P_2 \\ P_3 \end{pmatrix} + \begin{pmatrix} 0 & 0 \\ -b_1 C_2 & 0 \\ 0 & -b_2 C_3 \end{pmatrix} \begin{pmatrix} u_1 \\ u_2 \end{pmatrix} \right|$$

$$\leqslant M_1 |P| + M_2 |\upsilon|,$$

where M_1 and M_2 are the upper bound of the matrices. Hence, we see that the right–hand side is bounded by a sum of the state and the control variables. Therefore, condition (iii) is satisfied. The integrand in the objective functional, $A_1 P_2 + A_2 P_3 - B_1 P_1 A_3 u_1^2 + A_3 u_2^2$, is clearly

convex on u_1 and u_2, which gives the condition (iv). For the last condition (v),

$$A_1 P_2 + A_2 P_3 + \frac{1}{2}(B_1 u_1^2 + B_2 u_2^2) \geqslant B_1 u_1^2 + B_2 u_2^2,$$

$$\geqslant min(B_1, B_2)(u_1^2 + u_2^2),$$

$$\geqslant c_1(u_1^2 + u_2^2) - c_2.$$

Hence, $A_1 P_2 + A_2 P_3 + \frac{1}{2}(B_1 u_1^2 + B_2 u_2^2) \geqslant c_1(|u_1|^2 + |u_2|^2)^{\frac{n}{2}} - c_2$, where, $c_1 = min(B_1, B_2)$, c_2 is positive constant, and $n = 2 > 1$. Using all conditions we can conclude that there exists an optimal control (u_1^*, u_1^*) such that

$$J(u_1^*, u_2^*) = \min_{u_1, u_2 \in \Omega} J(u_1, u_2).$$

$\square$

6.7.2   Characterization of the Optimal Control

We characterize the time–dependent controls and the corresponding adjoint equations. To derive the necessary conditions for the optimal control pair, Pontryagins maximum principle [122] is used. The Hamiltonian is defined as follows:

$$H = A_1 P_2 + A_2 P_3 + \frac{1}{2}\left(B_1 u_1^2 + B_2 u_2^2\right)$$
$$+ \lambda_1 \left(-\frac{c P_3 P_1}{b + c_3 P_1 + d P_3} - c_1(1 - m_1)P_2 P_1 - i_1 P_1^2 + P_1 r_1\right)$$
$$+ \lambda_2 \left(-b_1 P_2 u_1 + c_2(1 - m_1)P_1 P_2 - i_2 P_2^2 + P_2 r_2\right) + \lambda_3 \left(-b_2 P_3 u_2 - \frac{e P_3^2}{K + P_1} + P_3 r_3\right) \quad (6.7.4)$$

where λ_1, λ_2, and λ_3 are adjoint functions associated with the state functions P_1, P_2, and P_3.

Theorem 6.7.2. If u_1^* and u_2^* be an optimal control which minimize $J(u_1, u_2)$. Let $P_1^*(t)$ and $P_2^*(t)$ are optimal state solutions for the control system (6.7.1), then there exist adjoint variables

$\lambda_1(t)$, $\lambda_2(t)$, and $\lambda_3(t)$, satisfying the following

$$
\begin{cases}
\frac{d\lambda_1}{dt} = \lambda_1 \left(-\frac{cc_3 P_3 P_1}{(b+c_3 P_1 + dP_3)^2} + \frac{cP_3}{b+c_3 P_1 + dP_3} + c_1(1-m_1)P_2 + 2i_1 P_1 - r_1 \right) - c_2\lambda_2(1-m_1)P_2 - \frac{e\lambda_3 P_3^2}{(K+P_1)^2}, \\
\frac{d\lambda_2}{dt} = -A_1 - \lambda_2(-b_1 u_1 + c_2(1-m_1)P_1 - 2i_2 P_2 + r_2) + c_1\lambda_1(1-m_1)P_1, \\
\frac{d\lambda_3}{dt} = -A_2 - \lambda_1 \left(\frac{cdP_1 P_3}{(b+c_3 P_1 + dP_3)^2} - \frac{cP_1}{b+c_3 P_1 + dP_3} \right) - \lambda_3 \left(-b_2 u_2 - \frac{2eP_3}{K+P_1} + r_3 \right).
\end{cases}
$$

$$(6.7.5)$$

with transversality conditions are

$$\lambda_i(T_f) = 0, \; i = 1,2,3.$$

Further, the optimal control variable $u_1^*(t)$ and $u_2^*(t)$ that minimize $J(u_1, u_2)$ are given by

$$u_1^*(t) = \min\left\{\max\left\{0, \frac{b_1\lambda_2 P_2}{B_1}\right\}, 1\right\}, \text{ and } u_2^*(t) = \min\left\{\max\left\{0, \frac{b_2\lambda_3 P_3}{B_2}\right\}, 1\right\}.$$

Proof. The adjoint equations are obtained from the partial derivatives of the Hamiltonian, H, with respect to each state variable. That is,

$$\lambda_1'(t) = -\frac{\partial H}{\partial P_1}, \; \lambda_2'(t) = -\frac{\partial H}{\partial P_2}, \; \lambda_3'(t) = -\frac{\partial H}{\partial P_3}.$$

The behaviour of the control can be determined by differentiating the Hamiltonian, H, with respect to the controls (u_1, u_2) at t. Where, $0 < u_j < 1$ for all $(j = 1, 2)$.

$\frac{\partial H}{\partial u_1} = 0 = -b_1\lambda_2 P_2 + B_1 u_1^*$ at $u_1 = u_1^*(t) \Rightarrow u_1^* = \frac{\lambda_2 b_1 P_2}{B_1}$,

$\frac{\partial H}{\partial u_2} = 0 = b_2\lambda_3 P_3 + B_2 u_2^*$, at $u_2 = u_2^*(t) \Rightarrow u_2^* = -\frac{\lambda_3 b_2 P_3}{B_2}$. Therefore, by using the bounds for the control [200], $u_1(t)$ and $u_2(t)$, we get

$$u_1^*(t) = \min\left\{\max\left\{0, \frac{b_1\lambda_2 P_2}{B_1}\right\}, 1\right\}, \text{ and } u_2^*(t) = \min\left\{\max\left\{0, \frac{b_2\lambda_3 P_3}{B_2}\right\}, 1\right\}.$$

$\square$

6.7.3   Optimality System.

The optimality system is made up of a state system and an adjoint system with starting and transversal conditions and the characterisation of optimal control. The

optimal control is represented by the optimality system shown below.

$$
\begin{cases}
\frac{dP_1(t)}{dt} &= r_1 P_1(t) - i_1 P_1^2(t) - c_1(1-m_1)P_2(t)P_1(t) - \frac{cP_1P_3}{b+c_3P_1(t)+dP_3(t)}, \\[2mm]
\frac{dP_2(t)}{dt} &= r_2 P_2(t) - i_2 P_2^2(t) + c_2(1-m_1)P_1(t)P_2(t) - b_1 \min\left\{\max\left\{0, \frac{b_1\lambda_2 P_2}{B_1}\right\}, 1\right\} P_2, \\[2mm]
\frac{dP_3(t)}{dt} &= r_3 P_3(t) - \frac{eP_3^2(t)}{P_1(t)+K} - b_2 \min\left\{\max\left\{0, \frac{b_2\lambda_3 P_3}{B_2}\right\}, 1\right\} P_3, \\[2mm]
\frac{d\lambda_1}{dt} &= \lambda_1\left(-\frac{cc_3P_3P_1}{(b+c_3P_1+dP_3)^2} + \frac{cP_3}{b+c_3P_1+dP_3} + c_1(1-m_1)P_2 + 2i_1P_1 - r_1\right) - c_2\lambda_2(1-m_1)P_2 - \frac{e\lambda_3 P_3^2}{(K+P_1)^2}, \\[2mm]
\frac{d\lambda_2}{dt} &= -A_1 - \lambda_2\left(-b_1 \min\left\{\max\left\{0, \frac{b_1\lambda_2 P_2}{B_1}\right\}, 1\right\} + c_2(1-m_1)P_1 - 2i_2P_2 + r_2\right) + c_1\lambda_1(1-m_1)P_1, \\[2mm]
\frac{d\lambda_3}{dt} &= -A_2 - \lambda_1\left(\frac{cdP_1P_3}{(b+c_3P_1+dP_3)^2} - \frac{cP_1}{b+c_3P_1+dP_3}\right) - \lambda_3\left(-b_2 \min\left\{\max\left\{0, \frac{b_2\lambda_3 P_3}{B_2}\right\}, 1\right\} - \frac{2eP_3}{K+P_1} + r_3\right).
\end{cases}
$$

$$(6.7.6)$$

with initial conditions

$$P_1(0) = P_{10} \geqslant 0,\ P_2(0) = P_{20} \geqslant 0,\ \text{and}\ P_3(0) = P_{30} \geqslant 0,$$

and transversality equations

$$\lambda_i(T_f) = 0,\ i = 1, 2, 3.$$

6.8 Numerical Simulations for Optimal Control Problem

Because this is a qualitative research, it is not based on a survey or a census. Therefore criteria cannot be measured in a meaningful way. We consider taking a simulated set of parameters for the objective of computation. This is one of the limitations of our model and the same is persistent in the huge published literature. We use Runge-Kutta fourth–order iterative method to numerically solve the optimality system (6.7.6). The forward–backward sweep method for the iterative procedure of the optimality system is given in [200, 218, 219]. The forward–backward sweep method convergence is based on the study done by [234]. The controls are updated at the end of each iteration using the formula for optimal controls. The iterations continue until convergence is achieved. Therefore, because our aim in this issue is to reduce pests and save crops, we assume that the initial values for the crop, pest, and locust swarms are $P_1(0) = 3$, $P_2(0) = 1.5$, and $P_3(0) = 1$ with appropriate units, respectively. We use this control within 2 unit time, which could be in

hours, days, weeks, or even months. Figure 6.8 is plotted using the parameter value $r_1 = 0.6$, $i_1 = 0.15$, $c_1 = 0.2$, $m_1 = 0.6$, $c = 0.5$, $b = 10$, $c_3 = 0.001$, $d = 0.1$, $r_2 = 0.5$, $i_2 = 0.4$, $c_2 = 0.3$, $r_3 = 0.35$, $e = 1$, $K = 5$, $b_1 = 1$, $b_2 = 1$, $A_1 = 1$, $A_2 = 1$, $B_1 = 1$, $B_2 = 1$, and $t = 2$. Figure 6.8 and Figure 6.8 describe the solution curves for the three–state variables, both in appearance and non–appearance of the control. Figure 6.8(a) indicates that the population density of crops is approximately 3.18 and 2.8 unit at 2 unit time in the presence of control and the absence of control, respectively. Similarly, Figure 6.8(b) and Figure 6.8(c) shows that the population density of P_2 and P_3 is approximately 1, 0.6 units in the presence of control and 2, 1.5 units in the absence of control, respectively. Figure 6.8(d) and Figure 6.8(e) represent the variation of controls u_1 and u_2 for application of pesticide and awareness. Figure 6.8(f) and Figure 6.8(g) represent the variation of adjoint variables. Figure 6.9 is plotted using the parameter values $i_1 = 0.1$, $c_1 = 0.1$, $c = 1$, $r_2 = 0.4$, $i_2 = 0.3$, $r_3 = 0.2$, $b_1 = 3$, $b_2 = 3$, $B_1 = 0.1$, $B_2 = 0.1$ and keeping the rest of the parameters unchanged of Figure 6.9. We see that the density of crops is approximately 4.5 and 3.6 unit in the presence of control and absence of control, respectively. Similarly, Figure 6.8(b) and Figure 6.8(c) shows that the population density of pest and locust swarms are approximately approach to zero in the presence of control and 2.3, 1.2 units in the absence of control, respectively. Figure 6.9 gives the batter output compared to Figure 6.8. In Figure 6.9, the cost of control is low because the value of B_1 and B_2 are 0.1.
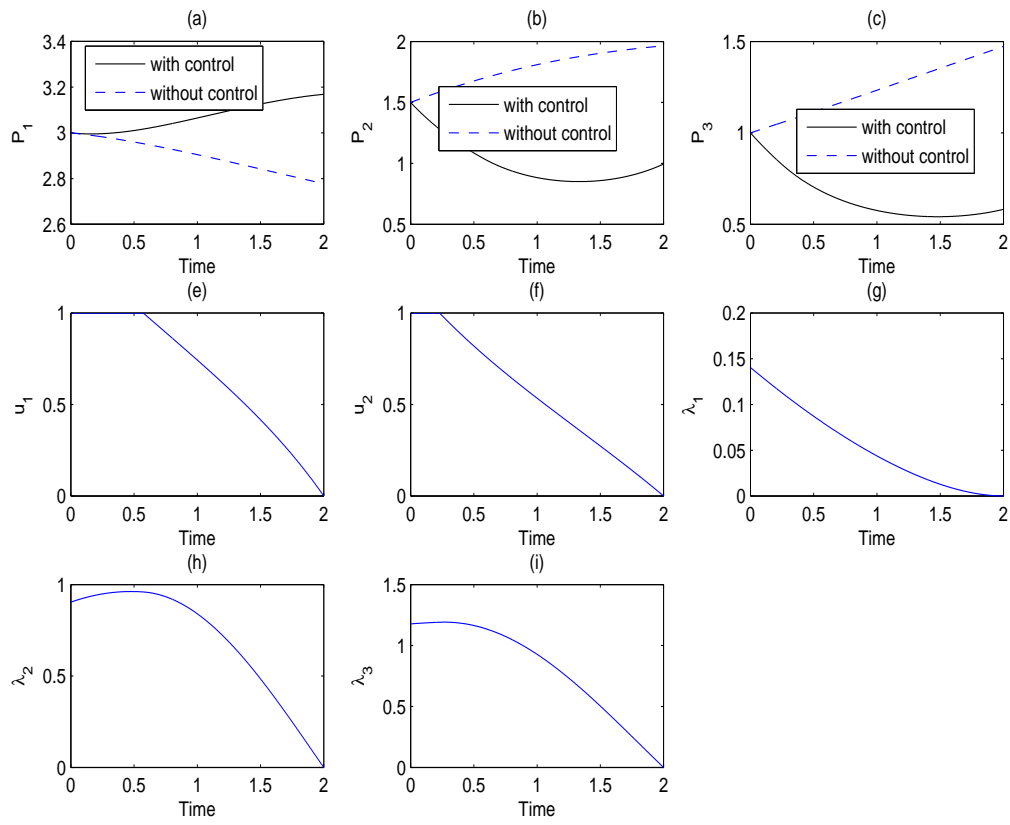
Figure 6.8: Comparison of population density with control versus without control
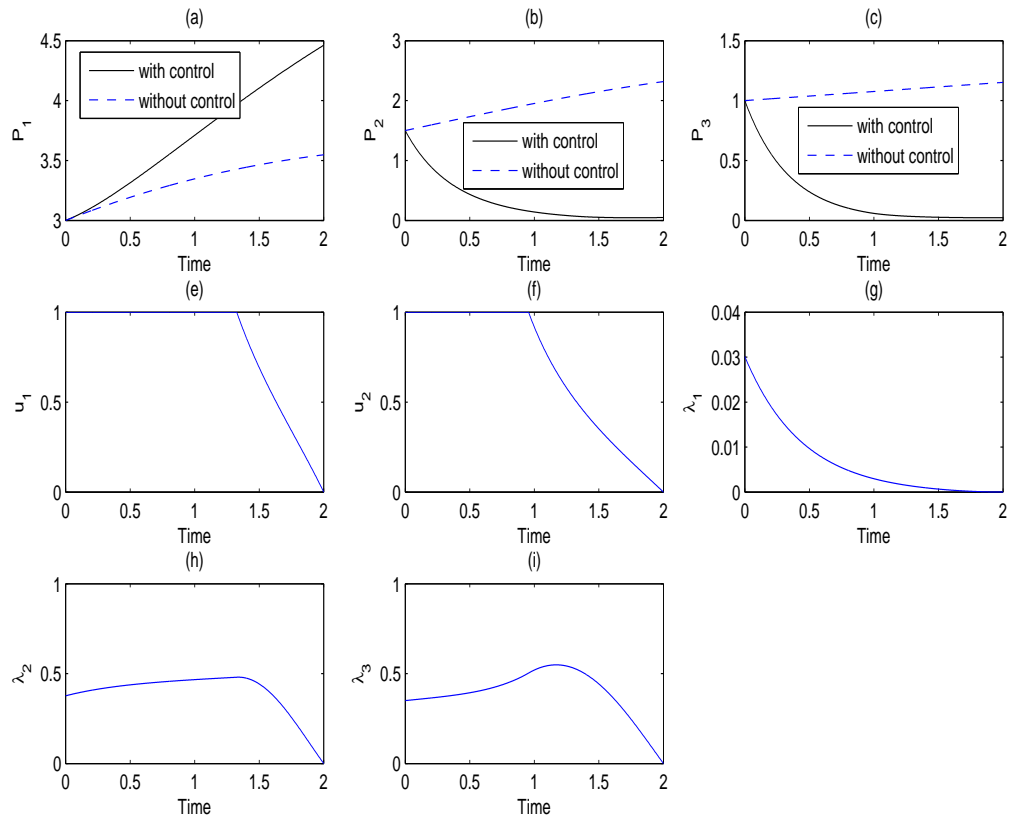
Figure 6.9: Comparison of population density with control versus without control

6.9 Discussion and Future Scope

In establishing population dynamics, environmental variations play an essential effect. In the instance, one of the essential links between populations that influence population dynamic is prey–predator interaction. In this work, a three–species crops, pest and locust swarms have been constructed. Moreover, the model based on the hypothesis of imprecision and description by appropriate parameters of the biological parameters in ecology. The Positivity and boundedness of the system (6.2.1) has been analysed. The possible presence of feasible biological equilibrium points of the system has been discussed. We also identified the local and global stability circumstances. By determining the suitable Lyapunov function, the global stability of the unique positive equilibrium has been evaluated. Further, the local asymptotic stability of several equilibrium points has been discussed to interpret the dynamics of the model system. In this way, Figure 6.2 showed the co–existence of the system.

Figure 6.5–Figure 6.7 showed the variation in population density and biological interpretation of the parameters when one parameter varies and keeping the rest of the parameters unchanged. Moreover, we have presented a prey–predator model with control and without control using a system of differential equations. Two controls have been introduced in the prey–predator model, in which one is the rate of application of pesticide and the other is the rate of application of awareness. In the examination of the effect of optimal control strategies, we have analysed the existence and conditions for optimal control. Further, the control model has been solved by numerical techniques by taking assumed suitable parameters and various numerical results, which were obtained with different values of parameters. In Figure 6.8 and Figure 6.9, it has been observed that control variables increased the density of crops while reducing the density of pests and locust swarm. This study is a new contribution in the area of prey–predator studies in agriculture. The results in this ecological paper have much potential in real–life farming communities and may be useful for decreasing reduction and systematic study for pest control management. This study may be a proven supplement to existing studies in this area of ecology. The results in this ecological paper have much potential in real–life farming communities and may be useful for decreasing reduction and systematic study for pest control management. This study may be a proven supplement to existing studies in this area of ecology. While this work represents an autonomous application to knowledge and practice within the industry, it promotes future research in this field using similar systems–based methodologies to make sustainable agricultural production processes and policies possible. A few new open challenges that can be performed in the coming years are (i) realistic systems are fitted with various requirements, (ii) the predator–prey system with mutual interference and an analysis of the impacts of appropriate monitoring and mutual interference may also become a viable and crucial further expansion of this work.

Chapter 7

Conclusion and Future Scope

7.1   Conclusion

In this thesis, we studied the principles, methodologies, and applications of mathematical models in agriculture. This thesis examines the interaction of a crop and pest, as well as the implementation of various functional responses. In ecological viewpoints, the dynamic behaviour of the prey and predator population displays seasonal changes on crop and pest. The dissertation is organized into six chapters. Chapter 1 introduces the motivation,biological backgrounds, mathematical model, significance of functional responses, various strategies associated with achieving stability, optimal control, and a numerical technique.

In Chapter 2, we look at a mathematical analysis of two prey and one predator models in agriculture. The model's boundedness and positivity of the solutions have been addressed. All equilibrium points have been found to be conditionally biologically acceptable, locally and globally asymptotically stable under specific circumstances. In addition, the mathematical effect has been demonstrated with and without control variables. For model verification, actual data and experimental data of parameters have been implemented. Our numerical study reveals that three control strategies, biomass, cassava mosaic virus control, and pesticides, have a massive impact on a-gricultural systems.

In Chapter 3 of the thesis, a three–dimensional model of prey (crop), pest (a predator

of prey), natural enemy of pest (a predator of pest) and a systematic technique have been used to control the pest population using a balanced mix of pesticide and a natural enemy of pest. The existence and stability conditions for the equilibrium point have been established. We have also numerically analyzed the significantly affect of the natural enemy on the pest population and agricultural productivity. In the presence of the natural enemy and control variables, the pest population declined and crop(prey) production has been enhanced in the prey–pest–natural enemy of pest model.

Chapter 4 illustrates how to represent agricultural processes better using dynamic simulation modelling. Three independent systems have been used to investigate interactions: integrated crops, pests, and natural enemies of the pest. It has been shown that the model is uniformly bounded and that all solutions are completely defined in the positive region. We perform a thorough analysis of the behavior of the system by examining the structure of the system through all its equilibria. The variables that have a major impact on the fundamental reproduction number have been identified. Furthermore, using the numerical values of the parameters, the sensitivity indices of the basic reproduction number have been calculated with regard to all of the parameters. The control variables improved soil fertility and crop yield, whereas the control variables diminished pest density. Our numerical results reveal that the use of control variables and pesticides has a significant influence on the agricultural control system.

In chapter 5, mathematical models have been addressed in order to better comprehend and give valuable biological abstractions and ecologically friendly interactions that occur in nematode pest management applications. The results pointed to a multi–seasonal structure as a possible explanation for the nematode invasion of banana roots. In addition, the types of pest control measures addressed in our study may be divided into the following categories: In this scenario, chemical insecticides and replanting are correctly blended. By examining the system's structure through all of its equilibriums, we became able to perform the behaviour of the system. We evaluated the resultant model using a qualitative optimal control study to see what conditions are best. Further, it has been observed that the optimal control worked as a break of the nematodes population and favorable conditions of the functional root of banana.

In Chapter 6, A three–species crop, pest, and locust swarm mathematical model has been developed. To analyse the dynamics of the model system, the positivity, boundedness, local and global stability of several equilibrium points have been studied. A prey-predator model has also been explored in the presence of two control variables, one of which is the rate of pesticide application and the other is the rate of awareness application. The control variables boosted crop density while decreasing pest and locust swarm density.

7.2   Future Scope

The motivation of studying of prey predator mathematical models is to develop ecological systems that describe the dynamics of crop and pest dynamics in agriculture, as well as to increase crop density while diminishing pest density. Modern agriculture necessitates high–resolution monitoring that is precise and effective. Control could be an effective solution to this problem because it is low–cost and covers a large area. They are concentrating on a proper fertilisation strategy that includes a uniform application of plant solutions to the field. As a result, the focus of this research is on the mathematical modelling and analysis of an intelligent airborne platform with capabilities for effective plant monitoring. It is hazardous to agricultural crops and nearby ecosystems. For many countries, detecting this damage is a major difficulty. The modelling of a real–world problem is done with the help of mathematical equations that use variables, parameters, and other factors, all of which are supported by scientific definitions, concepts, and affirmed assumptions that form the primary foundation of the reasoning used. Mathematical modelling, for example, is widely employed in a variety of issues, like:

- To depict the transmission of diseases in living beings.

- To learn more about how different organs work.

- To study the population dynamics.

- To research in order to make a design decision.

and many more.

The whole world is facing some of the serious environmental issues such as floods, global warming, drastic climate differences, increase in sea level etc. Future research in the field would involve a multidisciplinary interaction between agronomists, environmental modelers, and mathematical researchers, and computational experts, aimed at building Mathematical models which offer reliable outcomes and recognizing of field findings in actual environments so that all the models can be regarded as development tools. Finally, in order to apply optimal control techniques, the parameters need to be well known and this may increase the performance of our future optimal control systems. A few new open challenges that can be performed in the coming years are (i) realistic systems are fitted with various requirements, (ii) the predator–prey system with mutual interference and an analysis of the impacts of appropriate monitoring and mutual interference may also become a viable and crucial further expansion of this work. We expect that the decision–makers and farmers to consider the use of various modeling activities in the future. Researchers will give a more overview of the essential elements of farming system productivity and ecology and economic sustainability and will establish more flexible management practices and development strategies for truly sustainable agriculture.

Bibliography

[1] A.J. Lotka, Elements of Physical Biology, William and Wilkins, Baltimore, 1925.

[2] A. Lotka, Elements of Mathematical Biology, Dover, New York, 1956.

[3] A.A. Berryman, The origin and evolution of predator-prey theory, Ecology, 1992, 73, 1530–1535.

[4] A.M. Lyapunov, The General Problem of the Stability of Motion (In Russian), Doctoral dissertation, Univ. Kharkov 1892 English translations: (1) Stability of Motion, Academic Press, New–York & London, 1966 (2) The General Problem of the Stability of Motion, (A. T. Fuller trans.) Taylor & Francis, London 1992.

[5] A.E. Bryson, Optimal control–1950 to 1985, in IEEE Control Systems Magazine, 1996, 16(3), 26–33.

[6] A. Korobeinikov, Global properties of basic virus dynamics models. Bull. Math. Biol., 2004, 66, 879–883.

[7] A. Quarteroni, L. Formaggia, Mathematical Modelling and Numerical Simulation of the Cardiovascular System, Modelling of Living Systems, Handbook of Numerical Analysis Series. Amsterdam: Elsevier, 2004, 12, 3–127.

[8] A.B. Rai, J. Halder, and M.H. Kodandaram, Emerging insect pest problems in vegetable crops and their management in India: An appraisal. Pest Mgmt Hort Ecosyst., 2014, 20, 113–122.

[9] Agricultural Statistics at a Glance, Government of India Ministry of Agriculture & Farmers Welfare Department of Agriculture, Cooperation & Farmers Welfare Directorate of Economics and Statistics, 2015. (https://eands.dacnet.nic.in/PDF/Agricultural_Statistics_At_Glance-2015.pdf).

[10] A. Charu,V. Kumar, S. Kant, Dynamics of a High–Dimensional Stage–Structured Prey–Predator Model, International Journal of Applied and Computational Mathematics, 2017, 3(1), 427–445.

[11] A. Sabarwal, K. Kumar, R.P. Singh, Hazardous effects of chemical pesticides on human health–Cancer and other associated disorders, Environmental Toxicology and Pharmacology, 2018, 63, 103–114.

[12] A.B. Fahad, K.B. Blyuss, S. Ray, Modelling the effects of awareness-based interventions to control the mosaic disease of Jatropha curcas, Ecological Complexity, 2018, 36, 92–100.

[13] A. Jentsch, P. White, A theory of pulse dynamics and disturbance in ecology, Ecology, 2019, e02734.

[14] A.K. Misra, N. Jha, R. Patel, Modeling the effects of insects and insecticides on agricultural crops with NSFD method. J. Appl. Math. Comput., 2020, 63, 197–215.

[15] A.G. Garcia, J.B. Malaquias, C.P. Ferreira, et al. Ecological Modelling of Insect Movement in Cropping Systems. Neotrop Entomol., 2021, 50, 321–334.

[16] A. Sarkar, P.K. Tiwari, S. Pal, Effect of Additional Food on Predator–Prey Interactions With Water–Level Fluctuation, Journal of Biological Systems, 2021, 29(4), 995–1022.

[17] B. Moreau, J. Le Bourdelles, Etude du systéme racinaire du bananier Gros Michel en Equateur, Fruits, 1963, 18, 71-74.

[18] B.S. Goh, G. Leitman, T.L. Vicent, The optimal control of a prey-predator system. Math.Biosc., 1974, 19, 263–286.

[19] B.S. Goh, Management and analysis of biological populations, Elsevier Scietific Publishing Company: Amsterdam, 1980.

[20] B. Thalya, J. Ernstberger,& K.R. Fister, Optimal Control Applied to Immunotherapy. Discrete and Continuous Dynamical Systems B, 2004, 4(1), 135–146.‘

[21] B. Liu, L. Chen, Y. Zhang, The dynamics of a prey–dependent consumption model concerning impulsive control strategy, Appl Math Comput., 2005, 169(1), 305–320.

[22] B. Krauskopf, H.M. Osinga, J. Galan–Vioque, A continuing influence in dynamics, Numerical Continuation Methods for Dynamical Systems: Path following and boundary value problems, 2007, V–VII.

[23] B. Sahoo, S.Poria, Effects of supplying alternative food in a predatorprey model with harvesting, Applied Mathematics and Computation, 2014, 234, 150–166.

[24] Beyond Pesticides, Widely used pesticide in food production damages childrens brains. Pesticides and You, 2018, 16–19.

[25] Biomass–Energy Explained, Your Guide To Understanding Energy. U.S. Energy Information Administration, June 21, 2018.

[26] C.S. Holling, Some chararacteristics of simple types of predation and parasitism, Canad. Entomologist, 1959, 91, 385–398.

[27] C.S. Holling, The functional response of predators to prey density and its role in mimicory and population regulation, Memories of Entomological Society of Canada, 1965, 45, 1–60.

[28] C.S. Holling, The Functional Response of Invertebrate Predators to Prey Density, Memoirs of the Entomological Society of Canada, 1966, 98(48), 5-86.

[29] C. Shoemaker, Optimization of agricultural pest management II: formulation of a control model, Mathematical Biosciences, 1973, 17(34), 357–365.

[30] C.W. Clark, Mathematical Bioeconomics: The Optimal Management of Renewable Resources. Wiley, New York, 1990.

[31] C.A. Gilligan, Modelling soil–borne plant pathogens: reaction-diffusion models, Canadian Journal of Plant Pathology, 1995, 17(2), 96–108.

[32] C.R. Taylor and R. Rodrʻiguez-Kabana, Optimal rotation of peanuts and cotton to manage soil-borne organisms, Agricultural Systems, 1999, 61(1), 57–68.

[33] C. Chabrier, H. Mauléon, P. Bertrand, A. Lassoudière and P. Quénéhervé, Banane antillaise, les systèmes de culture évoluent: en Martinique, méthodes alternatives pour réduire íutilisation des nématicides et insecticides en bananeraies, Phytoma - La défense des végétaux, 2005, 584, 12–16.

[34] C. Nakul, J.M. Hyman, J.M. Cushing, Determining important parameters in the spread of malaria through the sensitivity analysis of a mathematical model. Bull Math Biol., 2008, 70, 1272–1296.

[35] C. Chabrier, P. Tixier, P. F. Duyck, Y. M. Cabidoche, P. Queneherve, Survival of the burrowing nematode Radopholus similis (Cobb) Thorne without food: Why do males survive so long?, Applied Soil Ecology, 2010, 45 (2), 85–91.

[36] C.C. Lo, Effect of pesticides on soil microbial community. Journal of Environmental Science and Health Part B, 2010, 45(5), 348–359.

[37] C. Arora and V. Kumar, Dynamics of a high–dimensional stage-structured prey–predator model International Journal of Applied and Computational Mathematics, 2017, 3(1), 427–445.

[38] D.S. Riggs, The mathematical approach to physiological problems, MIT Press, Cambridge, 1963.

[39] D.L. Jaquette, Mathematical models for controlling growing biological populations: a survey, Operations Research, 1972, 20(6), 1142–1151.

[40] D.L. DeAngelis, R.A. Goldstein, R.V. O'Neill, A model for trophic interaction. Ecology (Ecological Society of America), 1975, 56(4), 881–892.

[41] D.L. Lukes, Differential equations: classical to controlled. In:Mathematics in Science and Engineering, Academic Press, New York, 1982. vol. 162.

[42] D.S. Bhatti, R.K. Jain, Chemical control of root–knot nematode in India: A Review. Haryana J. Hort. Sci., 1984, 13, 6–68.

[43] D.J. Boethel, R.D. Eikenbary, Interactions of Plant Resistance and Parasitoids and Predator of Insects. Wiley, Chicheste, 1986.

[44] D.W. Jordan, P. Smith, Nonlinear Ordinary Differential Equations (Second edition), Clarendon Press, Oxford, 1987.

[45] D.D. Waele, R.G. Davide, The root–knot nematodes of banana. Musa Pest Factsheet No. 3. International Network for the Improvement of Banana and Plantain, Parc Scientifique Agropolis II, 34, Montpellier Cedex 5, FRANCE, 1998. .

[46] D.R. Powell, J. Fair, R.J. Le Claire, L.M. Moore, D. Thompson, Sensitivity analysis of an infectious disease model, in Proceedings of the International System Dynamics Conference, Boston, Mass, USA, 2005.

[47] D. Jana, J.P. Tripathi, Impact of generalist type sexually reproductive top predator interference on the dynamics of a food chain model, In. J. Dynam, 2016.

[48] D. Atwood, C.P. Jones, Pesticides Industry Sales and Usage: 2008–2012 Market Estimates. Environmental Protection Agency, 2017.

[49] E.J. Routh, A treatise on the stability of a given state of motion, particularly steady motion, Macmillan & Co., London, 1877.

[50] E. Jung, S. Lenhart, Z. Feng, Optimal control of treatments in a two–strain tuberculosis model. Discrete Contin. Dyn. Syst., Ser. B, 2002, 2–4, 473–482.

[51] E.C. OERKE, Crop losses to pests, Journal of Agricultural Science, 2005, 144, 31-43.

[52] E. Sli, D. Mayers, An Introduction to Numerical Analysis, New York, NY: Cambridge University Press, 2006.

[53] E.A. De Villiers, M.S. Daneel, P.S. Schoeman, J.C. Robinson and E.A. De Villiers, The cultivation of banana. Ingwe Print, Nelspruit, 2007, 194–219.

[54] E.N. Bodine, L.J. Gross, S. Lenhart, Optimal control applied to a model for species augmentation. Math. Biosci. Eng., 2008, 5(4), 669–680.

[55] E.C. Oerke, H.W. Dehne, Safeguarding production losses in major crops and the role of crop protection. Crop Prot, 2010, 23, 275–285.

[56] F. Chen, L. Chen, X. Xie, On a Leslie–Gower predator-prey model incorporating a prey refuge, Nonlinear Analysis: Real World Applications, 2009, 10, 2905–2908.

[57] F.G. Andrade, R.L. Pulles, and E. Estevez, Acute pesticide poisoning in Ecuador: A short epidemiological report, Journal of Public Health, 2010, 18 (5), 437–442.

[58] F.E. Uboh, E.N. Asuquo, M.U. Eteng, and E.O. Akpanyung, Endosulfan–induces renal toxicity independent of the route of exposure in rats. Am. J. Biochem. Mol. Biol., 2011, 1 (4), 359-367.

[59] F.M. Hamelin, M. Castel, S. Poggi, D. Andrivon, L. Mailleret, Seasonality and the evolutionary divergence of plant parasites, Ecology, 2011, 92 (12), 2159-2166.

[60] F. Affholder, P. Tittonell, M. Corbeels et al., Ad hoc modeling in agronomy: What have we learned in the last 15 years? Agronomy Journal, 2012, 104 (3), 735–748.

[61] FAOStat.,2011.`http://faostat.fao.org/site/567/DesktopDefault. aspx?PageID=567#ancoraccessedon3.1.2010.`

[62] F.M. Hilker, L.J. Allen, V.A. Bokil, C.J. Briggs, Z. Feng, K.A. Garrett, L.J. Gross, F.M. Hamelin, M.J. Jeger, C.A. Manore, A.G. Power, M.G. Redinbaugh, M.A. Ra, N.J. Cunniffe, Modeling virus coinfection to inform management of maize lethal necrosis in kenya, Phytopathology, 2017, 107, 1095–1108.

[63] F.A. Basir, A. Banerjee, S. Ray, Role of farming awareness in crop pest management–A mathematical model. Journal of Theoretical Biology, 2019, 461, 59–67.

[64] G.R. Conway, Mathematical Models in Applied Ecology. Nature, 1977, 269, 291–297.

[65] G. Birkhoff, G.C. Rota, Ordinary Differential Equations. Ginn, Boston, 1982.

[66] G.B. Schaalje, Dynamic Models of Pesticide Effectiveness, Environmental Entomology, 1990, 19(3), 439–447.

[67] G.I. Thaler, Automatic Control Systems. West Publishing, St. Paul, MN, 1990.

[68] G.S. Dhaliwal, R. Arora, An estimate of yield losses due to insect pests in Indian agriculture, Indian JEcol, 1996, 23, 70–73.

[69] G. Leitmann, The calculus of variations and optimal control. An introduction. Mathematical Concepts and Methods in Science and Engineering. New York: Plenum Press, 1997.

[70] G.T. Skalski, J.F. Gilliam, Functional responses with predator interference: viable alternatives to the Holling type II model, Ecology, 2001, 82, 3083–3092.

[71] G.S. Dhaliwal, R. Arora, A.K. Dhawan, Crop losses due to insect pests in Indian agriculture: An update. Indian JEcol., 2003, 31, 1–7.

[72] G.S. Dhaliwal, A.K. Dhawan, R. Singh, Biodiversity and ecological agriculture: Issues and perspectives. Indian JEcol., 2007, 34, 100–109.

[73] G.S. Dhaliwal, V. Jindal, A.K. Dhawan, Insect pest problems and crop losses: Changing trends. Indian J Ecol., 2010, 74, 1–7.

[74] G.P. Hu, X.L. Li, Stability and Hopf bifurcation for a delayed predator–prey model with disease in the prey. Chaos, Solitons and Fractals, 2012, 45(3), 229–237.

[75] G.S. Dhaliwal, V. Jindal, B. Mohindru, Crop losses due to insect pests: Global and Indian scenario. Indian J Ecol., 2015, 77, 165–168.

[76] Government of India Ministry Of Agriculture & Farmers Welfare Department Of Agriculture, Cooperation & Farmers Welfare Directorate Of Plant Protection, Quarantine & Storage Make In India `http://ppqs.gov.in/statistical-database`.

[77] H.D. Burges, N.W. Hussey, Microbial Control of Insects and Mites. Academic Press, New York, 1971.

[78] H.J. Barclay, Models for pest control using predator release, habitat management and pesticide release in combination, Journal of Applied Ecology, 1982 19 (2), 337–348.

[79] H.R. Joshi, Optimal control of an HIV immunology model. Optim. Control Appl. Methods, 2002, 23, 199–213.

[80] H.R. Joshi, S. Lenhart, M.Y. Li, L. Wang, Optimal control methods applied to disease models, in Mathematical studies on human disease dynamics, 2006, 410, 187–207.

[81] H. Zhang et al., An Impulsive Predator-Prey system with Beddington-DeAngelis functional response and time delay. Int. J. Biomath., 2008, 1(1).

[82] H. Mainul, Z. Jin, E. Venturino, An ecoepidemiological predator-prey model with standard disease incidence, Math. Meth. Appl. Sci., 2009, 32(7), 875–898.

[83] H.X. Hu, Z.D. Teng, S.J. Gao, Extinction in a non autonomous Lotka–Volterra competitive system with pure delays and feedback controls. Nonlinear Anal., Real World Appl., 2009, 10, 2508–2520.

[84] H. Gaff, F. Schaefer, Optimal control applied to vaccination and treatment strategies for various epidemiological models, Math Biosci Eng., 2009, 6, 469–492.

[85] H.W. McKenzie, M.A. Lewis, E.H. Merrill, First passage time analysis of animal movement and insights into the functional response, Bull. Math. Biol., 2009, 71, 107–129.

[86] H. Guo, L. Chen, Time–limited pest control of a Lotka Volterra model with impulsive harvest, Nonlinear Analysis. Real World Applications, 2009, 10(2), 840–848.

[87] H. Ritchie, M. Roser, Land Use, Published online at OurWorldInData.org. (https://ourworldindata.org/land-use), 2013.

[88] I.I.E. Slotine, L. Weiping, Applied Nonlinear Control. Prentice-Hall International, New York, 1991.

[89] I.K. Morton, L.S. Nancy, Dynamics Optimization: The Calculus of Variations and Optimal Control in Economics and Management. Elsevier Science, The Netherlands, 2000, 218–234.

[90] International Agency for Research on Cancer, IARC Monographs Volume 112: evaluation of five organophosphate insecticides and herbicides. World Health Organization, March 20, 2015.

[91] I. Tankam Chedjou, S. Touzeau, F. Grognard, L. Mailleret, J.J. Tewa, F. Grognard, Modelling and control of a banana soilborne pest in a multi-seasonal framework, Mathematical Biosciences, 2020.

[92] J.P. LaSalle, The Stability of Dynamical Systems, in: Regional Conference Series in Applied Mathematics, SIAM, Philedelphia, 1976.

[93] J.N. Sasser, W.D. Freckman, A world perspective on Nematology: the role of the society. In. Vistas on Nematology (Eds.Veech, J.A. and Dickson, D.W.), Society of Nematologists, Hyattsville, Maryland, USA, 1987, 7–14.

[94] J. Holt, M.J. Jeger, J.M. Thresh, G.W. Otim-Nape, An epidemiological model incorporating vector population dynamics applied to African cassava mosaic virus disease, J. Appl. Ecol., 1997, 34, 793–806.

[95] J.D. Murray, Mathematical biology, 2nd edn. Springer, Heidelberg, 1993.

[96] J.E. Brindley, Ocean plankton populations as excitable media, Bull Math Biol, 1994, 56(5), 981–998.

[97] J. Moore, Parasite and the Behavior of Animals. Oxford University Press, Oxford, 2002.

[98] J.H. Jones, Notes on R_0, Standford University, 2007.

[99] J.R. Rich, J.A. Brito, R. Kaur, J.A. Ferrell, Weed species as hosts of Meloidogyne : A review. Nematropica, 2008, 39, 157–185.

[100] J.C. Robinson, V.G. Sauco, Bananas and plantains, 2010, Vol 19.

[101] J.I. Ransom, J.G. Powers, N.T. Hobbs, D.L. Baker, Ecological feedbacks can reduce population-level efficacy of wildlife fertility control, Journal of Applied Ecology, 2014, 51, 259–269.

[102] J.P. Tripathi, S. Tyagi, S. Abbas, Global analysis of a delayed density dependent predatorprey model with Crowley-Martin functional response, Commun. Nonlinear Sci. Numer.Simulat., 2016, 30, 45–69.

[103] J.P. Tripathi, S.S. Meghwani, M. Thakur, S. Abbas, A modified Leslie–Gower predator–prey interaction model and parameter identifiability, Commun Nonlinear Sci. Numer. Simulat., 2018, 54, 331–346.

[104] I.R. Stella and M. Ghosh, Modeling plant disease with biological control of insect pests, Stochastic Analysis and Applications, 2019, 37(6), 1133–1154.

[105] I.R. Fitri,F. Hanum, A. Kusnanto, and T. Bakhtiar, Optimal pest control strategies with cost–effectiveness analysis. Sci. World J., 2021.

[106] J.B.S Haldane, Enzymes. London, New York, Longmans, Green, 1930.

[107] J. Macki, A. Strauss. Introduction to Optimal Control Theory. Springer-Verlag, New York, 1982.

[108] J. Chattopadhyay, O. Arino, A predator-prey model with disease in prey. Non Linear Analysis, 1999, 36(6), 747–766.

[109] J. M. Heffernan, R. J. Smith, and L. M. Wahl, Perspectives on the basic reproductive ratio, Journal of the Royal Society Interface, 2005, 2(4), 281–293, 2005.

[110] J.H. Jones, Notes on R_0, Standford University, 2007.

[111] J. Liang, S. Tanga, R.A. Cheke, An integrated pest management model with delayed responses to pesticide applications and its threshold dynamics. Nonlinear Anal., Real World Appl., 2012, 13, 2352–2374

[112] J.H. Dawes, M.O. Souza, A derivativation of Holling's type I,II and III functional responses in predator-prey system. J. Theor. Biol., 2013, 327, 11–22.

[113] J. Yang, S. Tang, Holling type II predator–prey model with nonlinear pulse as state-dependent feedback control. Journal of Computational and Applied Mathematics, 2016, 291, 225–241.

[114] K.E.F. Watt, A Mathematical model for the effect of densities of attacked and attacking species on the number attacked, The Canadian Entomologist, 1959, 91(3), 129–144.

[115] K. Wickwire, Mathematical models for the control of pests and infectious diseases: a survey, Theoretical Population Biology. An International Journal, 1977, 11(2), 182–238.

[116] K.P. Hadeler, H.I. Freedman, Predator–prey populations with parasitic infection. J. Math. Biol., 1989, 27, 609–631.

[117] K.D. Jager, M. S. Daneel, M. Desmet et al., Pathogenicity and distribution studies to determine threshold levels for nematodes on banana. Banana Grow Assoc S Afr Yearb, 1999, 3, 72–77.

[118] K. Eckstein, J.C. Robinson, The influence of the mother plant on sucker growth, development and photosynthesis in banana (Musa AAA; Dwarf Cavendish), The Journal of Horticultural Science and Biotechnology, 1999, 74(3), 347-350.

[119] K.O. Rauff, R. Bello, A review of crop growth simulation models as tools for agricultural meteorology. Agric. Sci., 2015, 6, 1098–1105.

[120] M.R. Kelly, J.H. Tien, M.C. Eisenberg, S. Lenhart, The impact of spatial arrangements on epidemic disease dynamics and intervention strategies, J. Biol.Dynam., 2016, 10, 222–249.

[121] M.H. Mohd, N.A.A. Rahman, N.N.A. Hamid, Y.M. Yatim, Dynamical Systems, Bifurcation Analysis and Applications, Springer Proceedings in Mathematics & Statistics, Penang, Malaysia, 2018, Vol. 295.

[122] L.S. Pontryagin, V.G. Boltyanskii, R.V. Gamkrelidze, E.F. Mishchenko, The Mathematical Theory of Optimal Processes. Wiley, New York, 1962.

[123] L. Cesari, Optimization Theory and Applications: Problems with Ordinary Differential Equations. Springer Verlag, New York, 1983.

[124] L. Edelstein–Keshet, Mathematical Models in Biology, McGraw–Hill, Inc., New York, 1987.

[125] L.W. Duncan, D.T. Kaplan, J.W. Noling, Maintaining barriers to the spread of Radopholus citrophilus in Florida citrus orchards, Nematropica, 1990, 20, 71-87.

[126] L.J.S. Allen, An introduction to mathematical biology. Pearson Prentice Hall, New Jersey, 2007.

[127] L. Mailleret, M. Castel, M. Montarry, F. Hamelin, From elaborate to compact seasonal plant epidemic models and back: Is competitive exclusion in the details?, Theoretical Ecology, 2011, 5, 311–324.

[128] L. Prost, M. Cerf, and M.H. Jeuffroy, Lack of consideration for end-users during the design of agronomic models. A review, Agronomy for Sustainable Development, 2012, 32(2), 581–594.

[129] L. Meng, K. Wang, Dynamics of a Leslie–Gower Holling-type II predatorprey system with Levy jumps, Nonlinear Analysis: Theory, Methods and Applications, 2013, 85, 204–213.

[130] L. Rasche, R.A.J. Taylor, EPIC–GILSYM: modelling crop–pest insect interactions and management with a novel coupled crop–insect model, Journal of Applied Ecology, 2019, 56(8), 2045–2056.

[131] M. Beugnon, J. Champion, Etude sur les racines du bananier, Fruits, 1966, 21(7), 309–327.

[132] M.P. Hassell, C.C. Varley, New inductive population model for insect parasites and its bearing on biological control. Nature, 1969, 223, 1133–1137.

[133] M. Braun, Differential equations and their applications, Springer–Verlag, New York, 1978.

[134] M.S. Swaminathan, Plant protection for global food security. In: Proceedings of 10th international congress on plant protection Brighton, British Crop Protection Council, Oxford, 1983, 1(1), 20–25.

[135] M. Araya, M. Centeno, Recuperacion de Radopholus similis, Helicotylenchus spp., Meloidogyne spp. y Pratylenchus spp. de raiz funcional, no funcional y combinada de banano (Musa AAA), Corbana, 1995, 20, 11–16.

[136] M. Kot, Elements of mathematical ecology. Cambridge University Press, Cambridge, 2001.

[137] M. Baalen, V. Krivan, P.C.J. van Rijn, M.W. Sabelis, Alternative food switching predators, and the persistence of predatorprey systems, Am. Nat., 2001, 157, 512–524.

[138] M. Gopal, A. Gupta, B. Sathiamma, C.P.R. Nair, Control of the coconut pest oryctes rhinoceros L. Using the oryctes virus. Insect Sci. Appl., 2001, 21(2), 93–101.

[139] M.A. Aziz–Alaoui, M.D. Okiye, Boundedness and global stability for a predator-prey model with modified Leslie–Gower and Holling–type II schemes, Appl. Math. Lett., 2003, 16, 1069–1075.

[140] M.J. Jeger, J. Holt, F. Van Den Bosch, L.V. Madden, Epidemiology of insect–transmitted plant viruses, modelling disease dynamics and control interventions, Physiol. Entomol., 2004, 29, 291–304.

[141] M. Arshad, A. Khalid, Impact of Pesticides on Soil Microbial Diversity, Enzymes, and Biochemical Reactions. Advances in Agronomy., 2009, 102, 159–200.

[142] Ministry of Health and Family Welfare, Family Welfare Statistics in India, Statistics Division, Government of India, New Delhi, 2011.

[143] M.V. Cook, Flight Dynamics Principles (Third Edition), Butterworth–Heinemann, 2013.

[144] M. Mehra, R.K. Malik, Solutions of differential–difference equations arising from mathematical models of granulocytopoiesis, differential equations and dynamical systems, 2014, 22(1), 33–49.

[145] M.S. Daneel, K. De Jager, I. Van den Bergh et al, Occurrence and Pathogenicity of Plantparasitic Nematodes on Commonly Grown Banana Cultivars in South Africa. Nematropica, 2015, 45, 118–127.

[146] M. Schuster, M. Torero, Towards a sustainable food system: reducing food loss and waste. In: 2016 Global food policy report, International Food Policy Research Institute. Available via `http://ebrary.ifpri.org/cdm/ref/collection/p15738coll2/id/130211`. Accessed 28 June, 2016.

[147] M. Sen, A. Simha, S. Raha, Adaptive Control Based Harvesting Strategy for a Predator–Prey Dynamical System", Acta Biotheor, 2018, 66, 293–313.

[148] M.R. Kelly Jr, J.H. Tien, M.C. Eisenberg, S. Lenhart, The impact of spatial arrangements on epidemic disease dynamics and intervention strategies, J. Biol.Dynam., 2016, 10, 222–249.

[149] N. Parolini, A. Quarteroni, Mathematical Models and Numerical Simulations for the America"s Cup. Computer Methods in Applied Mechanics and Engineering, 2005, 194(11), 1001–1026.

[150] N. Bairagi, P.K. Roy, J. Chattopadhyay, Role of infection on the stability of a predator–prey system with several response functions a comparative study, J. Theor. Biol., 2007, 248, 10–25.

[151] N. Chitnis, J.M. Hyman, J.M. Cushing, Determining important parameters in the spread of malaria through the sensitivity analysis of a mathematical model, Bulletin of Mathematical Biology, 2008, 70(5), 1272–1296.

[152] Nemabase, 2010. http://plpnemweb.ucdavis.edu/nemaplexNemabase2010/GenusHostRangeResul

[153] N.C. Apreutesei, An optimal control problem for a pest, predator, and plant system. Nonlinear Anal., Real World Appl., 2012, 13, 1391-1400.

[154] N.J. Cunniffe, B. Koskella, C.J.E. Metcalf, S. Parnell, T.R. Gottwald, C.A. Gilligan, Thirteen challenges in modelling plant diseases, Epidemics, 2015, 10, 6–10.

[155] N.N. Khondoker, C.N. Podder, Sensitivity Analysis of Chronic Hepatitis C Virus Infection with Immune Response and Cell Proliferation. International Journal of Biomathematics, 13, 2020.

[156] O. Diekmann, K. Dietz, J.A.P. Heesterbeek, The basic reproduction ratio for sexually transmitted diseases: theoretical considerations. Math Biosci., 1991, 107, 325–339.

[157] O.P. Lal, Recent advances in Indian entomology. APC, New Delhi, 1996.

[158] O. Diekmann, J.A.P. Heesterbeek, M.G. Roberts, The construction of next–generation matrices for compartmental epidemic models, J. R. Soc. Interface, 2010, 7, 873–885.

[159] O. Diekmann, H. Heesterbeek, T. Britton, Mathematical tools for understanding infectious disease dynamics. Princeton University Press, New Jersey, 2013.

[160] P.F. Verhulst, Notice sur la loi que la population suit dans son accroissement, Correspondance Mathmatique et Physique Publie par A. Quetelet, 1838, 10, 113–121.

[161] P.H. Leslie, Some further notes on the use of matrices in population mathematics, Biometrica, 1948, 35, 213–245.

[162] P.C. Trivedi, B. Tiagi, Control of root-knot of chilli with nematicides. J. Res. Assam Agric. Univ., 1985, 4, 65–66.

[163] P.H. Crowley, E.K. Martin, Functional responses and interference within and between year classes of a dragonfly population. J. North American Benthological Society, 1989, 8(3), 211–221.

[164] P.J. Hudson, A. Dobson, D. Newborn, Do parasites make prey vulnerable to predation? Red grouse and parasites. J. Anim. Ecol., 1992, 61, 681–692.

[165] P.G. Darzin, Nonlinear Systems. Cambridge University Press, 1992.

[166] P.A. Abrams, C.J. Walters, Invulnerable prey and the paradox of enrichment. Ecology, 1996, 77(4), 1125–1133.

[167] P.V.D. Driessche, J. Watmough, Reproduction numbers and sub–threshold endemic equilibria for compartmental models of disease transmission. Math Biosci., 2002, 180, 29–4.

[168] P. Tixier, J.M. Ris‘ede, M. Dorel, E. Malezieux, Modelling population dynamics of banana plant–parasitic nematodes: A contribution to the design of sustainable cropping systems, Ecological Modelling, 2006, 198(3), 321–331.

[169] P. Gregory, Plant Roots: Growth Activity and Interactions with Soils, Bio–Green Elsevier (Exc), 2006.

[170] P.D.N. Srinivasu, B.S.R.V. Prasad, M. Venkatesulu, Biological control through provision of additional food to predators: a theoretical study. Theor. Popul. Biol., 2007, 72, 111–120.

[171] P. Thota, H. Dankowicz, TC–HAT: A Novel Toolbox for the Continuation of Periodic Trajectories in Hybrid Dynamical Systems, SIAM Journal on Applied Dynamical Systems, 2008, 7(4), 1283–1322.

[172] P. Liu, Certification in the value chain for fresh fruits: The example of banana industry, FAO, 2009.

[173] P. Yongzhen, P. Xuehuia, and L. Changguo, Pest regulation by means of continuous and impulsive nonlinear controls. Math. Comput. Model., 2010, 51, 810–822.

[174] P.K. Mondal, S. Jana, T.K. Kar, A theoretical approach on controlling agricultural pest by biological controls, Acta Biotheoretica, 2014, 62(1), 47–67.

[175] P.K. Rice, Pests and pathogens place global burden on major food crops, UC Division of Agriculture and Natural Resources, february 8, 2019 (`https://ucanr.edu/blogs/blogcore/postdetail.cfm?postnum=29354`).

[176] Q. Wang, B.X. Dai, Almost periodic solution for n-species Lotka-Volterra competitive systems and feedback controls, Appl. Math. Comput., 2008, 200, 133–146.

[177] R.M. May, Stability and complexity in model ecosystems, Princeton University Press, Princeton, 1973.

[178] R.K. Jones, D.L. Milne, Nematode pests of bananas. In: Keetch DP, Heyns J (eds) Nematology in southern Africa. Science Bulletin No. 400, Department of Agriculture and Fisheries, Pretoria, 1982, 30–37.

[179] R.M. Anderson, R.M. May, The invasion, persistence and spread of infectious diseases within animal and plant communities, Philosophical Transactions of the Royal Society B: Biological Sciences, 1986, 314(1167), 533–570.

[180] R. Hugon, H. Picard, Relations spatiales entre taches et necroses racinaires et nematodes endoparasites chez le bananier, Fruits., 1988, 43(9), 491–498.

[181] R. Arditi, L.R. Ginzburg, Coupling in predator-prey dynamics: ratio-dependence, Journal of Theoretical Biology, 1989, 139(3), 311–326.

[182] R.L Baldwin, Modeling ruminant digestion and metabolism, Chapman and Hall, Great Britain, 1995.

[183] R.S. Cantrell, C. Cosner, On the Dynamics of Predator–Prey Models with the Beddington-DeAngelis Functional Response, Journal of Mathematical Analysis and Applications, 2001, 257(1), 206–222.

[184] R.S. Hussey, J.G.W. Janssen, In: Plant Resistance to Parasitic Nematodes (J.L. Starr, R. Cook and J. Bridge, eds.) CAB International, Wallingford Oxon, UK, 2002, 43–70.

[185] R.K. Jain, K.N. Mathur, R. V. Singh, Estimation of Losses due to Plant Parasitic Nematodes on different crops in India. Indian J. Nematol., 2007, 37, 219–21.

[186] R.K. Upadhyay, N. Kumari, V. Rai, Wave of chaos and pattern formation in spatial predator-prey systems with Holling type IV predator response, Mathematical modeling of Natural phenomena, 2008, 3(4), 71–95.

[187] R. Shi, X. Jiang, L. Chen, A predator–prey model with disease in the prey and two impulses for integrated pest management, Appl Math Model, 2009, 3(5), 2248–2256.

[188] R. Peshin, A.K. Dhawan, Integrated Pest Management: Innovation–Development Process, Springer Netherlands, Dordrecht, 2009.

[189] R.K. Upadhyey, R.K. Iyenger, Introduction to Mathematical Modeling and Chaotic Dynamics, Chapman and Hall/CRC, 2013.

[190] S. Pradhan, Assessment of losses caused by insect pests of crops and estimation of insect population. In: Pant NC (ed) Entomology in India. Entomological Society of India, New Delhi, 1964, 17–58.

[191] S. Gubbins, C.A. Gilligan, Biological control in a disturbed environment, Philosophical Transactions of the Royal Society of London. Series B: Biological Sciences, 1997, 352(1364), 1935-1949.

[192] S. Pradhan, Agricultural entomology and pest control. Indian Council of Agricultural Research, New Delhi, 1983.

[193] S. Jayaraj, Biopesticides and integrated pest management for sustainable crop production, 1993.

[194] S. Gowen, Chemical control of nematodes: efficiency and side-effects, in: M. A. Maqbool, B. Kerry (Eds.), Plant nematode problems and their control in the Near East region, FAO, 1997, 59–65.

[195] S. Ahmad, M.R.M. Rao, The theory of ordinary differential equations with applications in biology and engineering. East–West Press Pvt. Ltd., New Delhi, 1999.

[196] S. Tang, Y. Xiao, L. Chen, R.A. Cheke, Integrated pest management models and their dynamical behaviour. Bull. Math. Biol., 2005, 67, 115-135.

[197] S. Tang, R.A. Cheke, State–dependent impulsive models of integrated pest management (IPM) strategies and their dynamic consequences, J Math Biol., 2005, 50(3), 257–292.

[198] S.E. Seal, M.J. Jeger, F. Van den Bosch, Begomovirus evolution and disease management, Adv. Virus Res., 2006, 67, 297–316.

[199] S.E. Seal, F. VandenBosch, M.J. Jeger, Factors influencing begomovirus evolution and their increasing global significance: implications for sustainable control, Crit. Rev. Plant Sci., 2006, 25, 23–46.

[200] S. Lenhart, J.T. Workman, Optimal Control Applied to Biological Models. Mathematical and Computational Biology Series. Chapman & Hall/CRC, London, 2007.

[201] S. Ghosh, S. Bhattacharyya, D.K. Bhattacharya, The role of viral infection in pest control: a mathematical study, Bulletin of Mathematical Biology, 2007, 69(8), 2649–2691.

[202] S.N. Puri, V.V. Ramamurthy, Insects and integrated pest management in the context of climate change–an overview. In: Ramamurthy VV, Gupta GP and Puri SN (eds) Proceedings of national symposium on IPM strategies to combat emerging pests in the current scenario of climate change, Pasighat, 2009, Jan 28–30, 1–7.

[203] S. Ghosh, D.K. Bhattacharya, Optimization in microbial pest control: an integrated approach. Appl. Math. Model., 2010, 34, 1382–1395.

[204] S. Tang, Y. Tan, L. Juhua, A. Cheke, R., Threshold conditions for in tegrated pest management models with pesticides that have residual effect, Journal of Mathematical Biology, 2011, 66 (1), 1–35.

[205] S. Jana, T.K. Kar, A mathematical study of a prey–predator model in relevance to pest control. Nonlinear Dynamics, 2013, 74, 667–683.

[206] S. Tanure, C. Nabinger, J.L. Becker, Bioeconomic model of decision support system for farm management: proposal of a mathematical model. Syst. Res. Behav. Sci., 2014, 32(6), 658–671.

[207] S. Sharma, G.P. Samanta, A Leslie–Gower predator–prey model with disease in prey incorporating a prey refuge, Chaos, Solitons & Fractals, 2015, 70(1), 69–84.

[208] S. Kant, V. Kumar, Analysis of an eco–epidemiological model with migrating and refuging prey, Mathematical Analysis and its Applications, 2015, 17–36.

[209] S. Kant, and V. Kumar, Dynamical behavior of a stage structured eco–epidemiological model, Differential Equations & Applications, 2015, 7(4), 503–515.

[210] S. Kant, V. Kumar, Dynamical behavior of a stage structured prey–predator model, International Journal of Nonlinear Analysis and Applications, 2016, 7(1), 231–241.

[211] S. Kant, V. Kumar, Dynamics of a prey–predator system with infection in prey, Electronic Journal of Differential Equations, 2017, 209, 1–27.

[212] S. Savary, L. Willocquet, S.J. Pethybridge, et al., The global burden of pathogens and pests on major food crops. Nat Ecol Evol., 2019, 3, 430–439.

[213] S. Yadav, S. and V. Kumar, Study of a prey–predator model with preventing crop pest using natural enemies and control, AIP Conference Proceedings, 2021, 2336(1), 020002.

[214] S. Yadav, S. and V. Kumar, A prey–predator model and control of a nematodes pest using control in banana: Mathematical modeling and qualitative analysis, International Journal of Biomathematics, 2021, 2150089.

[215] T. Malthus, An essay on the principal of population, 1798.

[216] T.K. Kar, K.S. Chaudhuri, Harvesting in a two prey one predator fishery: a bioeconomic model, The ANZIAM Journal, 2004, 45(3), 443–456.

[217] T.K. Kar, A. Ghorai, and S. Jana, Dynamics of pest and its predator model with disease in the pest and optimal use of pesticide. J. Theor. Biol., 2012, 310, 187–198.

[218] T.K. Kar, S. Jana, A theoretical study on mathematical modelling of an infectious disease with application of optimal control. Biosystems, 2013, 111, 37–50.

[219] T.K. Kar, S. Jana, Application of three controls optimally in a vector–borne disease–a mathematical study. Commun. Nonlinear Sci. Numer. Simul., 2013, 18 (10), 2868–2884.

[220] T. Culliney, Crop losses to arthropods. In: Pimentel D, Peshin R, Integrated pest management reviews, vol 3. Chapman & Hall, London, 2014, 201–225.

[221] T.S. Dhadialla, R. Ross, L.E. Gomez, Bisacylhydrazines: novel chemistry for insect control, in Modern Crop Protection Compounds, Wiley–VCH Verlag, Weinheim, Germany, 2019, 1013–1049.

[222] The Food and Agriculture Organization of the United Nations(`http://www.fao.org/faostat/en/#data/RP`).

[223] The Fertiliser Association of India.
`https://www.indiastat.com/table/agriculture-data/2/`
`consumption-of-fertilisers/206871/7949/data.aspx`.

[224] U.D. Ancona, The struggle of existence, E.J. Brill, Leiden, 1954.

[225] U.K. Pahari, T.K. Kar, Conservation of a resource based fishery through optimal taxation. Nonlinear Dyn., 2013, 72, 591–603.

[226] United Nations, Concise Report on the World Population Situation, New York, NY, USA, 2014.

[227] US Environmental Protection Agency. "EPA Takes Next Step in Review Process for Herbicide Glyphosate, Reaffirms No Risk to Public Health". EPA, April 30, 2019.

[228] V. Volterra, Fluctuations in the abundance of a species considered mathematically, Nature, 1926, 118, 558–560.

[229] V. Volterra, Variazioni e fluttuazionidel numero d'indidui in specie animali conviventi. Memoria R.Comita to talassografica Italiano., 1927, 131, 1–142.

[230] V. Kumar, M. Mehra, Wavelet optimized finite difference method using interpolating wavelets for solving singularly perturbed problems, Journal of Wavelet Theory and Applications, 2007, 1(1), 83–96.

[231] W.C. Allee, Animal Aggregations. University of Chicago Press, Chicago Illinois, 1931.

[232] W.C Allee, Cooperation among Animals with Human Implications, Henry Schuman, New York, 1951.

[233] W.H. Fleming and R. W. Rishel, Deterministic and Stochastic Optimal Control,Springer–Verlag, New York, 1975.

[234] W.K. Hackbusch, A Numerical Method for Solving Parabolic Equations with Opposite Orientations, Computing, 1978, 20, 229–240.

[235] W.L. Brogan, Modern Control Theory. Prentice Hall, Englewood Cliffs, NJ, 1991.

[236] W.I. Bajwa, M. Kogan, Compendium of IPM Definitions (CID), What is IPM and how is it defined in the Worldwide Literature? 2002, 19.

[237] W. Van den Berg, W. Rossing, Generalized linear dynamics of a plantparasitic nematode population and the economic evaluation of crop rotations, Journal of nematology, 2005, 37, 55–65.

[238] W. Ko, K. Ryu, Qualitative analysis of a predator–prey model with Holling type II functional response incorporating a prey refuge. Journal of Differential Equations, 2006, 231(2), 534–550.

[239] W.R. Cookson, D.V. Murphy, and M. Roper, Characterising the relationships between soil organic matter components and microbial function and composition along a tillage disturbance gradient. Soil Biology and Biochemistry, 2008, 40, 763–777.

[240] W.H. Fleming, R.W. Rishel, Deterministic and Stochastic Optimal Control, Springer Science & Business Media, New York, NY, 2012, 1.

[241] Y.M. Svirezhev, Nonlinearities in mathematical ecology: Phenomena and models. Would we live in Volterras world? Ecological Modelling, 2008, 216(2), 89–101.

[242] Y. Hsieh, S. Sheu, The effect of density–dependent treatment and behaviour change on the dynamics of HIV trans–mission, Journal of Mathematical Biology, 2001, 43, 69–80.

[243] Z. Lu, X. Chi, L. Chen, Impulsive control strategies in biological control of pesticide. Theor Popul Biol, 2003, 64(1), 39–47.

[244] `https://en.wikipedia.org/wiki/Biomass#cite_note-2`.

[245] `https://www.statista.com/statistics/271943/total-world-grain-production-since-2008-2009/`.

[246] `http://www.fao.org/economic/est/est-commodities/bananas/bananafacts/en/#.Xuuz1ZozbIU`

[247] `https://en.wikipedia.org/wiki/Banana_industry`

[248] `https://www.statista.com/statistics/264003/production-of-bananas-worldwide-by-region/`

[249] `https://www.indiafoodbanking.org/hunger`.

[250] `https://www.businessinsider.in/india/news/pictures-of-locust-attacks-in-jaipur-rajasthan-madhya-pradesh-uttar-pradesh/articleshow/76032310.cms`

[251] `http://www.fao.org/resilience/resources/resources-detail/en/c/278608/`

[252] Directorate of Plant Protection and Quarantine Faridabad, Govt of India `http://ppqs.gov.in/sites/default/files/contingency_plan_0.pdf`

List of Publications

1. Sudhakar Yadav, Vivek Kumar, A Prey–Predator Model Approach to Increase the Production of Crops: Mathematical Modelling and Qualitative Analysis, *International Journal of Biomathematics, World Scientific* (SCIE), (I.F: 2.053), (2022) `https://doi.org/10.1142/S1793524522500425`.

2. Sudhakar Yadav, Vivek Kumar, A Prey Predator Model and Control of a Nematodes Pest Using Control in Banana: Mathematical Modelling and Qualitative Analysis, *International Journal of Biomathematics, World Scientific* (SCIE),(I.F: 2.053), (2021) `https://doi.org/10.1142/S1793524521500893`.

3. Sudhakar Yadav, Vivek Kumar, Study of a PreyPredator Model with Preventing Crop Pest Using Natural Enemies and Control *American Institute of Physics, Conference Proceedings* (Scopus), (2020) `https://doi.org/10.1063/5.0045745`.

Communicated Papers

1. Sudhakar Yadav, Vivek Kumar, Study of Prey Predator System with Additional Food and Effective Pest Control Techniques in Agriculture.

2. Sudhakar Yadav, Vivek Kumar, Preventing the Spread of Locust Swarm and Pest in Agriculture: Mathematical Modeling and Qualitative Analysis.

3. Sudhakar Yadav, Vivek Kumar, Mathematical Analysis of A Prey-Predator Model in Presence of Two Controls.